

Studies of the stability and metabolism  
of tumour inhibitory tetrazinones

Lincoln Ling Hong Tsang  
Doctor of Philosophy

THE UNIVERSITY OF ASTON IN BIRMINGHAM  
October, 1989

This copy of the thesis has been supplied on condition that anyone who consults it is understood to recognize that its copyright rests with its author and that no quotation from the thesis and no information derived from it may be published without the author's prior, written consent.

The University of Aston in Birmingham

Studies of the stability and metabolism of  
tumour inhibitory tetrazinones

by

Lincoln Ling Hong Tsang

submitted for the degree of Doctor of Philosophy, 1989

Temozolomide is an imidazotetrazinone with antineoplastic properties. It is structurally related to dacarbazine. Temozolomide was not metabolized in vitro by liver fractions. Chemical decomposition appears to play an important rôle in its in vitro and in vivo disposition. In contrast, 3-methylbenzotriazinone, a structural analogue, was metabolized by hepatic microsomes to afford benzotriazinone and a hydrophilic metabolite. The cytotoxicity of temozolomide, dacarbazine, 5-[3-(hydroxy-methyl-3-methyl-triazene-1-yl)]imidazole-5-carboxamide (HMMTIC) and 3-monomethyl-(triazene-1-yl)imidazole-4-carboxamide (MTIC) were investigated in TLX5 murine lymphoma cells. Unlike dacarbazine, which was not toxic, MTIC, HMMTIC and temozolomide were cytotoxic in the absence of microsomes. Dacarbazine was only cytotoxic in the presence of microsomes. The formation of MTIC from dacarbazine, HMMTIC and temozolomide was determined by reversed phase high performance liquid chromatography in mixtures incubated under conditions identical to those described before. MTIC was generated chemically from temozolomide and HMMTIC metabolically from dacarbazine. Using [<sup>14</sup>C]temozolomide, it was found that, in mice, the major route of excretion of the drug is via the kidneys. An acidic metabolite (metabolite I) was found in the urine of mice which had received temozolomide but its identity has not been established. <sup>1</sup>H NMR, UV and chemical analyses revealed that Metabolite I possesses an intact NNN linkage and the site of metabolism is at the N<sub>3</sub> methyl group. A further acidic metabolite (metabolite II) was found in the urine of patients. Metabolite II was unambiguously identified as the 8-carboxylic acid derivative of temozolomide. In vitro cytotoxicity assay showed that only metabolite II is cytotoxic but not metabolite I. Pharmacokinetic studies of temozolomide and MTIC in vivo were performed on mice bearing TLX5 tumour. Temozolomide was eliminated from the plasma monophasically with a  $t_{1/2}$  of 0.7hr. MTIC was identified as a product of decomposition. MTIC was eliminated rapidly with a  $t_{1/2}$  of 2min. Though temozolomide shares many biochemical and biological similarities with clinically used dacarbazine, the results obtained in this study show that it differs markedly in its pharmacokinetic properties from dacarbazine, as temozolomide produced relatively sustained plasma levels which were reflected by drug concentrations in the tumour.

Keywords: imidazotetrazinones, triazenes, metabolism, pharmacokinetics, cytotoxicity.

To my parents with love

### Acknowledgements

I would like to express my sincere thanks to Dr. Andreas Gescher and Dr. John Slack for their guidance, stimulating discussion and unceasing encouragement throughout this project and production of this thesis.

I would also like to acknowledge the practical assistance of many colleagues at Aston University especially to Dr. Charmaine Quarterman, Dr. Keith Horspool, Mrs. Jan Pageter, Mr. Michael Wynter, Dr. Michael Perry, Ms. Hilary Cross, Dr. Igor Linhart, Dr. Paul Groundwater and Mrs. Karen Farrow. Thanks are also due to Dr. Julian Foster and Mr. Graham Smith for their superb artistic endeavours.

I am indebted to Dr. Peter Farmer and Mr. John Lamb at the Medical Research Council, Toxicology Unit, Carshalton, Dr. Herbie Newell, Dr. Brenda Foster and Dr. Chris Ruddy at the Institute for Cancer Research, Sutton, for their interest, advice and hospitality.

Finally, I wish to extend my appreciation to my friends and colleagues at Aston University for making these three years worthwhile. I am also grateful to the Cancer Research Campaign and Committee of University Vice Chancellors and Principals for financial support.

Contents

	Page
Summary	2
Acknowledgements	4
Contents	5
List of figures	12
List of tables	24
Abbreviations	25
Section 1: INTRODUCTION	
1.1 General Introduction	29
1.2 Development of dacarbazine (DTIC)	30
1.2.1 Metabolism and pharmacokinetics of DTIC	34
and related 1-aryl-3,3-dimethyltriazenes	44
1.2.2 Structure-activity relationships for	45
imidazo- and related aryl-	
dialkyltriazenes	
1.2.3 Antitumour activity of DTIC on experimental	45
tumour models	
1.3 Development of imidazotetrazinones	46
1.3.1 Chemical synthesis and properties of	48
imidazotetrazinones	
1.3.2 Metabolism and pharmacokinetics of	55
mitozolomide	
1.3.3 Antitumour activity and clinical property	58
of imidazotetrazinones	
1.3.3.1 Antitumour evaluation of mitozolomide	58
1.3.3.2 Clinical investigation on mitozolomide	61
1.3.3.3 Antitumour activity of temozolomide	61

1.3.4	Mode of action of imidazotetrazinones	64
1.4	Aims and Objectives	73
Section 2: MATERIALS AND METHODS		
2.1	Materials	77
2.1.1	Chemicals	77
2.1.2	Buffer solutions	78
2.1.3	Animals	79
2.1.4	Synthesis	80
2.1.4.1	Synthesis of 3-methyl-2,3-dihydro-4-oxoimidazo[5,1-d]tetrazine-4-carboxylic acid	80
2.1.4.2	Synthesis of S-methyl-N-acetyl-cysteine (methyl-mercapturic acid)	80
2.1.4.3	Synthesis of 3-monomethyl(triazene-1-yl)imidazole-4-carboxamide (MTIC), 3,3-dimethyl-(triazene-1-yl)imidazole-4-carboxamide (DTIC) and 3-monoethyl (triazene-1-yl)imidazole-4-carboxamide (METIC)	81
2.2	Weighings and measurement of volumes	82
2.3	Measurement of pH	83
2.4	Development of analytical methods	83
2.4.1	HPLC analysis of temozolomide and its urinary metabolites	83
2.4.1.1	Extraction efficiency of temozolomide and ethazolastone	84
2.4.1.2	Reproducibility of the HPLC method	84
2.4.1.3	Reproducibility of the instrument	84

2.4.2	HPLC analyses of MTIC, temozolomide, HMMTIC and DTIC	85
2.4.2.1	Recovery after protein precipitation	86
2.4.2.2	Reproducibility of the HPLC method	86
2.4.2.3	Reproducibility of the instrument and accuracy of manual injection	86
2.4.3	HPLC analysis of benzotriazinones	87
2.4.4	GC analysis of methyl isocyanate	87
2.4.5	Thin layer chromatography (TLC)	87
2.4.5.1	TLC solvent systems	88
2.4.5.2	Spray reagents	88
2.4.6	Mass spectral (MS) analysis	89
2.4.7	Nuclear Magnetic Resonance (NMR) analysis	89
2.4.8	Infra-red (IR) spectroscopic analysis	91
2.4.9	Ultraviolet (UV) spectroscopic analysis	91
2.5	<u>In vitro</u> stability studies	91
2.5.1	Determination of the stability of temozolomide and MTIC by UV spectroscopy	91
2.5.2	<u>In vitro</u> investigation of the release of methyl isocyanate from temozolomide	92
2.6	<u>In vitro</u> metabolism	93
2.6.1	Preparation of liver homogenate and subcellular fractions for <u>in vitro</u> metabolic studies on temozolomide and 3-methylbenzotriazinone	93
2.6.2	Protein determination	94
2.6.3	Analysis for formaldehyde	95
2.7	Cell culture	96
2.7.1	Coulter counter settings	96

2.7.2	TLX5 cell culture	96
2.7.3	Storage of cells in liquid nitrogen	97
2.7.4	Characterization of cell growth	97
2.8	<u>In vitro</u> cytotoxicity assays	98
2.8.1	Cell growth assay	98
2.8.2	Clonogenic assay	98
2.9	<u>In vitro</u> cytotoxicity assay including liver microsomes	98
2.10	<u>In vitro</u> metabolic studies of temozolomide, DTIC, MTIC and HMMTIC	99
2.11	<u>In vivo</u> metabolic studies	100
2.11.1	Metabolism and total excretion balance studies in mice	100
2.11.1.1	Quality control on the purity and specific radioactivity of [ <sup>14</sup> C methyl]temozolomide	100
2.11.1.2	Drug solutions	101
2.11.1.3	Experimental protocol	101
2.11.1.4	Sample preparation	104
2.11.2	<u>In vivo</u> murine metabolic studies at LD <sub>10</sub> dose	105
2.11.2.1	Preparation of suspension	105
2.11.2.2	Experimental protocol	105
2.11.2.3	Urine collection	105
2.11.3	Pharmacokinetics and metabolic studies of patients	106
2.11.3.1	Eligibility of patients	106
2.11.3.2	Treatment of patients	106
2.11.3.3	Collection of blood samples	106
2.11.3.4	Collection of urine samples	107



2.11.4	Enzymic hydrolysis of urinary metabolites	107
2.11.5	Colour test for the presence of glucuronides	108
2.11.6	Isolation of metabolites	109
2.11.6.1	Isolation of metabolites II	109
2.11.6.2	Isolation of metabolite I	111
2.11.7	Methylation of metabolite I	112
2.11.7.1	Preparation of diazomethane	112
2.11.7.2	Methylation procedure	113
2.12	<u>In vivo</u> pharmacokinetics of temozolomide and MTIC in tumour bearing mice	114
2.12.1	Innoculation of mice with TLX5 lymphoma cells	114
2.12.2	Experimental protocol	115
2.12.3	Collection of blood	115
2.12.4	Collection of tissues	116
2.12.5	Homogenization of tumour tissue	116
2.12.6	Mathematical analysis of pharmacokinetic data	118
2.12.7	Statistical analysis	118

Section 3: RESULTS AND DISCUSSION

3.1	Analysis of temozolomide in biological fluids	120
3.1.1	Development of an HPLC assay	120
3.1.2	Validation of the method	120
3.2	Analysis of benzotriazinone	124
3.3	Analyses of MTIC, HMMTIC, DTIC and temozolomide in biological fluids	127
3.3.1	Validation of the analytical methods	144
3.4	Stability of temozolomide and MTIC in biological media	151
3.5	Comparison of the <u>in vitro</u> cytotoxicity of temozolomide and its metabonates MTIC and AIC	157
3.6	Comparative <u>in vitro</u> metabolism of temozolomide and 3-methylbenzotriazinone	160
3.6.1	Introduction	160
3.6.2	Results	163
3.6.3	Discussion	176
3.7	<u>In vitro</u> cytotoxicity bioassay in the presence of liver microsomes	178
3.7.1	<u>In vitro</u> cytotoxicity of formaldehyde towards TLX5 cells	184
3.7.2	Discussion	186
3.8	<u>In vitro</u> metabolism studies	188
3.8.1	Investigation of the release of methyl isocyanate from temozolomide	198
3.8.2	Discussion	202
3.9	Studies of metabolism of temozolomide	207

	<u>in vivo</u>	
3.9.1	Excretion of drug-derived radioactivity	207
3.9.2	Characterization of urinary metabolites	211
3.9.2.1	Isolation and structural characterization of metabolite II	227
3.9.2.2	Isolation and structural characterization of metabolite I	242
3.9.3	Investigation of the cytotoxicity of metabolite I and II towards TLX5 cells	263
3.9.4	Discussion	266
3.10	Murine pharmacokinetics <u>in vivo</u>	271
3.10.1	Discussion	281
Section 4: GENERAL DISCUSSION		285
Section 5: APPENDICES		
	Appendix I	300
	Appendix II	301
	Appendix III	310
	appendix IV	318
Section 6: REFERENCES		322

LIST OF FIGURES

Figure		Page
1	<u>De novo</u> biosynthesis of purine nucleotides	31
2	Synthesis of dialkylimidazotriazenes	32
3	Photolytic decomposition pathway of DTIC	33
4	Proposed metabolic pathway of DTIC	36
5	Structure of NEDA	37
6	Proposed metabolic pathway of dialkyl-substituted phenyltriazenes	41
7	Formation of the $\beta$ -glucuronic acid metabolite from 1-(2,4,6-trichlorophenyl)3,3-dimethyl-triazene	43
8	Structures of mitozolomide, temozolomide and ethazolastone	47
9	Finger's reaction	49
10	Decomposition of 1,2,3-triazinone and 1,2,3,5-tetrazinone	49
11	Synthetic pathway of imidazotetrazinones	51
12	Decomposition of mitozolomide in the presence of methanol	54
13	Mechanism of DNA-crosslinking by a bifunctional alkylating agent	66
14	Chemical decomposition of the nitrosoureas	71
15	Structures of pyrazolotetrazinones	72
16	Principle of the analysis of methyl isocyanate	92
17	Principle of Nash reaction	95
18	Diagram of the apparatus for total excretion balance study	103

19	Principle of Tollen's reaction	108
20	Diagram of the apparatus for continuous solvent excretion	110
21	Diagrammatic representation showing the site of tumour inoculation	114
22	Diagrams of the centrifugal micro-homogenizer system	117
23	HPLC chromatogram showing the separation of ethazolastone (internal standard) and temozolomide	122
24	Calibration curve for temozolomide using ethazolastone as the internal standard	123
25	Structures of the benzotriazinones and anthranilic acid	124
26	UV chromatograms of the benzotriazinones	125
27	HPLC chromatogram showing the separation of the benzotriazinones	126
28	A plot of stability constant ( $k_{ob}$ ) <u>versus</u> pH of temozolomide and MTIC	129
29	UV chromatograms of temozolomide and MTIC	131
30	UV chromatograms of DTIC and HMMTIC	132
31	A plot of capacity factor <u>versus</u> percentage of acetonitrile	134
32	HPLC chromatograms showing the separation of temozolomide, MTIC and internal standard	135
33	Structures of hydroxyethylbenzotriazinone metronidazole	136
34	HPLC chromatogram showing the separation of MTIC, HMMTIC, DTIC	137

35	HPLC chromatogram showing the separation of MTIC, HMMTIC, DTIC and internal standard	137
36	HPLC chromatogram showing the separation of MTIC, HMMTIC, metronidazole and DTIC using 5% MeCN in ammonium acetate (0.05M) and 5% MeOH in 0.05M ammonium acetate (0.05M)	140
37	HPLC chromatograms showing the separation of MTIC, HMMTIC, metronidazole and DTIC using a) 1% MeCN/4% MeOH in ammonium acetate (0.05M), b) 3.25% MeCN/1.75% MeOH in ammonium acetate (0.05M), c) 3.75%MeCN/1.25% MeOH in ammonium acetate (0.05M)	141
38	HPLC chromatogram showing the separation of MTIC, HMMTIC, metronidazole and DTIC using 1.25% MeOH/3.75% MeCN in ammonium acetate (0.05M)	142
39	Calibration curves for a) temozolomide and b) DTIC	147
40	Calibration curves for a) HMMTIC and b) MTIC	148
41	Stability of temozolomide, MTIC, HMMTIC and DTIC at -20°C after sample preparation	150
42	Stability of temozolomide in phosphate buffer, RPMI supplemented with 17% horse serum and plasma	152
43	Stability of MTIC in phosphate buffer and RPMI supplemented with 17% horse serum	152
44	UV chromatogram of temozolomide recorded at	154

	pH10 showing its degradation	
45	UV chromatogram of MTIC recorded at pH7.5 showing its degradation	155
46	UV chromatogram of DTIC recorded at pH1 in the absence of light	156
47	Growth curve of TLX5 cells at 2 different initial seeding densities	158
48	Effect of 72hr continuous exposure to temozolomide, MTIC and AIC on TLX5 lymphoma cell growth	159
49	Proposed metabolic pathway of 1-(4-acetylphenyl)-3,3-dimethyltriazene	162
50	HPLC chromatogram showing the degradation of temozolomide in the presence of liver microsomes fortified with NADPH after a) 0min, b) 20min incubation	164
51	Time course of disappearance of temozolomide in the presence of a) viable microsomes, b) boiled microsomes and c) in phosphate buffer at 37°C	165
52	Time course of disappearance of temozolomide in the presence of viable and deactivated 10,000g fortified with NADPH	166
53	Time course of disappearance of temozolomide in the presence of viable and deactivated whole liver homogenates fortified with NADPH	167
54	Proposed chemical reaction of MTIC with Nash reagent (Dr. M.D. Threadgill)	168
55	HPLC chromatograms of a) a mixture of standards	171

	of benzotriazinones, and of extracts of suspensions of fortified microsomes with 3-methylbenzotriazinone after a) 5min b) 20min incubation	
56	HPLC chromatograms of a) an acidic extract of an incubation of 3-methylbenzotriazinone and b) an incubation of 3-methylbenzotriazinone in the presence of deactivated microsomes	172
57	Time course of the metabolic formation of a metabolite from 3-methylbenzotriazinone with a R.T. identical to the authentic benzotriazinone	173
58	Time course of the metabolic formation of a metabolite from 3-methylbenzotriazinone with a R.T. 1.8min	173
59	CIMS spectra of a) authentic benzotriazinone and b) the metabolite with an identical R.T. isolated from the microsomal incubations	174
60	CIMS spectrum of the metabolite with a R.T. 1.8min isolated from the microsomal incubations	175
61	Proposed metabolic pathway of 3-methylbenzotriazinone	177
62	Cytotoxicity of temozolomide, DTIC, HMMTIC and MTIC against TLX5 lymphoma cells in the presence and absence of microsomes	180
63	Cytotoxicity of temozolomide and cyclophosphamide against TLX5 lymphoma cells in the presence and absence of 10,000g supernatant	181
64	Proposed metabolic pathway of cyclophosphamide	182



65	Cytotoxicity of DTIC and cyclophosphamide against TLX5 lymphoma cells in the presence and absence of NADPH	183
66	Effect of formaldehyde on TLX5 lymphoma cell growth	185
67	HPLC chromatograms of a microsomal incubation a) omitting, b) in the presence of temozolomide (20mg/L) c) of an incubation of temozolomide in the absence of microsomes	189
68	Time course of the disappearance of temozolomide and the appearance of MTIC in the presence of microsomes	190
69	HPLC chromatograms of a microsomal incubation a) omitting, b) in the presence of DTIC (40mg/L) showing the presence of HMMTIC and MTIC	192
70	Time course of the metabolic formation of MTIC from DTIC in the presence of mouse and human microsomes	193
71	Time course of the metabolic formation of MTIC from DTIC at different substrate concentrations	193
72	Time course of the disappearance of HMMTIC and the appearance of MTIC	195
73	Time course of the disappearance of MTIC in the presence and absence of microsomes	197
74	Structure of a) S-(N-methyl-carbamoyl) glutathione, b) N-methylformamide and c) methyl isocyanate	198

75	Proposed chemical generation of methyl isocyanate from caracemide (NSC-253272)	199
76	GC chromatograms of an incubation of a) DMSO, b) caracemide (20mM) and c) temozolomide (20mM)	201
77	Correlation between TLX5 cell growth and [AUC] <sub>MTIC</sub>	204
78	Proposed metabolic pathway of oxidative N-demethylation	205
79	Proposed mechanism of the formation of an iminium ion from an N-(acyloxymethyl)triazene	206
80	Cumulative amount of radioactivity excreted in urine and exhaled in breath over 72hr followed by an i.p. injection of <sup>14</sup> C labelled temozolomide (40mg/Kg)	209
81	Cumulative amount of unchanged temozolomide excreted in urine over 72hr followed by an i.p. injection	209
82	Total excretion balance of temozolomide	210
83	HPLC chromatograms of an ethylacetate extract of a urine sample a) collected 24hr prior to drug administration, b) collected 24hr after dosing omitting the internal standard c) with the internal standard	212
84	HPLC radiochromatography of a) [ <sup>14</sup> C] labelled temozolomide b) a pooled urine extract of 6 mice which had received the labelled material	213
85	Structure of S-methylglutathione	214
86	High field <sup>1</sup> H NMR spectrum of S-methyl-N-acetyl-cysteine	215

87	HPLC chromatogram of a pooled urine extract of 12 mice which had received LD <sub>10</sub> dose of temozolomide <u>via</u> p.o. route	218
88	HPLC chromatogram of an ethylacetate extract of a urine sample of a patient (V.S.) who had received 700mg/m <sup>2</sup> of temozolomide <u>via</u> p.o. route	220
89	HPLC chromatograms of an ethylacetate extract of a urine sample of a) a patient (V.S.) prior to temozolomide treatment and after receiving dexamethazone (8mg) and metoclopramide (100mg), b)after administration of temozolomide c,d) of 2 healthy subjects	221
90	HPLC chromatograms showing the degradation of temozolomide after 12hr incubation with urine at 37°C	222
91	Effect of pH in the urine layer on the extraction efficiency of the metabolites at pH a) 1-2, b) 3 , c) 4, d) 5 and e) re-acidified the urine with 1N HCl(pH2)	225
92	HPLC chromatogram of a) an acidic extract of a patient's urine, b) after pre-treatment with 4N NaOH for 2min at room temperature and the aqueous layer was re-acidified for solvent extraction and analyzed by HPLC	226
93	Structures of rilnazafone and its metabolites	228
94	Proposed metabolic pathway of dimethyl-mitozolomide	229

95	HPLC chromatogram of an ethylacetate extract of a) a patient's urine (V.S.) and b) of the authentic 3-methyl-2,3-dihydro-4-oxoimidazo[5,1-d]tetrazine-8-carboxylic acid	230
96	HPLC chromatogram of the ethylacetate layer of a urine sample (200-300ml) after 72hr continuous extraction	232
97	HPLC chromatogram of the urine layer after 72hr continuous extraction	233
98	HPLC chromatogram of metabolite II isolated from urine detected by UV at a) 325nm and b) 205nm	234
99	High field <sup>1</sup> H NMR spectrum of temozolomide	236
100	High field <sup>1</sup> H NMR spectra of a) the authentic 3-methyl-2,3-dihydro-4-oxoimidazo[5,1-d]tetrazine-8-carboxylic acid and b) metabolite II	237
101	EIMS spectrum of temozolomide	239
102	EIMS spectra of a) the authentic 3-methyl-2,3-dihydro-4-oxoimidazo[5,1-d]tetrazine-8-carboxylic acid and b) metabolite II	240
103	UV spectrum of metabolite II	241
104	Principle of Pauly's reaction	244
105	UV spectra of a) acid hydrolysis of temozolomide and b) metabolite II showing an absorbance at 570nm	244
106	HPLC chromatogram of metabolite I a) before and b) after acid hydrolysis	245
107	HPLC chromatogram of an ethylacetate extract of patient's urine a) before and b) after the treatment with glucuronidase and sulphatase	246

108	Structures of meprobamate and its glucuronic acid metabolite	247
109	HPLC chromatogram of metabolite I a) before and b) after derivatizing with diazomethane	249
110	HPLC chromatogram of the eluents from the anionic exchange column at pH a,b) 6 and c,d) 5	252
111	HPLC chromatogram of the eluents from the anionic exchange column at pH a) 5 and b) 4	253
112	HPLC chromatogram of eluents from the anionic column at pH a) 4 and b) 3	254
113	High field <sup>1</sup> H NMR of the freeze dried extract collected from the anionic and cationic exchange columns	255
114	HPLC chromatogram of metabolite I eluted with 0.5% acetic acid using a 12.5cm RP select B column	256
115	HPLC chromatogram of metabolite I eluted with 0.5% acetic acid using a 25cm RP select B column	257
116	HPLC chromatogram of metabolite I after repeated HPLC purification detected by UV at a) 325nm and b) 205nm	258
117	High field <sup>1</sup> H NMR of metabolite I; water peak was suppressed by continuous secondary irradiation	260
118	UV spectrum of metabolite I	262
119	Cytotoxicity of temozolomide and metabolite II against TLX5 lymphoma cells	264
120	Lack of cytotoxicity of metabolite I against TLX5 lymphoma cells	265

121	Structures of metopimazine and LY195448	267
122	HPLC chromatograms of a sample of plasma of a mouse which had received a) DMSO/normal saline, b) temozolomide 5min and c) 10min after drug administration	273
123	<u>In vivo</u> murine plasma pharmacokinetics of temozolomide and its major metabolite MTIC after a single i.v. bolus injection at 40mg/Kg	274
124	HPLC chromatograms of a sample of plasma of a mouse which had received MTIC a) 5min b) 10min after drug administration	276
125	<u>In vivo</u> plasma pharmacokinetics of MTIC after a single i.v. bolus injection at 40mg/Kg	277
126	HPLC chromatograms showing the stability of MTIC in normal saline on ice/water	278
127	HPLC chromatograms of a) a sample of tumour of a mouse received DMSO/normal saline, b) 5min and c) 10min after the administration of temozolomide	279
128	<u>In vivo</u> tumour and plasma pharmacokinetics of temozolomide after a single i.v. bolus injection at 40mg/Kg	280
129	Proposed metabolic and decomposition pathways of temozolomide and DTIC	287
130	Time course of disappearance of ethazolastone in the presence of viable and deactivated 10,000g supernatant	291
131	Computer simulation of the amount of MTIC generated from temozolomide in plasma and tumour	295

132 Computer simulation of the amount of MTIC 296  
generated metabolically from DTIC and  
chemically from temozolomide

LIST OF TABLES

<u>Table</u>		Page
1	Antitumour activity of mitozolomide against the NCI murine tumour panel	60
2	Antitumour activity of temozolomide against the NCI murine tumour panel	63
3	Inter- and within day reproducibility of temozolomide analysis	121
4	Percentage recovery of temozolomide, DTIC, MTIC and HMMTIC after protein precipitation	143
5	Inter- and within-day reproducibility of temozolomide, DTIC, MTIC and HMMTIC	145
6	Limits of detection of temozolomide, DTIC, MTIC and HMMTIC	149
7	Rf values for the standard S-methyl-N- acetyl-cysteine, S-methyl-cysteine, temozolomide and the urinary product	216
8	Summary of the pharmacokinetic parameters of temozolomide	284
9	Summary of the pharmacokinetic parameters of MTIC	284



ABBREVIATIONS

ACNU	1-(4-amino-2-methyl-pyrimidin-5-yl)- methyl-3-(2-chloroethyl)-3-nitrosoureas
AIC	5-amino-imidazole-4-carboxamide
AUC	area under plasma concentration <u>versus</u> time curve
BCNU	1-3-bis(2-chloroethyl)-1-nitrosourea
BIC	5-[3,3-bis(2-chloroethyl)triazen-1-yl] imidazole-4-carboxamide
CCNU	1-(2-chloroethyl)-3-cyclohexyl-1- nitrosourea
CIMS	chemical ionization mass spectrometry
Cl	clearance
CPA	cyclophosphamide
Cpmax	maximum concentration of drug in plasma
C.V.	coefficient of variation
Diazald	N-methyl-N-nitroso-p-toluene sulphonamide
DiazoIC	diazoimidazole-4-carboxamide
DMSO	dimethylsulphoxide
DMSO <sub>d</sub> <sub>6</sub>	deuterated dimethylsulphoxide
dpm	disintegration per minute
DTIC	5-(3,3-dimethyl-triazen-1-yl)imidazole- 4-carboxamide
DNA	deoxyribose nucleic acid
D <sub>2</sub> O	deuterated water
EIMS	electron impact mass spectrometry
FABMS	fast atom bombardment mass spectrometry

FDCIMS	field desorption chemical ionization mass spectrometry
FID	field induction decay
fm	fraction of drug absorbed that is converted to a metabolite/metabonate
g	acceleration due to gravity
GC	gas chromatography
$^1\text{H}$ NMR	proton nuclear magnetic resonance
HMMTIC	5-[3-(hydroxymethyl-3-methyl-triazen-1-yl)]imidazole-5-carboxamide
HPLC	high performance liquid chromatography
hr	hour
i.p.	intra-peritoneally
IR	infra red
I.S.	internal standard
i.v.	intravenously
J	coupling constant
k'	capacity factor
$k_{e1}$	elimination constant
$k_{ob}$	apparent degradation constant
LD <sub>10</sub>	lethal dose for 10% of test population
MeCN	acetonitrile
MeOH	methanol
METIC	3-monoethyl(triazen-1-yl)imidazole-4-carboxamide
min	minute
MTIC	3-monomethyl(triazen-1-yl)imidazole-4-carboxamide
M	molar

m/z	mass per charge
N	normal
n	number of experiments
NADPH	nicotinamide adenine dinucleotide phosphate reduced form
NCI	National Cancer Institute
NEDA	N-(naphth-1-yl)ethylenediamine
p	probability
p.o.	orally
ppm	chemical shift part per million
Rf	relative index of movement from origin in TLC
RP-HPLC	reversed phase high performance liquid chromatography
RPMI	Roswell Park Memorial Institute
rpm	revolution per minute
R.T.	retention time
s	second
s.c.	subcutaneously
S.D.	standard deviation
$t_{1/2}$	half life
$t_{max}$	time at which maximum concentration is attained
TLX5	X-irradiation-induced thymus lymphoma
Tris	tris(hydroxymethyl)methylamine
UV	ultraviolet
Vd	apparent volume of distribution

Section 1  
Introduction

## 1 Introduction

### 1.1 General

Modern cancer chemotherapy started with the initial clinical trials of antifolates, steroids and alkylating agents in the 1940's (Pratt and Ruddon, 1979; Mihich, 1981). Since then, many new therapeutic agents have emerged from the laboratories and gone into the clinic. However, no single agent used to date in the clinic is completely devoid of deleterious side-effects on patients. This is because most of these drugs are antiproliferative agents and they cause indiscriminate toxicity to rapidly dividing cells by interfering with cell division. Hence, normal tissues with rapidly growing cells such as bone marrow, cells lining the oropharynx and gastrointestinal tract, hair follicles and the gonads are susceptible to this toxicity, usually at high doses. However, the nature of side effects varies considerably between drugs (Pratt and Ruddon, 1979). In order to improve the therapeutic benefit and decrease the toxicity of cancer chemotherapy in patients, there is an urgent need to develop new agents and drug delivery systems with high selectivity for tumour cells. Mihich (1981) outlined the following strategies and approaches upon which the development of new drug entities with improved selectivity towards tumour cells is based:

- a) A better understanding of the biology and biochemistry of tumour cells so that new targets can be identified. This may lead to the discovery of new types of drugs which can act selectively upon these newly identified targets.

b) The development of new analogues of existing active agents which might possess more favourable pharmacological properties than the parent compounds.

c) The development of new agents and treatments which can augment the physiological response of the host to malignant growth, thus constituting an indirect action against the tumours.

This thesis is concerned with the comparative metabolic evaluation of clinically related agents, a 3,3-dimethyltriazene in clinical use and a novel imidazotetrazinone. Therefore, in this section the development and pharmacology of these two classes of antitumour agents are reviewed.

#### 1.2.1 Development of dacarbazine (DTIC)

DTIC is an imidazotriazene which was developed in 1962 by Shealy and co-workers at Southern Research Institute as a structural analogue of 5-amino-imidazole-4-carboxamide (AIC), an intermediate in purine biosynthesis (Shealy et al, 1962a,b)(fig.1). At that time, most of the known inhibitors of this pathway were analogues of the naturally occurring purines or pyrimidines (Montgomery, 1959).

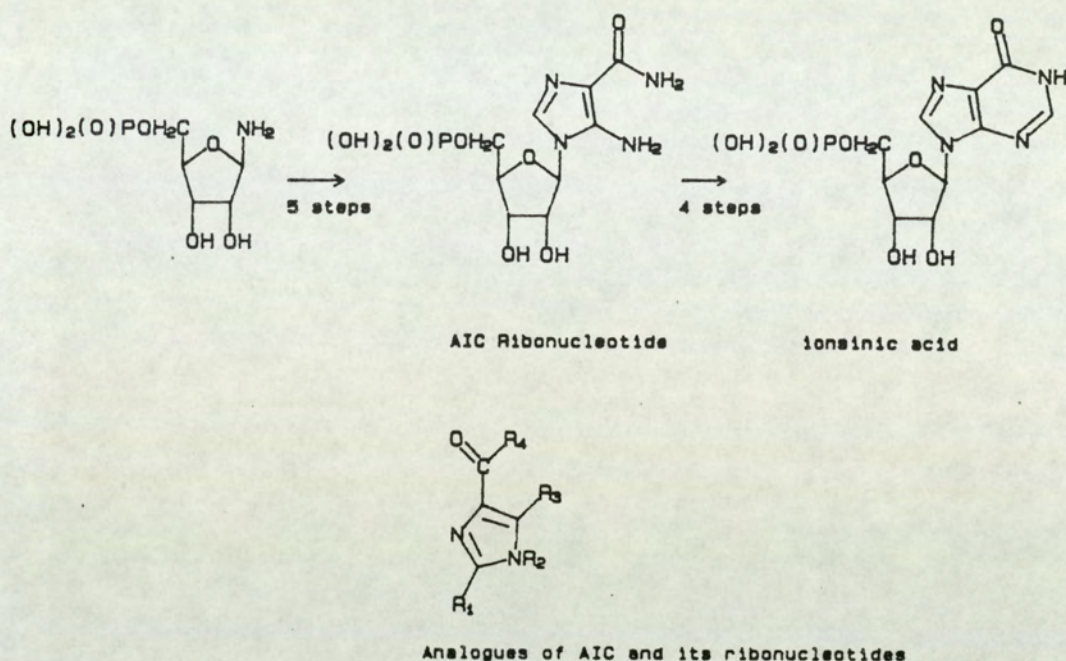
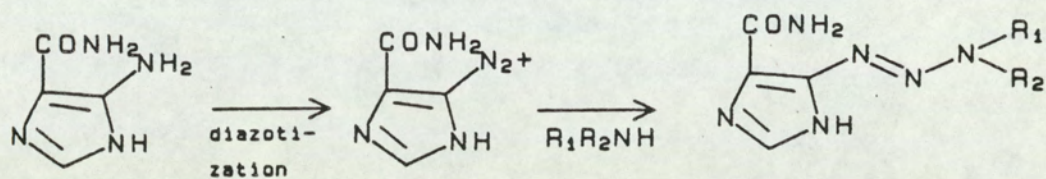


Fig.1 De novo biosynthesis of purine nucleotides

In an attempt to synthesize 2-azahypoxanthine, Shealy et al (1961) utilized the method by Woolley and Shaw (1951), which involved the treatment of AIC with nitrous acid. The initial product of the diazotization reaction as observed by Shealy et al (1961) was diazoimidazole-4-carboxamide (diazoIC), which undergoes intramolecular cyclization to yield 2-azahypoxanthine. In vitro and in vivo screenings revealed that diazoIC was active against a panel of murine tumours, but of insufficient activity to render the compound potentially useful for the treatment of human cancers. Therefore, the research for more stable and more active derivatives led to the synthesis of reaction products of diazoIC with aliphatic amines and most notably 5-(3,3-dimethyl-1-triazene-1-yl)imidazole-4-carboxamide (DTIC).



R <sub>1</sub>	R <sub>2</sub>	Compound
CH <sub>3</sub>	CH <sub>3</sub>	DTIC
H	CH <sub>3</sub>	MTIC
C <sub>2</sub> H <sub>5</sub>	C <sub>2</sub> H <sub>5</sub>	DETIC
H	C <sub>2</sub> H <sub>5</sub>	METIC

Fig.2 Synthesis of dialkylimidazotriazenes

DTIC has been shown to undergo photolytic decomposition. Such a reaction can lead to the formation of at least 5 different imidazoles (Horton and Stevens, 1981a,b) (fig.3) and one of these products was diazoIC (Horton and Stevens, 1981 a,b and Shealy et al, 1962a).



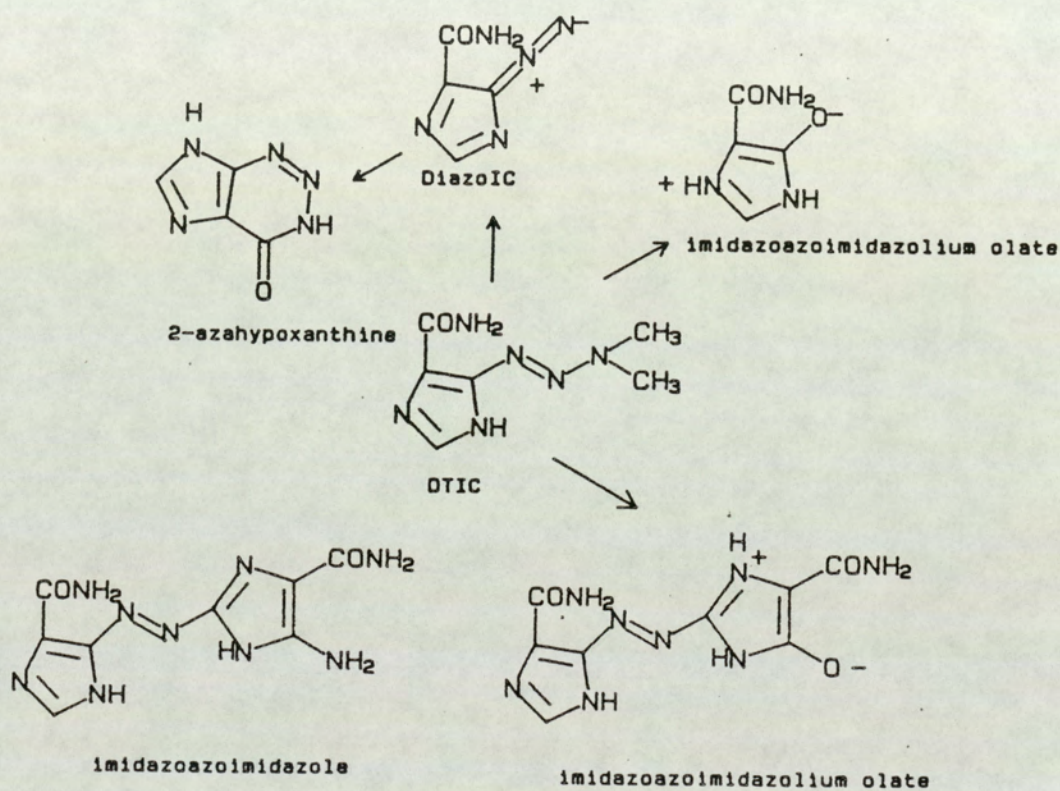


Fig.3 Photolytic decomposition pathway of DTIC

### 1.2.2 Metabolism and pharmacokinetics of DTIC and related 1-aryl-3,3-dimethyltriazenes

Though diazoIC was found to be a product of the light-catalyzed decomposition of DTIC, it is now accepted that the generation of this species cannot be responsible for the antineoplastic activity of DTIC in vivo (reviewed by Stevens, 1983). The monomethyl analogue of DTIC, MTIC, was found to be as active in vivo as DTIC, even though MTIC was much more labile than DTIC (Shealy et al, 1962a). This observation was important in elucidating the metabolism and mechanism of action of DTIC. DTIC undergoes oxidative demethylation in vitro and in vivo to give, presumably, MTIC, which decomposes leading to the formation of AIC (reviewed by Newell et al, 1987; Gescher and Threadgill, 1987; Stevens, 1983). Indeed, AIC has been identified as the major urinary metabolite of DTIC in man and also as a product of metabolism of DTIC in vitro in incubations with mouse liver microsomes (Hill, 1975) and with human and animal tumour tissues (Gerulath and Loo, 1972; Mizumo and Humphrey, 1972). In living cells, the production of reactive species, such as MTIC, leads to the interaction of the reactive species with bionucleophiles, for example, nucleic acids. This is exemplified by a study conducted by Meers et al (1986) in which following a single i.p. injection of [<sup>14</sup>C]-methyl-DTIC to rats, the highest levels of methylation of DNA were found in the liver and kidneys, which are known to be most actively engaged in the metabolism of dialkyltriazenes (Preussmann et al, 1970; Kolar, 1984). It has been suggested that the methylation

of DNA, in particular in the O<sup>6</sup> position of guanine residues, is thought to be responsible for the cytotoxic activity of MTIC (Gibson et al, 1986a; Meers et al, 1984; Montgomery, 1976; Tisdale, 1987; Lunn and Harris, 1988). Further evidence to support the contention that DTIC undergoes oxidative demethylation was the identification of 5-[3-(hydroxymethyl)-3-methyltriazene-1-yl]imidazole-4-carboxamide (HMMTIC) as an urinary metabolite in rats (Kolar et al 1980) (fig.4). Surprisingly, this metabolite was found to be more stable than MTIC in polar solvents, an observation which has led to the hypothesis that HMMTIC might act as a relatively stable transport carrier of MTIC to the target tissues (Kolar et al, 1980).

The pharmacokinetics of DTIC have been studied in both patients and in animals (Breithaupt et al, 1982; Skibba et al, 1969; Loo et al, 1968a,b). The data obtained in the early studies revealed that the disappearance of DTIC in plasma could be described by a two compartment model (Loo et al, 1968a). In dogs, after an intravenous injection of DTIC at 20mg/kg (400mg/m<sup>2</sup>), the plasma clearance of the drug was relatively fast with a t<sub>1/2</sub> of approximately 36min. The cumulative excretion of parent drug in 6hr was only 17% of the injected dose (Loo et al, 1968a,b).

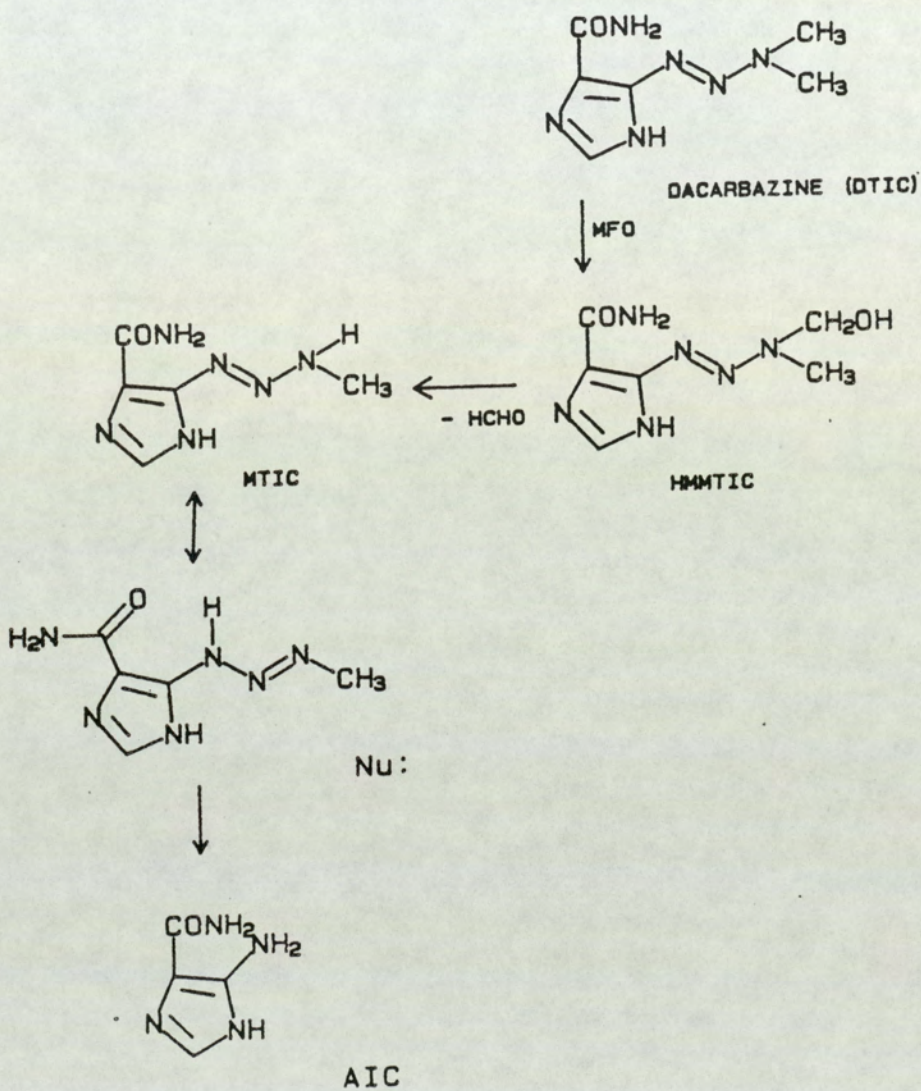


Fig.4 Proposed metabolic pathway of DTIC

When the drug was administered intravenously to patients at doses ranging from 133 to 270 mg/m<sup>2</sup>, the disappearance of DTIC from the plasma was similar to that seen in dogs: the plasma  $t_{1/2}$  was 35 min. In patients, the cumulative urinary excretion of DTIC in 6hr was 43%. This data seems to suggest that DTIC undergoes extensive degradation in the body and probably more so in dogs than in humans (Loo et al, 1969). This contention was supported by the observation that at least one biotransformation product of DTIC was detected by chromatography in the urine of dogs and patients who had received the drug. The nature of the metabolite(s) was tentatively elucidated using the Bratton-Marshall reagent (Bratton and Marshall, 1939). This colorimetric reaction involves the interaction of N-(naph-1-yl)ethylenediamine (NEDA) with diazoIC. Since the metabolite reacted with the reagent, it could possess an intact 5-diazo-imidazole moiety.

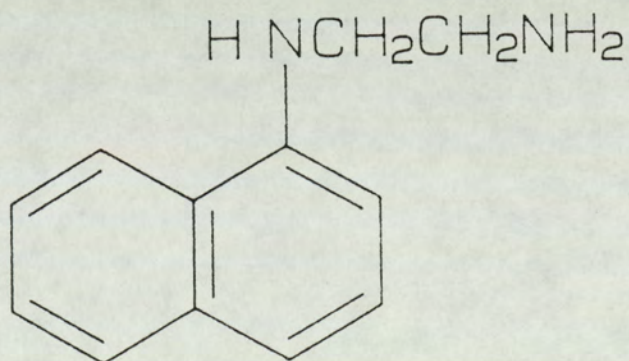


Fig.5 Structure of NEDA

When the drug was administered orally to patients at doses ranging from 30 to 260mg/m<sup>2</sup>, the plasma  $t_{1/2}$  of

DTIC was 111 min. The sustained level of the drug in plasma and the variable cumulative excretion of DTIC in urine led to the suggestion that gastrointestinal absorption of DTIC was slow, incomplete and erratic (Loo et al, 1968). These findings were in disagreement with the results obtained from another study conducted by Skibba et al, 1969 (a), in which it was found that an acceptable plasma level of DTIC was obtained after oral administration. After an oral dose of 4.5mg/kg,  $2.4 \pm 0.9 \mu\text{g/ml}$  and  $2.0 \pm 0.8 \mu\text{g/ml}$  were present in the plasma after 30 and 60min respectively. In the same patients given the same intravenous dose, the plasma levels of DTIC were  $3.3 \pm 1.3 \mu\text{g/ml}$  after 30 min and  $2.2 \pm 1.0 \mu\text{g/ml}$  after 60 min. The authors concluded that multiple daily dose therapy by oral route could be used.

Breithaupt et al (1982) utilized a more sensitive HPLC method to measure the concentration of DTIC and its major metabolite, AIC in the plasma. The pharmacokinetic data were in broad agreement with those obtained earlier from the studies using relatively less specific colorimetric analytical methods. (Householder and Loo, 1969, 1971; Loo et al, 1968, 1971, 1976 and Skibba et al, 1969).

DTIC has shown good activity against certain murine tumours in vivo but has very limited therapeutic application in the clinic (reviewed by Comis, 1976; Spassova and Golvinsky, 1985). On the basis of a preliminary pharmacokinetic study of DTIC and its putative active metabolite, MTIC, in rodents and patients, Ruddy et al (1980) suggested that lack of clinical activity of DTIC

may be at least in part due to poorer N-demethylation of the drug to MTIC in man than in rodents.

Interestingly, though DTIC is the only triazene used in the clinic, most studies of the metabolism and mechanism of the antineoplastic action of dimethyltriazenes have been carried out using substituted dimethylphenyltriazenes rather than DTIC. Dialkylaryltriazenes are known carcinogens (Preussmann et al, 1969 a,b, 1970; Druckery, 1973) and the dimethylaryltriazenes have demonstrated pronounced antitumour activity against murine leukaemias and sarcomas (Clarke et al, 1955; Burchenal et al, 1956). In the original in vitro metabolic study, Preussman, Von Hodenberg and Hengy (1969a), chose sixteen dialkylaryltriazenes as substrates to investigate the in vitro biotransformation by microsomal enzymes prepared from rat livers. The potent carcinogens 3,3-dimethyl-1-phenyltriene, 3,3-dimethyl-1-(pyrid-3-yl)triene and several other triazenes were shown to undergo oxidative dealkylation to form the corresponding aldehydes (fig.5). In the case of 3,3-dimethyl-1-phenyltriene, aniline was formed as a metabolite. The authors suggested that 3-methyl-1-phenyltriene was formed as an intermediate product. In a later study conducted by Pool (1979a), incubation of four haloaryldimethyltriazenes and unsubstituted 3,3-dimethyl-1-phenyltriene with microsomes showed that 3,3-dimethyl-1-phenyltriene yielded the lowest whilst 3,3-dimethyl-1-(2,4,6-trichlorophenyl)triene yielded the highest extent of oxidative N-demethylation. Furthermore, there was some

tentative evidence to suggest that haloaryl-monomethyltriazenes might undergo further oxidative N-demethylation.

Direct identification of a monomethyltriazene as a metabolite of 1-aryl-3,3-dimethyltriazene by comparative chromatography has only been reported once in the literature (Farina et al, 1982 and 1983). Metabolites with the same retention times and mass spectral fragmentations as the authentic synthetic compounds, 1-(4-acetyl-phenyl)-3-methyltriazene and 4-amino-acetophenone, were found as metabolites of 1-(4-acetyl-phenyl)-3,3-dimethyltriazene in vivo in the plasma of mice and in vitro in incubations with 9,000g fractions of mouse liver homogenate (Farina et al, 1982 and 1983). Isolation of 3-acetyl-3-methyl-1-phenyl-triazene in incubations of 3,3-dimethyl-1-phenyltriazene with rat liver microsomes provided further indirect evidence that dimethyltriazenes undergo N-demethylation to the corresponding monomethyltriazenes. The formation of this N-acyltriazene may involve the monomethyltriazene as a metabolic intermediate which is subsequently acetylated (Pool, 1979b).



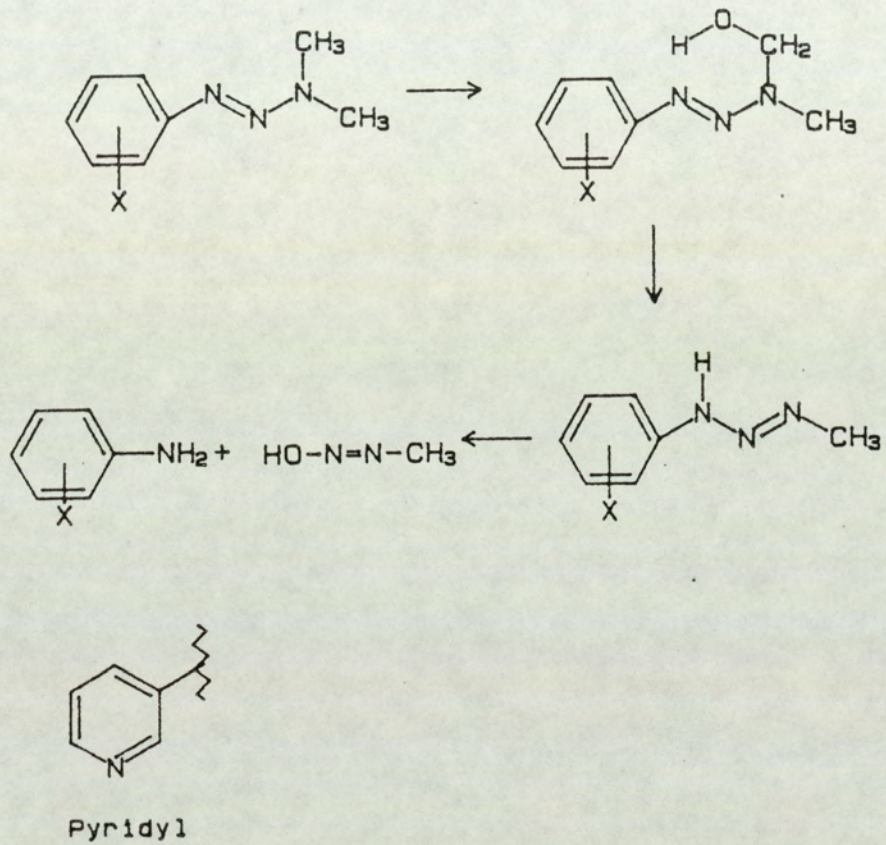


Fig.6 Proposed metabolic pathway of dialkyl-substituted phenyltriazenes

Subcutaneous administration of [<sup>14</sup>C] 3,3-dimethyl-1-phenyltriazene to rats resulted in the exhalation of <sup>14</sup>CO<sub>2</sub> which accounted for 40% of the injected radioactivity, and the formation of 7-[<sup>14</sup>C]methylguanine and other alkylated DNA and RNA bases (Kleihues et al, 1976). These results are consistent with the interpretation that dimethylphenyltriazenes are metabolized by oxidative N-demethylation to form alkylating agents; it has been observed previously by Preussman and Hodenberg (1970) that monomethyltriazenes are powerful alkylating agents, capable of methylating bionucleophiles, such as nucleic acids in the absence of drug-metabolizing enzymes. Stevens (1983) suggested that this methylation reaction proceeds via an SN<sub>2</sub> reaction mechanism and not via a "free" methyl carbonium ion as frequently quoted in papers. In the intact animal, the release of formaldehyde as a result of the initial oxidation would be expected to enter the one carbon pool and the labelled carbon atom can be incorporated into various intermediary products including purine bases, amino acids and CO<sub>2</sub> (Krüger et al, 1970; Kleihues et al, 1976). 7-[<sup>14</sup>C methyl]guanine adducts were found in various organs such as the brain and the spleen of animals exposed to labelled dimethylphenyltriazene and these tissues, distal to the sites of metabolizing activity, are presumably unable to catalyze N-demethylation (Kleihues et al, 1976). The authors suggested that dimethyltriazenes may be metabolized to a stable transport form which subsequently undergoes chemical decomposition to generate the monomethyltriazene. The immediate metabolic

precursors of 1-aryl-3-methyltriazenes, the 3-(hydroxymethyl)-3-methyltriazenes have been synthesized (Gescher et al, 1978; Juilliad et al, 1980) but have not been identified as metabolites of aryl dimethyltriazenes. Kolar and Carubelli (1979) isolated and identified 1-[3-methyl-1-(2,4,6-trichlorophenyl)-triazene-1-yl]-methyl- $\beta$ -D-glucuronic acid as a metabolite in the urine of rats which had received 1-(2,4,6-trichlorophenyl)-3,3-dimethyltriazene. The authors suggested that this glucuronide might be one of the transport forms of the triazene capable of carrying monomethyltriazene to the target tissue where enzymic hydrolysis takes place to release the methylating agent and formaldehyde.

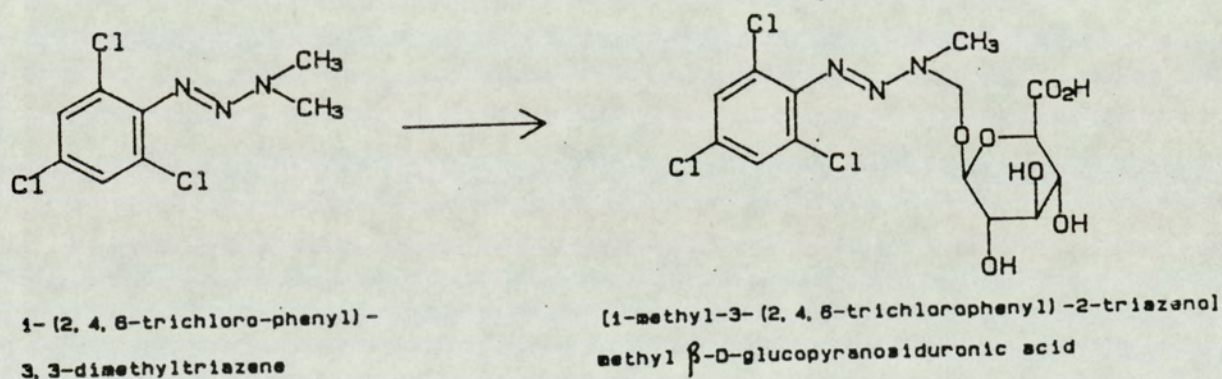


Fig.7 Formation of the  $\beta$ -glucuronic acid metabolite from 1-(2,4,6-trichlorophenyl)3,3-dimethyl-triazene

### 1.2.3 Structure activity relationships for imidazo- and related aryl- dialkyltriazenes

Structure activity analyses on imidazo- and phenyl-triazenes demonstrate that at least one methyl group at the N<sub>3</sub> position is necessary for antitumour activity (Audette et al, 1963; Connors et al, 1965; Hano et al, 1965; Shealy et al, 1968; Hansch et al, 1972; Hatheway et al, 1978; Wilman and Goddard, 1980). In a series of 3,3,dialkylimidazoletriazenes, the dimethyl derivative possessed the highest antitumour effect against Ehrlich solid carcinoma in mice (Hano et al, 1965). An increase in the chain length of the 2 alkyl groups in the N<sub>3</sub> position resulted in a decrease in antitumour activity. In another series of triazenes with differing alkyl groups, it was shown that at least one methyl group was necessary to exert the greatest antitumour activity (Hansch et al, 1972). Varying the chain length of the second alkyl group did not result in a significant difference in antitumour activity (Shealy et al, 1968).

Similar results were obtained in a series of dialkylphenyltriazenes (Hatheway et al, 1978; Audette et al, 1963; Connors et al, 1973). Of the series of compounds investigated, only those which could be metabolized in vivo to an 1-aryl-3-monomethyltriazene possessed antitumour properties (Connors et al, 1973; Wilman and Goddard, 1980). This may explain the inactivity of a methyl-tert-butyl triazene as the tert-butyl substituent has no alpha-CH group amenable to metabolic oxidation and therefore cannot be metabolized to a monomethyltriazene. The nature of the

substituent in the phenyl ring had little effect on the overall antitumour activity at least against the TLX5 lymphoma and L1210 leukaemia in mice (Lin and Loo, 1972; Connors et al, 1973; Audette et al, 1963).

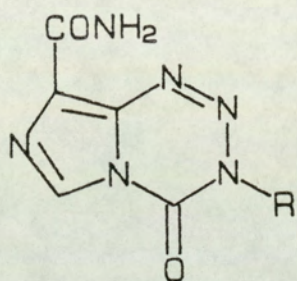
#### 1.2.4 Antitumour activity of DTIC on experimental tumour models

The introduction of DTIC into clinical trials was based on its activity against i.p. implanted leukaemia L1210 in mice. DTIC was found to be active against L1210 and the cell lines of L1210 which were resistant to antimetabolites, for examples, methotrexate, 6-mercaptopurine and 6-thioguanine. The treatment of mice bearing leukaemia P815 or a 5-fluorouracil-resistant variant of P815 resulted in a number of cures (reviewed by Venditti, 1976; Montgomery, 1976). These results seem to suggest that the mechanisms of antitumour activity of DTIC are different from that of antimetabolites. In addition, DTIC was also active against solid tumours, such as sarcoma 180 and adenocarcinoma 755 and lymphosarcoma P1798 but only slightly effective against B16 melanoma, Lewis lung carcinoma and Ridgway osteogenic sarcoma and against Walker 256 carcinoma in rats.

### 1.3. Development of imidazotetrazinones

The imidazotetrazinones are a group of new antitumour agents, which are structurally similar to the 3,3-dialkyltriazenylimidazoles. Amongst them, the lead compound, mitozolomide (CCRG 81010, M&B 39565, 8-carbamoyl-3-(2-chloroethyl)imidazo[5,1-d]-1,2,3,5-tetrazin-4(3H)one) displays potent antitumour activity against a broad spectrum of murine tumours (Hickman et al, 1985) and human xenografts (Fodstad et al, 1985). The drug completed phase I clinical evaluation in 1985 (Newlands et al, 1985) and phase II trials in 1988 (Gundersen et al, 1987; Harding et al, 1988; Van Oosterom et al, 1989). The 3-methyl analogue of mitozolomide, temozolomide (CCRG 81045, M&B 39831, 8-carbamoyl-3-methyl-imidazo-[5,1-d]-1,2,3,5-tetrazin-4(3H)-one) began phase I clinical evaluation in the United Kingdom in 1987.

In the following sections, the i) synthesis ii) chemical decomposition iii) metabolism and pharmacokinetics and iv) biological and clinical evaluations of these compounds are reviewed.



R	Compound
CH <sub>2</sub> CH <sub>2</sub> Cl	mitozolomide
CH <sub>3</sub>	temozolomide
CH <sub>2</sub> CH <sub>3</sub>	ethazolastone

Fig.8 Structures of mitozolomide, temozolomide and ethazolastone

1.3.1 Chemical synthesis and properties of imidazotetrazinones

The rationale of the synthesis of imidazotetrazinones stemmed from detailed chemical studies on molecules bearing NNN linkages- in cyclic or acyclic structures or in bicyclic heterocycles with bridgehead nitrogen atoms (Stevens, et al, 1984). It was found that 1,2,3-benzotriazin-4(3H)-one undergoes ring-opening in the presence of aqueous alkali to yield anthranilic acid (Finger's reaction)(fig.8). Although the 1,2,3-triazinones can decompose to give a variety of products, dominated by cleavage of the 1,8a; 2,3; or 3,4 bonds, antitumour activity is not exhibited by these compounds (Stevens et al, 1984; reviewed by Stevens, 1987, fig.9).



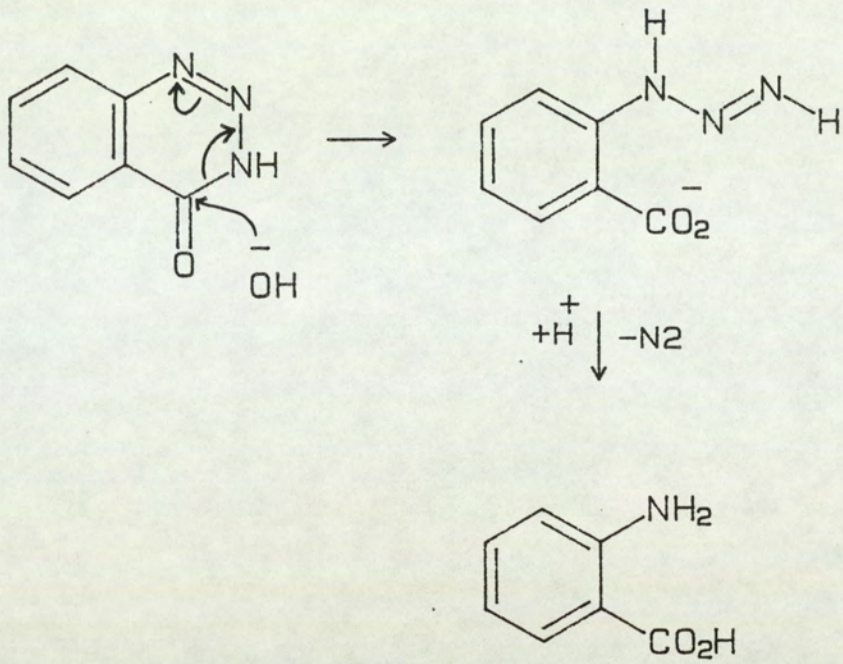


Fig.9 Finger's reaction

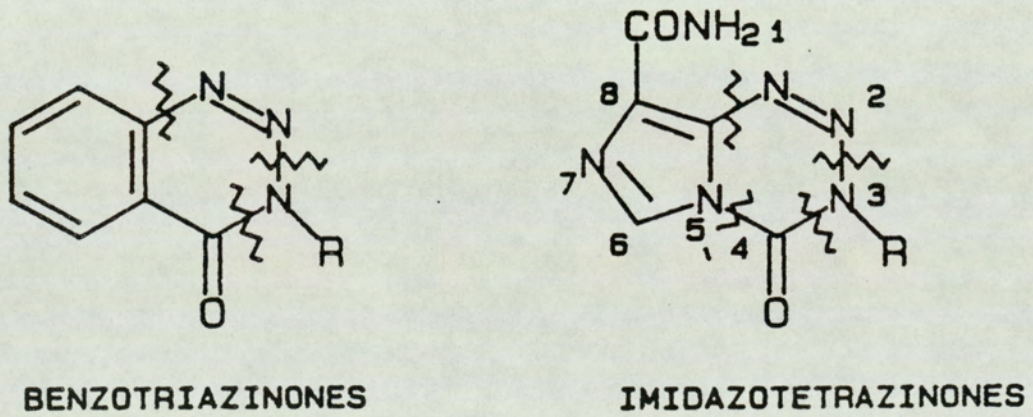


Fig.10 Decomposition of 1,2,3-triazinone and 1,2,3,5-tetrazinone

In accordance with a new general synthetic route devised by Ege and Gilbert (1979), a series of 8-carbamoyl-3-substituted-imidazo[5,1-d]-1,2,3,5-tetrazin-4(3H)ones could be prepared by reacting 5-diazoimidazole-4-carboxamide with aryl and alkyl isocyanates. On the basis of the chemistry of 1,2,3 and 1,2,4-triazines, Stevens et al (1984) predicted that incorporation of an extra heteroatom in a bicyclic 1,2,3,5-tetrazine would induce lability in four different bonds, namely 1,8a; 2,3; 3,4 and 4,5 (fig.9). It was suggested that such fragmentations might generate a cascade of reactive products, some of which are known to possess antitumour activity. For example, cleavage of the 2,3 and 4,5 bonds in mitozolomide would generate diazoimidazole and 2-chloroethyl isocyanate respectively; the latter species has been shown to play a rôle in modulating the biological activity of the nitrosourea BCNU against TLX5 lymphoma in mice (Gibson and Hickman, 1982). However, hydrolytic attack at the C<sub>4</sub> position, with subsequent cleavage of the 3,4 or 4,5 bonds would liberate MCTIC which is a potent antitumour agent in its own right (Shealey et al, 1975; Stevens et al, 1984; Stone, 1981). There has been some evidence to substantiate the existence of both decomposition routes for mitozolomide (Stevens et al, 1984; Stone, 1981).

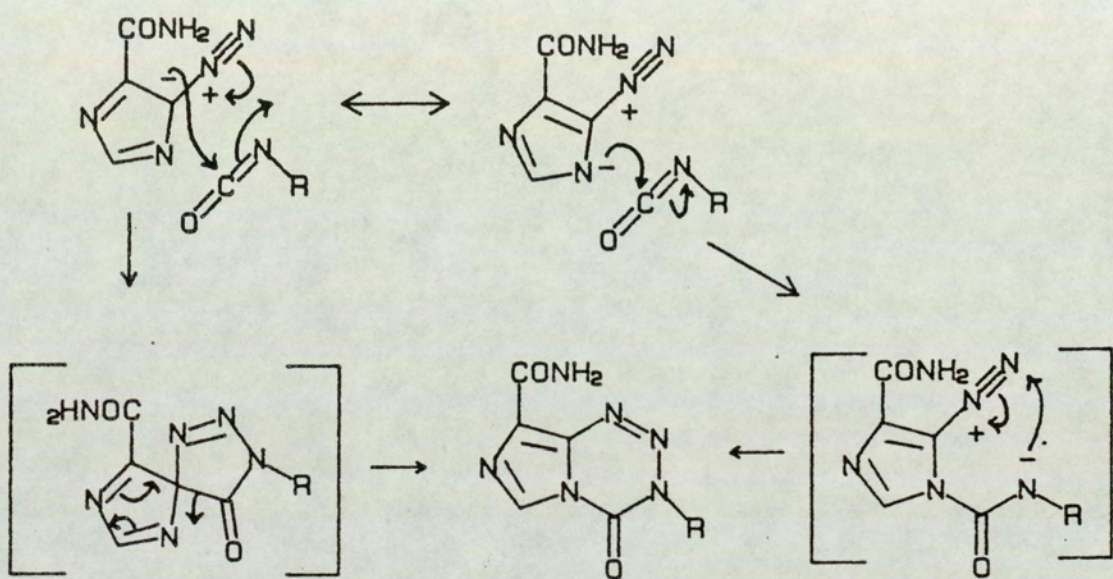


Fig.11 Synthetic pathway of imidazotetrazinones

Indeed, the nature and the route of decomposition of mitozolomide and its 3-methyl and 3-ethyl analogues were extremely sensitive to the reaction conditions (Baig and Stevens, 1987; Baig, 1986).

Mitozolomide was unstable in boiling methanol or ethanol and yielded 2-azahypoxanthine and N-(2-chloroethyl)carbamates. The mechanism of decomposition is thought to involve the initial attack at C<sub>4</sub> to generate hemiacetals; loss of a proton from this intermediate leads to cleavage of the 4,5 bond to produce the unstable triazenes. The formation of 2-azahypoxanthine and the carbamates is probably achieved via intramolecular cyclization with subsequent loss of the isocyanate moiety (fig.11). In contrast, both the 3-methyl and 3-ethyl analogues were more stable in boiling methanol than mitozolomide; after 10 days, 2-azahypoxanthine (80%) and a colourless solid (20%) were obtained; the latter was identified as 5-amino-1-methoxycarbamoylimidazole-4-carboxamide. Therefore, there are apparent differences in the chemistry of mitozolomide and its 3-alkyl derivatives. Evidence obtained in the investigation by Baig and Stevens (1987) suggests that in the presence of nucleophiles containing oxygen or nitrogen atoms, mitozolomide undergoes fission of the 4,5 bond whereas 3-methyl and 3-ethyl analogues also undergo fragmentations at the 3,4 bond to a minor extent.

When mitozolomide and its 3-alkyl homologues were boiled in water, the main product was AIC (Baig and Stevens, 1987). The rate of decomposition of mitozolomide was greatly influenced by pH: mitozolomide, temozolomide and the 3-ethyl analogue were stable in warm concentrated sulphuric acid. However, at higher values of pH, for example in an aqueous 5% sodium carbonate solution, these 3 compounds undergo ring-opening to give the corresponding linear triazene (Baig and Stevens, 1987; Stevens et al, 1984). At physiological pHs, for instance, in phosphate buffer (0.2M, pH 7.4) at 37°C, mitozolomide and temozolomide undergo decomposition with a  $t_{1/2}$  0.9 and 1.24hr respectively (Goddard, 1985, Slack et al, 1986; Slack and Goddard, 1986). The slightly greater stability of temozolomide when compared with mitozolomide was also observed in physiological fluids (Goddard, 1985). AIC and N-(hydroxyethyl)-AIC have been tentatively identified by HPLC and TLC as 2 of the principal decomposition products of mitozolomide (Goddard, 1985).

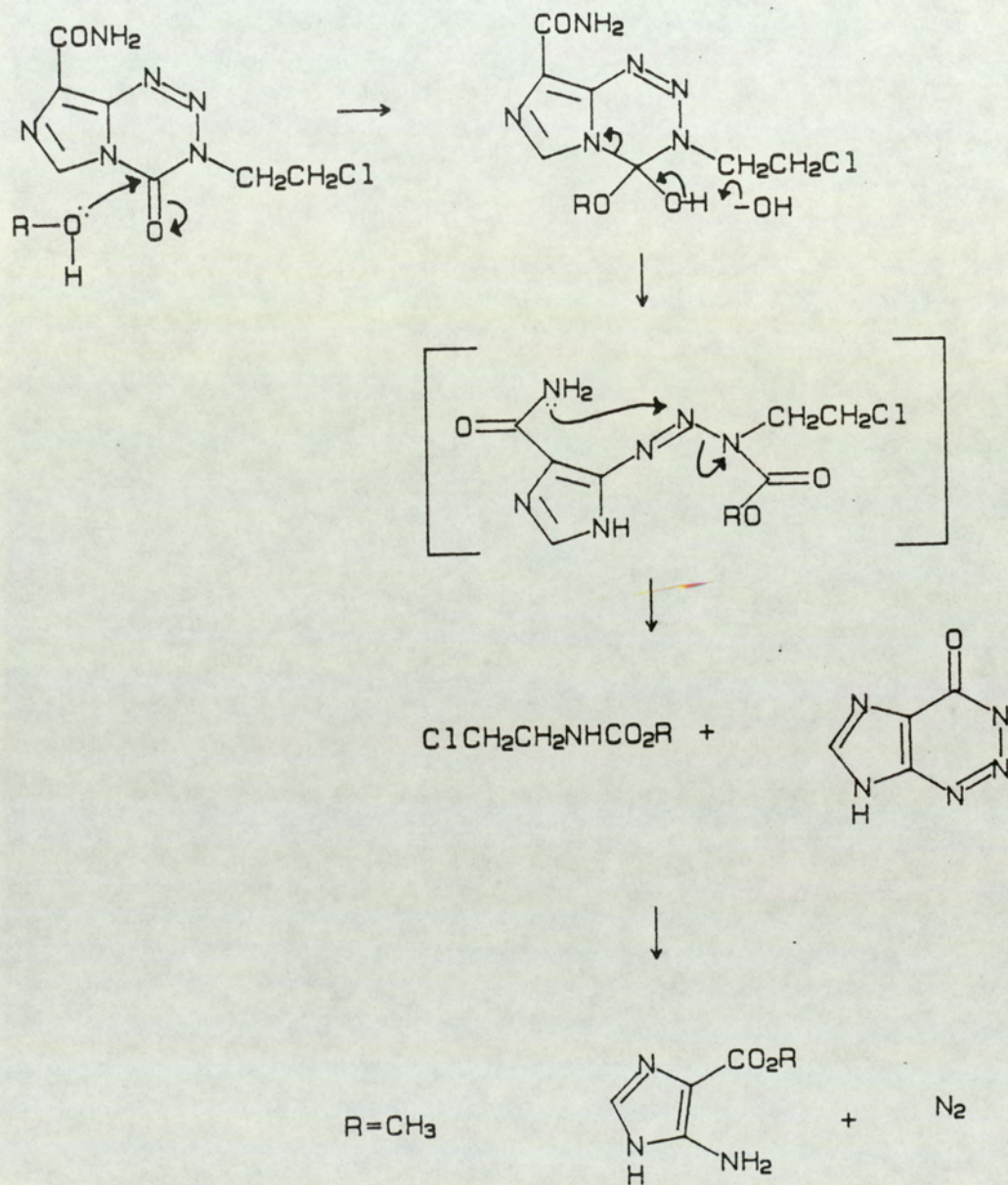


Fig.12 Decomposition of mitozolomide in the presence of methanol

### 1.3.2 Metabolism and pharmacokinetics of mitozolomide

The pharmacokinetic properties of mitozolomide have been studied in both mice and humans (Goddard et al, 1985; Goddard, 1985, Newlands et al, 1985; Slack et al, 1985). Measurement of plasma drug concentrations, in the phase I trial of mitozolomide, using HPLC (Slack and Goddard, 1985), yielded a monophasic elimination profile with a plasma  $t_{1/2}$  of between 1 and 1.3hr after administration of the drug by a 1hr i.v. infusion; and the drug was undetectable 12hr after administration. The plasma  $t_{1/2}$  was in broad agreement with that predicted from animal studies (Goddard et al, 1985; Newlands et al, 1985; Slack et al, 1985). There was no evidence of dose dependency in the pharmacokinetics of mitozolomide over the range of doses examined (8 to 153 mg/m<sup>2</sup>). Mitozolomide was well absorbed after oral administration, with a mean bioavailability of 95%.

The drug shares certain biochemical and biological similarities with the nitrosoureas BCNU and CCNU (Gibson et al, 1984 a,b; 1985). However, relatively sustained levels of mitozolomide were found in the plasma when compared with those of BCNU and CCNU (Goddard et al, 1985; Levin, 1979, 1981). The pharmacokinetic differences observed between these nitrosoureas and mitozolomide may be of therapeutic importance in that they may indicate a pharmacokinetic advantage over the nitrosoureas if they reflect similarly sustained tumour concentrations (Goddard et al, 1985). Brindley et al (1986) have demonstrated that when mice bearing ROS osteosarcoma received mitozolomide by the i.p.

route, the drug was rapidly and extensively distributed into tissues including the tumour.

The in vivo metabolism of mitozolomide has been studied in mice (Goddard, 1985) but no metabolic studies have yet been conducted in patients. In that study, mitozolomide radiolabelled in either the imidazole ring or the chloroethyl moiety was injected into mice intraperitoneally. It was found that kidneys were the major organs of drug excretion for both labelled materials, urinary excretion accounted for 58 and 88% of the injected radioactivity. The urine of mice obtained 12hr after the administration of the drug was analyzed by TLC autoradiography. Four principal bands were apparent in the case of the urine from the mice which received material radiolabelled in the imidazole ring: they were mitozolomide, AIC, N-(2-hydroxyethyl)-AIC and an unknown urinary product. Six main bands were seen in the autoradiogram of the urine obtained from the mice treated with [<sup>14</sup>C]chloroethyl-mitozolomide, one of them was identified as mitozolomide. No attempt was made to identify and characterize the other urinary products. None of these unidentified urinary products were found in the autoradiogram obtained in a parallel drug decomposition study.

Some radioactivity (6.5-22% of the injected radioactivity) derived from mitozolomide labelled <sup>14</sup>C in the imidazole ring and the chloroethyl moiety was found in the faeces. This finding suggests the possibility of biliary excretion; but since administration of the drug was



by the i.p. route, a general diffusion of the drug into the gastro-intestinal tract is an alternative possibility. Therefore, the chemical nature of the faecal radioactivity remains speculative. The amount of carbon dioxide exhaled was relatively insignificant, 5% after administration of [<sup>14</sup>C]chloroethyl-mitozolomide and 1.8% after receiving material labelled in the imidazole ring.

In addition, there is some evidence to suggest that metabolism is an important determinant of the rate of deactivation of mitozolomide. It has been shown that pretreatment of mice with phenobarbital reduces the activity of mitozolomide against the KHT sarcoma (Workman and Lee, 1984). Furthermore, the plasma AUC of mitozolomide determined in mice, which had been pretreated with phenobarbital, was significantly smaller than that in control animals (Brindley et al, 1986).

### 1.3.3 Antitumour activity and clinical property of imidazotetrazinones

#### 1.3.3.1 Antitumour evaluation of mitozolomide

Mitozolomide demonstrated potent antitumour activity against a broad spectrum of murine tumours (Hickman et al, 1985). In animal screening models, mitozolomide at single doses between 20 and 40 mg/kg elicited curative activity against L1210 and P388 leukaemias irrespective of the route of tumour implantation and drug administration. Potent antitumour activity was also observed against the TLX5 lymphoma (s.c.) and B16 melanoma (i.p.) and various solid tumour models, for examples, Lewis lung carcinoma, colon 38 carcinoma (Hickman et al, 1985). These results suggested that mitozolomide is one of the most potent compounds screened against the "old" National Cancer Institute murine tumour panel (Geran et al, 1972). When the antitumour activity of mitozolomide was compared with that of other widely studied agents in these animal models, it was shown that it was equally active with cis-platinum, BCNU, cyclophosphamide and adriamycin and more active than DTIC (Hickman et al, 1985).

In cross resistance studies, mitozolomide was inactive against L1210 leukaemia made resistant to BCNU and against a TLX5 lymphoma resistant to dimethyltriazenes such as DTIC. However, mice bearing the L1210 Leukaemia with derived resistance to cyclophosphamide retained their sensitivity to mitozolomide.

Fodstad et al (1985) investigated the antitumour

activity of mitozolomide against several human tumour lines which were grown as xenograft. In that report, mitozolomide displayed pronounced antitumour activity against xenografts from human sarcomas, melanomas and colon cancers. It was, therefore, suggested that mitozolomide might elicit clinical responses in these types of cancer (Fodstad et al, 1985).

Drug	L1210 leukaemia	P388 leukaemia	B16 melanoma
Mitozolomide	++	++	++
Nitrogen mustard	++	+	++
BCNU	++	++	++
DTIC	++	+	+
Cisplatin	++	++	++
Cyclophosphamide	++	++	++
Methotrexate	++	++	inactive
Adriamycin	++	++	++
<hr/>			
% T/C activity criteria (++)	>150	>175	>150
(+)	>125	>120	>125

Table 1. Antitumour activity of mitozolomide against the NCI murine tumour model

### 1.3.3.2 Clinical investigation on mitozolomide

In the phase I clinical trial of mitozolomide (Newlands et al, 1985), it was found that the dose-limiting toxicity was thrombocytopenia at doses greater than 115mg/m<sup>2</sup>, and recovery from the thrombocytopenia was delayed for up to 8 weeks. This observation was similar to that made with the nitrosoureas (Schein, 1981).

Similar haematological adverse reactions were also encountered in the phase II clinical trials (Harding et al, 1988, Gundersen et al, 1987). However, mitozolomide was active against malignant melanomas and seemed to have a response rate comparable to those of the most active established drugs (Gundersen et al, 1987). The apparent nature of selective toxicity towards the bone marrow has led to the suggestion that mitozolomide might be used in conjunction with bone marrow transplantation; the rationale being that after aspiration of bone marrow, the patient could be treated with high doses of the drug before re-infusion of the bone marrow. (Gundersen et al, 1987)

### 1.3.3.3 Antitumour activity of temozolomide

A number of 3-alkyl analogues of mitozolomide were screened against murine tumours in vivo (Stevens et al, 1987). Amongst them, only the 3-methyl, temozolomide, and 3-bromoethyl analogues showed antitumour activity. Compounds with an increase in carbon chain length were almost devoid of any activity. This is a result reminiscent of the structure activity relationships amongst the alkyaryltriazenes (Audette et al, 1973; Connors et al,

1976) (see section 1.2.3).

Temozolomide was active against L1210, P388 leukaemias, the M5076 reticulum cell sarcoma, B16 melanoma and ADJ/PC6A plasmacytoma. In contrast to mitozolomide, which displayed optimal activity on a single dose schedule, temozolomide was most active on a divided dose schedule. Temozolomide has demonstrated cross resistance to a P388 line resistant to mitozolomide and an L1210 cell line resistant to DTIC (Stevens et al, 1987). Therefore, temozolomide might act via a mechanism similar to that by which DTIC exerts its effect.

	Schedule (day of injection)	Optimum dose (mg/kg/day)	Optimal T/C Assessment (%)
P388 leukaemia	1	200	+
	1-4	100	++
	1-5	200	+++
P388/mitozolomide	1	200	-
	1-4	100	-
L1210 leukaemia	1	200	+
	1-4	100	++
L1210/DTIC	1	200	-
	1-4	100	-
L1210/BCNU	1	200	+
	1-4	100	++
B16 melanoma	1-9	100	++
	1,5,9,13	200	++
TLX5 lymphoma	3	160	++
	3,6,9	80	++
	3-7	40	++

Table 2. Antitumour activity of temozolomide against the NCI murine tumour panel

+++ , T/C > 150% with cures at one or more dose  
 ++ , T/C > 150% with no cures  
 + , T/C > 125%

#### 1.3.4 Mode of action of imidazotetrazinones

One of the objectives of this project is to elucidate the mechanism of action of temozolomide (see section 1.4). In the following section of the thesis, the findings obtained from the biochemical mechanistic studies conducted previously on the imidazotetrazinones are reviewed.

Most of the earlier work on elucidating the mode of action of imidazotetrazinones was centred on the lead compound, mitozolomide. The generation of 2-chloroethyl isocyanate by cleavage of the 2,3 and 4,5 bonds in mitozolomide is theoretically possible (section 1.3.1). However, evidence accrued from both biochemical and mechanistic chemical studies on mitozolomide have suggested that the antitumour activity of mitozolomide may be mediated via MCTIC, by cleavage of the 3,4 or 4,5 bonds (Finger's reaction, section 1.3.1) (Stevens et al, 1984; Lowe et al, 1985,a,b; Baig and Stevens, 1987; Horgan and Tisdale, 1984, 1985; Gibson et al, 1984 a,b, 1985; Hickman et al, 1985).

MCTIC is a chloroethylating agent which is capable of alkylating nucleophiles such as DNA via an  $SN_2$  mechanism (Shealey et al, 1975). There are a variety of potential sites for alkylation. Amongst them, the  $O^6$  position of guanine residues of DNA is of particular biological interest. There is cumulative evidence that  $O^6$  alkylation plays a rôle in carcinogenicity and mutagenesis (Singer, 1979; Rajewsky, 1982; Guttenplan, 1974; Goth and Rajewsky, 1974). Alkylation of  $O^6$  guanine is a pro-mutagenic lesion leading to the misreading of the genetic code. This is



because guanine alkylated at O<sup>6</sup> is read as adenine and consequently, a GC-AT single point mutation occurs. In addition, Kohn (1977) proposed that the mechanism by which chloroethylating agents kill tumour cells might be due to their ability to cross-link DNA. It is postulated that initial chloroethylation occurs at the O<sup>6</sup> position of guanine followed by intramolecular reaction of the chloroethyl group at the O<sup>6</sup> with N<sup>1</sup> position of guanine. This is accompanied by the completion of the interstrand link to the N<sup>3</sup> position of the complementary cytosine residues (fig.13). This type of cross-linking has been observed in DNA treated with the nitrosourea BCNU (Tong et al, 1982) and in murine L1210 leukaemia cells treated with mitozolomide and MCTIC (Gibson et al, 1984a). In the latter study, it was demonstrated that mitozolomide and MCTIC possessed similar cytotoxicity towards L1210 cells, and at equitoxic concentration, similar levels of DNA interstrand cross-linking were also observed. These results suggest that mitozolomide is cytotoxic to L1210 leukaemic cells as a result of DNA interstrand cross-link formation, probably via MCTIC, which is generated upon chemical decomposition. DNA cross-linking and cytotoxicity of mitozolomide was further studied by examining its

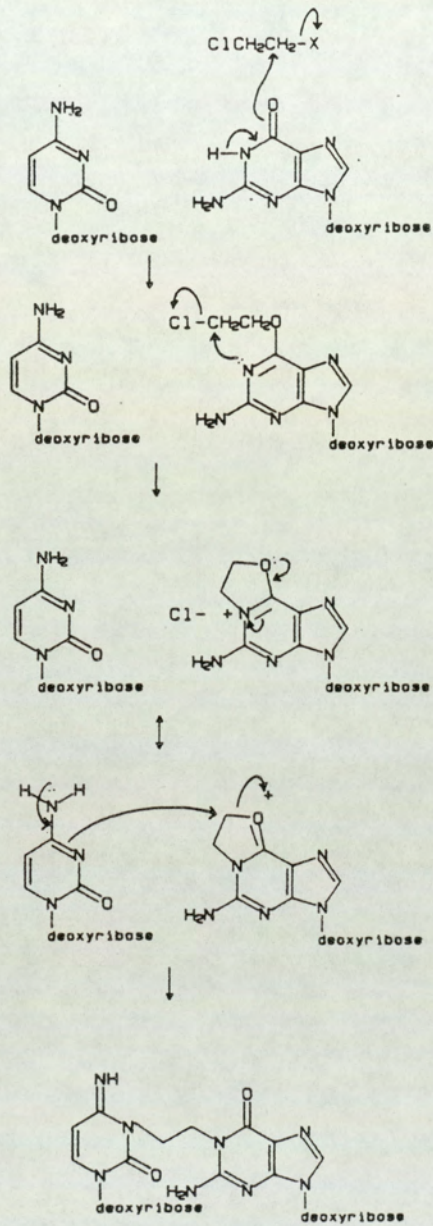


Fig.13 Mechanism of interstrand cross-link

effect on cell viability and cellular DNA integrity of two cell lines, IMR-90 (Mer<sup>+</sup>) and SV-40 transformed (VA-13, Mer<sup>-</sup>) embryo cells. These two cell lines differ in their response to chloroethylnitrosoureas (Erickson et al, 1980), possibly because of a difference in their ability to repair the O<sup>6</sup>-alkyl guanine lesion due to the presence of a repair enzyme, O<sup>6</sup>-alkylguanine DNA-alkyltransferase (Olsson et al, 1980; Harris et al 1983; Hora et al, 1983). It has been demonstrated that the removal of an O<sup>6</sup> chloroethyl-monoadduct by a Mer<sup>+</sup> cell would prevent subsequent cross-linking and therefore enhance the survival of the cells which possess this enzyme in abundance. Gibson et al (1984b) demonstrated a similar differential response in the same cell lines with both mitozolomide and MCTIC. Mitozolomide and MCTIC were 5 to 6 fold more toxic to VA-13 cells than to IMR-90 cells, as measured by their ability to form colonies. The level of formation of DNA-protein cross-links was similar in both cell lines for each drug examined, suggesting that drug penetration and intracellular drug reactivity were similar in both cell types. Both mitozolomide and MCTIC produced insignificant levels of DNA interstrand cross-links in the Mer<sup>+</sup> cell line even at a concentration that gave more than 1.5 log cell kill whereas a large degree of interstrand cross-links were found in the Mer<sup>-</sup> cell line. The interstrand cross-link formation in the Mer<sup>-</sup> cell line was concentration dependent and a linear correlation between the formation of cross-linking and log cell kill was observed. However, no such correlation was obtained with the Mer<sup>+</sup> cell line. It

was suggested that mitozolomide might produce a chloroethyldiazo species analogous to chloroethylnitrosoureas, previously implicated in the formation of chloroethyl-DNA adducts leading to the formation of interstrand cross-links (Erickson et al, 1980b; Mehta et al, 1981). These results led to the suggestion that DNA interstrand cross-link formation might be a common mechanism for the cytotoxicity in vitro of mitozolomide and MCTIC.

The importance of DNA-interstrand cross-links in causing cell death has been questioned by Gibson et al (1986). Using a series of alkyltriazenyylimidazoles against HT-29 colon carcinoma cells (Mer<sup>+</sup>) and BE colon cells (Mer<sup>-</sup>), it was found that chloroethyl and monomethyl analogues of this series of imidazotriazenes produced a differential toxicity between Mer<sup>+</sup> and Mer<sup>-</sup> cell lines; however, unlike chloroethyl analogues, monomethyltriazenes were unable to cross link. It was, therefore, argued that monoalkylation of guanine of DNA at the O<sup>6</sup> position is sufficient to account for the differential cytotoxicity.

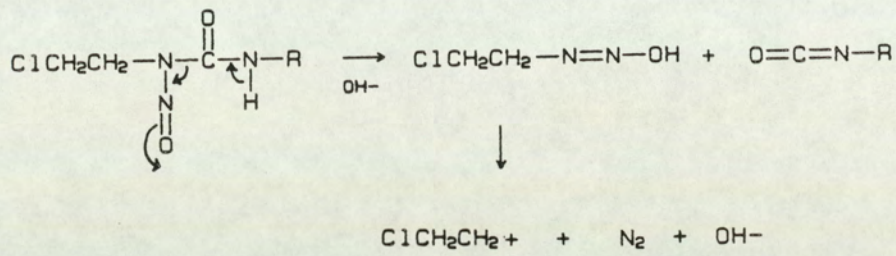
Tisdale (1987) investigated the rôle of alkylation at O<sup>6</sup> position of guanine in the mechanism of cytotoxicity of imidazotetrazinones, mitozolomide, temozolomide and the 3-ethyl analogue of mitozolomide. The results of that study suggest that mitozolomide and temozolomide are similar to the nitrosoureas and triazenes because cytotoxicity was correlated with alkylation of O<sup>6</sup> of guanine. It was postulated that in the case of temozolomide, cytotoxicity is probably mediated via the

formation of MTIC (Tisdale, 1987; Stevens et al, 1987; Stevens, 1987). Furthermore, distinct from mitozolomide and its 3-ethyl analogue, temozolomide promotes erythroid differentiation in K562 erythroleukaemia cells (Tisdale, 1985) after exposure to the drug for 3 days. In addition, the concentration of 5-methylcytosine in the DNA of temozolomide treated cells decreased 3 days after beginning of treatment and was directly proportional to the number of haemoglobin producing cells. These results suggest that a methylating agent is more effective than chloroethylating agent in altering gene expression.

Upon chemical decomposition, the antitumour nitrosoureas, such as BCNU, can liberate isocyanates (fig.13). The organic isocyanate moieties generated are characterized by the ability to carbamoylate intracellular proteins (Schein, 1981; Mitchell and Schein, 1986; Schmall et al, 1973; Wheeler, 1974), mainly at amino acids at sites such as ε amino groups of lysine or arginine. The production of isocyanates might be of minor importance in the cytotoxicity of nitrosoureas. This is because nitrosoureas such as ACNU and chlorozotocin, despite negligible carbamoylating properties, possess excellent antitumour activity (Panasci et al, 1975; Anderson et al, 1975; reviewed by Mitchell and Schein, 1986). Interestingly, Gibson and Hickman (1982) showed that isocyanates generated from BCNU and CCNU might be responsible for the cytotoxicity of nitrosoureas towards TLX5 lymphoma. Horgan and Tisdale (1984) studied the potential carbomoylating property of mitozolomide by

comparing its effect with that of BCNU and of 2-chlorethyl isocyanate on enzymes known to be inhibited by carbamoylation. The enzymes examined were glutathione reductase, gamma-glutamylpeptidase and alpha-chymotrypsin. At equitoxic concentration of mitozolomide and BCNU, BCNU and 2-chloroethyl isocyanate produced complete inhibition of activity of glutathione reductase in intact TLX5 cells within 2hr. In contrast, mitozolomide, MCTIC and chlorambucil did not show any significant inhibitory effect on enzyme activity even after 24hr incubation. Similar differential effects of mitozolomide and BCNU on the activity of gamma-glutamyltranspeptidase and chymotrypsin was observed. These results suggest that the generation of isocyanate is unlikely to occur during decomposition of mitozolomide. Intriguingly, using a novel flow cytoenzymological method, Dive et al (1987) demonstrated that mitozolomide might possess some carbamoylating activity. This data is in disagreement with that obtained by Horgan and Tisdale (1984).

McKeage and Roberts (1989) recently reported that mitozolomide might have the potential to enhance radiation damage.



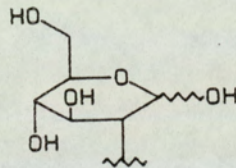
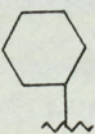
R	Compound
	Chlorozotocin
	CCNU
$\text{ClCH}_2\text{CH}_2$	BCNU

Fig.14 Chemical decomposition of the nitrosoureas

Recently, two derivatives of pyrazolotetrazine were synthesized as prodrugs analogous to the light-sensitive antineoplastic agents DTIC and BIC (Cheng et al, 1986). In contrast to the imidazotetrazine series, it was found that only the chloroethyl analogue displayed antineoplastic activity whereas the methyl analogue was inactive. This observation suggests that the chloroethyl analogue is active per se.

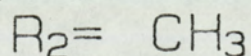
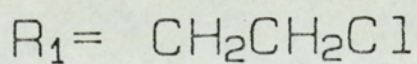
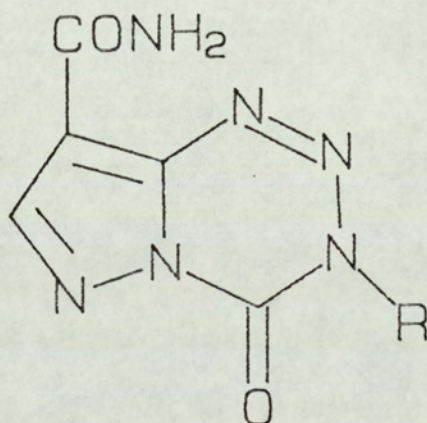


Fig.15 Structures of pyrazolotetrazinones



#### 1.4 Aims and objectives

As part of a programme to develop imidazo[5,1-d]-1,2,3,5-tetrazin-4(3H)ones as potential anticancer drugs, the work described in this thesis is concerned with the pharmacokinetic and metabolic aspects of one such compound, temozolomide. The overall aim of this project is as follows:-

i) The stability, cytotoxicity in vitro and disposition in vivo of temozolomide are compared with those of DTIC, an established anticancer drug, which is structurally related to temozolomide (see section 1.3). It is thought that a better understanding of the relative stability, cytotoxicity and biodisposition of temozolomide as compared with those of an existing drug might assist with the planning of the details pertinent to its clinical trials. Moreover, the results obtained from these studies might help to provide an indication of potential therapeutic advantages associated with the administration of temozolomide in comparison to therapy with DTIC.

ii) The biotransformation of aryltetrazinones and aryltriazinones is virtually unknown (see section 1.3.3). Therefore, in this thesis, the metabolism of two such compounds, temozolomide and 3-methylbenzotriazinone is investigated. In particular, the hypothesis is tested that the N-methyl moiety attached to the triazene part of the molecule is susceptible to oxidation catalyzed by mixed function oxygenases. It is considered that this part of the study constitutes a contribution towards the general knowledge of how chemicals are metabolized. A better

understanding of the metabolic pathways, which novel drugs might undergo, will perhaps help, in the future, to predict, within limits, the metabolism of newly designed drug molecules.

Even though the metabolism of temozolomide is unknown, it is unlikely that the drug requires metabolic activation to exert its antineoplastic activity, because it is likely to undergo chemical decomposition to generate MTIC, the putative cytotoxic species (see section 1.3.2). Nevertheless, potential metabolism of temozolomide to deactivation products might be an important determinant in the antitumour activity, toxicity and clinical usefulness of this drug. The work presented in this thesis can be divided into two parts i) in vitro studies and ii) in vivo investigations. Initial experiments are focussed on the i) the nature and rate of in vitro decomposition of temozolomide in comparison with that of its putative metabolite, MTIC, and that of DTIC ii) the disposition and cytotoxicity of temozolomide in comparison with those of MTIC, HMMTIC and DTIC in the presence and absence of drug metabolizing enzymes and the amount of MTIC generated either metabolically or chemically will be quantified. The results obtained from these experiments may provide preliminary data i) to indicate if temozolomide possesses therapeutic advantages over DTIC and ii) to support or refute the hypothesis that imidazotriazines, such as DTIC, HMMTIC and MTIC share the same mechanism of action as temozolomide.

Using [<sup>14</sup>C methyl]temozolomide, the in vivo metabolism

of temozolomide in mice is investigated in order to identify i) the major route of excretion and ii) the nature of potential biotransformation products of the drug. The metabolism is also studied in patients using unlabelled temozolomide.

The in vivo pharmacokinetics of temozolomide and DTIC are investigated in mice bearing a murine lymphoma. The results obtained from these studies are considered to provide further information to ascertain whether temozolomide might possess any pharmacokinetic and hence therapeutic advantages over DTIC.

3-Methylbenzotriazinone resembles temozolomide in structure, but is devoid of antitumour activity (see section 1.3.2). Since it is chemically stable (Stevens M.F.G., personal communication), it is useful as a model compound to study the metabolic fate of molecules bearing NNN linkages in a cyclic arrangement. In this part of the study, the hypothesis is tested that this model compound undergoes similar metabolism in vitro as temozolomide.

Section 2  
Materials and Methods

## 2.1 Materials

### 2.1.1 Chemicals

All the purchased chemicals were of analytical grade and the solvents were of HPLC grade.

Acetylacetone, acetonitrile, ammonium acetate, benzoic acid, DMSO, ethylacetate, magnesium chloride hexahydrate, methanol potassium dihydrogen orthophosphate, potassium iodide, sodium acetate trihydrate, trichloroacetic acid were obtained from British Drug House (BDH), Atherstone, Warwickshire, United Kingdom.

Anthranilic acid, sulphanilic acid, naphthoresorcinol, methylamine solution (40% w/v in water) iodine crystal, DMSO-d<sub>6</sub> were obtained from Aldrich Chemical Company, Gillingham, Dorset, United Kingdom.

Bovine serum albumin, heparin, hydrogen peroxide (30%) solution, NADPH, trizma base, chloroplatinic acid were obtained from Sigma Chemical Company, Poole, Dorset, United Kingdom.

Acetic acid and chloroform were obtained from May and Baker Ltd., Dagenham, United Kingdom.

RPMT 1640 with 25mmol hepes and glutamine, donor horse serum were obtained from Gibco Laboratories, Paisley, Scotland, United Kingdom.

S-Methyl-L-cysteine was obtained from Fluka Chemicals, Glossop, Derbyshire, United Kingdom.

Beckman Redissolve E.P. scintillation gel was obtained from Beckman RIIC Ltd., High Wycombe, United Kingdom.

Optiphase MP scintillation gel was obtained from FSA

Laboratory Supplies, Loughborough, Leicestershire, United Kingdom.

Fluothane was purchased from ICI, Macclesfield, U.K.

5-[3-(Hydroxymethyl)-3-methyltriazene-1-yl]imidazole-5-carboxamide (HMMTIC) was synthesized by Drs. Keith Vaughan and Ronald LaFrance at St. Mary's University, Halifax, Canada.

Benzotriazinone, N-hydroxymethyl-benzotriazinone, N-methyl-benzotriazinone, N-hydroxy-ethyl-benzotriazinone and 8-carbamoyl-3-ethylimidazo[5,1-d]-1,2,3,5-tetrazin-4(3H)-one (ethazolastone) were synthesized by Drs. Michael Threadgill and Ghouse Baig in the CRC Experimental Chemotherapy Group, Aston University.

[<sup>14</sup>C]methyl labelled and unlabelled temozolomide and 5-amino-imidazole-4-carboxamide were supplied by Dr. Chris Newton, May Baker Ltd, Dagenham, United Kingdom.

#### 2.1.2 Buffer solutions

All the buffer solutions (0.1M) pH 1-2, hydrochloric acid buffer; pH 3-4, acid phthalate buffer; pH 5-6, neutralized phthalate buffer; pH 7-8, phosphate buffer; pH 9-10, alkaline borate buffer) used in the chemical degradation experiments and in vitro metabolic studies were prepared in accordance with the United States Pharmacopoeia (USP) (The United States Pharmacopoeia, National Formulary, 1985).

Erythrocyte cell lysis buffer was prepared by dissolving ammonium chloride (7.5g/l) in Tris buffer (0.016M) and the pH was adjusted to 7.2 using HCl (Boyle et

al, 1968).

### 2.1.3 Animals

CBA/CA (female) and Balb C (male) mice (18-25g) were obtained from Bantin and Kingman Ltd., Hull and were maintained in the university animal house for one week prior to use. Animals were fed on Heygates modified 41B breeding diet pellets and allowed access to water ad libitum.

## 2.1.4 Synthesis

### 2.1.4.1 Synthesis of 3-methyl-2,3-dihydro-4-oxoimidazo[5,1-d]tetrazine-8-carboxylic acid

To a solution of temozolomide (0.5g) in concentrated sulphuric acid (4ml), sodium nitrite (0.5g) in water (4ml) was added slowly at room temperature. The reaction mixture was then stirred at 35°C for 2.5hr and was then poured onto crushed ice. The solid was filtered off, washed well with water and dried in vacuo to give 3-methyl-2,3-dihydro-4-oxoimidazo[5,1-d]tetrazine-8-carboxylic acid as a white powder. (first crop 0.26g, second crop 0.23g) 93% yield. m/z, 195; DMSO-d<sub>6</sub>, 3.90ppm (3H,s,CH<sub>3</sub>), 8.62ppm (1H,s,H-6)

### 2.1.4.2 Synthesis of S-methyl N-acetyl cysteine (methyl mercapturic acid)

S-Methyl-L-cysteine (1g) was dissolved in ice cold 4N NaOH (28ml) and acetic anhydride (1.8 to 2.0ml) was added dropwise with vigorous stirring and continuous cooling in an ice bath. More ice cold 4N NaOH (14ml) was added followed by the addition of acetic anhydride (1.8 to 2.0ml). After the mixture had been stirred for 5min, the solution was brought to pH1 by the addition of concentrated H<sub>2</sub>SO<sub>4</sub>. The solution was left overnight at 5°C and then shaken at least six times with portions of chloroform. the combined chloroform extracts were evaporated to dryness. The residue (yellow glue) was crystallized by trituration with petroleum ether (60-80°C) previously distilled



containing a little ethanol and recrystallized from a mixture of ethylacetate and light petroleum ether (60-80°C). DMSO-d<sub>6</sub>, 1.85ppm (3H,s,COCH<sub>3</sub>), 2.06ppm (3H,s,SCH<sub>3</sub>), 2.7ppm (1H,q,H<sub>b</sub>), 2.84ppm (1H,q,H<sub>a</sub>), 4.38ppm (1H,multiplet,H<sub>c</sub>), 8.25ppm (1H,d,NH).

2.1.4.3 Synthesis of 3-monomethyl(triazen-1-yl)imidazole-4-carboxamide (MTIC), 3,3-dimethyl-(triazen-1-yl)imidazole-4-carboxamide (DTIC) and 3-monomethyl (triazen-1-yl)imidazole-4-carboxamide (METIC)

A solution of 5-amino-imidazole-4-carboxamide (4g) in 1N HCl (32ml) was added dropwise to a solution of sodium nitrite (1.88g) in water (48ml) at -5°C to 0°C. A crystalline precipitate began to form after a small portion of the amino-imidazole solution had been added; after the addition of about 90% of the amino-imidazole solution, the reaction mixture turned pink. Addition was discontinued and the solid was removed by filtration, washed three times with 20ml portions of water, dried in vacuo over phosphorous pentoxide overnight (m.p.207-210°C) decomposed explosively. I.R. spectrum was then compared with the published data (Shealy et al, 1961). V<sub>max</sub> (Nujol) 2160cm<sup>-1</sup> (N<sub>2</sub><sup>+</sup>).

Ethylacetate (40ml) was mixed with aqueous methylamine (40% w/v aq solution. 40ml) (or methylamine hydrochloride) and stirred with some anhydrous potassium carbonate (20g) at 0°C for at least 15min. The mixture was then filtered. Diazo-imidazole-4-carboxamide(1g) was suspended in ethylacetate/methylamine mixture (25ml) which was stirred

at 0°C for 1hr. A white solid was then filtered and dried in vacuo or over dried silica gel at 5°C (70% yield).  $\nu_{\max}$  (Nujol), 3450 $\text{cm}^{-1}$ , 3200 $\text{cm}^{-1}$  (NH), 1680 $\text{cm}^{-1}$  (C=O); DMSO- $d_6$ , 3.0ppm (3H,s,CH<sub>3</sub>), 7.5ppm (1H,s,H-2), 7.6ppm (4H,br,NH and NH<sub>2</sub>). DTIC and METIC were synthesized in a similar manner by using the corresponding alkylamine: dimethylamine and ethylamine, respectively.

## 2.2 Weighings and measurement of volumes

All weighings were performed on a Mettler AE163 balance. Amounts over 100g, a Mettler PE360 balance was used. The balances were calibrated daily prior to use.

Gilson pipette man pipettes (maximum volumes of 0.25, 1 and 5ml) were used in the quantification of small volumes. Volumes of 0.02ml or less were measured using a Gilson microman positive displacement pipette. All pipettes were calibrated regularly by dispensing volumes of water at room temperature and weighing them.

### 2.3 Measurement of pH

All measurements of were performed on a H18520 bench pH meter with automatic temperature compensation facility (Hanna Instruments).

### 2.4 Development of analytical methods

#### 2.4.1 HPLC analysis of temozolomide and its urinary metabolites

HPLC assays were performed on a Waters Associates system comprising a Waters 840 Data and Chromatography Control Station, M710B WISP (autosampler), M510 solvent delivery systems and a Lambda max 480 variable wavelength detector. A Lichrosorb C18 RP select B column with a Lichrocart RP-18 pre-column were used. The HPLC analysis of temozolomide was based on the published method (Slack et al, 1986) with slight modifications. For in vitro metabolism experiments, the mobile phase was 10% methanol in 0.5% acetic acid at a flow rate of 1.5ml/min. For in vivo urine analysis, the mobile phase was 5% methanol in 0.5% acetic acid at a flow rate of 1ml/min and the total run time was 15min; a washing period (20min) with 40% methanol in 0.5% acetic acid was incorporated between each run, followed by an equilibration period (10min). Detection was achieved by UV detection at 325nm. Samples of urine or liver homogenates were acidified with 1N HCl and extracted twice with ethylacetate (3ml). The organic extracts were then concentrated and re-constituted with methanol (0.125ml), followed by 0.5% acetic acid (0.125ml).

six points was constructed in each HPLC assay covering the required range for quantification, by spiking known amount of drug into either urine or liver homogenates. Each standard sample contained exactly 1% v/v DMSO in 1N HCl. Glass-distilled water was used throughout.

#### 2.4.1.1 Extraction efficiency of temozolomide and ethazolastone

To determine the efficiency of the ethylacetate extraction, aliquots of the stock solution of drug (10mg/ml) were added to a mixture of methanol (0.125ml) and 0.5% acetic acid (0.125ml) to give a concentration of 4mg/L. Tubes containing equal amounts of drug were prepared and extracted with ethylacetate twice and reconstituted with same proportion of methanol and 0.5% acetic acid. The peak heights were compared with the unextracted samples to evaluate the percentage of recovery.

#### 2.4.1.2 Reproducibility of the HPLC method

The reproducibility of the HPLC assay was assessed by preparing six separate stock solutions of each of the following concentrations of temozolomide: 35mg/L, 5mg/L and 0.2mg/L. Aliquots of these solutions (0.5ml) were prepared and analyzed as described in section 2.4.1.

#### 2.4.1.3 Reproducibility of the instrument

The reproducibility of the instrument was established by six replicate injections from a single sample.

#### 2.4.2 HPLC analysis of MTIC, temozolomide, HMMTIC and DTIC

HPLC analysis was performed on the system as described previously in Section 2.4.1 equipped with a 0.02ml injection loop. UV detection at 323nm was achieved for detection and quantification.

For sample preparation, incubation mixtures, plasma or tumour homogenates were allowed to thaw slowly at room temperature. Before completely thawed, they were placed in an ice/water bath at 0-4°C. An aliquot of the sample (0.1ml) was pipetted into a pre-chilled polypropylene centrifuge tube followed by the addition of cool acetonitrile or a mixture of acetonitrile and methanol containing the internal standard (0.2ml) and vigorously mixed with a vortex mixer. The precipitated protein was then removed by centrifugation at -20°C, 2,500rpm for 10min. The clear supernatant was then analyzed by HPLC.

MTIC and temozolomide were separated using a 12.5cm Lichrosorb C18 RP select B column with a PVDF guard column and a mobile phase containing 5% acetonitrile in 0.05M ammonium acetate (pH 6.7) at a flow rate of 1.5ml/min. Hydroxyethylbenzotriazinone was used as an internal standard for quantifying the amount of MTIC and temozolomide present.

Separation of MTIC, HMMTIC and DTIC was achieved using a 25cm Lichrosorb C18 RP C<sub>18</sub> column with a PVDF guard column and a mobile phase containing 3.25% acetonitrile/1.75% methanol in 0.05M ammonium acetate with a flow rate of 1.5ml/min. Metronidazole was used as an

internal standard to quantify the amount of MTIC, HMMTIC and DTIC present.

#### 2.4.2.1 Recovery after protein precipitation

To determine the recovery of the compounds after protein precipitation, aliquots of the stock solutions of temozolomide, MTIC, DTIC and HMMTIC were added in plasma and phosphate buffer solutions (0.1ml) followed by the addition of cold acetonitrile to give a final concentration of 4mg/L. Equal concentration of the drug solutions were spiked in clear supernatant of plasma prepared by precipitating plasma protein with acetonitrile. The peak heights were compared to determine the percentage of recovery.

#### 2.4.2.2 Reproducibility of the HPLC method

The reproducibility of the HPLC method was examined by preparing six separate solutions of each concentration of the following concentrations of MTIC, HMMTIC, DTIC and temozolomide: 20mg/L, 7.5mg/L and 5mg/L. Aliquots of these solutions were prepared and analyzed in an identical manner to that described in section 2.4.2.

#### 2.4.2.3 Reproducibility of the instrument and accuracy of manual injection

The reproducibility of the instrument and accuracy of manual injection was assessed by performing six replicate manual injections from a single sample.

#### 2.4.3 HPLC analysis of benzotriazinones

Separation of benzotriazinone and 3-methylbenzotriazinone was accomplished using a 12.5cm Lichrosorb C18 RP select B column on a Waters Associates system. The mobile phase system was 25% methanol and 75% water with a flow rate of 1.5ml/min. Quantification of the metabolites was determined by peak height ratio of the sample peaks to the internal standard (anthranilic acid) at 284 nm.

#### 2.4.4 GC analysis of methyl isocyanate

All analyses were performed on a Pye Unicam GC instrument. Methyl isocyanate was analyzed using the published method by Mraz and Turecek, 1987 for the determination of N-acetyl-S-(N-methylcarbamoyl)cysteine in urine. The GC analytical conditions were as follows: glass column (1.5m x 2mm) was packed with 5% KOH, 10% carbowax 20M and silanized chromsorb W 80-100 mesh; detector and injection temperature, 200°C; column temperature, 170°C. Nitrogen was used as the carrier gas (50ml/min). Detection was achieved by a nitrogen sensitive detector. Injection volume was 0.001ml.

#### 2.4.5 Thin layer chromatography

Thin layer chromatographic separation of temozolomide and metabolite(s) was accomplished using plastic sheets coated with silicagel (Kieselgel 60 F254, 0.2mm). The samples were applied as 1cm bands positioned 2cm above the

plate. A minimum gap of 1 cm separated adjacent bands. Samples were applied using a Hamilton microsyringe and the solvent or urine was evaporated by applying cool air between successive applications to each band. For autoradiograms samples were applied such that an equivalent of 5,000 dpm of radioactivity was applied to each band. Chromatography was performed in a standard TLC tank with plates being run over a distance of 15cm.

#### 2.4.5.1 TLC solvent systems

- 1) acetone:acetic acid:water (7:1:2)
- 2) benzene:methanol:acetic acid (45:8:8)
- 3) chloroform:methanol:acetic acid (3.5:1.5:1% v/v)
- 4) butan-1-ol:acetic acid:water (3:1:1)

#### 2.4.5.2 Spray reagents

Pauly's reagent was used for detecting the presence of imidazole ring.

solution(a): sulphanilic acid (1g) in concentrated HCl (10ml) and water( 50ml)

solution(b): 5% aqueous sodium nitrite

solution(c): 10% aqueous sodium carbonate

The spray reagent was made up by mixing one part of solution (a) with one part solution (b). The mixture was allowed to stand for 5 minutes. Then 2 parts of solution (c) were added and the final mixture was allowed to cool at room temperature.

Chloroplatinate reagent was used for detecting sulphur containing compounds.



solution(a): 5% chloroplatinic acid in water

solution(b): 10% aqueous potassium iodide

Solution(a) (5ml) was mixed with solution (b) (45ml), then diluted to 100ml with water, followed by the addition of concentrated HCl (1 part to 10 parts).

#### 2.4.6 Mass spectral (MS) analysis

Preliminary and routine mass spectral analyses were measured on a VG micromass 12B single focussing spectrometer in the Pharmaceutical Sciences Institute, Aston University by Mrs. Karen Farrow. For final structural determination, mass spectra were measured on a VG 11/250 mass spectrometer by Dr. Peter Farmer and Mr. John Lamb at the MRC Toxicology Unit, Carshalton using a direct insertion probe and data were processed using a VG 70 SEQ data system. Isobutane was used as reagent gas in the chemical ionization mass spectral (CIMS) analysis. For electron impact method, mass spectra were measured at 70eV with an inlet temperature 230°C. For field desorption/chemical ionization (FDCI), sample was dissolved in the appropriate solvent, either water or methanol, and applied direct onto the probe filament. For fast atomic bombardment (FAB), sample was dissolved in the matrix which was either glycerol or thiodiglycol. The spectra were run at a scan rate of 3 sec/decade.

#### 2.4.7 Nuclear Magnetic Resonance (NMR) analysis

Routine NMR analyses were performed on a Varian EM360 (60 MHz) spectrometer. High field NMR analyses were

performed on Bruker (400 MHz) at the Department of Chemistry, University of Warwick by Dr. Oliver Howarth or Bruker AL 300 (300 MHz) by Dr. Michael Perry in the Pharmaceutical Sciences Institute of Aston University. The compounds were dissolved in DMSO- $d_6$  or  $D_2O$  prior to NMR analysis; the prepared solutions were always filtered via a glass wool plug in a pasteur pipette in order to remove particulate matters. All spectra were recorded at room temperature using 32768 data points over a 2994.012Hz sweep width and an acquisition time of 5.472s. In case of the identification of metabolite II, the spectrum was obtained by collecting up to 48 FID's using  $45^\circ$  pulses with a relaxation delay of 0.2s between pulses. In case of the identification of metabolite I, the water signal was suppressed with continuous secondary irradiation. The spectrum was obtained by collecting a total of 2484 FID's using  $45^\circ$  pulses with a relaxation delay of 0.5s between pulses.

#### 2.4.8 Infra-red (IR) spectroscopic analysis

IR spectroscopic analyses were performed on a Perkin Elmer double beam IR spectrometer. Samples were prepared by either suspending in Nujol solution or compressing with KBr powders.

#### 2.4.9 Ultraviolet (UV) spectroscopic analysis

Ultraviolet spectroscopic analyses were performed on Diode array UV spectrometer (Hewlett Packard, HP 8451A) equipped with a microcomputer built in display screen and printer/plotter.

### 2.5 In vitro stability studies

#### 2.5.1 Determination of the stability of temozolomide and MTIC by UV spectroscopy

Decomposition studies were performed using a Diode array UV spectrometer as described in section 2.4.9. Samples were excluded from light and maintained at 37°C. Solutions of temozolomide, DTIC and MTIC were prepared in DMSO (10mg/ml). Aliquots (0.01ml) of the stock solutions were added to silica cuvettes (1cm path length) containing 0.1M buffer solutions (3ml) (section 2.1.2). The decrease in absorbance with time was measured at the maximum absorbance wavelength of the compound under investigation at 37°C. No measurable difference in pH of the samples was found before and after each experiment.

### 2.5.2 In vitro investigation of the release of methyl isocyanate from temozolomide

Temozolomide (approximately 20mM) in 0.2M phosphate buffer (pH8.0) was placed in a tube. The tube was connected through a side arm containing a glass wool plug to a pasteur pipette which was immersed in a mixture of potassium hydroxide (3.3mg/ml) and propanol (6ml). The principle of this method is encapsulated in the following reaction scheme:

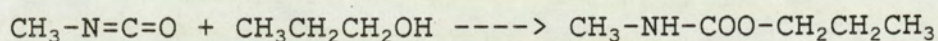


Fig.16 Principle of the analysis of methyl isocyanate

The tube was placed in a water bath at 37°C and a slow stream of nitrogen was continuously bubbled through the drug solution to serve as an inert carrier gas for the released methyl isocyanate. After an incubation period of 30min, the KOH/PROH mixture (6ml) was removed from the receptor vessel and shaken thoroughly with saturated NaCl solution (6ml). The organic layer was then removed and analyzed by GC as described in section 2.4.4. Caracemide [N-acetyl-N-(methylcarbamoyloxy)-N-methylurea [NSC 253272], an antitumour agent capable of generating methyl isocyanate (Newman and Farquhar, 1987), was used as a positive control. DMSO, the solvent temozolomide was dissolved in, was used as a negative control.

## 2.6 In vitro metabolism

### 2.6.1 Preparation of liver homogenate and subcellular fractions for in vitro metabolic studies on temozolomide and 3-methylbenzotriazinone

The mice were killed by cervical dislocation. Livers were excised and weighed at 9.00am. A homogenate (1g/ml) was made in ice cold phosphate buffer (pH 7.4, 0.1M) using a coulab 563 homogenizer (speed 5) fitted with a teflon pestle. The resulting suspension was centrifuged at 10,000g for 10min in a MSE/Fison Hispin 21 Centrifuge at 4°C. The 10,000g supernatant was used directly or further centrifuged at 100,000g for 1hr to prepare microsomes. The pellets were resuspended in 0.1M phosphate buffer (1g of wet liver weight per ml of buffer solution).

Glass scintillation vials (10ml) were used in the metabolic studies in vitro. Incubations using liver fractions were performed in phosphate buffer (5ml pH 7.4, 0.1M) in the presence of 16.4µmole of  $MgCl_2 \cdot 6H_2O$ , 2.4µmole of NADPH and 0.25ml (equivalent to 5-6mg of microsomal protein in the final incubation mixtures) of the liver homogenate suspension. Reactions were initiated by addition of substrate dissolved in DMSO (0.04ml). The reaction mixtures were gently shaken at 37°C and exposed to atmospheric air. Aliquots of the reaction mixtures were taken at several time intervals, deproteinized by addition of 0.5ml of 1N HCl, which can also stabilize temozolomide. In case of the experiments on 3-methylbenzotriazinone, the

ice. Control incubates contained liver inactivated by heating at 85-90°C for 15min. The pH of the incubation mixtures was measured before and after each experiment, and no change was observed. Disappearance of the substrate and appearance of the metabolites were compared chromatographically in experimental and control incubates.

### 2.6.2 Protein determination

The amount of protein present in the incubation medium was determined according to Lowry's method (1951).

solution(a): sodium carbonate (2%w/w) in sodium hydroxide (0.1M)

solution(b<sub>1</sub>) : copper sulphate(1% w/v) in water

solution(b<sub>2</sub>) : sodium potassium tartrate (2% w/v) in water

solution(b) : equal parts of b<sub>1</sub> and b<sub>2</sub>

Folin's reagent: Folin and Ciocalteu's phenol reagent diluted with equal volume of distilled water

solution(c) solution(a) (50ml) and solution(b) (1ml)

Diluted microsomal suspension (1ml) was added to solution C (5ml) and was then mixed thoroughly. After allowing to stand at room temperature for 10min, Folin's reagent (0.5ml) was added and the mixture was vortexed and allowed to stand for further 30min. The absorbance at 750nm was measured. Bovine serum albumin was used for the

preparation of standard solutions.

### 2.6.3 Analysis for formaldehyde

The amount of formaldehyde generated metabolically was quantified by the colorimetric procedure of Nash (1953) based on Hantzsch reaction. Aliquots (1ml) of incubation medium or formaldehyde standard solutions was added to trichloroacetic acid (TCA) (12.5%, 1.5ml). The mixture was mixed thoroughly and centrifuged at 4,000g for 20min. The clear supernatant was transferred to a test tube followed by the addition of Nash reagent (1ml), mixed well and heated for 10min at 60°C in a water bath. The reaction mixture was then allowed to cool and the absorbance was read at 414nm. The standard curve was constructed using freshly prepared formaldehyde solution by dissolving paraformaldehyde in 1N NaOH.

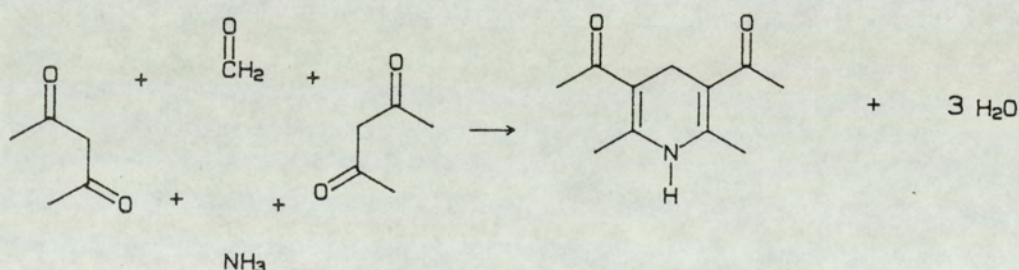


Fig.17 Principle of Nash reaction

## 2.7 Cell Culture

### 2.7.1 Coulter counter settings

All cell countings were performed on ZM counter (Coulter, Bedfordshire, United Kingdom). The settings were as follows:

Current: 200

Attenuation: 8

Lower threshold: 10

Upper threshold: 99.9

### 2.7.2 TLX5 cell culture

TLX5 murine lymphoma cells ( $2 \times 10^5$ /ml) were injected into CBA/CA mice intraperitoneally, and cells were passaged each week. For in vitro culture, ascites cells ( $2 \times 10^6$ /ml) were harvested from animals and rinsed with erythrocyte cell lysis buffer, as described in section 2.1.2. The cells were vortexed and centrifuged at 2000 rpm for 5min. The supernatant was decanted and the cell pellet was gently suspended to yield a cell density of  $1 \times 10^5$  cells/ml in RPMI 1640 medium supplemented with 17% horse serum. Cells were maintained at 37°C under an atmosphere of air with 10% CO<sub>2</sub>. Cells were grown for at least 10 subcultures in order to obtain a steady doubling time in vitro. For all experiments, cells were taken from subcultures 10 to 20. The sterility of the culture medium was always controlled prior to use by incubating an aliquot (5ml) at 37°C for 72 hours to assess for bacterial growth.



### 2.7.3 Storage of cells in liquid Nitrogen

Confluent cultures of cells were pelleted on a bench centrifuge at 2000 rpm for 5min. The supernatant was then carefully decanted and the pellet was gently resuspended to give a cell density of  $2 \times 10^6$ /ml in culture medium with 10% DMSO. Aliquots (1ml) of the cell suspensions were transferred to cryogenic vials and cooled to  $-8^\circ\text{C}$  for 7hr prior to immersion in liquid nitrogen. To reculture the banked cells, vials were rapidly thawed and the contents were seeded into culture flasks with an addition of 1ml culture medium.

### 2.7.4 Characterization of cell growth

Cells ( $1$  or  $2 \times 10^4$ /ml) were seeded into Nunc 24 multiwell dishes with medium (2ml). Cells were counted every day for 6 days using a ZM coulter counter. A semi-logarithmic plot of cell number against time was constructed to characterize the pattern of growth of TLX5 cell line in vitro. The doubling time of TLX5 murine lymphoma cells was between 12-14 hr.

## 2.8 In vitro cytotoxicity assay

### 2.8.1 Cell growth assay

The effect of temozolomide and its metabolites and metabonates on cell growth was evaluated as follows: Cells ( $2 \times 10^4$ /ml) were seeded in 24 multiwell dishes (Nunc). Drug solutions were made up in DMSO at different concentrations such that the final concentration of DMSO in the culture medium was always 0.2% (v/v). Cells were incubated and counted after 72hr exposure to the drugs.

### 2.8.2 Clonogenic assay

The clonogenic assay in soft agar was performed according to Bill et al (1988) with slight modifications. An aliquot of cell suspension (500/ml, 2ml) was seeded into Nunc 35mm six multiwell dish containing RPMI 1640 medium supplemented with 17% horse serum (3ml) and 12% noble agar, the final agar concentration in the well was 0.36 and 0.4%.

## 2.9 In vitro cytotoxicity assay including a liver microsomes

Cells ( $4 \times 10^4$ /ml) were incubated with temozolomide and liver microsomes fortified with co-factors (section 2.6.1) in RPMI medium with 17% horse serum. Reaction mixtures were gently shaken and gassed with sterile air with 10% CO<sub>2</sub> every 15-20min. The cells were washed 2 to 3 times with the culture medium to remove the drug, and plated out into 24 multi-well dishes. Cells were counted as described above (section 2.7.4). The results were expressed as

percentage of the respective controls which were in the presence or absence of microsomes. The whole procedure was performed under aseptic conditions. The dissection instruments were sterilized by autoclaving. The sterility of the microsomal suspension was assessed after incubation with medium for 72hr. Cyclophosphamide was used as positive control to validate that the liver homogenate fractions were metabolically active.

#### 2.10 In vitro metabolic studies of temozolomide, DTIC, MTIC and HMMTIC

The experimental protocol was identical to that described for the in vitro cytotoxicity assay (section 2.9). Aliquots (0.5ml) of the incubation mixtures were taken, processed and analyzed as described in section 2.4.2.

In case of the experiments using human microsomes, human livers were obtained from Dr. Kevin Chipman, Department of Biochemistry, University of Birmingham. The livers were stored at -20°C and used within one week.

## 2.11 In vivo metabolic studies

### 2.11.1 Metabolism and total excretion balance studies in mice

#### 2.11.1.1 Quality control on the purity and specific radioactivity of [<sup>14</sup>C methyl]temozolomide

The HPLC method described in section 2.4.1 was employed to determine the purity and specific radioactivity of [<sup>14</sup>Cmethyl]temozolomide.

[<sup>14</sup>C]Temozolomide (4mg) was dissolved in DMSO (0.25ml). This solution was diluted (1:1000) with distilled water. The diluted solution (0.05ml) was injected onto the HPLC.

For fraction collection, the HPLC eluent outlet from the U.V. detector was connected to a 211-Redirac fraction collector (LKB Bromma). Between 100-120 fractions (0.3-0.5ml per fraction) were collected. The radioactivity of each fraction was counted after the addition of Optiphase MP scintillant gel (2ml) using a 2000CA Tri-carb liquid scintillation analyzer (United Technologies Packard). The presence of the impurities was determined by HPLC (section 2.4.1) and by plotting the radioactivity measured against the fraction number.

The purity of the labelled drug was determined by collecting the fraction corresponding to [<sup>14</sup>C]temozolomide detected by UV (325nm). The eluent was diluted with distilled water to which Optiphase MP scintillant gel was added for the determination of the radioactivity. Total

radioactivity of the eluant was determined by disconnecting the column from the detector and injecting the diluted stock solution (0.05ml) onto the HPLC. The eluant over the ensuing 10min was collected and diluted to 10ml with distilled water. The diluted solution (2ml) was mixed with Optiphase scintillant gel (10-15ml) for the determination of the radioactivity.

#### 2.11.1.2 Drug solution

Samples of the stock solution of [ $^{14}\text{C}$ ]temozolomide (approximately 0.016ml) were diluted with a solution of unlabelled temozolomide in sterile normal saline (BP) immediately before administration to give a final concentration of drug 5mg/ml containing 40 $\mu\text{Ci/ml}$  radioactivity.

#### 2.11.1.3 Experimental Protocol

Six (Balb/C, male) mice were housed in metabolic cages in groups of 2 or individually at 24hr prior to dosing. Urine was collected as control. Mice received via the i.p. route unlabelled or [ $^{14}\text{C}$ ]temozolomide (40mg/kg, 6-8 $\mu\text{Ci}$  per mouse) (injection volume 0.2ml, based on a 25g mouse). Dosing was performed at 9.00 am. Collection flasks were immersed in a solution of antifreeze (-5°C to -15°C) and HCl (1N, 0.5ml) was added to stabilize the imidazotetrazinones. Urine and faeces were collected at 8 hourly intervals for 72hr. To study the excretion balance of radioactivity, air was drawn through by a pump, inlet air was filtered by calcium sulphate to remove

moisture and soda lime to remove CO<sub>2</sub>. <sup>14</sup>CO<sub>2</sub> was trapped by 2 consecutive flasks with a mixture (20ml) of ethanolamine/ethoxyethanol (1:4). The system was maintained airtight throughout the experimental period. Each dose formulation was subjected to quality control by scintillation counting.

The amount of temozolomide excreted in the urine was analyzed by HPLC method as described in section 2.2.1. Total radioactivity excreted in urine, faeces, breath and remaining in the carcasses was analyzed by scintillation counting. Counts obtained were corrected for quenching by the external standard ratio, external standard used was [<sup>14</sup>C] hexadecane (Amersham).

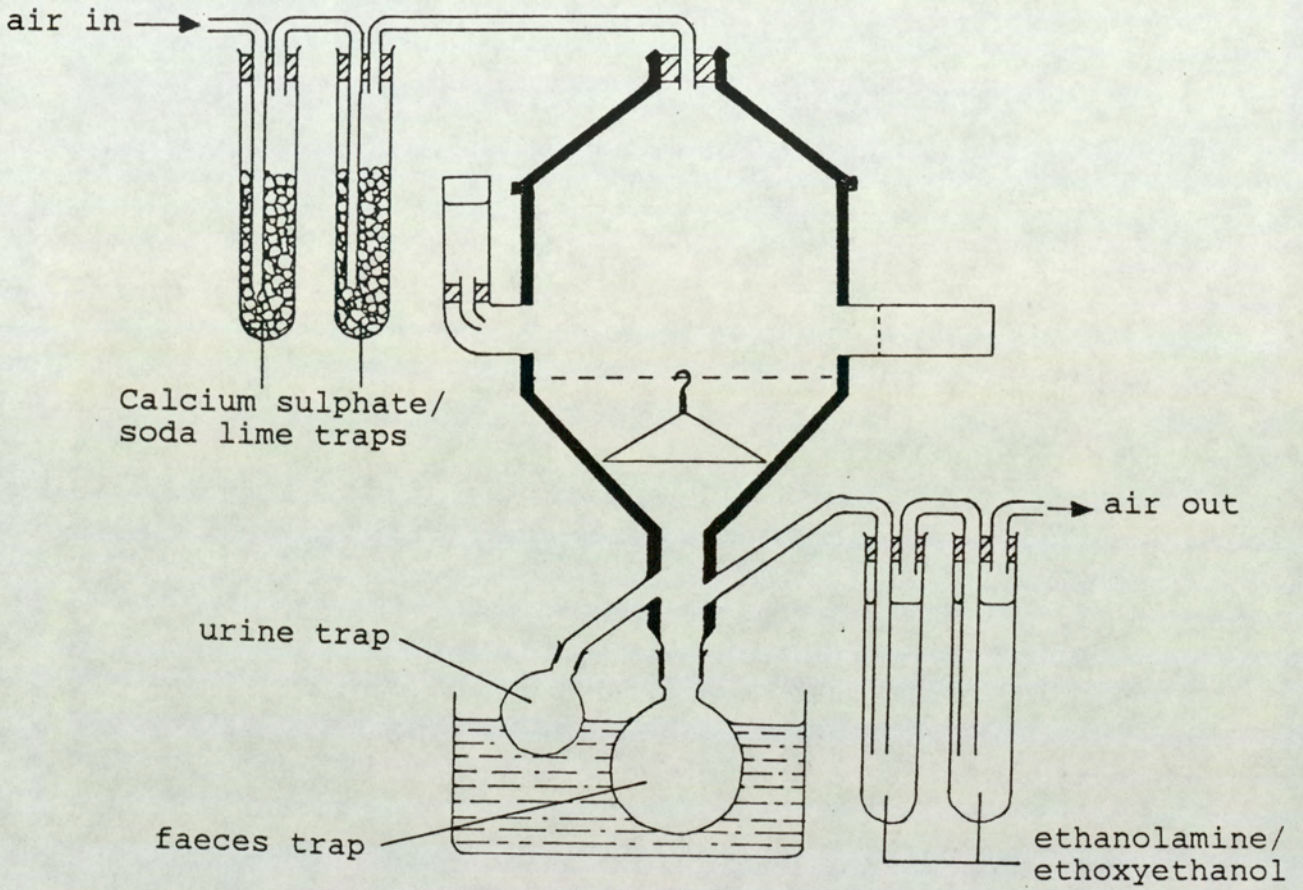


Fig.18 Diagram of the apparatus for total excretion balance study

#### 2.11.1.4 Sample Preparation

Prior to scintillation counting, urine samples (0.05ml) or samples of CO<sub>2</sub> (0.1ml) were diluted to 1ml with water, Optiphase MP scintillant (10ml) was added for counting.

In the case of tissue and faeces, the following method of solubilization was employed for sample preparation: faeces or carcasses (which had been cut into smaller fragments) were weighed and mixed with twice the amount of water in a homogenizer bottle. The diluted samples were homogenized using a Sorval tissue homogenizer. Samples of tissue homogenates (0.05ml) were weighed into glass scintillation counting vials. Soluene tissue solubilizer (1ml) (Packard Ltd., Caversham, U.K.) was added and the vials were heated to 50°C in an oven for 2hr. After the vials were completely cooled, propan-2-ol (0.2ml) and hydrogen peroxide (0.2ml) were added to each vial. Once the effervescence had subsided, the vials were heated for a further 2hr at 50°C. After cooling, Beckman E.P. Redissolve scintillation fluid (10ml) was added to each vial. Samples were counted after 12hr to minimize chemoluminescence.



## 2.11.2 In vivo murine metabolic studies at LD10 dose

### 2.11.2.1 Preparation of suspension for oral dosing

Temozolomide (225mg) was accurately weighed and immediately transferred to a mortar. The powder was then gradually ground into a paste with Tween 80 (0.5ml). 0.9% saline (4.5ml) was added to a pre-weighed bijoux pot. The suspension was then transferred to a Universal container and vigorously agitated in order to attain homogeneity.

### 2.11.2.2 Experimental protocol

Each mouse received a dose of temozolomide equivalent to 450mg/kg (LD<sub>10</sub> dose) by gastric intubation using a curved 18G dosing needle of length 1.5 inches fitted to a 1ml syringe. The dose was taken up into the syringe immediately prior to dosing and only after the suspension had been vigorously agitated. A control mouse was dosed with 10% Tween 80 in 0.9% sterile saline (the volume was based on a 20g mouse receiving a volume of 0.2ml).

### 2.11.2.3 Urine collection

After dosing, mice were housed in a cage and were provided with food and water ad libitum. Urine was collected over a 12hr period using a purpose-made urine contraption situated beneath the cage and direct from the mice which underwent cardiac puncture procedure for pharmacokinetic experiments.

### 2.11.3 Pharmacokinetic and metabolic studies of patients

#### 2.11.3.1 Eligibility of patients

Patients entering the studies were those who had progressive disease after all established therapies for that tumour have failed. The age of patients was between 16-75 years. The performance status of patients was between 0-2 on WHO scale (or >60 on Karnofsky scale) and the expected survival time should be more than 2 months. The minimum haematological requirements were: white blood cells count was greater than 4,000/mm<sup>3</sup> and platelets greater than 100,000/mm<sup>3</sup>. Normal hepatic and renal function as defined by standard liver function tests and urea and electrolytes and creatinine. Patients should be off all anticancer therapy for a least three weeks (6 weeks for nitrosoureas and mitomycin C) and had recovered from the toxic effects of prior treatment.

#### 2.11.3.2 Treatment of patients

Temozolomide was administered to patients i.v. as bolous or orally. In case of i.v. bolous infusion, temozolomide was provided as a 30mg/ml solution in DMSO in sterile ampoules containing 120mg of the drug. Oral capsules containing 20mg, 50mg and 100mg were used for doses at 200 mg/m<sup>2</sup> or more.

#### 2.11.3.3 Collection of blood samples

The following procedures were carried out by Dr. Charmaine Quarterman of Aston University. All syringes and

tubes for the collection of blood samples were pre-cooled to 4°C. Blood samples (10ml) were taken via the Venflon, an intravenous cannula. Samples were immediately transferred to 10ml lithium-heparin tubes. After each sampling the cannula was kept patent by the introduction of Hepflush (1ml). Prior to subsequent sampling the first 2ml of blood was discarded to avoid the possibility of sample dilution or contamination. Whole blood or plasma samples were acidified with 1N HCl to stabilize temozolomide. The samples were then stored at -20°C prior to analysis.

#### 2.11.3.4 Collection of urine samples

Urine was only collected from patients receiving temozolomide by the oral route. The collected urine was acidified with 1N HCl (20ml) and stored at -20°C prior to analysis.

#### 2.11.4 Enzymic hydrolysis of urinary metabolites

Enzymic hydrolysis of urinary metabolites was performed using urine samples (1ml) diluted and adjusted to pH5 with 0.2M acetate buffer containing  $\beta$ -glucuronidase (10,000U) or sulphatase (300U). Samples were then incubated at 37°C for 17-24 hours.

### 2.11.5 Colour test for the presence of glucuronides

The eluent corresponding to the peak of metabolite I obtained on HPLC was collected. Naphthorescorcinol crystals (approximately 2mg) and concentrated HCl (1ml) were added and heated for 3 min. The mixture was cooled. Ethylacetate (3ml) was added and the mixture was vortexed for 1min. The organic layer was analyzed by U.V. spectroscopy (190-820nm). A purple coloration at 570nm would indicate the presence of glucuronides.

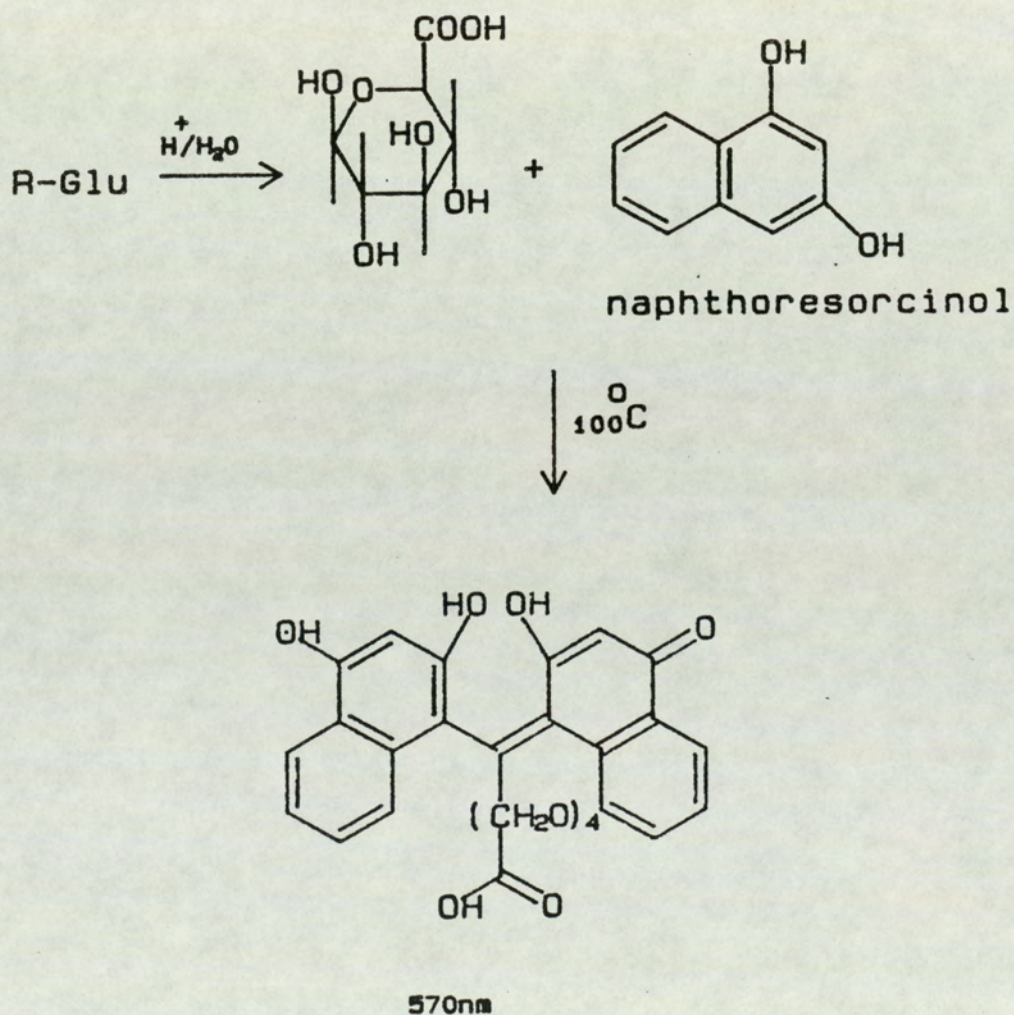


Fig.19 Principle of Tollen's reaction

## 2.11.6 Isolation of metabolites

### 2.11.6.1 Isolation of metabolite II

Samples (200-300ml) of acidified urine from the patient were continuously extracted for three days with ethylacetate (see fig.20). The ethylacetate extract was concentrated in vacuo and reconstituted with 0.5% acetic acid (10ml). Urinary pigments were removed using C<sub>18</sub> Sep-pak cartridges, pre-conditioned with methanol (2ml) and 0.5% acetic acid (5ml). The crude extract was applied onto the cartridges and eluted initially with 0.5% acetic acid then 5% methanol: 95% acetic acid (0.5%) and eventually 50% methanol: 50% acetic acid (0.5%). Each fraction was analyzed by the HPLC method as described in section 2.4.1. Fractions containing metabolite II were pooled. Methanol was removed by rotary evaporation in vacuo and acetic acid was removed by freeze-drying. The residue were then dissolved in 0.5% acetic acid (between 1-3ml). Effective purification was achieved by repeated HPLC separations using two RP select B column (12.5cm and 25cm).

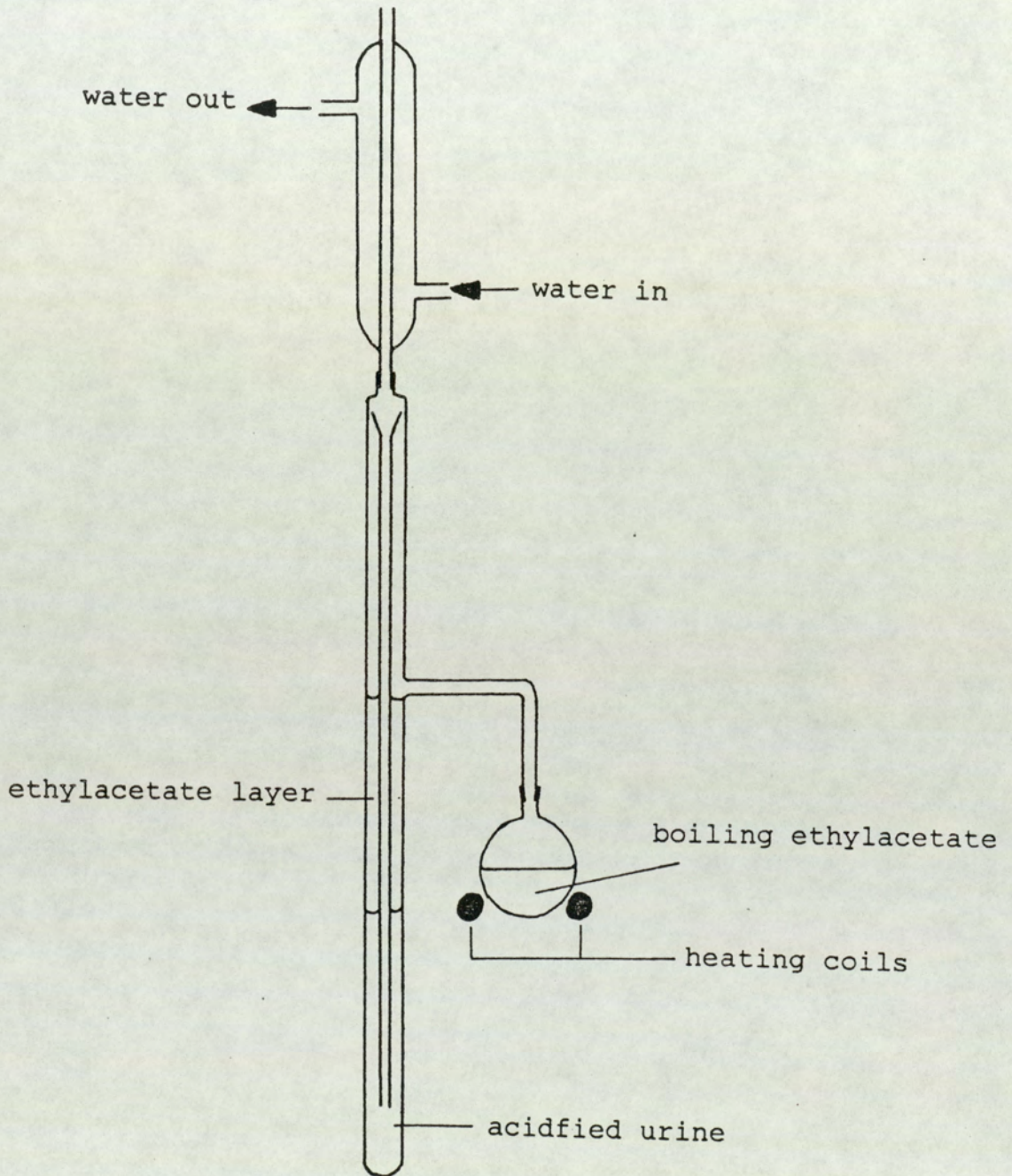


Fig.20 Diagram of the apparatus for continuous solvent extraction

#### 2.11.6.2 Isolation of metabolite I

Samples of acidified patient urine (200-400ml) were lyophilized by freeze-drying. The brown residues were reconstituted with 0.5% acetic acid (between 10-20ml) and extracted 7 to 10 times with ethylacetate at room temperature. The ethylacetate extract was concentrated in vacuo and reconstituted with 0.5% acetic acid (10ml). Urinary pigments were removed by repeated solid phase extraction using C<sub>18</sub> Sep-pak cartridges, which had been pre-conditioned as described previously. The crude extract was applied onto the cartridges and eluted initially with 0.5% acetic acid, then 5% methanol in 0.5% acetic acid. The presence of the metabolite was confirmed by HPLC. The fractions containing the metabolite were pooled, freeze-dried and reconstituted with 0.5% acetic acid in preparation for further HPLC separation and purification as described in section 2.4.1.

The eluant from the HPLC containing the metabolite was freeze-dried and the yellow oily isolate was further purified using an anionic exchange column. Dowex I (Cl<sup>-</sup>, mesh size 100-200) was dissolved in HPLC grade water (5ml) and applied to a column (8cm). The resin was washed with 1N HCl (5ml). The anion on the resin was replaced by formate by equilibrating the resin with 20 bed volumes of 1N ammonium formate solution. The column was then adjusted to pH6 using formate buffer (0.1N). To assure the equilibration, the pH of the eluent from the column was measured.

The metabolite in formate buffer (1ml, pH6) was

applied to the column. The column was sequentially washed with formate buffers (0.1M) with pH values of 6 to 3: firstly with buffer (10ml, pH6) followed by (10ml, pH5). Two fractions (5ml) of were collected from these two steps; finally washed with the buffer (10ml, pH4) and five fractions (2ml) were collected. Each fraction was analyzed by HPLC. The fractions containing the metabolite were pooled and freeze-dried. Ammonium formate was removed using a Dowex 50W (H<sup>+</sup>) cation exchange resin which had been pre-conditioned with HPLC grade water (20ml), then by reverse phase HPLC utilizing initially a 12.5cm followed by a 25cm RP select B columns. The mobile phase was 0.5% acetic acid.

#### 2.11.7 Methylation of Metabolite I

##### 2.11.7.1 Preparation of diazomethane

The following procedures were performed under the supervision of Dr. Igor Linhart. Absolute alcohol (5ml) was added to a solution of potassium hydroxide (1g) in water (1.6ml) in a 100ml round bottom flask fitted with a dropping funnel and a condenser. The condenser was connected to two receiving flasks in series, the second of which contained ether (20ml). The inlet tube of the second receiver was placed below the surface of the ether, and both receivers were cooled to 0°C.

The flask containing the alkali solution was heated in a water bath to 65°C, and a solution of Diazald (4.3g) (Aldrich) in ether (20ml) was added slowly through the



dropping funnel. When the dropping funnel was empty, another portion of ether (20ml) was added slowly and the distillation was continued until the distilling ether was colourless.

#### 2.11.7.2 Methylation procedure

The metabolite was dissolved in methanol (1ml) and this solution of diazomethane in ether was added. Excess amount of diazomethane ethereal mixture was added so that the colour of the resultant solution was yellow. A small amount of anhydrous calcium chloride was then added and the mixture was allowed to stand at 0°C for 1hr until the solution was clear. The solution was then filtered through glass wool in a pasteur pipette. The organic solvents were removed in vacuo. The resultant residue was dissolved in the mobile phase for isolation by HPLC.

## 2.12 In vivo pharmacokinetics of temozolomide and DTIC in tumour bearing mice

### 2.12.1 Innoculation of mice with TLX5 lymphoma cells

Cells were passaged as described in section 2.5.2. In this study, ascitic fluid (0.05ml) from a mouse was taken from the intra-peritoneal cavity. The fluid was then diluted to 10mls with sterile saline in order to obtain the required cell density ( $2 \times 10^6/\text{ml}$ ) which was verified by counting the cells using a Coulter Counter ZM model. On Day 0 of each experiment, eleven CBA/CA female mice were inoculated subcutaneously in the left hind leg with the final cell suspension (0.1ml). Under these conditions, a solid TLX5 tumour was developed at the site of the inoculation. The mice were then housed in the Animal Unit of the institute and provided with food and water ad libitum.

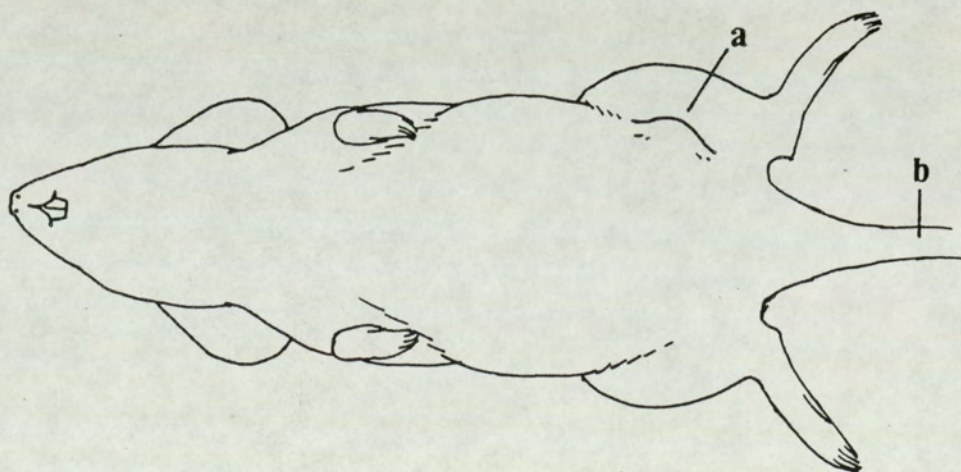


Fig.21 Diagrammatic representation showing the sites of(a) tumour inoculation and injection(b)

### 2.12.2 Experimental protocol

Mice were dosed intravenously via the tail vein with the drug solutions. A control mouse was dosed with 0.9% sterile saline, the volume of which was based on a 20g mouse receiving a volume of 0.2ml. In case of the early time points, the animals were anaesthetized prior to dosing and immediately transferred to the operating theatre for cardiac puncture as described below.

### 2.12.3 Collection of blood

All blood samples were collected by cardiac puncture of the right ventricle. Approximately 7min prior to the sample being due, the appropriate mouse was anaesthetized using a Boyles Apparatus set to administer fluothane (4%) with an oxygen flow rate of 500cc/min and a nitrous oxide flow rate of 500cc/min. When the animal no longer responds to pressure applied to its hind foot pads with blunt forceps, the fluothane composition was reduced to 2%. Blood samples were collected at 0.08, 0.17, 0.33, 0.5, 1.0, 1.5, 2.0, 2.5 and 3.0hr after administration of the drug.

An area of skin covering the thoracic and abdominal regions were removed and a transverse cut was made along the right abdominal wall immediately below the diaphragm. Following this, a cut was made through the right anterior diaphragm. Whilst holding the sternum, a vertical cut was made along the centre of the thorax so that the heart became visible. A syringe (1ml), previously rinsed with heparin solution (1000U/ml), was inserted into the right ventricle and the blood was slowly withdrawn. The mouse

was killed by dislocation of its neck. Blood samples were immediately transferred to microfuge vials (1.5ml) previously rinsed with heparin solution (1000U/ml). Samples were then immediately centrifuged in a Minifuge at  $-20^{\circ}\text{C}$  at 3500rpm for 2min. A known volume of plasma was removed and transferred to microfuge vials which were frozen at  $-20^{\circ}\text{C}$  prior to analysis (section 2.4.2).

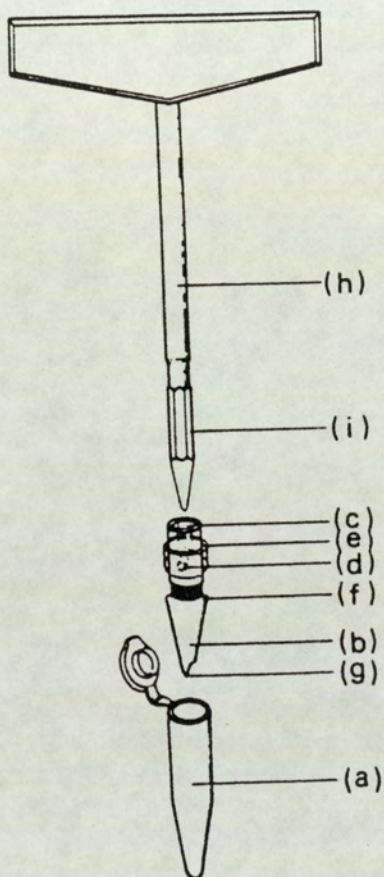
#### 2.12.4 Collection of tissues

After dislocation of the neck, the tumour surrounding the muscle attached to the left femor were removed for analysis. Tissues were immediately transferred into a bijoux pots previously weighed and tared. Samples were then frozen at  $-20^{\circ}\text{C}$  until analysis (2.4.2).

#### 2.12.5 Homogenization of tumour tissue

Preliminary experiments were to determine the presence of MTIC in tumour tissue. Sample preparation procedure was performed according to that described by Hearse (1984). Tumour tissue (0.02-0.05g) was transferred to microfuge vials (1.5ml) which had been pre-cooled in liquid nitrogen. The tissue was then pulverized using the apparatus (Biomedix, 2 West Avenue, Pinner, Middlesex) as illustrated in fig.22. The pulverized cold tissue from the previous preparative step was homogenized in ammonium acetate buffer (0.05M, pH6.7, 1ml). The tumour homogenate (0.1ml) was then used for analysis (see 2.4.2). Since MTIC was not detected in the tumour tissue, the subsequent experiments were designed solely to detect and quantify temozolomide.

The sample preparation procedure was modified so as to avoid potential degradation of temozolomide at room temperature. This was achieved by adding 0.1N HCl (0.5ml) to the tumour tissue. Tumour tissue (0.2-0.3g) in 0.1N HCl was then homogenized with distilled water (1.5ml). Tissue homogenate (0.25ml) was then extracted twice with ethylacetate as described in section 2.4.1.



Centrifugal micro-homogeniser system. The drawings illustrate the polypropylene tube (a) in which pulverisation, homogenisation, extraction and centrifugation of a tissue sample is accomplished. The polypropylene pestle (b), which is moulded with the identical profile of the lower part of the tube is characterised by a hollow shaft with hexagonal core (c), a spin support bar hole (d) which is covered by removable rubber sleeve (e), a tapered shoulder (f) on the body of the pestle and a cutting step (g) at its tip. The pestle can be attached to a mandrel (h) via a hexagonal pin (i).

Fig.22 Diagrams of the centrifugal micro-homogenizer system

### 2.12.6 Mathematical analysis of pharmacokinetic data

The calculation of the pharmacokinetic parameters are described as follows: the rate constants for the elimination ( $k_{e1}$ ) were estimated from the gradients generated by linear regression analysis of log concentration versus time. The AUC values were estimated by trapezoidal method from 0 to 3hr. Other pharmacokinetic parameters for the model were determined from the following equations:

$$\text{elimination } t_{1/2} = 0.693/k_{e1}$$

$$\text{clearance (Cl)} = \text{dose/AUC}$$

$$\text{volume of distribution (Vd)} = \text{Cl}/k_{e1}$$

Fraction of MTIC generated from temozolomide ( $f_m$ ) was estimated by comparison of the AUC and clearance obtained for MTIC and temozolomide (Rowlands and Tozer, 1980; Gibaldi and Perrier, 1982)

$$\text{AUC}_{\text{MTIC}}/\text{AUC}_{\text{tem}} = f_m - \text{Cl}_{\text{tem}}/\text{Cl}_{\text{MTIC}}$$

### 2.12.7 Statistical analysis

The analysis of variance was used to test the degree of significance.

Section 3

Results and Discussion

### 3 Results and Discussion

#### 3.1 Analysis of temozolomide in biological fluids

##### 3.1.1 Development of an HPLC assay

In order to study the metabolism and pharmacokinetics of temozolomide in vitro and in vivo, an HPLC method was used to detect and quantify temozolomide and metabolic species possessing an intact tetrazinone ring in biological fluids. The HPLC analysis was based on the published method developed by Slack et al (1986) with slight modifications.

##### 3.1.2 Validation of the method

In this section of the thesis, the results of the experiments are discussed which were designed to establish the extraction efficiency, reproducibility, linearity and detection limits of the assay.

The extraction efficiency was  $58.4 \pm 2.3\%$  (n=6) for temozolomide and  $93.9 \pm 2.6\%$  (n=6) for ethazolastone (expressed as percentage of temozolomide being extracted in ethylacetate  $\pm$  one standard deviation). The coefficients of variation (C.V.) obtained for inter-day and the within-day reproducibility of the analysis of temozolomide at 35mg/L, 5mg/L and 0.2mg/L were less than 10% , and the C.V. for replicate injections for a single sample was 0.52%.



conc (mg/L)	within day C.V.	inter-day C.V.
35.35	1.82%	7.5%
4.29	1.54%	6.8%
0.35	3.67%	8.2%

Table 3. Inter- and within-day reproducibility of temozolomide

All the quoted values in table 3 are the means of six different determinations. The limit of detection of temozolomide was 0.2mg/L in plasma and liver homogenates and 0.5mg/L in urine with a signal-to-noise ratio of greater than 3.0. The calibration curve was linear between 0.2mg/L to 40mg/L with the correlation coefficient greater than 0.99. A typical calibration curve is shown in fig.24. The results presented here suggest that this analysis can be used to quantify temozolomide reproducibly in biological media.

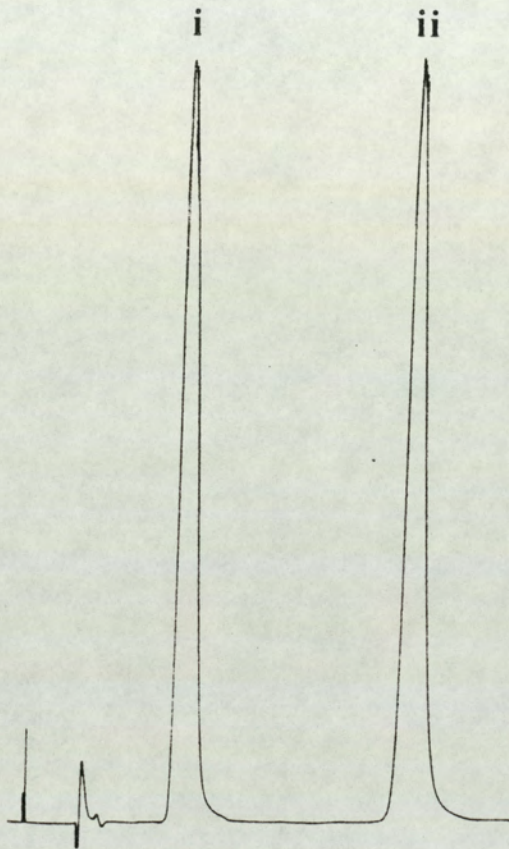


Fig.23 HPLC chromatogram showing the separation of temozolomide (i) and ethazolastone (ii).  
Mobile phase, 7% methanol in 0.5% acetic acid  
Detection wavelength, 325nm. Flow rate, 1.5ml/min

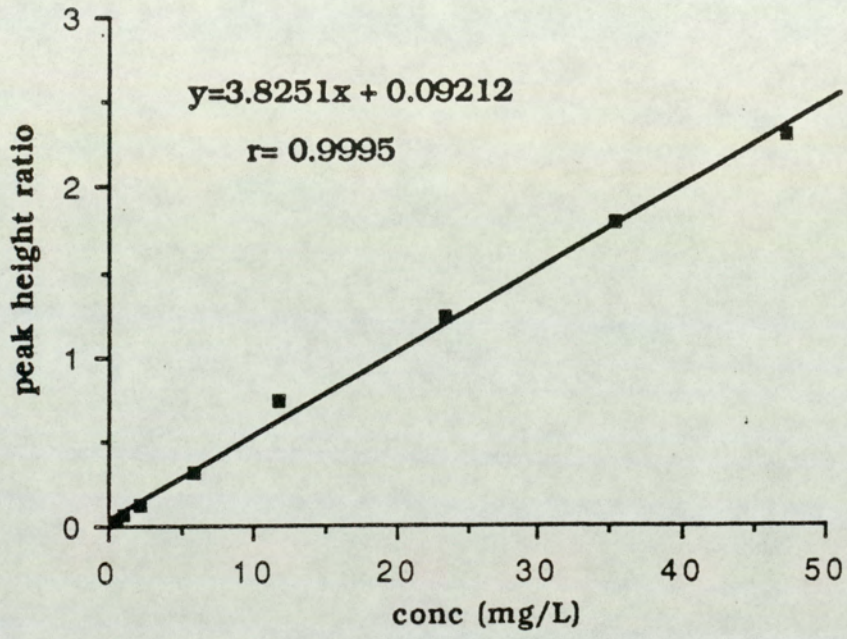


Fig.24 Calibration curve for temozolomide using ethazolastone as the internal standard

### 3.2 Analysis of the benzotriazinones

3-Methylbenzotriazinone is a structural analogue of temozolomide. In order to investigate its metabolism in vitro, an HPLC method was developed to detect and separate the parent substrate and its putative metabolites, namely benzotriazinone, hydroxymethyl- benzotriazinone.

The benzotriazinones have a  $\lambda_{\max}$  between 280 and 286nm (see fig.26). Therefore, the wavelength 284nm was chosen to detect these compounds. Good separation was achieved with an isocratic reversed phase HPLC method which employed 75% water and 25% methanol. This method was also used for isolating the metabolites for subsequent mass spectral analyses. Due to its inherent instability in aqueous solution, where it readily decomposed to benzotriazinone, hydroxymethylbenzotriazinone was not detected by this method.

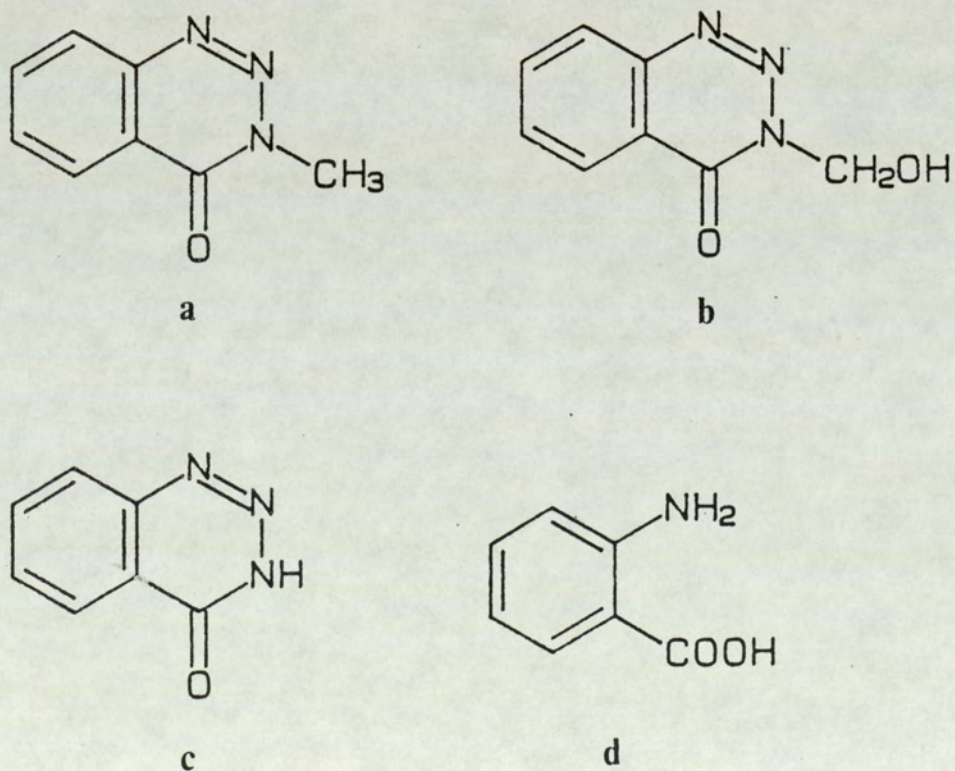


Fig.25 Structures of the benzotriazinones  
a) 3-methylbenzotriazinone, b) hydroxymethyl-  
benzotriazinone, c) benzotriazinone  
d) antronic acid (internal standard)

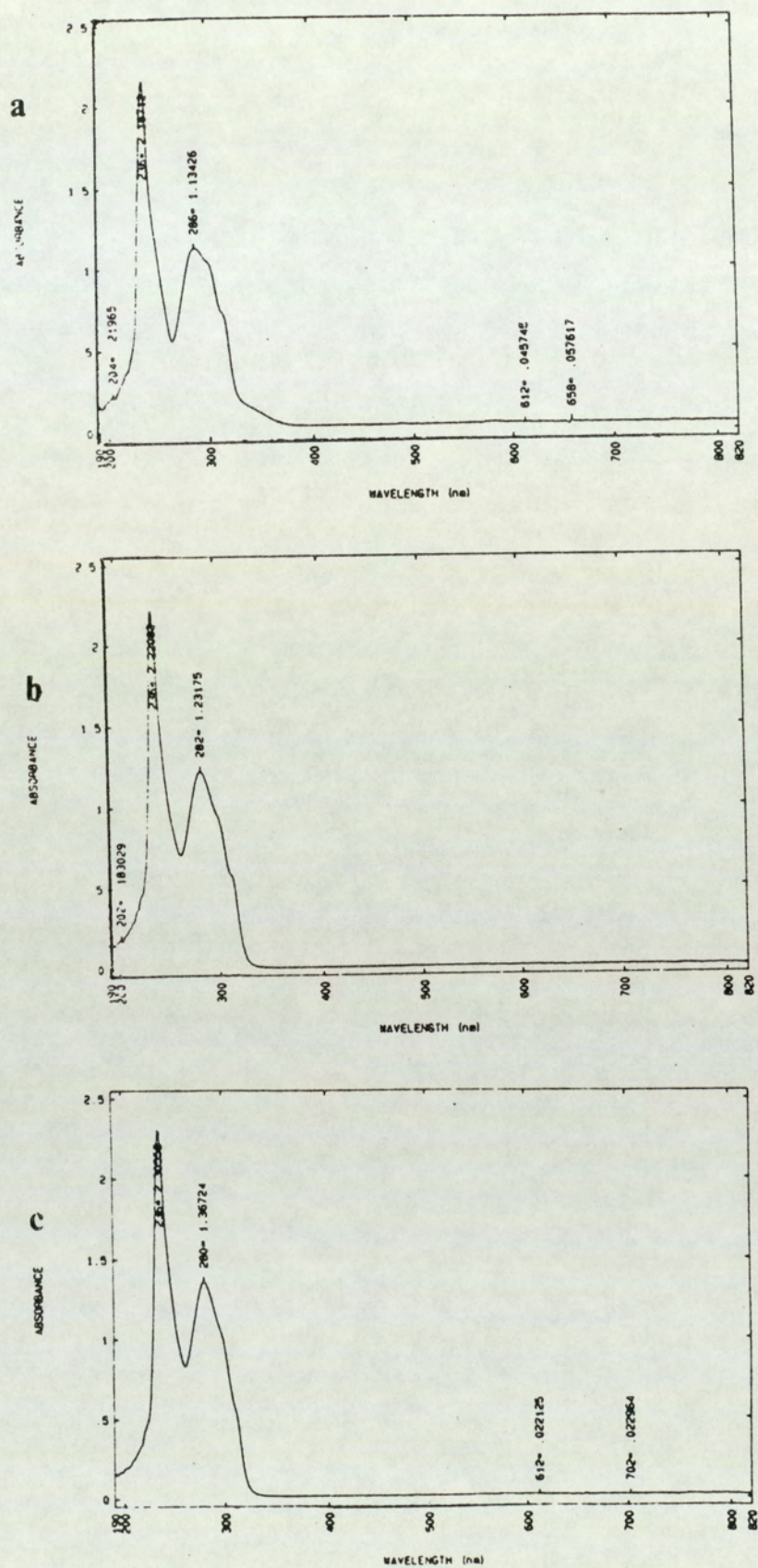


Fig.26 UV spectra of the benzotriazinones  
a) 3-methylbenzotriazinone, b) hydroxymethylbenzotriazinone, c) benzotriazinone

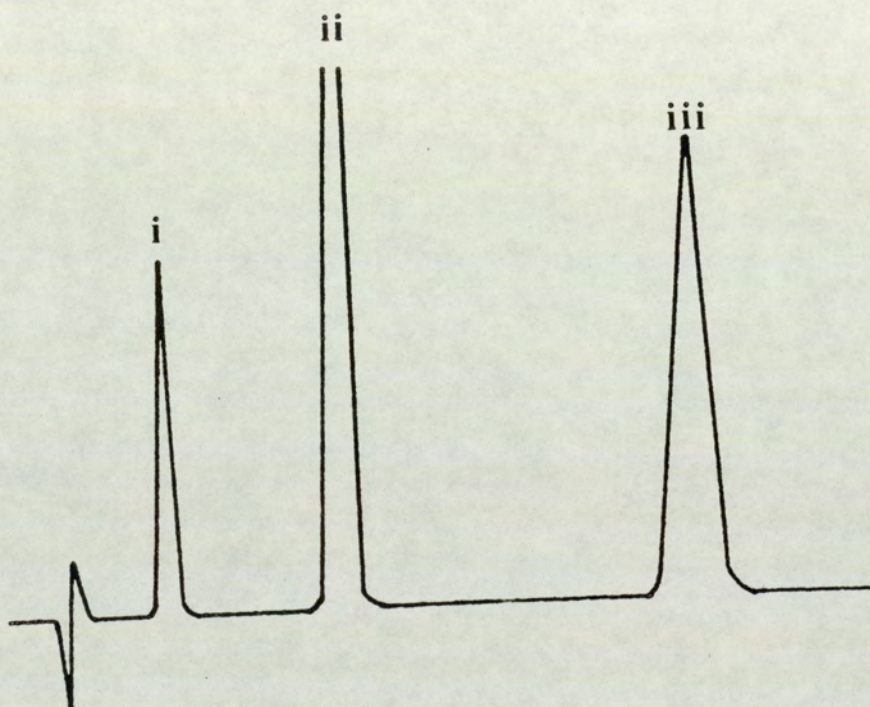


Fig.27 HPLC chromatograms showing the separation of the benzotriazinones i) benzotriazinone, ii) internal standard, iii) 3-methylbenzotriazinone. Mobile phase, 25% methanol and 75% water. Detection wavelength, 284nm. Flow rate, 1.5ml/min

### 3.3 Analysis of MTIC, HMMTIC, DTIC and temozolomide in biological fluids

One of the objectives of this thesis is to study the mechanism of action of temozolomide (see section 1.4). It is postulated that temozolomide is a stable prodrug of MTIC (see section 1.3.4). However, direct identification of MTIC as an intermediate product of chemical degradation of temozolomide has not yet been accomplished by chromatographic means. In order to study the disposition of temozolomide and DTIC in vitro and in vivo, two HPLC methods were developed to allow simultaneous separation, detection and quantitation of MTIC, temozolomide, HMMTIC and DTIC.

Initial experiments were conducted to establish the relative stability of temozolomide, MTIC and DTIC at different pH values in order to choose suitable conditions under which the labile imidazotriazines and tetrazinone can be analyzed with sufficient stability. The stability of temozolomide and its putative metabonate, MTIC, was monitored by diode-array UV spectrometry (section 2.5.1) and HPLC (section 2.4.1). Fig.28 shows a plot of degradation constant ( $k_{ob}$ ) versus pH. It is shown that the degradation of temozolomide and MTIC was pH-dependent. At 37°C, temozolomide was relatively stable at acidic to neutral pH (1-7). The rate of degradation increased in an exponential manner when the pH exceeded 8. MTIC exhibited a triphasic log  $k_{ob}$ -pH profile at 37°C. In a solution of low pH, the drug was extremely unstable, half-life was less than 2min. As the pH increased, the rate of degradation of

MTIC decreased, MTIC was seen to be relatively stable at alkaline pH. Previous studies (Horton, 1982) have shown that DTIC was stable under acidic and alkaline conditions in the absence of light. The results presented here indicate that a pH value between 6 to 7 is optimum for the analyses of temozolomide, DTIC and MTIC. In the actual analyses, 0.05M ammonium acetate buffer adjusted to pH 6.7 was used.



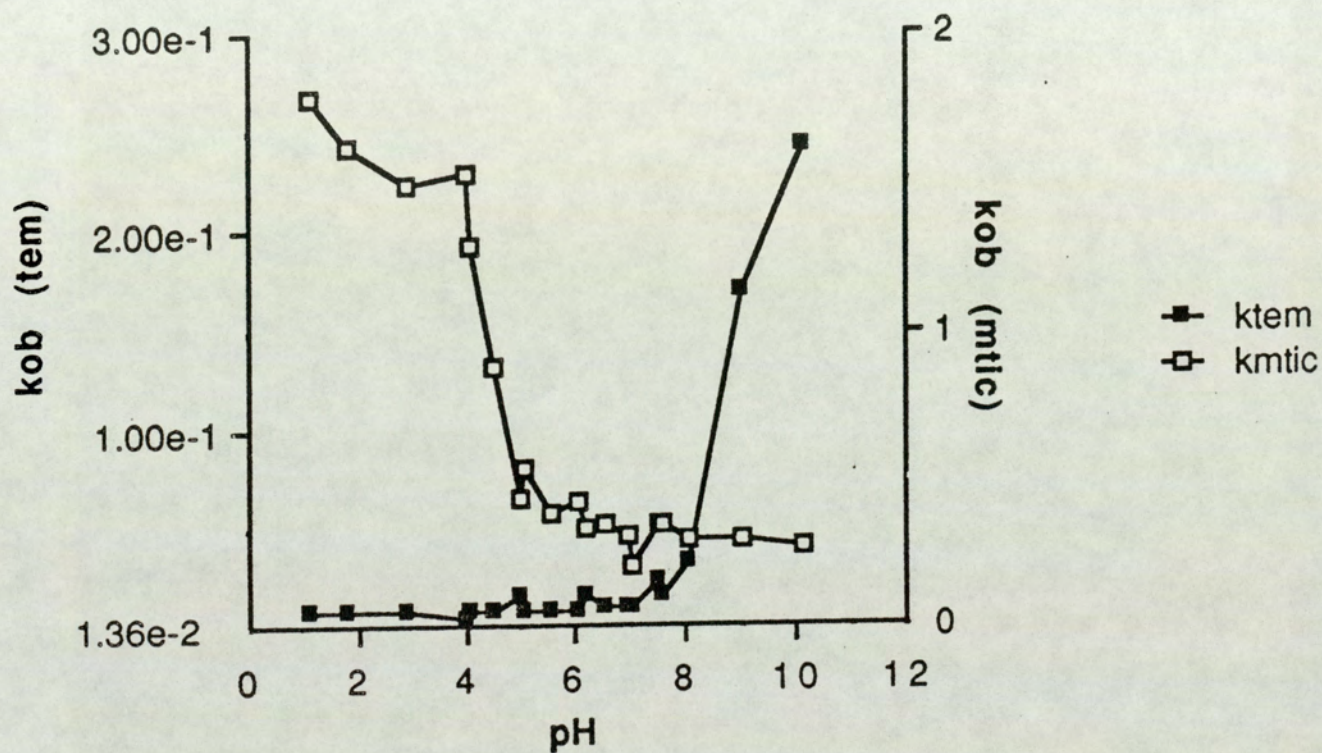


Fig.28 A plot of stability constant ( $k_{ob}$ ) versus pH of temozolomide and MTIC

A C<sub>18</sub> reversed-phase column has been used previously to detect temozolomide (Slack et al, 1986; Goddard, 1985) (see section 3.1) and DTIC (Fiore et al, 1985). Farina et al (1982, 1985) also successfully separated dimethyl and monomethyl triazenes using this column chemistry. In preliminary experiments, the peaks corresponding to the respective triazenes and tetrazinone were resolved using a C<sub>18</sub> RP-select B column (12.5cm). Since MTIC, temozolomide, HMMTIC and DTIC all possess a  $\lambda_{\text{max}}$  in the region of 320nm, a wavelength 323nm was chosen for detection (figs.29&30).

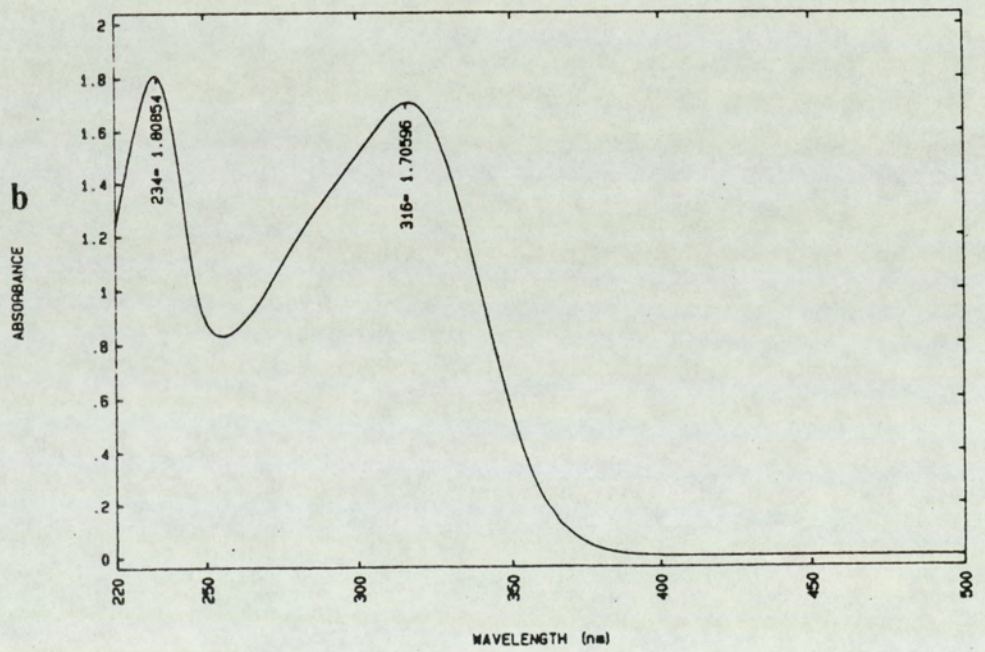
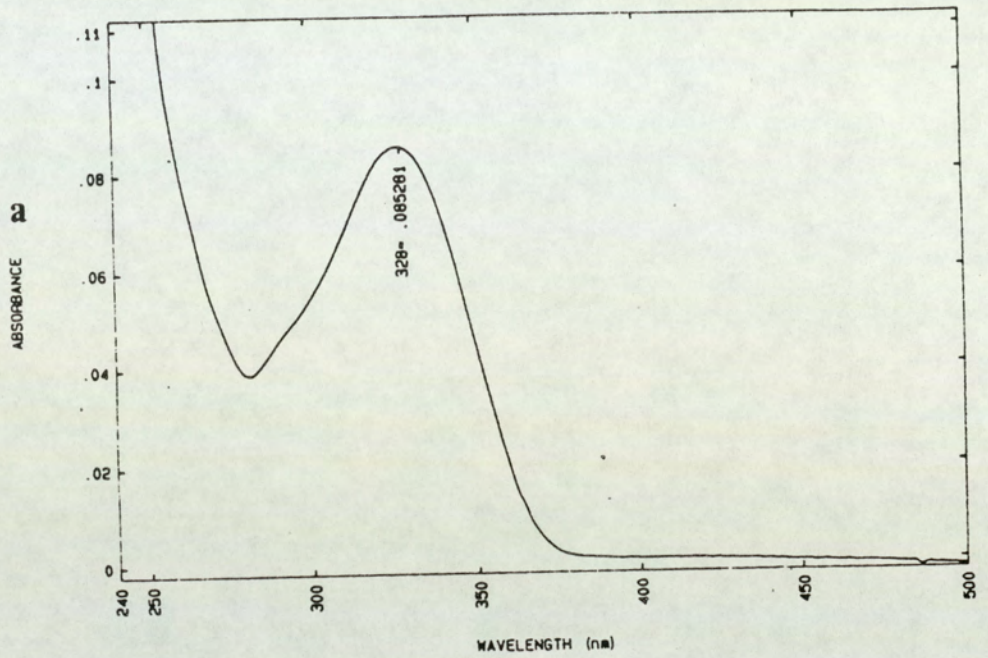


Fig.29 UV spectra of a) temozolomide, b) MTIC

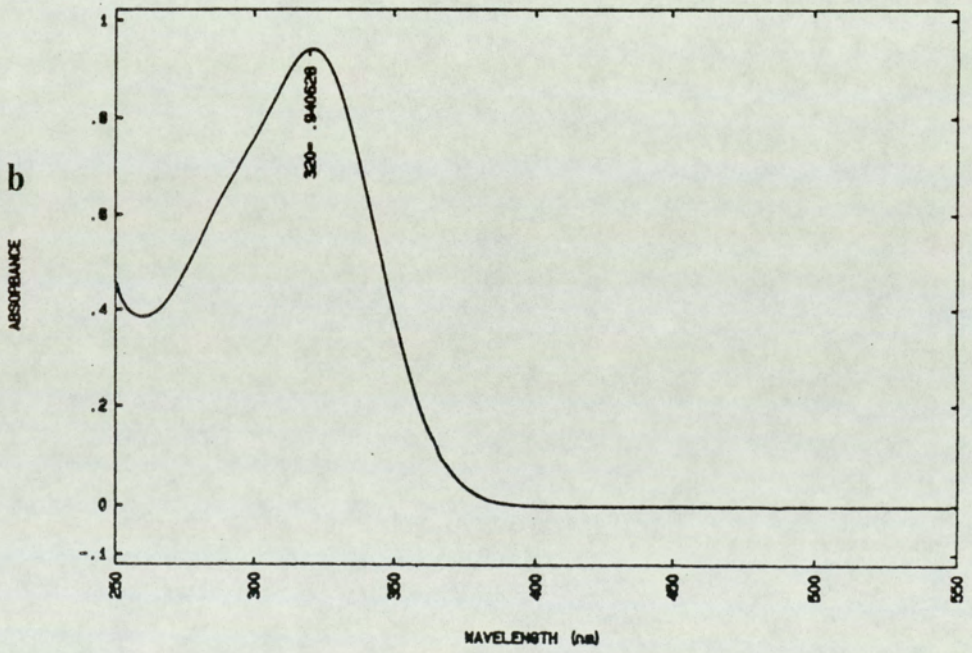
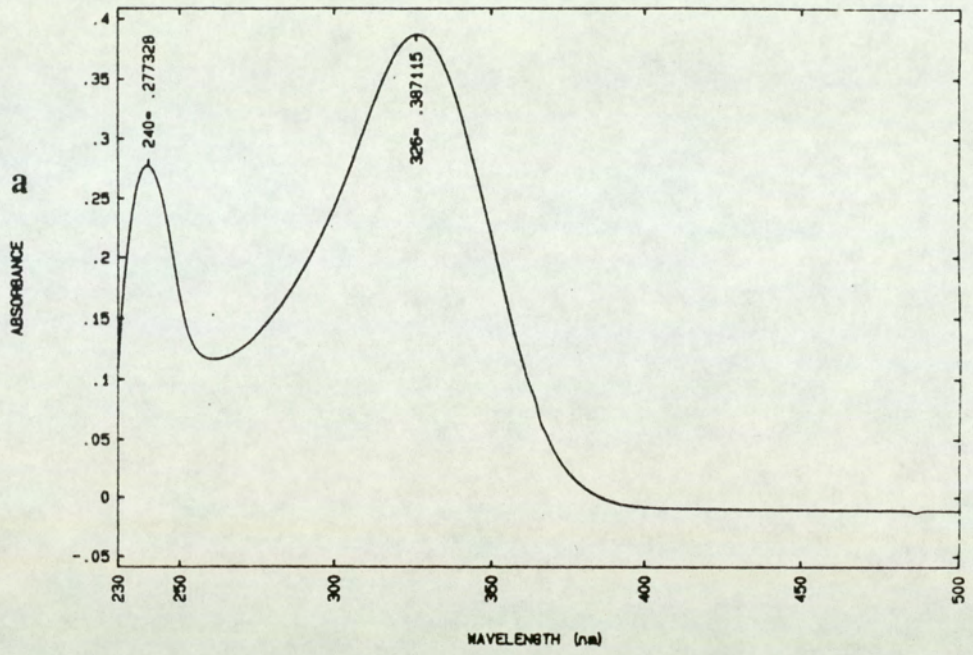


Fig.30 UV spectra of a) DTIC, b) HMMTIC

Fig. 31 shows a plot of capacity factor ( $k'$ ) versus the percentage of acetonitrile present in the mobile phase. Methanol was not used as the organic solvent because preliminary experiments have shown that temozolomide is not stable in the presence of methanol at this pH. It was shown that MTIC, temozolomide and DTIC were resolved using acetonitrile (5-8%) in ammonium acetate buffer (0.05M, pH 6.7). However, under these conditions, the peaks corresponding to MTIC and HMMTIC were not resolved. Since MTIC and HMMTIC were sufficiently retained on the column as characterized by their capacity factor ( $k'= 5$ ), a longer column was chosen to increase the theoretical plates in order to achieve increased resolution (Bombaugh, 1978). In order to achieve this goal, a 25cm column was used to optimize the separation of MTIC, HMMTIC and DTIC (fig.34).

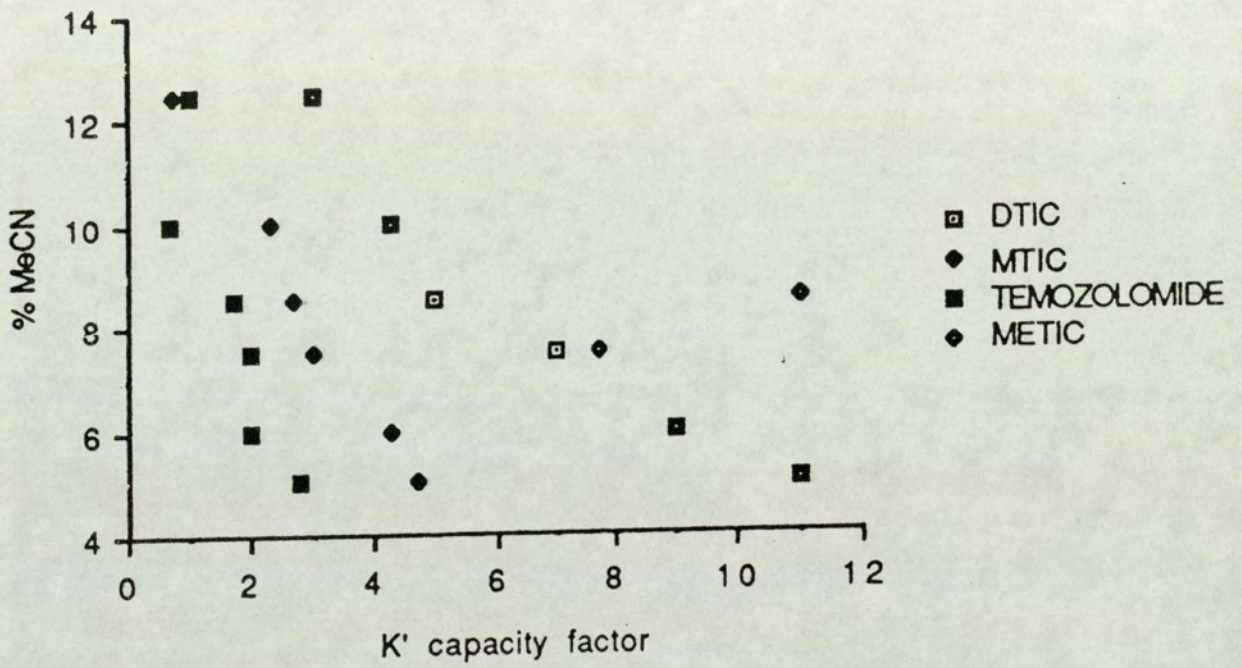


Fig.31 A plot of capacity factor versus percentage of acetonitrile

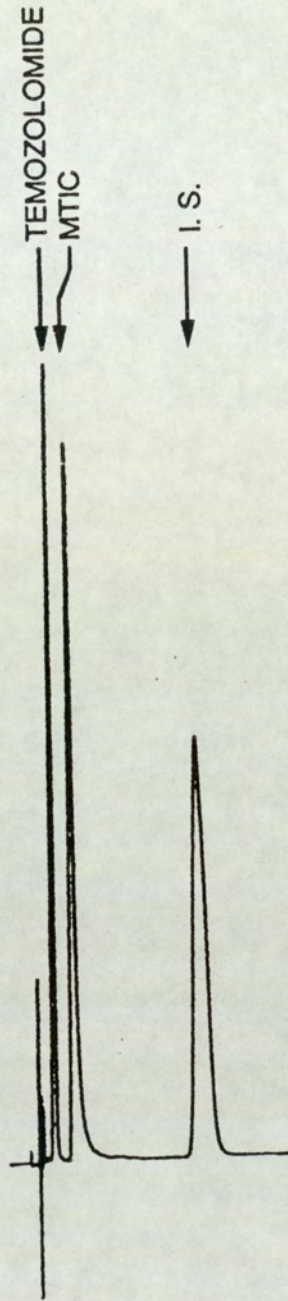
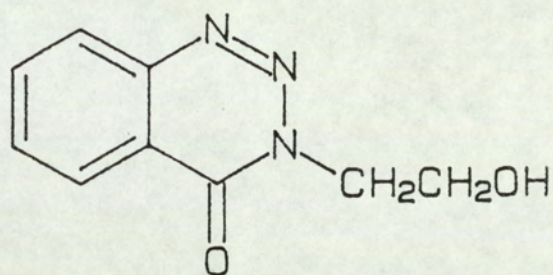
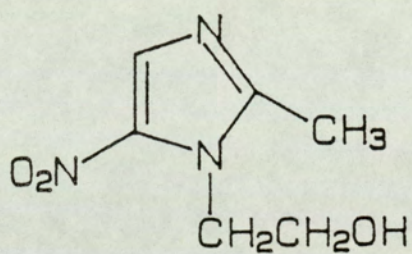


Fig.32 HPLC chromatograms showing the separation of  
i) temozolomide, ii) MTIC, iii) internal standard  
Mobile phase, 5% acetonitrile in 0.05M ammonium  
acetate. Detection wavelength, 323nm. Flow rate,  
1.5ml/min



Hydroxyethylbenzotriazinone



Metronidazole

Fig.33 Structures of hydroxyethylbenzotriazinone and metronidazole



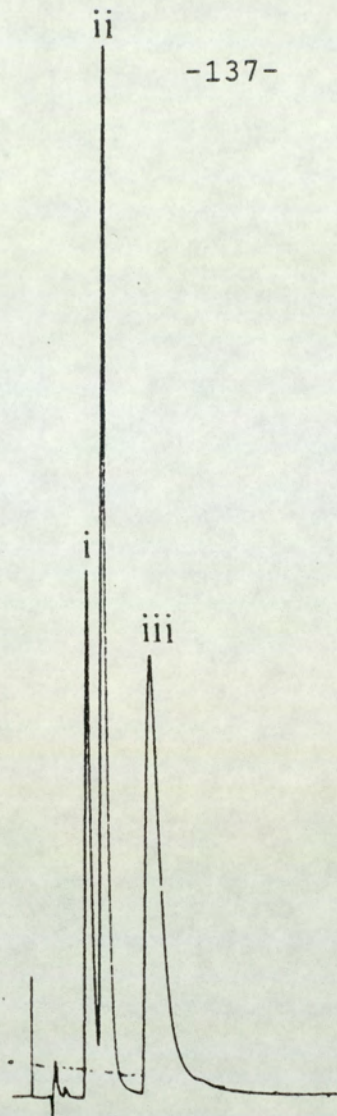


Fig.34 HPLC chromatogram showing the separation of  
 i) MTIC, ii) HMMTIC, iii) DTIC using a 25cm  
 Lichrosorb RP C<sub>18</sub> column

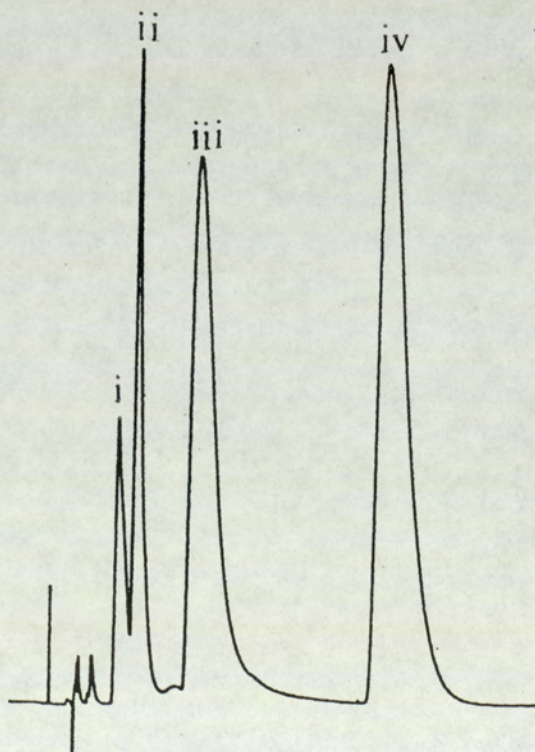


Fig.35 HPLC chromatogram showing the separation of  
 i) MTIC, ii) HMMTIC, iii) DTIC, iv) hydroxyethyl-  
 benzotriazinone. Detection wavelength, 323nm.  
 Flow rate, 1.5ml/min

For accurate quantitative analysis, the addition of an internal standard is desirable. Ideally, the standard should be a substance not present endogenously in the biological fluids and structurally similar to the compounds under examination. In the case of the analysis of temozolomide and MTIC, 3-hydroxyethylbenzotriazinone was chosen as the internal standard. This compound was, however, not suitable as an internal standard for the analysis of DTIC and its metabolites because under these conditions, 3-hydroxyethylbenzotriazinone was retained on the column, thus increasing the total time for analysis to exceed 35min (fig.35). Therefore, an alternative internal standard was looked for. METIC and ethazolastone (the ethyl analogues of MTIC and temozolomide) were unsuitable because they co-eluted with DTIC and MTIC. Metronidazole is an antimicrobial agent, structurally similar to the imidazotriazines (see fig.33) and has a  $\lambda_{max}$  at 277nm (B.P., 1980). Fig.36a&b show the separation of MTIC, HMMTIC, metronidazole and DTIC using 5% acetonitrile or 5% methanol as organic solvent. Using 5% acetonitrile as an organic solvent, the peaks of MTIC, HMMTIC, metronidazole and DTIC were not well resolved, whereas 5% methanol gave a better resolution of these four component peaks but poor peak shape. Often, optimal separation can be achieved by a binary organic solvent mixtures (Major, 1976; Krstulovic and Brown, 1982). Therefore, by varying the amount of acetonitrile and methanol in the organic solvent in the mobile phase, an optimal separation of these four component peaks could be achieved. Fig.37 shows the separation of

MTIC, HMMTIC, metronidazole and DTIC using different proportion of acetonitrile and methanol in the mobile phase. Optimal separation was achieved with 1.75% methanol, 3.75% acetonitrile and 95% ammonium acetate buffer (0.05M, pH 6.7).

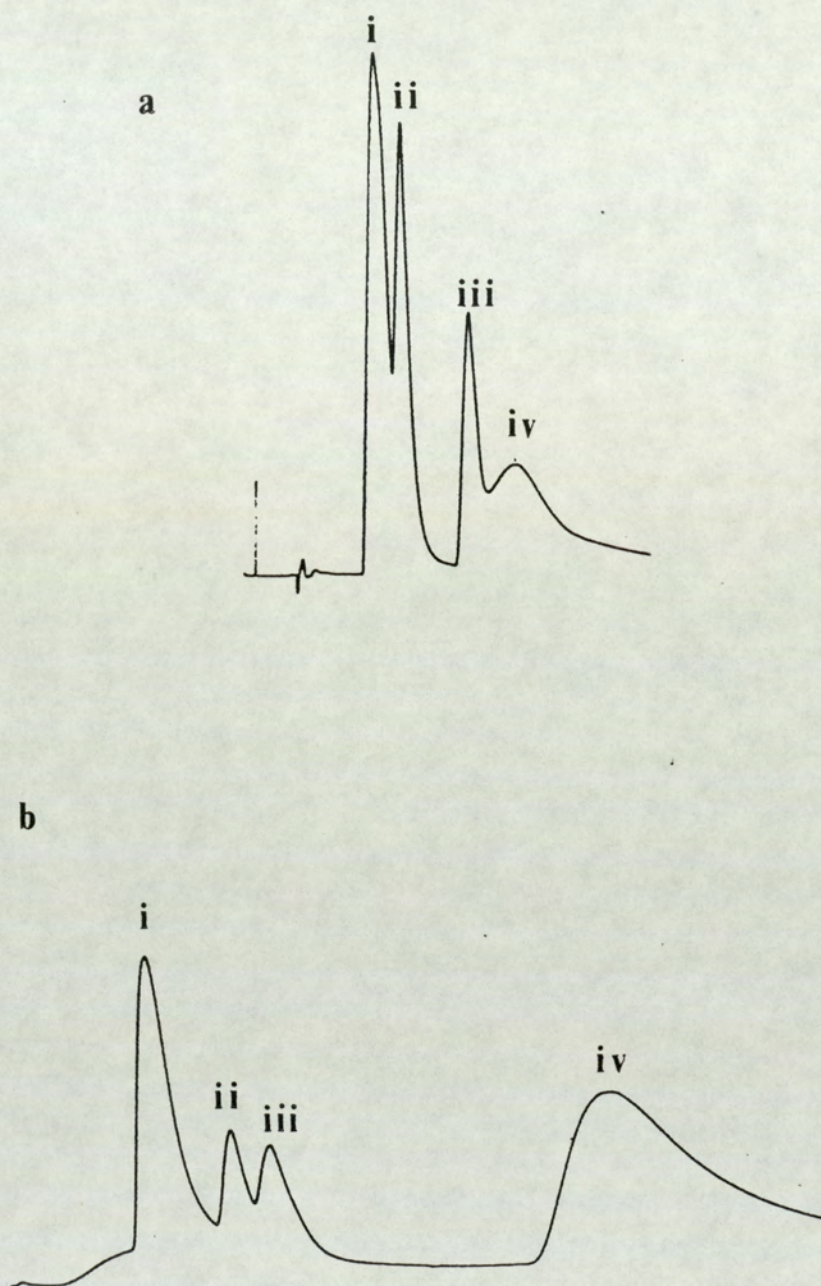


Fig.36 HPLC chromatogram showing the separation of i) MTIC, ii) HMMTIC, iii) metronidazole, iv) DTIC using a) 5% MeCN in ammonium acetate (0.05M) b) 5% MeOH in ammonium acetate (0.05M) Detection wavelength, 323nm. Flow rate, 1.5ml/min

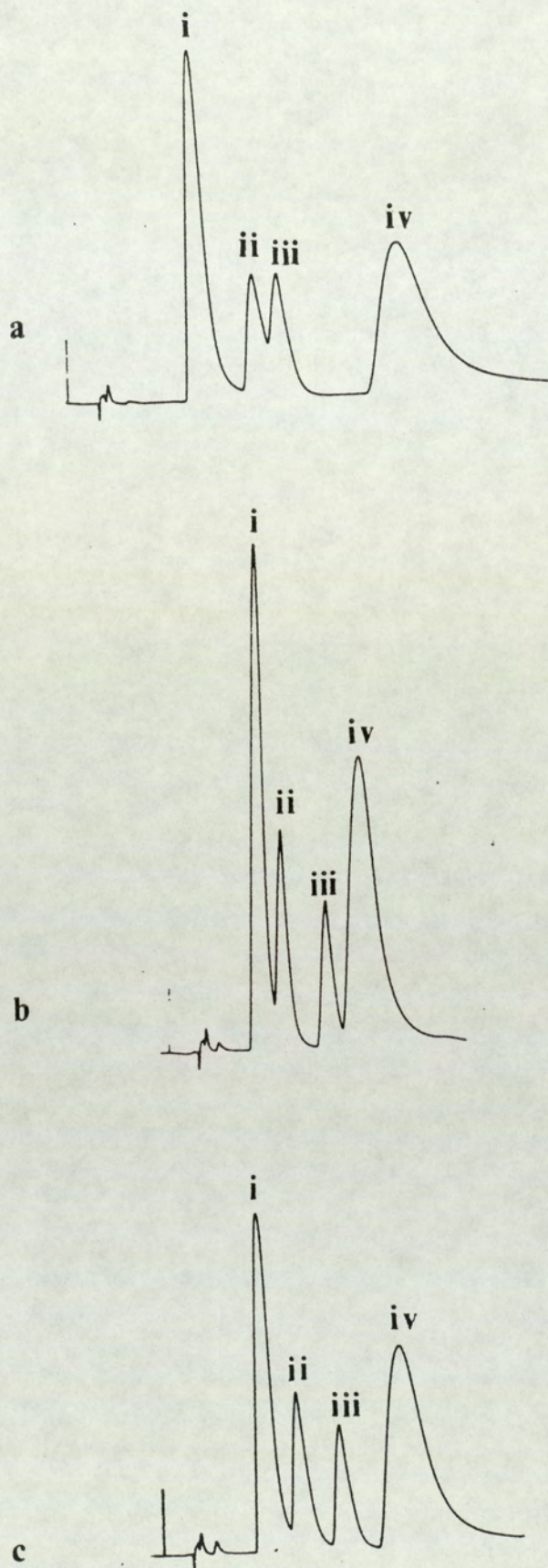


Fig.37 HPLC chromatograms showing the separation of i) MTIC, ii) HMMTIC, iii) metronidazole iv) DTIC using a) 1% MeCN/4% MeOH in ammonium acetate (0.05M), b) 3.25% MeCN/ 1.75% MeOH in ammonium acetate (0.05M). Detection wavelength, 323nm. Flow rate, 1.5ml/min

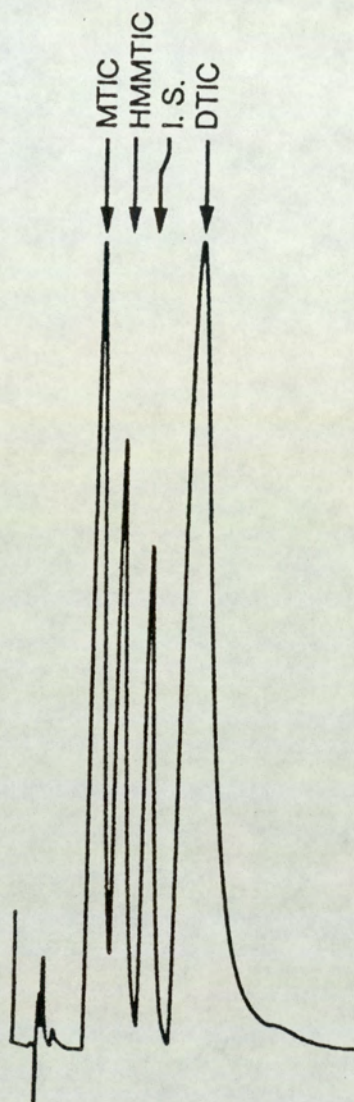


Fig.38 HPLC chromatogram showing the separation of i) MTIC, ii) HMMTIC, iii) metronidazole iv) DTIC using 1.25% MeOH/3.75% MeCN in ammonium acetate (0.05M). Detection wavelength: 323nm Flow rate: 1.5ml/min

In order to separate temozolomide and the imidazotriazenes from the plasma and to render them amenable to analysis by HPLC, a protein-precipitation procedure was incorporated in the sample preparation stage. The method used was similar to that used by Farina et al (1982, 1985) for the analysis of labile dimethyl and monomethyl triazenes. Protein precipitation was achieved by the addition of ice cold acetonitrile (0.2ml) containing the internal standard whilst in the case of the analysis of MTIC, HMMTIC and DTIC, an aliquot (0.2ml) of a mixture of ice cold acetonitrile and methanol (65:35) containing the internal standard was added to precipitate protein. Table 4 shows the percentage recovery of the drugs after protein precipitation. The individual percentages of recovery was between 80 to 90%.

Drugs	Percentage Recovery (%)
temozolomide	93 <sub>±</sub> 10% (n=6)
DTIC	90 <sub>±</sub> 7% (n=6)
MTIC	96 <sub>±</sub> 9% (n=6)
HMMTIC	94 <sub>±</sub> 8% (n=6)

Table 4. Percentage recovery of temozolomide, DTIC MTIC and HMMTIC after protein precipitation

To verify that drug was not adsorbed onto the precipitated proteins, the percentage of recovery of the drugs after protein precipitation was compared with those standards prepared by the addition of derivatives to a centrifuged plasma-acetonitrile or acetonitrile/methanol mixtures. The results obtained showed that adsorption did not occur.

### 3.3.1 Validation of the analytical methods

The reproducibility of the analytical assays was determined by analyzing each compound at concentrations of 20mg/L, 10mg/L and 2.5mg/L. The results are tabulated in table 5.



Drugs	mg/L conc	Coefficient of Variation		n
		within-day	between-day	
temozolomide	20.26	12%	12%	6
	10.13	4.6%	8%	6
	2.53	9.4%	10%	6
MTIC	20.44	16%	15%	6
	10.22	11%	11%	6
	2.55	14%	18%	6
DTIC	20	11%	10%	6
	10	8%	10%	6
	2.5	11%	13%	6
HMMTIC	20.3	13%	14%	6
	10.15	10%	7%	6
	2.53	15%	17%	6

Table 5. Inter- and within day reproducibility of temozolomide, DTIC, MTIC and HMMTIC

The coefficient of variation for replicate injections from a single sample for temozolomide, MTIC, DTIC and HMMTIC were, respectively, 2, 4, 4 and 5% of the mean (n=6). The high values of coefficient of variation derived from temozolomide, HMMTIC, MTIC could possibly be due to their inherent instability.

Examples of the calibration curves of temozolomide, MTIC, HMMTIC and DTIC are shown in figs. 39&40. In every case, the correlation coefficient for a fit to a straight line was greater than 0.98.

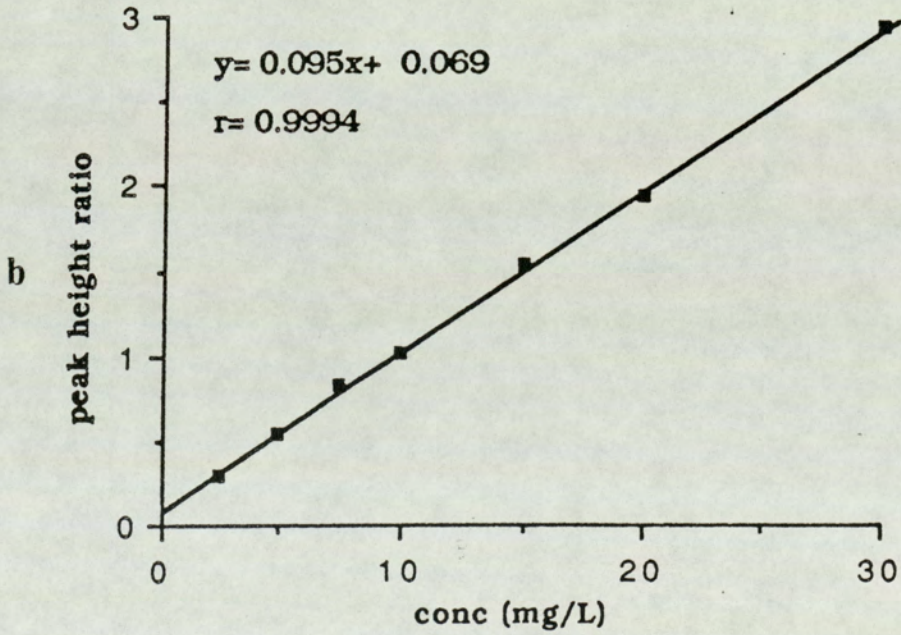
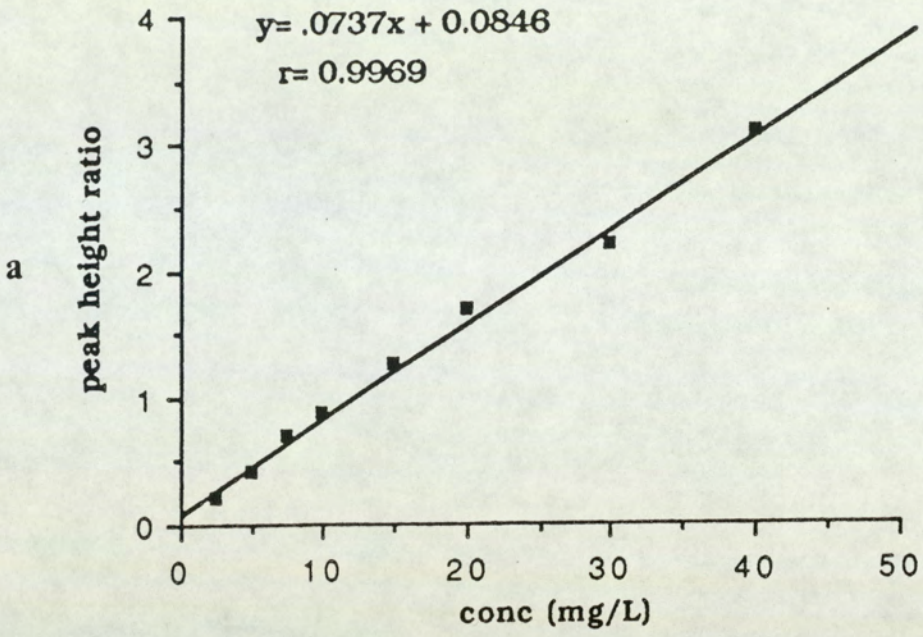


Fig.39 Calibration curves for a) temozolomide and b) DTIC

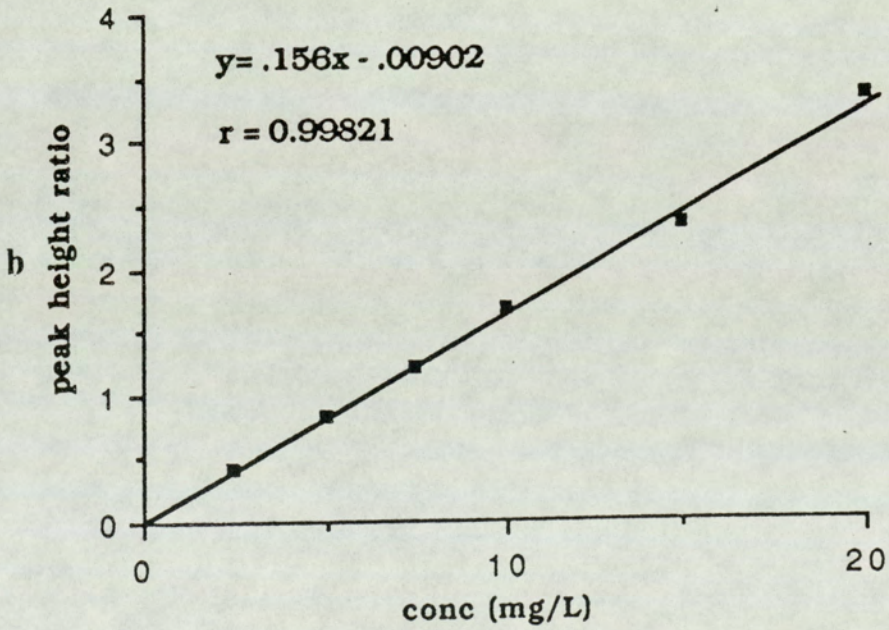
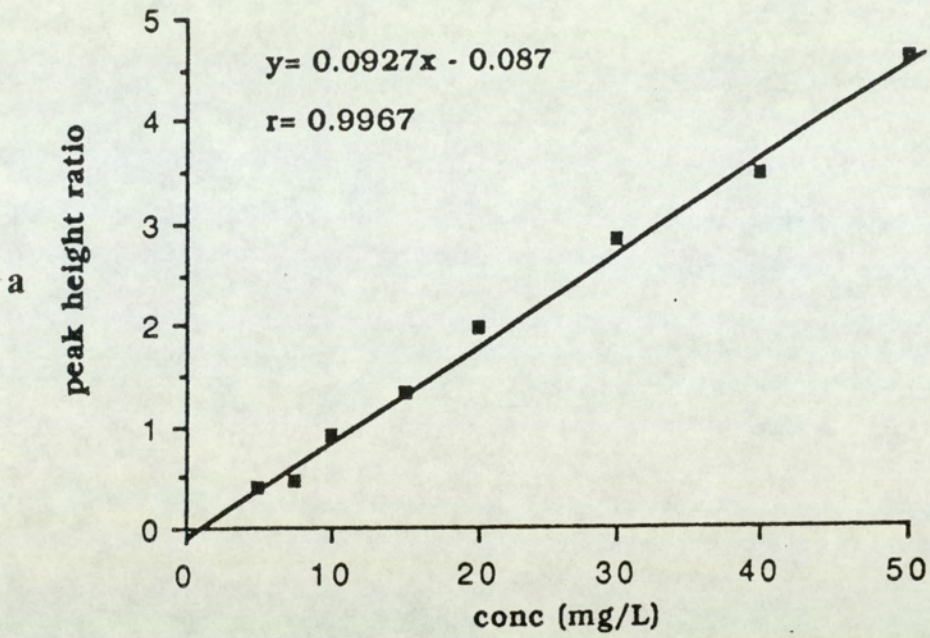


Fig.40 Calibration curves for a) HMMTIC and b) MTIC

The limits of detection of the compounds under examination was established by serially diluting a solution of the drug in plasma and assaying the diluted samples with the LM480 detector at maximum sensitivity. The results are shown in table 6.

drugs	conc (mg/L)	ng on column
temozolomide	0.2	4
MTIC	0.25	5
DTIC	0.2	4
HMMTIC	0.3	6

Table 6. Limits of detection of temozolomide, DTIC, MTIC and HMMTIC

As shown above, in general, the minimum concentration that could be detected was between 0.2 to 0.3mg/L with a signal to noise ratio of greater than 3. This corresponds to 4 to 6ng on column.

The principal problems associated with the development of the quantitative assay was the inherent instability of the compounds in biological media. The problem was largely overcome by keeping the time for analysis to a minimum. In the case of temozolomide and MTIC, the retention times were 3 and 5min respectively. HMMTIC and DTIC had the retention times of 6 and 8min respectively. To increase stability, the samples were processed in ice/water and stored at -20°C after sample preparation. In all analyses, the samples were manually injected onto the HPLC column instead of

using the autosampler, which was not equipped with a refrigeration unit. Fig. 41 shows that temozolomide, MTIC, HMMTIC and DTIC were stable even 8hr after sample preparation at  $-20^{\circ}\text{C}$ . The HPLC methods described in this section are specific, reproducible and sensitive for the analysis of temozolomide and labile imidazotriazines such as MTIC and HMMTIC. The total run time for both analysis was 20min and the component peaks were sufficiently resolved.

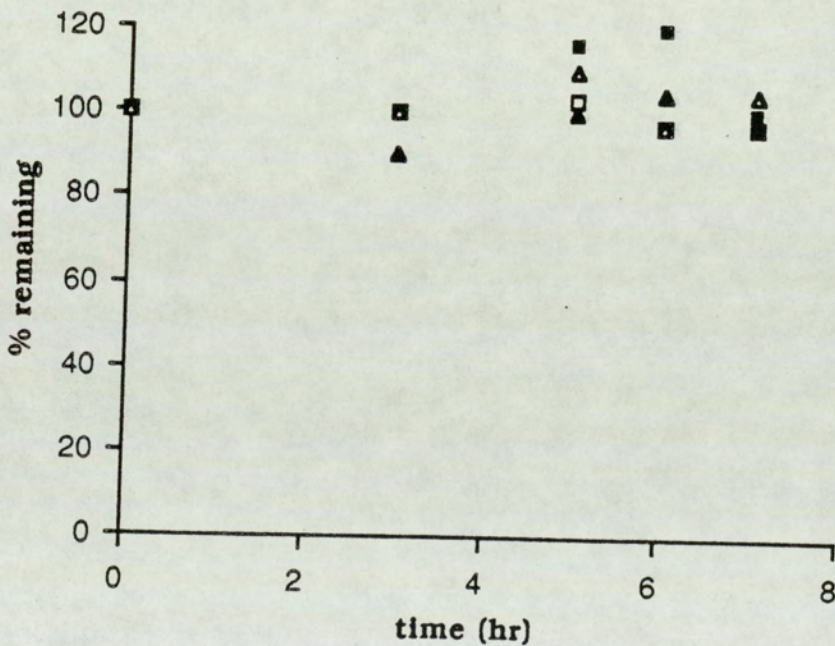


Fig.41 Stability of temozolomide (□), MTIC (■), HMMTIC (▲), DTIC (△) at  $-20^{\circ}\text{C}$  after sample preparation (n=2)

### 3.4 Stability of temozolomide and MTIC in biological media

The stability of temozolomide and its metabonate, MTIC was monitored by diode array UV spectrometry or HPLC as described in the methods and materials section (2.4.1). Figs 42 and 43, show the degradation at 37°C of temozolomide and MTIC in phosphate buffer (pH 7.4, 0.1M), RPMI supplemented with 17% horse serum, the tissue culture medium for TLX5 cells and human plasma. In phosphate buffer, temozolomide decomposed according to first order kinetics which was confirmed by regression analysis (fig.42). The apparent  $t_{1/2}$  of temozolomide in phosphate buffer was 100min. The degradation of temozolomide in tissue culture medium and human plasma deviates slightly from first order kinetics. In both cases, the residual points were not randomly scattered along the regression line. This result indicates that there is a greater standard error of the estimate along the regression lines of y (percentage of temozolomide remaining) and on x (time) of these two media when compared with that phosphate buffer. Since the calculated correlation coefficient was greater than 0.98, the data obtained were treated mathematically as if they followed first order kinetics. The apparent  $t_{1/2}$  thus calculated were 50min for tissue culture medium and 30min for human plasma. The  $t_{1/2}$  of MTIC computed in this study was 2min for both phosphate buffer and tissue culture medium.

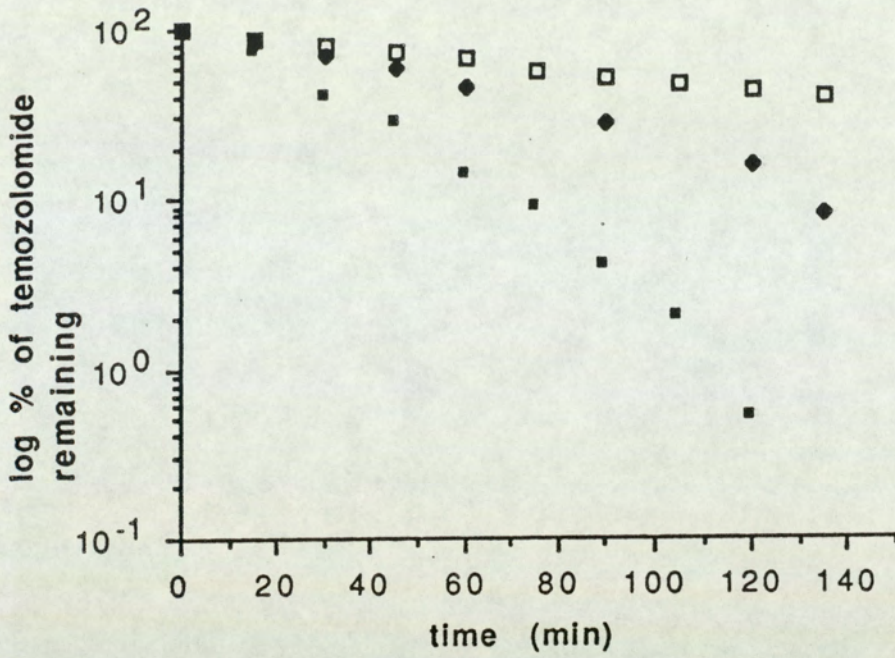


Fig.42 Stability of temozolomide in phosphate buffer (□), RPMI supplemented with 17% horse serum (◆) and plasma (■) (n=3)

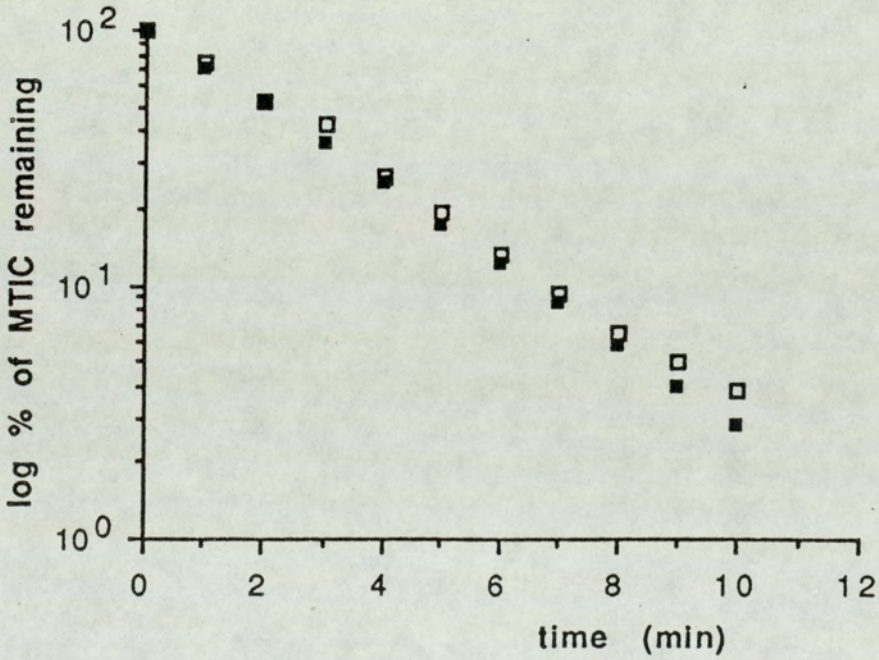


Fig.43 Stability of MTIC in phosphate buffer (□), and RPMI supplemented with 17% horse serum (■) (n=3)



Figs. 44 and 45 show the UV spectra of temozolomide and MTIC. The spectra were recorded in the dark, the one of temozolomide at pH10 (fig.44) and the one of MTIC at pH7.5 (fig.45). On the basis of what is known about the chemistry of imidazotetrazinones (Stevens et al, 1984; Baig and Stevens, 1987) and of the arylalkyltriazenes (Vaughan and Stevens, 1978), one can assume that the degradation end-product of both compounds is AIC. AIC possesses a UV  $\lambda_{max}$  at 270nm. Such a maximal wavelength is observed in the solutions of both degraded temozolomide and MTIC (figs.44 and 45). In the case of temozolomide, decomposition occurs rapidly at alkaline pH (fig.44). During decomposition, the  $\lambda_{max}$  of temozolomide appears to undergo a slight shift to 324nm. Also the position of the isobestic point changes during degradation of temozolomide. It has been outlined previously in the introduction that chemical experiments have suggested the intermediary of MTIC in the decomposition of temozolomide (see also section 3.8). MTIC has a UV  $\lambda_{max}$  at 320nm (fig.29). The shift in wavelength by 4nm observed in the spectra of temozolomide during decomposition is consistent with the interpretation that the spectrometer records the absorption of a mixture of temozolomide and MTIC during temozolomide decomposition and that the resultant spectrum is the envelope of the spectra of both compounds at rapidly changing concentration ratio.

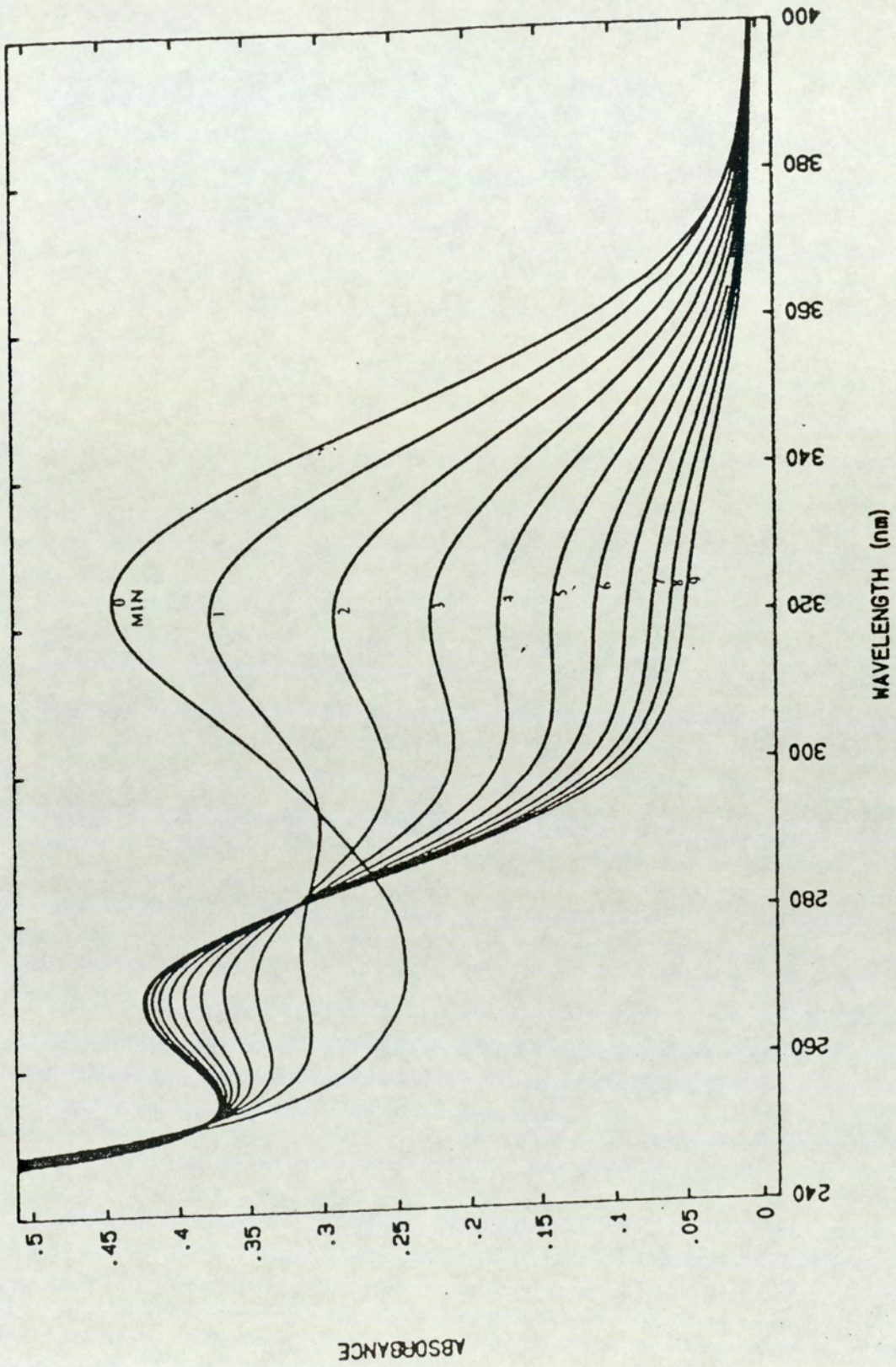


Fig.44 UV spectrum of temozolomide recorded at pH10 showing its degradation

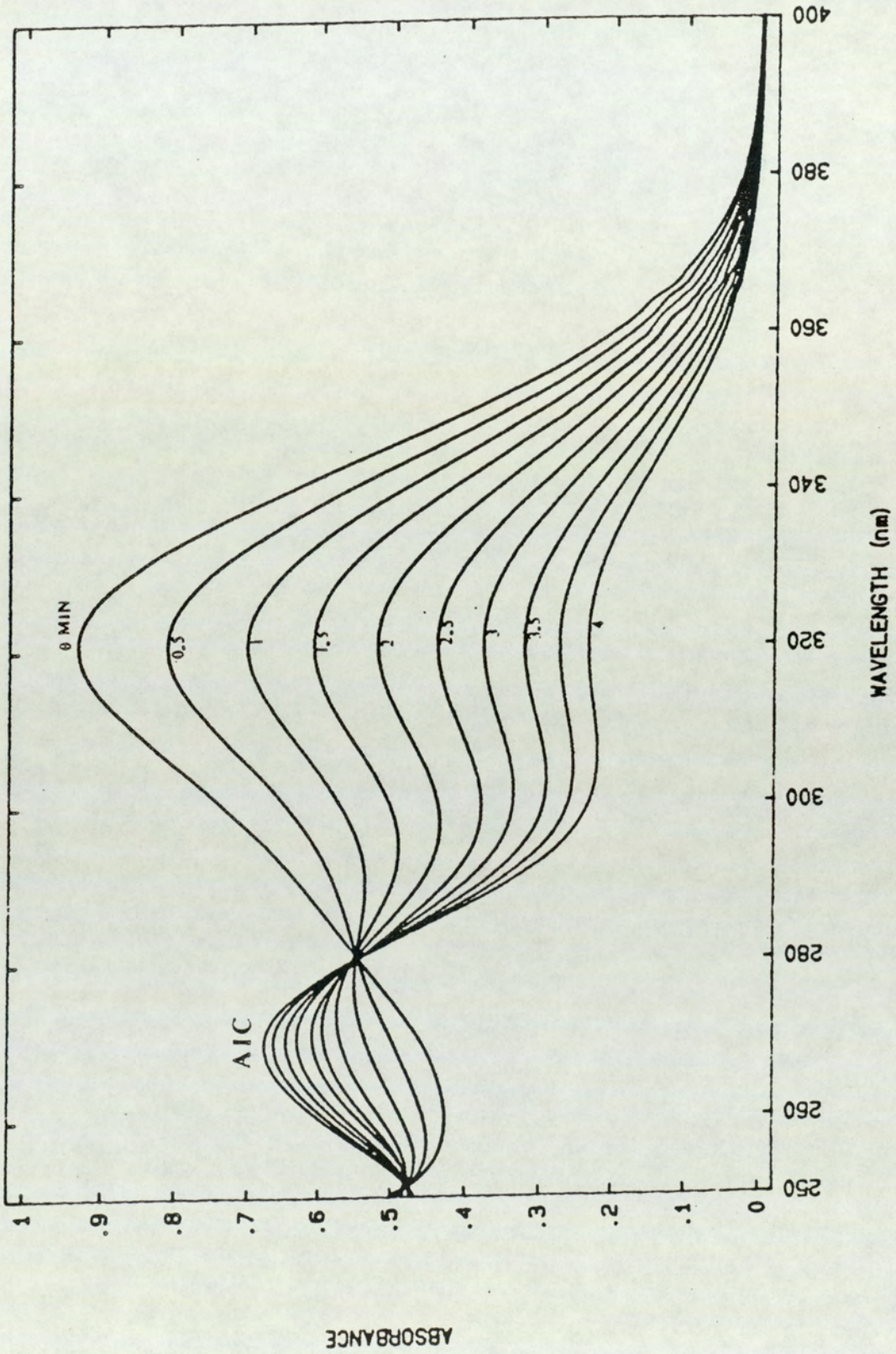


Fig.45 UV spectrum of MTIC recorded at pH7.5 showing its degradation

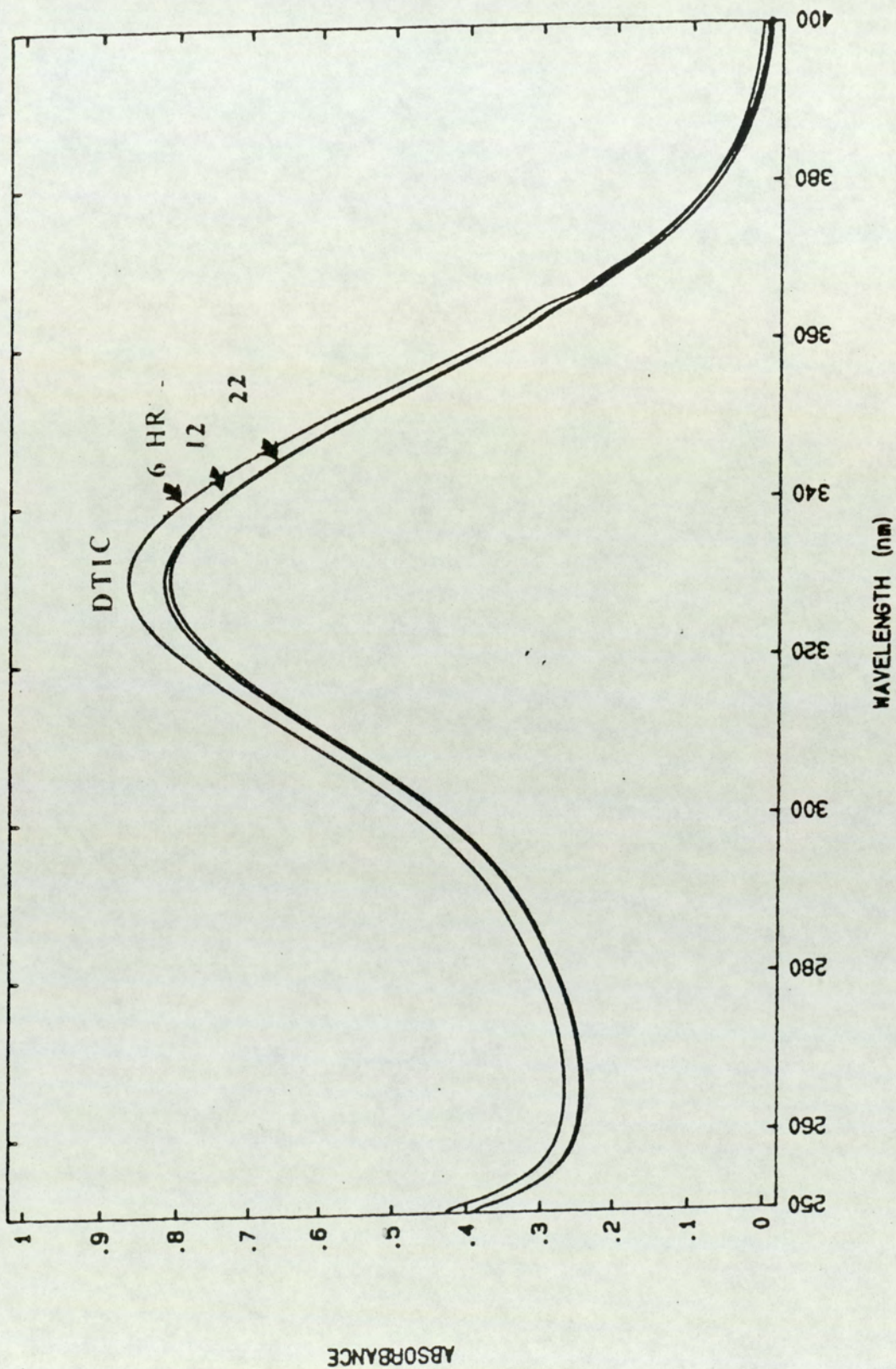


Fig.46 UV spectrum of DTIC recorded at pH1 in the absence of light

### 3.5 Comparison of the in vitro cytotoxicity of temozolomide and its metabonates, MTIC and AIC

In this part of the thesis, the in vitro cytotoxicity of the putative metabonates of temozolomide is described. Fig.47 shows the growth curve of TLX5 murine lymphoma cell in vitro at different initial seeding cell densities. The doubling time calculated from the growth curve was between 14<sub>±</sub>2hr. Fig.48 shows the effect of continuous exposure for 72hr to temozolomide, MTIC and AIC on TLX5 cell growth. In fig.48, temozolomide, MTIC are shown to inhibit cell growth in a dose-dependent manner. The IC<sub>50</sub>, obtained graphically, of temozolomide and MTIC were 5.8<sub>±</sub>1.7mg/L (30<sub>±</sub>6 $\mu$ M) and 12.5<sub>±</sub>4mg/L (75<sub>±</sub>24 $\mu$ M) respectively. AIC had little effect on cell growth. One possible explanation for the difference in cytotoxicity between MTIC and temozolomide is that MTIC is even more labile than temozolomide, t<sub>1/2</sub> is 2min at 37°C in tissue culture medium, compared with 50min for temozolomide.

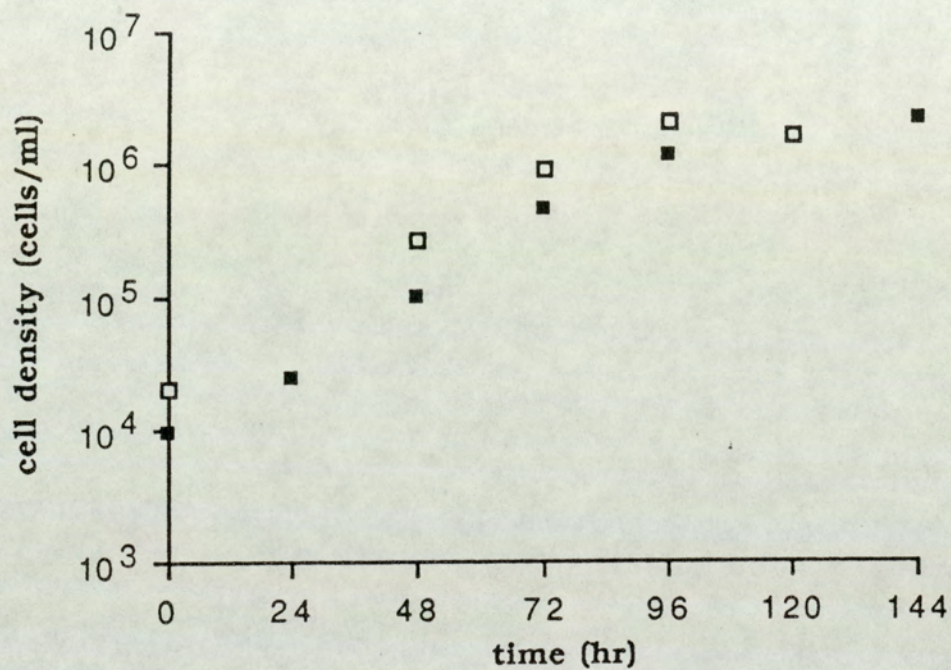


Fig.47 Growth curve of TLX5 cells at 2 different initial seeding densities (n=4)

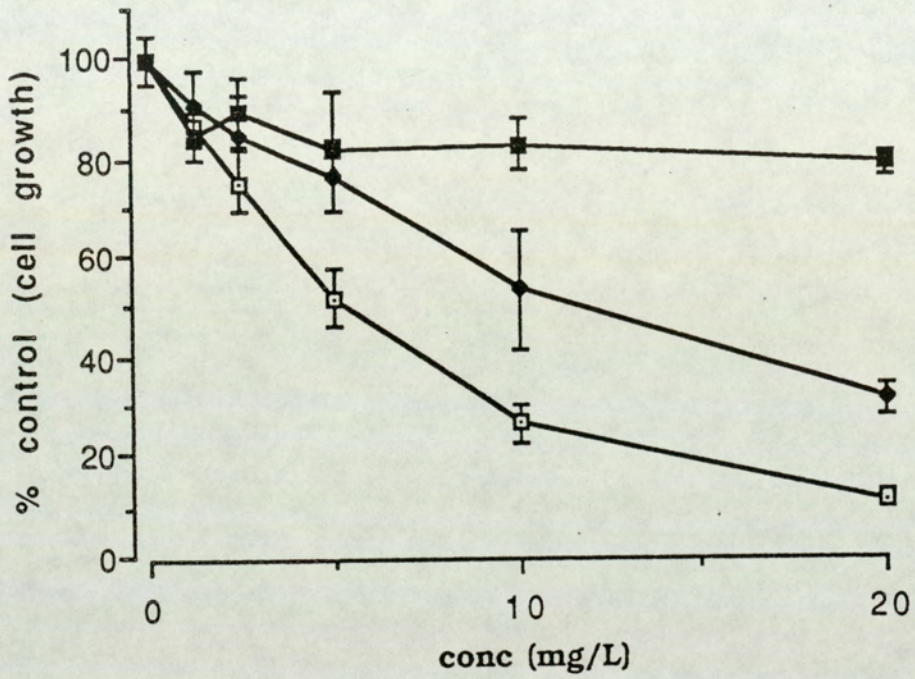


Fig.48 Effect of 72hr continuous exposure to temozolomide (-□-), MTIC (-◆-), and AIC (-■-) on TLX5 lymphoma cell growth (n=4 ± 1 S.D.)

### 3.6 Comparative in vitro metabolism of temozolomide and 3-methylbenzotriazinone

#### 3.6.1 Introduction

The in vitro biotransformation of aryltetrazinone and aryltriazinone is virtually unknown (see section 1.4). In this section of the thesis, the in vitro metabolism of temozolomide and its structural analogue, 3-methylbenzotriazinone is discussed. In particular, the hypothesis is tested that the N-methyl group undergoes metabolism to the corresponding stable N-hydroxymethyl derivative. It is well-documented that N-methyl compounds are metabolized by oxidation of the methyl group to generate a carbinolamine (reviewed by Ross, 1982; Overton et al, 1985). The monomethyltriazene, derived from the metabolism of 1-(4-acetyl-phenyl)-3,3-dimethyltriazene has been shown to undergo further metabolism when incubated with 9,000g supernatant fortified with co-factors (Farina et al 1982, 1985) (see fig.49). It was speculated that the monohydroxymethyltriazene might be a metabolite but this species has not been identified. Farina et al (1982) suggested that such a species may be a candidate for the "truly ultimate selective toxic species". The cytotoxicity of such a species can be explained by that certain N-(hydroxymethyl)-amines and -amides can form potentially electrophilic imines or iminium ions (reviewed by Overton et al, 1985, see section 3.8.2) and therefore, can react with nucleophiles present in target tissues, for example, tumour tissue. Both temozolomide and 3-methylbenzotriazinone are structural analogues of a



monomethyltriazene arranged in a stable cyclic form. It is, therefore, of interest to investigate the in vitro biotransformation of these two compounds in order to support or refute the hypothesis that N-hydroxymethyl derivative is formed.

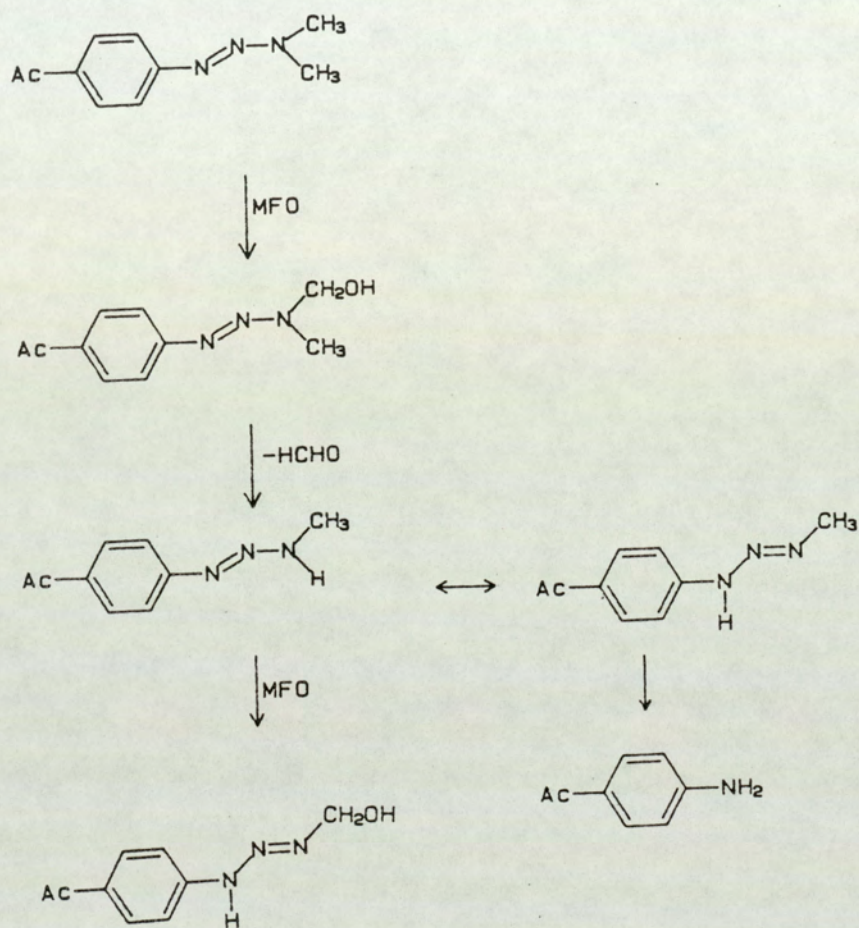


Fig.49 Proposed metabolic pathway of 1-(4-acetylphenyl)-3,3-dimethyltriazene

### 3.6.2 Results

Microsomes, 10,000g post-mitochondrial cytosolic fraction and whole liver homogenate were used to investigate the in vitro metabolic fate of temozolomide. The disappearance of the substrate with time was measured by reversed phase HPLC as described in section 2.4.1. It was found that there was no difference between degradation rate of temozolomide in the presence or absence of viable liver preparations (figs.51, 52 and 53). The disappearance of the substrate due to chemical degradation was shown in a parallel study in which the disappearance of the substrate in the mixtures containing phosphate buffer with or without deactivated liver preparations were compared. Using this HPLC assay, the degradation end-product, AIC, could not be detected because the incubation mixture was deproteinized and quenched by acid prior to extraction, therefore AIC would remain in the aqueous phase during the extraction process.

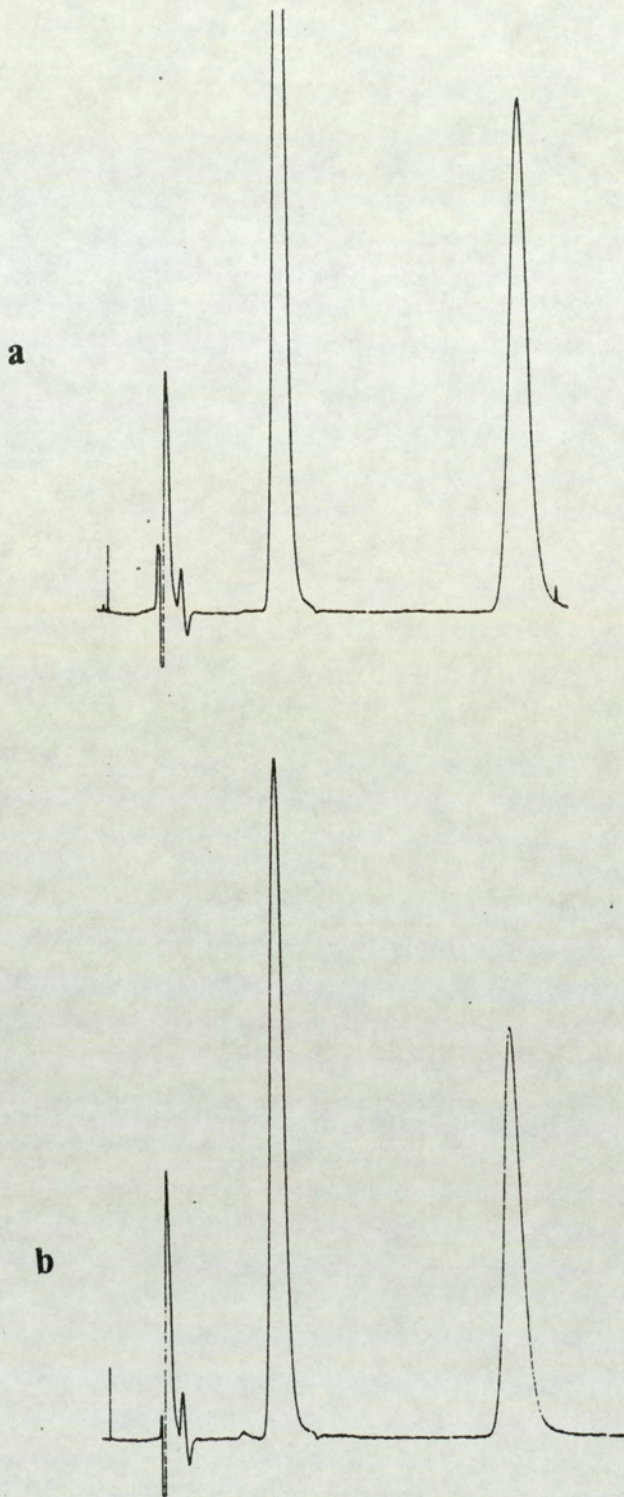


Fig.50 HPLC chromatogram showing the degradation of temozolomide in the presence of liver microsomes fortified with NADPH after a) 0min, b) 20min incubation

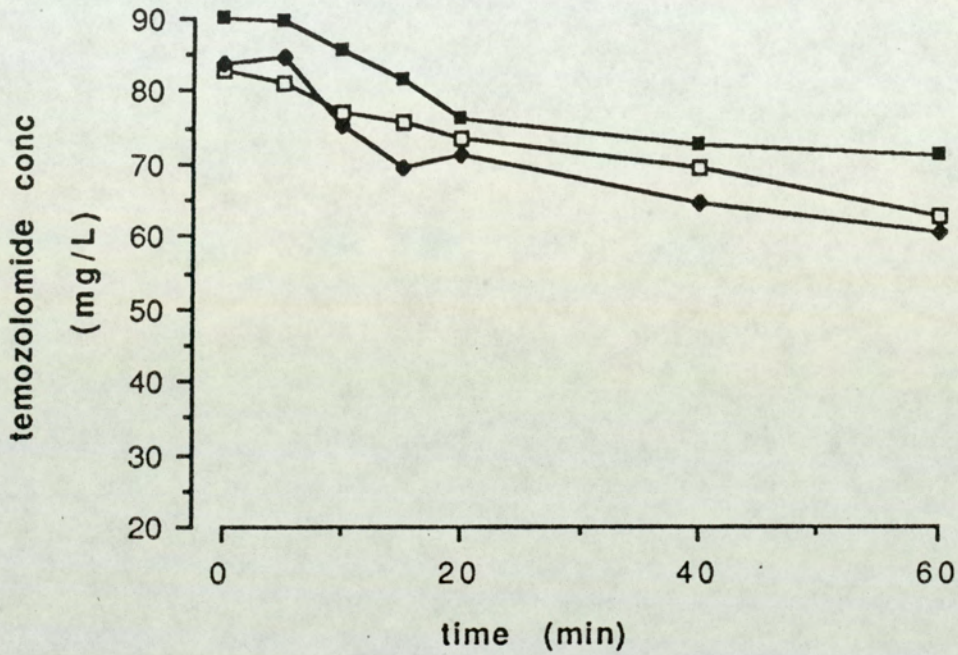


Fig.51 Time course of disappearance of temozolomide in the presence of a) viable microsomes ( $\square$ ), b) boiled microsomes ( $\blacklozenge$ ), c) in phosphate buffer ( $\blacksquare$ ) at 37°C (n=4). C.V. of each data point was less than 10%

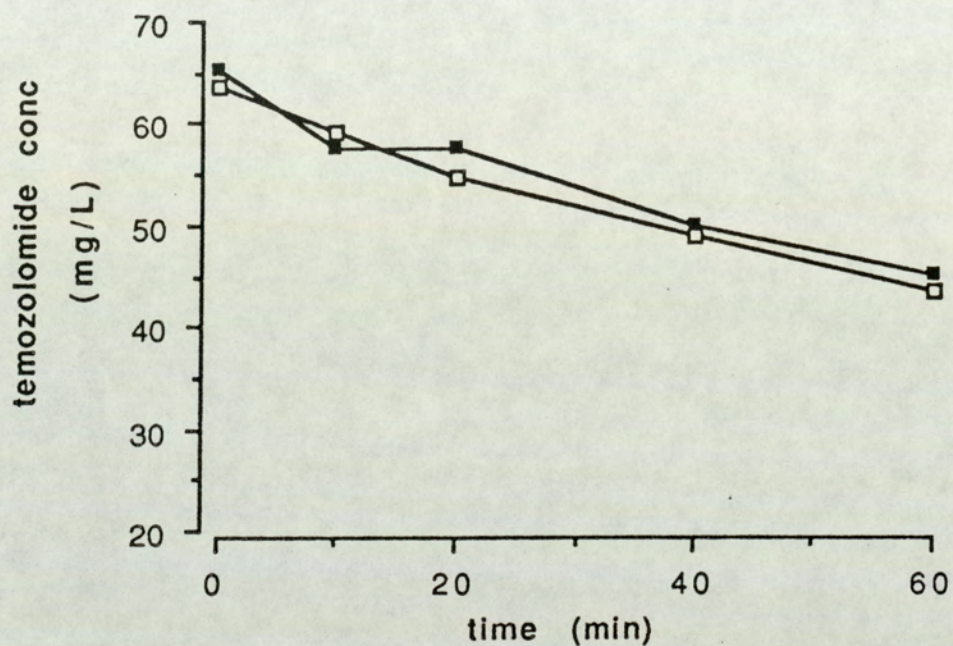


Fig.52 Time course of disappearance of temozolomide in the presence of viable (□) and deactivated (■) post-mitochondrial supernatant fortified with NADPH (n=4). C.V. of each data point was less than 10%

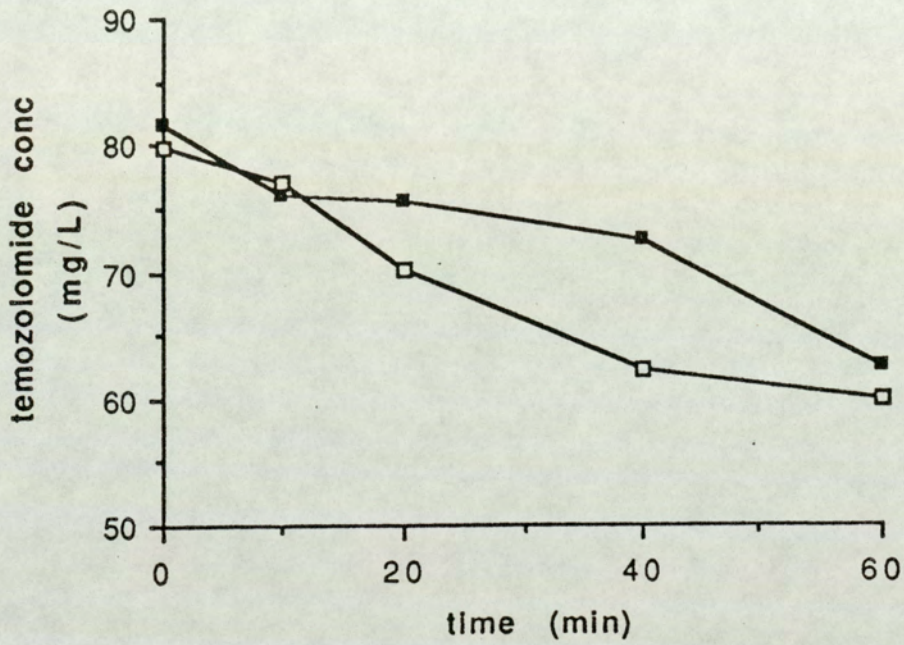


Fig.53 Time course of disappearance of temozolomide in the presence of viable (-□-) and deactivated (-■-) whole liver homogenate fortified with NADPH (n=4). C.V. of each data point was less than 10%

The production of formaldehyde during N-demethylation is conveniently measured by the colorimetric procedure described by Nash (1953). In this study, it was impossible to measure the amount of formaldehyde found during the *in vitro* metabolism of temozolomide possibly because MTIC and diazoIC interfered with the the Nash reagent in that they yielded a yellow colour solution. A speculative mechanism by which triazene could react with Nash reagent has been proposed by M.D. Threadgill (personal communication) and outlined in fig.54.

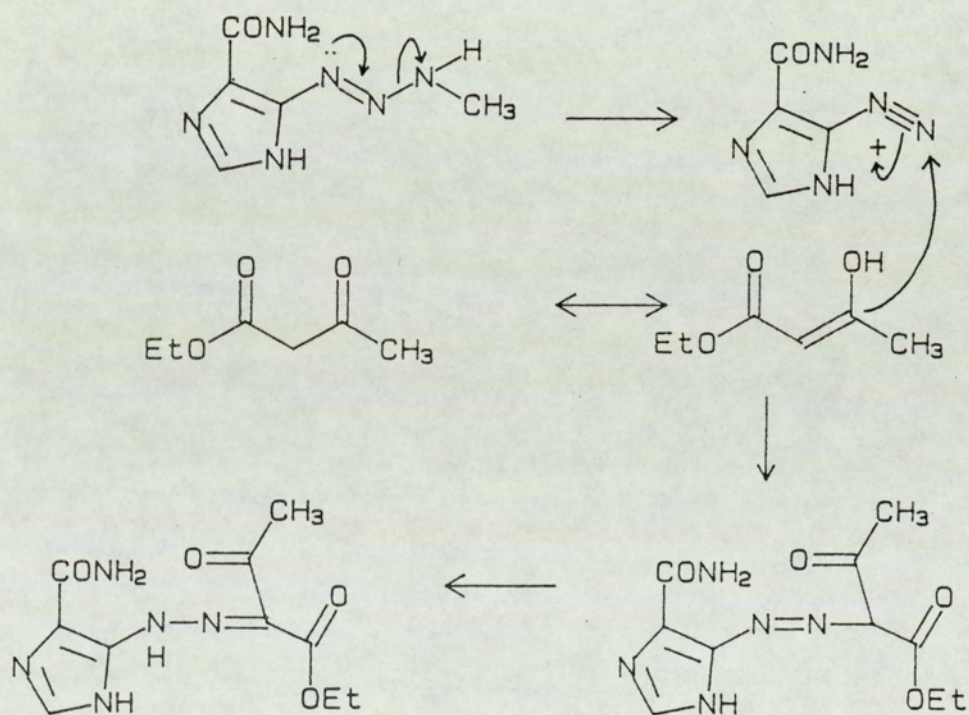


Fig.54 Proposed chemical reaction of MTIC with Nash reagent (Dr. M.D. Threadgill)



Under conditions identical to those described in the case of temozolomide, the incubation of 3-methylbenzotriazinone with microsomes fortified with co-factors produced two metabolites. One of them had the retention time identical to that of benzotriazinone (5min). Figs.57 shows the generation of this metabolite over 60min incubation time. The identity of this metabolite was confirmed by comparison with authentic benzotriazinone using CIMS analysis (fig.59). Benzotriazinone possesses a molecular weight of 147, as shown by the molecular ion  $MH^+148$ . The fragment  $m/z$  120 indicates a loss of 28 mass unit from the molecular ion  $MH^+148$ ; probably as a result of the cleavage of the triazinone ring leading to the loss of  $C=O$  (fig.59). A metabolite, with a retention time of 1.8min was also found in the incubation mixtures. It is apparent that its formation is enzymically catalyzed because the metabolite was not present in the incubations with deactivated microsomes. The identity of this metabolite was elucidated by collecting the eluent from the HPLC for CIMS analysis. As shown in fig.60, the metabolite gave a fragment ion with the highest intensity value 123 identical to benzoic acid. The presence of the fragment ion  $m/z$  106 indicates the loss of a hydroxy group, presumably from the carboxylic acid group. Benzoic acid had a retention time of 8.5min using the same HPLC method, suggesting this metabolite is not benzoic acid. The ion  $m/z$  123 might be a stable fragment of the metabolite on the CIMS. High field NMR analysis was attempted but failed to give an interpretable spectrum due to insufficient

material. No further attempt was made to characterize this metabolite. In all in vitro incubations, other metabolites were not identified when the pH of the incubation mixtures were adjusted to pH 2-3 and re-extracted after the initial extraction at pH 7.4 had been performed. This result implies the absence of phenolic metabolites which may have been ionized at pH 7.4 and thus may not have been removed during the first extraction. The metabolite with a retention time of 1.8min was not extractable into the ethylacetate layer under the acidic condition (fig.56).

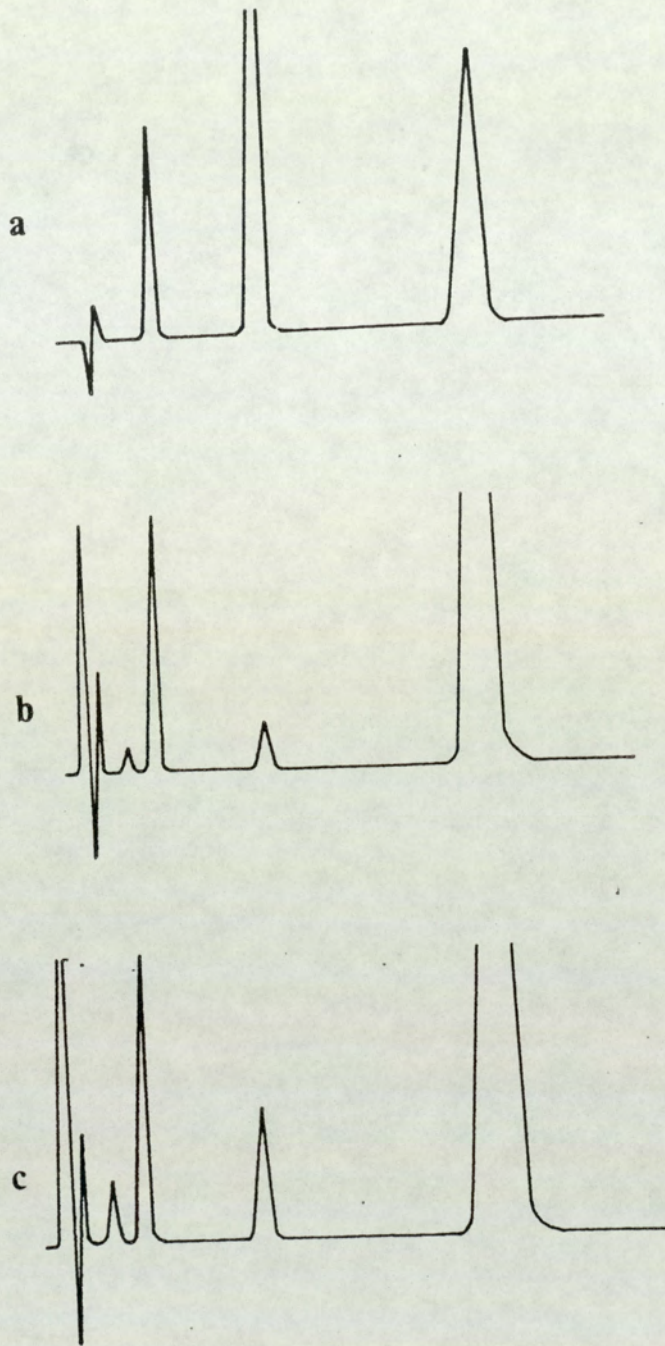


Fig.55 HPLC chromatograms of a) a mixture of standards of benzotriazinones, and of extracts of suspensions of fortified microsomes with 3-methylbenzotriazinone after b) 5min and c) 10min incubation

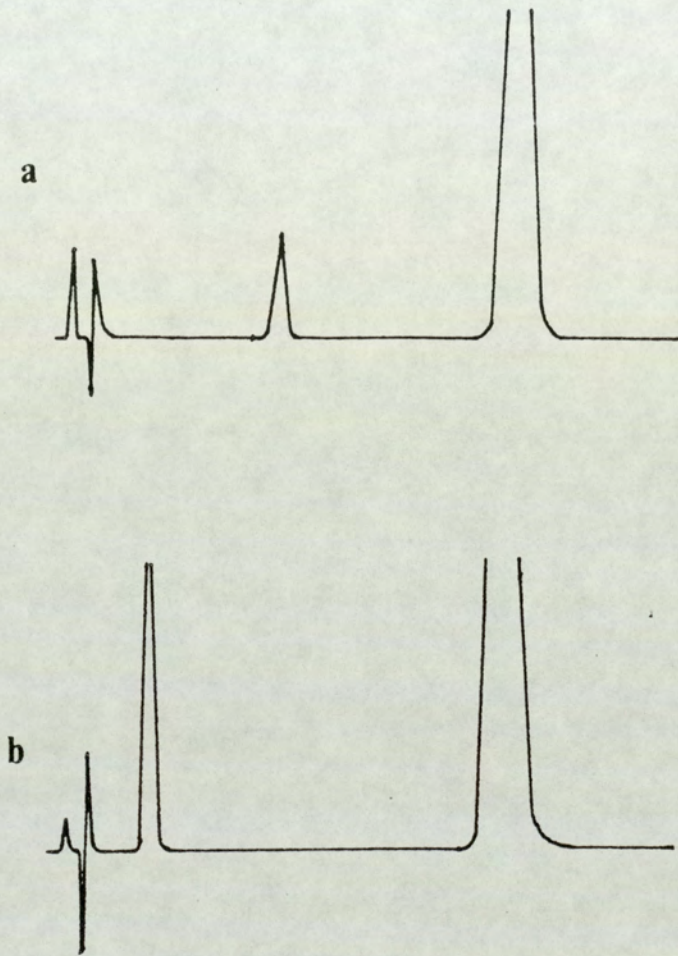


Fig.56 HPLC chromatograms of a) an acidic extract of an incubation of 3-methylbenzotriazinone and b) an incubation of 3-methylbenzotriazinone in the presence of deactivated microsomes

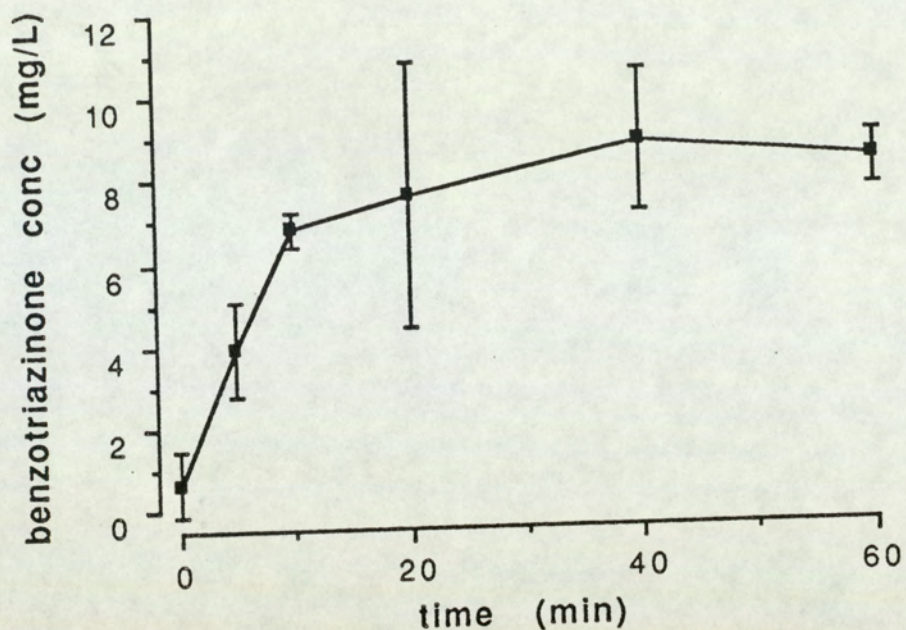


Fig.57 Time course of the metabolic formation of a metabolite from 3-methylbenzotriazinone with a R.T. identical to the authentic benzotriazinone (n=4 ± 1 S.D.)

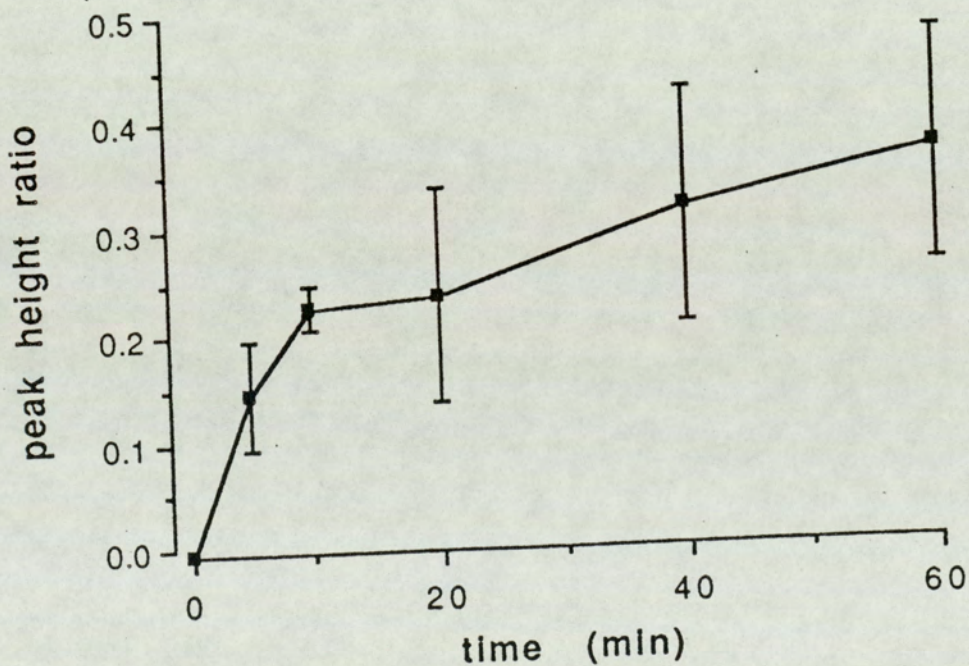


Fig.58 Time course of the metabolic formation of a metabolite from 3-methylbenzotriazinone with a R.T.=1.8min. (n=4 ± 1 S.D.)

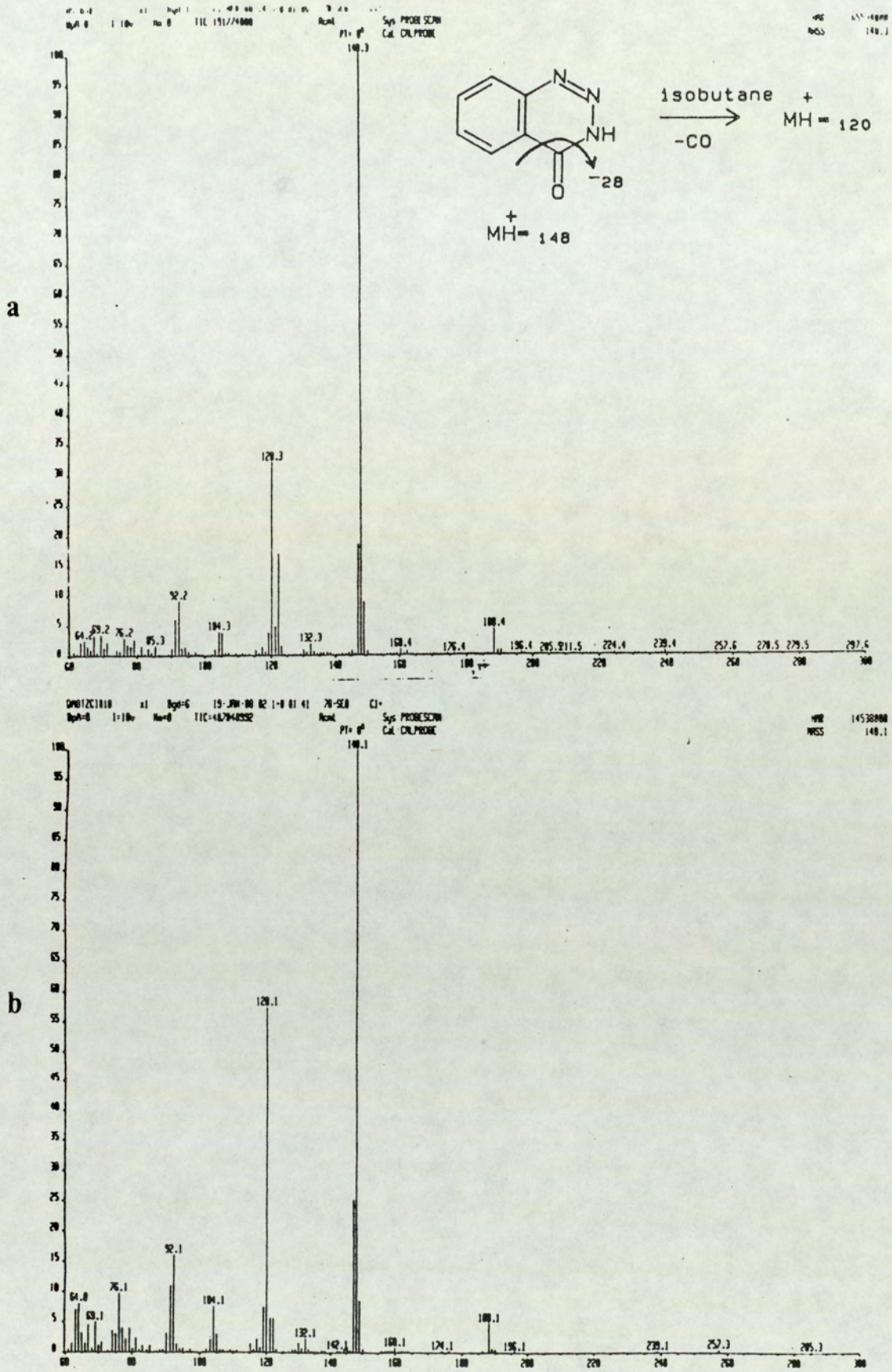


Fig.59 CIMS spectra of a) authentic benzotriazinone and b) the metabolite with an identical R.T. isolated from the microsomal incubations

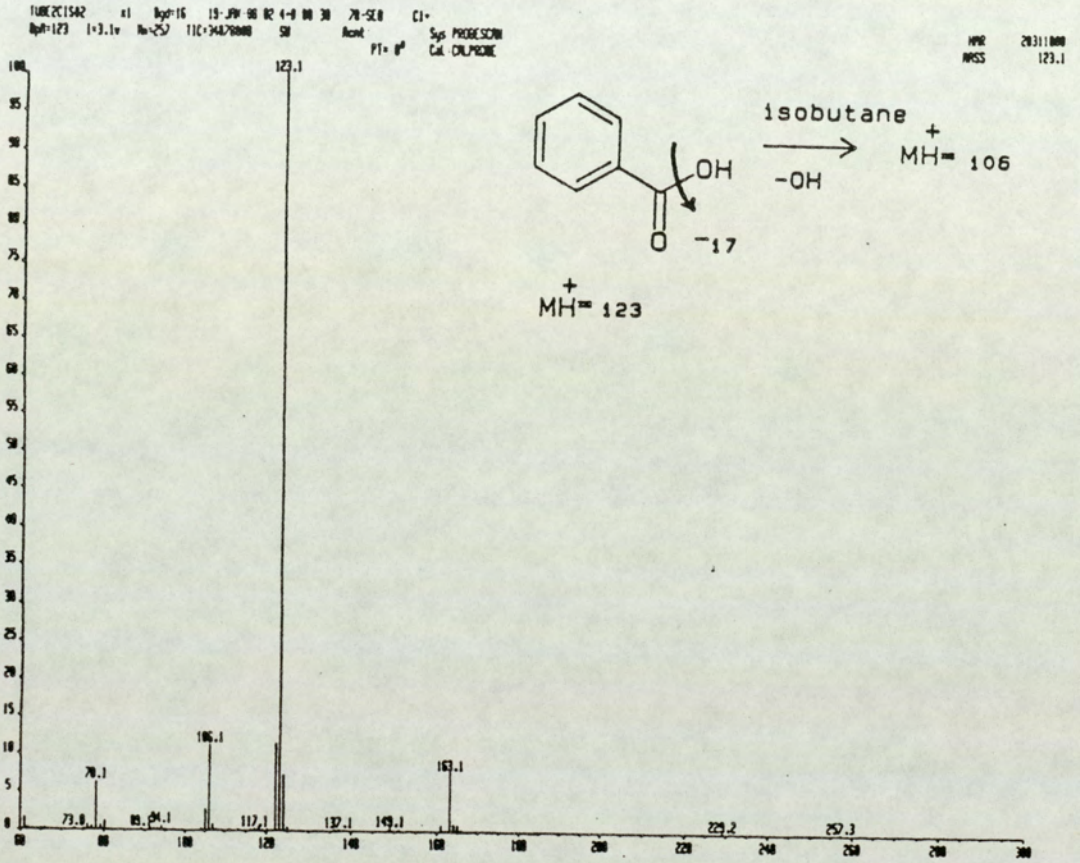


Fig.60 CIMS spectrum of the metabolite with a R.T.=1.8min isolated from the microsomal incubations

### 3.6.3 Discussion

In this study, it was found that temozolomide is not metabolized in vitro by liver fractions and that chemical degradation plays a vital rôle in the in vitro fate of the drug. In contrast, under incubation conditions as the those described for temozolomide, 3-methylbenzotriazinone was metabolized in vitro by microsomal enzymes to afford benzotriazinone, presumably via the unstable intermediate hydroxymethylbenzotriazinone (fig.61). Preliminary experiments have shown that authentic hydroxymethylbenzotriazinone was not stable in aqueous medium and readily decomposes to form benzotriazinone. Therefore, it is conceivable that the hydroxymethyl species generated as a result of initial hydroxylation of the methyl carbon undergoes the same reaction in vitro. The mechanism possibly involves the transfer of the hydroxyl proton to the carbonyl oxygen via a six membered cyclic transition state resulting in the elimination of formaldehyde (fig.61), a mechanism which has been proposed previously by Ross et al (1983) and Tanaka et al (1972).



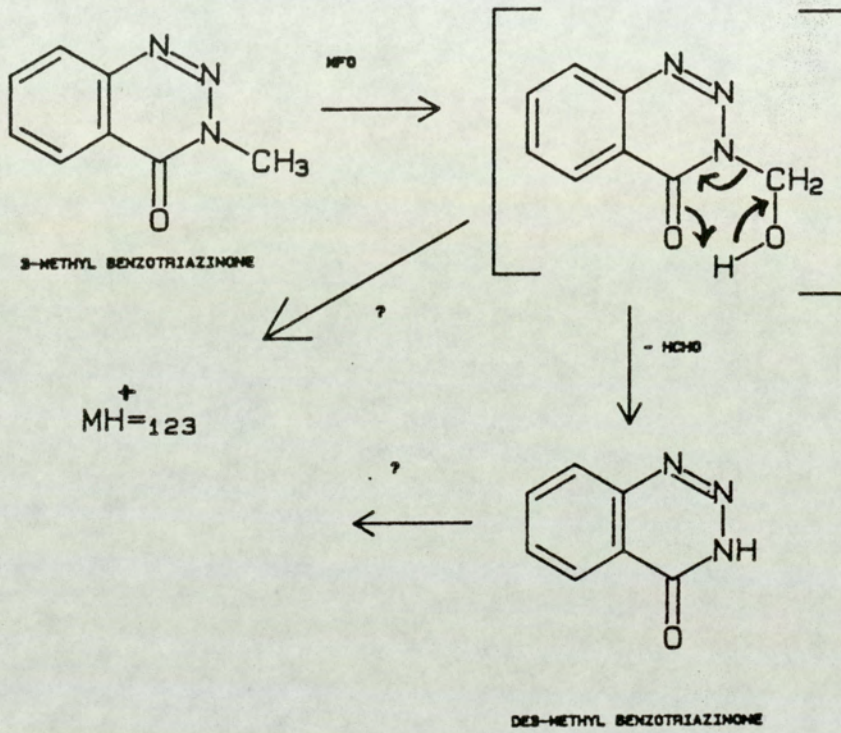


Fig.61 Proposed metabolic pathway of 3-methylbenzotriazinone

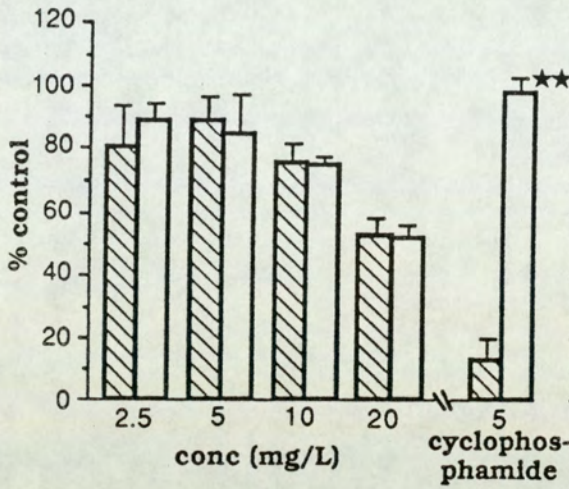
### 3.7.1 In vitro cytotoxicity bioassay in the presence of liver microsomes

The in vitro cytotoxicity bioassay used in this study was a modification of that devised by Dolfini et al (1973) and Horspool (1988) (see section 2.9). This bioassay is designed to test if a compound undergoes bioactivation mediated by the liver mixed function oxygenases. In this case, the bioassay was performed using temozolomide, DTIC, HMMTIC and MTIC as substrates. Fig.62a shows the results of the cytotoxicity bioassay of temozolomide in the presence of microsomes. Cyclophosphamide was used as the positive control in all experiments. It was shown that an incubation of the cells with temozolomide and microsomes did not result in a significant difference in inhibitory effect on cell growth when compared with the the cells incubated without microsomes. Cyclophosphamide was activated by microsomes causing a decrease in cell number by 87±7% (fig.62). Incubating temozolomide with the 10,000g supernatant resulted in a significant decrease in cytotoxicity when compared with cells treated with the drug in the absence of the 10,000g supernatant (fig.63). The likely explanation for the decrease in cytotoxicity is that the toxic metabolites of cyclophosphamide and temozolomide are inactivated by glutathione or proteins in the cytosolic fraction. The results presented here show unambiguously that temozolomide does not undergo metabolism in vitro by liver fractions to generate a more cytotoxic species.

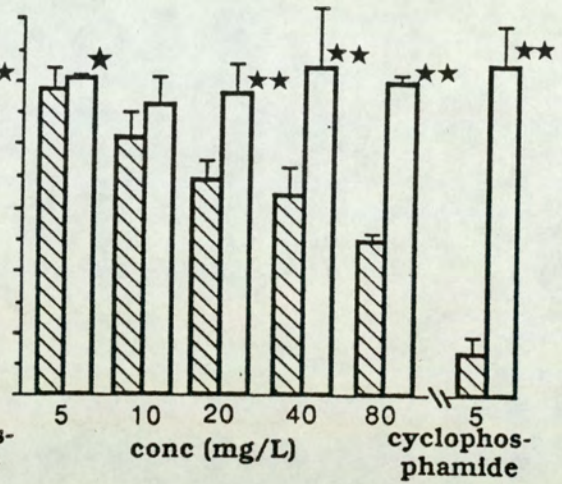
Unlike temozolomide, DTIC requires metabolism to exert its antineoplastic activity in vitro. In the absence of

microsomes, DTIC was not toxic but in their presence, DTIC brought about a significant decrease in cell growth in a concentration-dependent manner (fig.62). In addition, like cyclophosphamide, the cytotoxicity of DTIC towards TLX5 cells was an NADPH-dependent reaction (fig.65). This result strongly suggests the involvement of hepatic mixed function oxygenases (MFO) in the bioactivation of DTIC and cyclophosphamide (fig.64) because during MFO reaction, reducing equivalents derived from NADPH and H<sup>+</sup> are required to catalyze the hydroxylation reaction (Gibson and Skett, 1986). The metabolites of DTIC, namely HMMTIC and MTIC do not require metabolic activation to exert their antineoplastic action in vitro. These results seem to suggest HMMTIC is either active itself or may be a stable prodrug of MTIC- that is, upon chemical decomposition, MTIC is generated with the concomitant release of formaldehyde (see sections 1.2.2 and 3.8). As outlined earlier, Farina et al (1982 and 1986) suggested that 1-(4-acetyl-phenyl)-3-methyltriazene was metabolized and possibly bioactivated by liver monooxygenases. On the basis of the results obtained in this study, it seems that the hypothesis postulated by Farina et al (1982,1986) does not hold true for the monomethyltriazene, i.e. MTIC, used in this study.

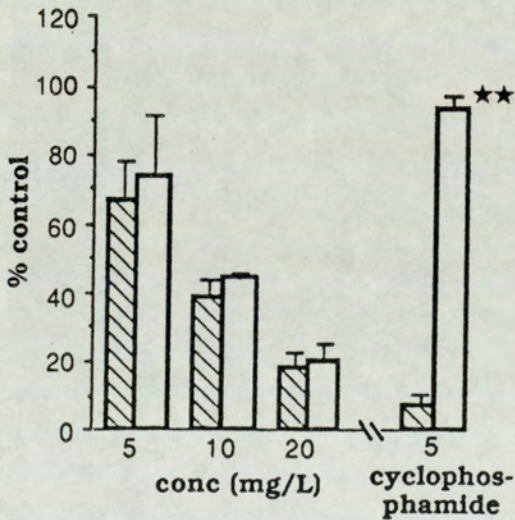
**A.**  
**EFFECT OF TEMOZOLOMIDE**  
**ON TLX5 CELL GROWTH**



**B.**  
**EFFECT OF DTIC ON**  
**TLX5 CELL GROWTH**



**C.**  
**EFFECT OF HMMTIC ON**  
**TLX5 CELL GROWTH**



**D.**  
**EFFECT OF MTIC ON**  
**TLX5 CELL GROWTH**

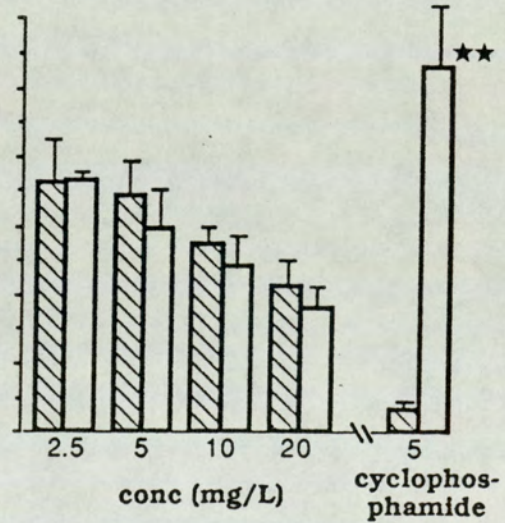
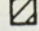
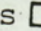


Fig.62 Cytotoxicity of A) temozolomide, B) DTIC  
C) HMMTIC, D) MTIC against TLX5 lymphoma cells  
in the presence  and absence of microsomes   
(n=4-16  $\pm$  1 S.D.). \* p<0.05, \*\* p<0.001

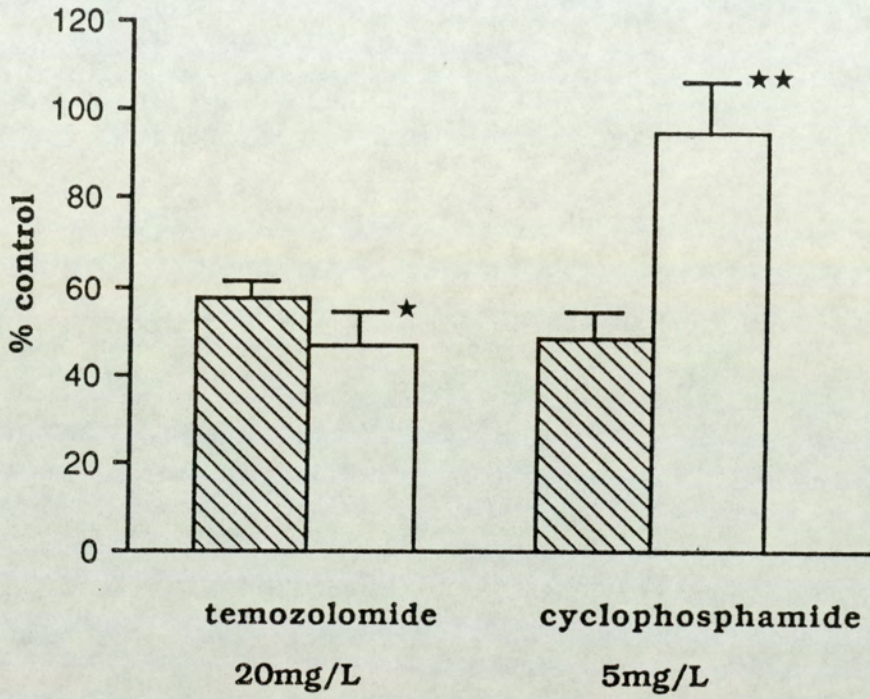


Fig.63 Cytotoxicity of temozolomide and cyclophosphamide against TLX5 lymphoma cells in the presence (▨) and absence (□) of post-mitochondrial supernatant (n=8 ± 1 S.D.). ★ p<0.05, ★★ p<0.001

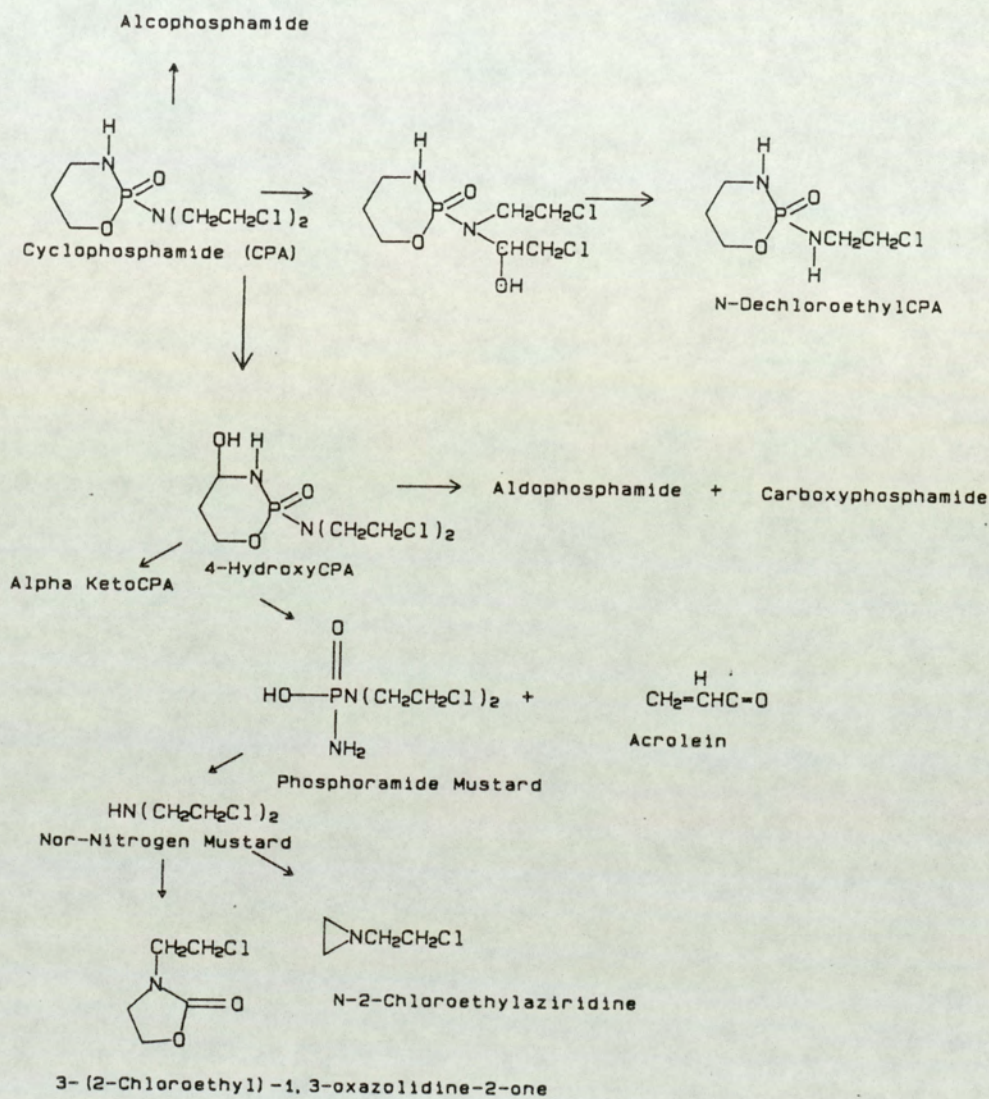


Fig.64 Proposed metabolic pathway of cyclophosphamide (De Bruijn et al, 1987)

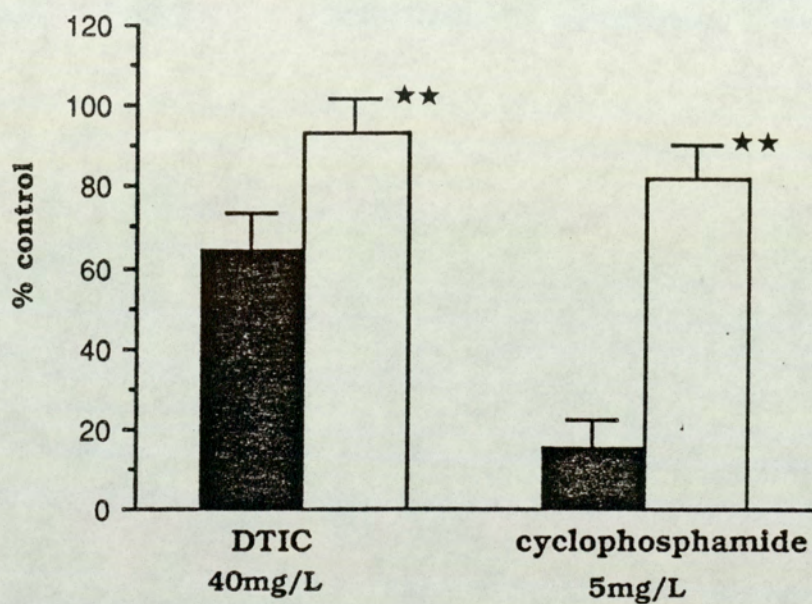


Fig.65 Cytotoxicity of DTIC and cyclophosphamide against TLX5 lymphoma cells in the presence (■) and absence of NADPH (□). \*\* p<0.001

### 3.7.2 In vitro cytotoxicity of formaldehyde towards TLX5 cells

The oxidative metabolism of N-methyl compounds leads ultimately to the generation of formaldehyde. Formaldehyde is mutagenic (Rapoport, 1946; Auerbach et al, 1977) and carcinogenic (Nature, 1979; Swenberg et al, 1980). Furthermore, it has been shown that formaldehyde is cytotoxic in vitro towards the murine L1210 leukaemia, causes DNA strand-breaks and DNA-protein cross links (Ross et al, 1980). The metabolically-generated release of formaldehyde has been implicated in the antitumour activity of some N-methyl antineoplastic agents (Rutty and Connors, 1977; Rutty and Abel, 1980). It was, therefore, thought that the increase in cytotoxicity of DTIC observed in the presence of microsomes and co-factors may be at least in part due to the production of formaldehyde generated as the product of the oxidation of one of the N-methyl groups. In order to test this hypothesis, the cytotoxicity of formaldehyde towards TLX5 cells was evaluated. The experimental protocol was identical to that conducted in section 3.7.1. Formaldehyde was generated in situ by treatment of paraformaldehyde with NaOH. The concentration of formaldehyde present was established by using a colorimetric method based on that by Nash (1953)(see section 2.6.3). As seen in fig.66, the growth of cells was not affected by exposure to formaldehyde up to 132 $\mu$ M: this is a concentration higher than that would be theoretically achievable when 20-25% of DTIC at 80mg/L was metabolized. This result suggests that formaldehyde does not cause the



increased cytotoxicity of DTIC when incubated with microsomes.

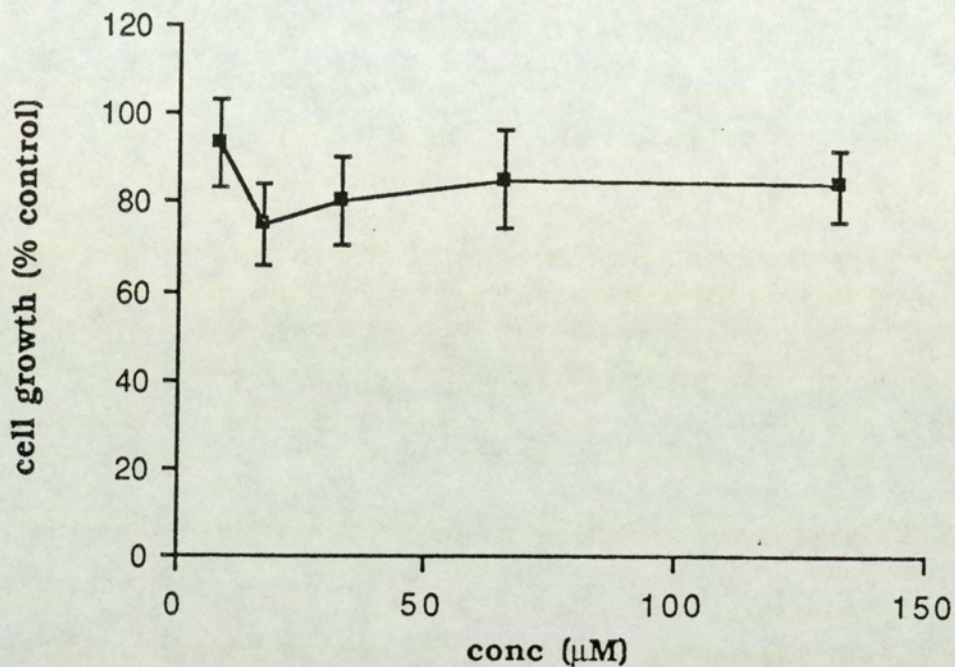


Fig.66 Effect of formaldehyde on TLX5 lymphoma cell growth

### 3.7.3 Discussion

The use of this in vitro model system provides some useful information of cytotoxicity of drugs which require metabolic activation by hepatic mixed function oxygenases. However, the use of this in vitro model is open to criticism because there are often other metabolic processes in vivo which are not present in vitro. In the present study, it is clearly demonstrated that temozolomide, MTIC and HMMTIC do not require bioactivation to exert their antineoplastic activity in vitro. DTIC, in contrast, is metabolically activated to a cytotoxic species in vitro. In addition, the cytotoxicity of DTIC, when incubated with hepatic microsomes, cannot be accounted for by the production of formaldehyde. It has been postulated HMMTIC and MTIC are the products of metabolism of DTIC (see introduction 1.2.2). Therefore, it is likely that these metabolites are produced in vitro. Since HMMTIC and MTIC are cytotoxic species in their own right, it could be via either one or both of these compounds DTIC exerts its cytotoxicity in vitro. The result obtained in this study concerning DTIC broadly concurs with that obtained by Metelmann and Von Hoff (1983). In that study, the authors used L1210, B16 and human malignant melanoma cells to evaluate the cytotoxicity DTIC in the presence of microsomes as determined by colony formation. In the presence of microsomes and co-factors, it was found that DTIC caused a decrease in formation of colonies by more than 10% (L1210), 11% (B16) and 26% (human malignant

melanoma) at a concentration 1µg/ml. Light was apparently not excluded in that study. It seems that DTIC appears to be more cytotoxic towards these cells than TLX5 cells or alternatively the observed cytotoxicity is a composite effect of microsomal activation and light, which was excluded in the work described here. The results described above suggest that temozolomide exerts its antineoplastic activity via MTIC, and the identification of this species was attempted to support this contention.

### 3.8 In vitro metabolism studies

In this part of the thesis, the hypothesis was tested, by HPLC methods (see section 2.4.2), that MTIC is responsible for the in vitro cytotoxicity of DTIC and temozolomide. Fig.67 shows the HPLC chromatogram of an extract of the products of the microsomal incubation of temozolomide. One of the peaks was unchanged temozolomide. In addition, a peak had a retention time identical to that of authentic MTIC was present on the chromatogram. MTIC was also found in the incubations omitting microsomes. Figs.68a&b show the time course of degradation of temozolomide and production of MTIC. The  $t_{1/2}$  of temozolomide obtained in this study was in agreement with that obtained in the chemical stability studies (see section 3.4). The AUC, calculated by trapezoidal rule, of temozolomide (20mg/L) in the presence and absence of microsomes were  $990 \pm 97$  and  $1026 \pm 30$  mg.min/L respectively. The AUC of MTIC produced over 60min incubation time were  $67 \pm 9$  mg.min/L in the presence of microsomes and  $73 \pm 10$  mg.min/L in the absence of microsomes. Since the rate of degradation of temozolomide, and the AUC of temozolomide and generated MTIC were identical under both conditions, the generation of MTIC from temozolomide seems to be chemically mediated.

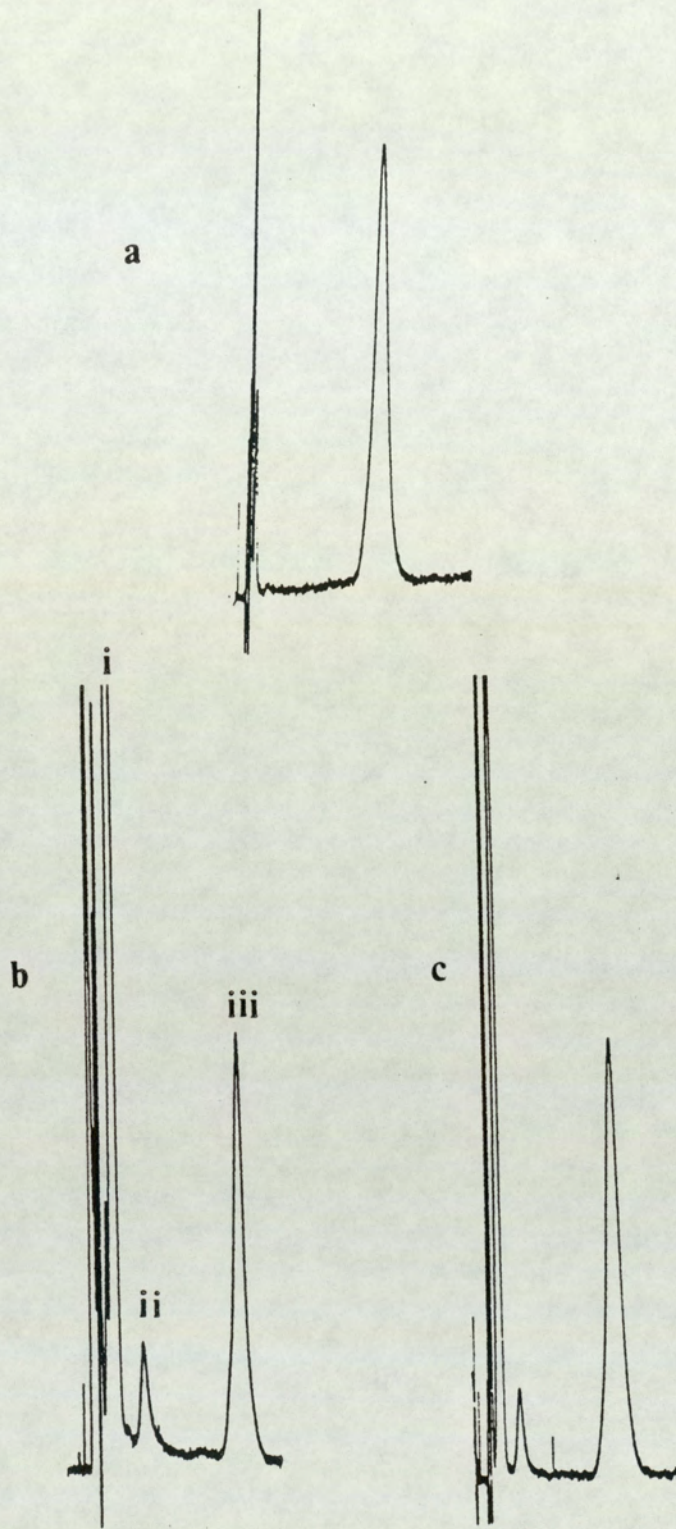


Fig.67 HPLC chromatograms of a microsomal incubation a) omitting, b) in the presence of temozolomide (20mg/L), c) of an incubation of temozolomide in the absence of microsomes. i) temozolomide, ii) MTIC and iii) internal standard

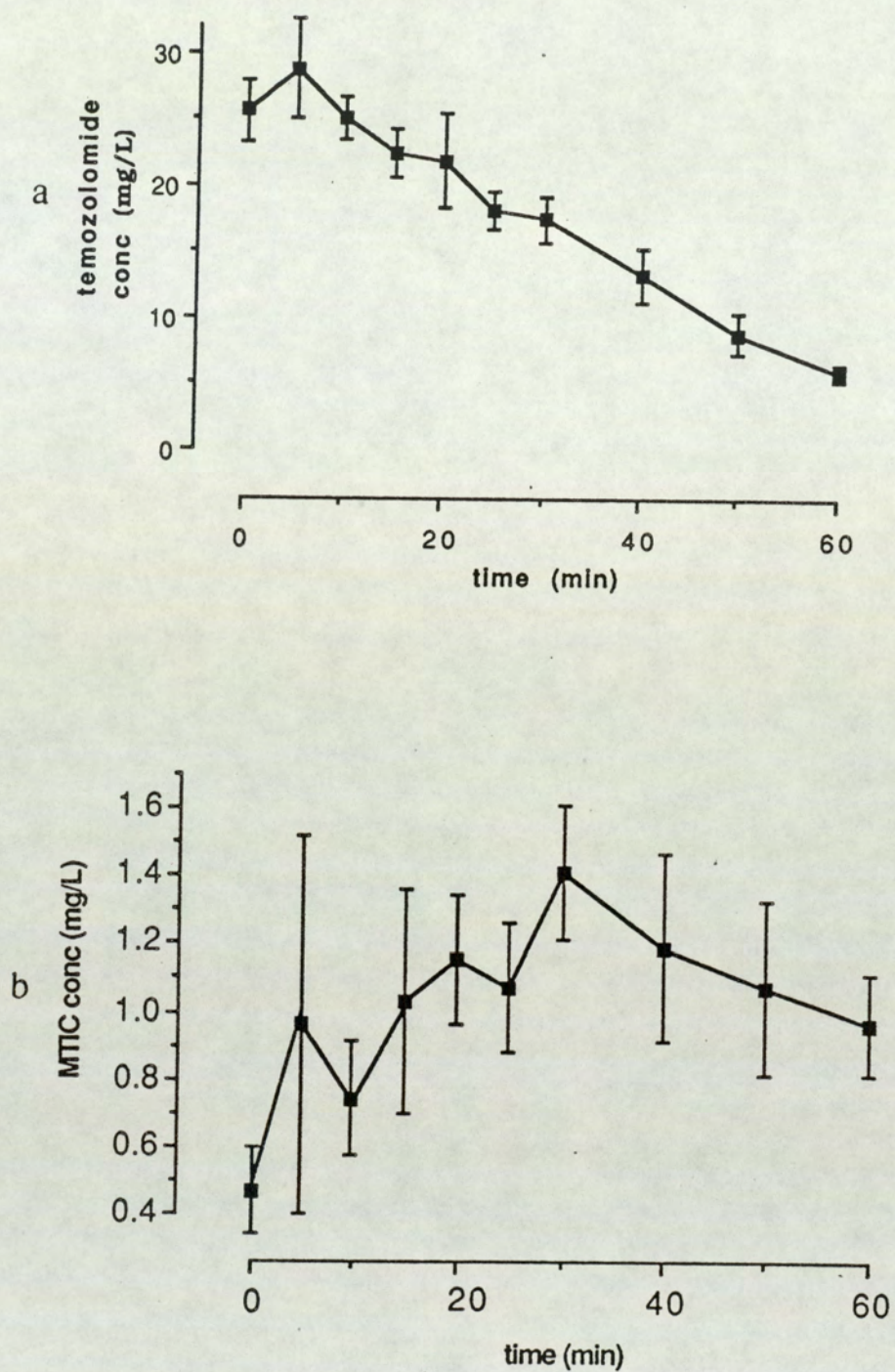


Fig.68 Time course of the disappearance of a)temozolomide b) and the appearance of MTIC in the presence of microsomes (n=4  $\pm$  1 S.D.)

Analysis of microsomal incubation mixtures of DTIC afforded three peaks (fig.69), one of which co-eluted with unchanged DTIC. Another two co-eluted with HMMTIC and MTIC. The production of these metabolites was dependent upon the presence of O<sub>2</sub> and NADPH. Fig.70 shows the time course for the production of MTIC using mouse and human microsomes. The AUC of MTIC produced from DTIC (40mg/L) were 11<sub>±</sub>2 mg.min/L/mg of microsomal protein (108<sub>±</sub>19 mg.min/L) and 7<sub>±</sub>1 mg.min/L/mg of microsomal protein (78<sub>±</sub>6 mg.min/L) respectively in mouse and human microsomal incubations. The data presented here indicates that mouse microsomal enzymes might be more efficient in catalyzing N-demethylation in comparison with human preparations. Certainly, more experiments are required to support this contention. Nevertheless, these results are broadly in agreement with the in vivo data obtained by Ruddy et al (1981).

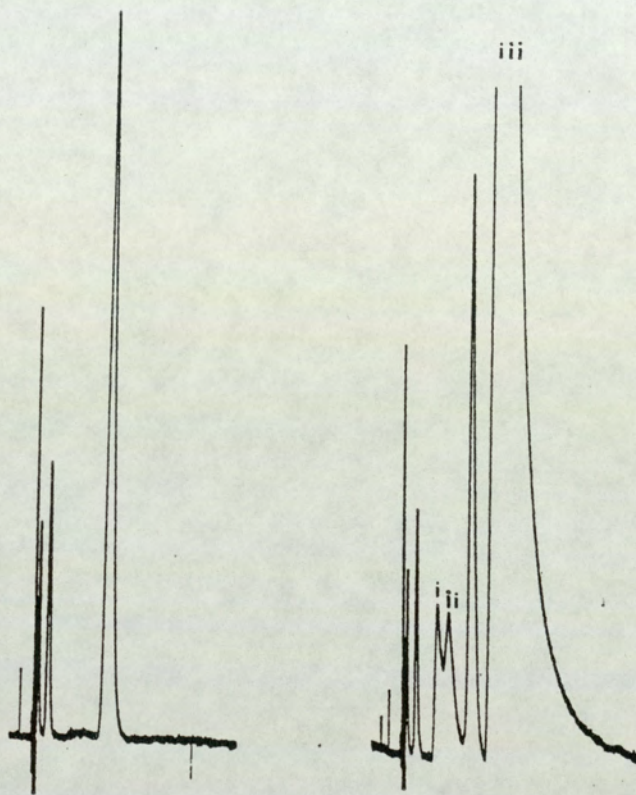


Fig.69 HPLC chromatograms of a microsomal incubation  
a) omitting, b) in the presence of DTIC (iii)  
(40mg/L) showing the presence of HMMTIC (ii)  
and MTIC (i)



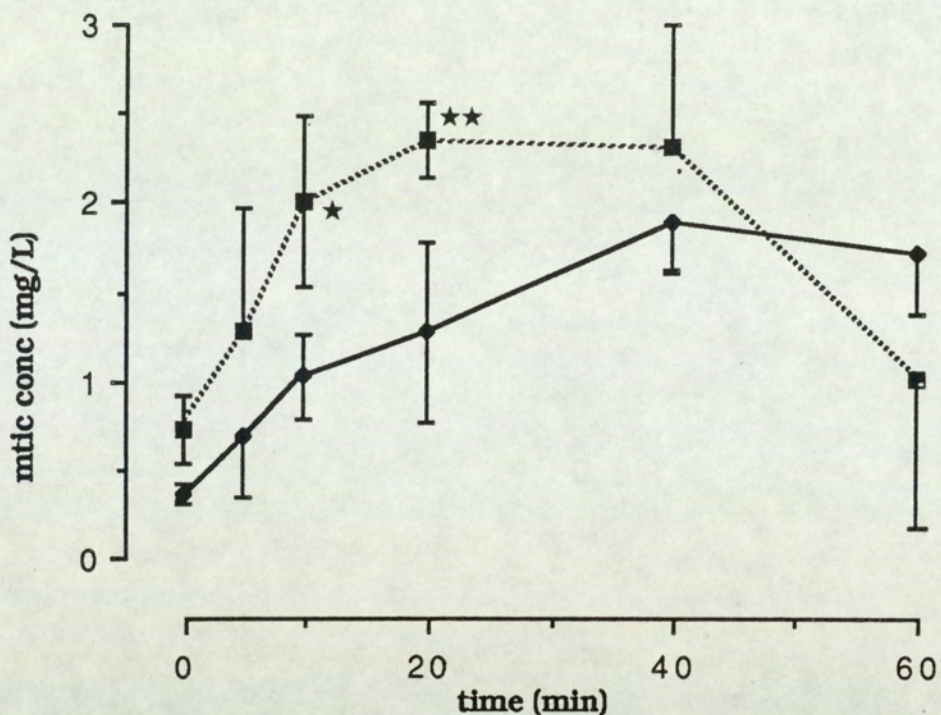


Fig.70 Time course of the metabolic formation of MTIC from DTIC in the presence of mouse (■) and human (●) microsomes (n=4 + 1 S.D.).  
 \* p < 0.05, \*\* p < 0.01

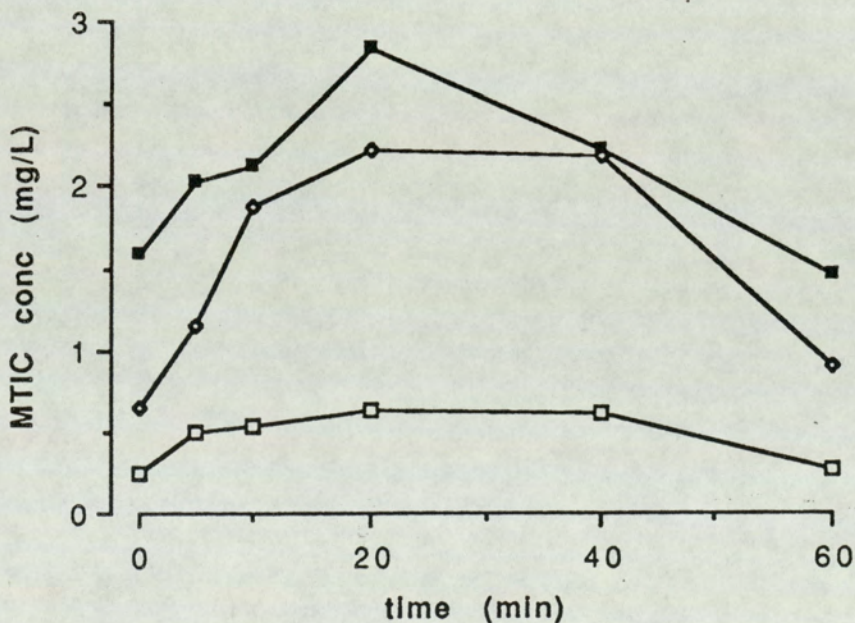


Fig.71 Time course of the metabolic formation of MTIC from DTIC at different substrate concentrations 20mg/L (□), 40mg/L (○), 80mg/L (■) (n=4). C.V. of data point was less than 28%

Incubation HMMTIC in tissue culture medium afforded two peaks which co-eluted with MTIC and HMMTIC. Fig.72b shows the time course of production of MTIC from HMMTIC and fig.72a shows the degradation of HMMTIC. The  $t_{1/2}$  of HMMTIC in tissue culture medium was  $16 \pm 2$ min.

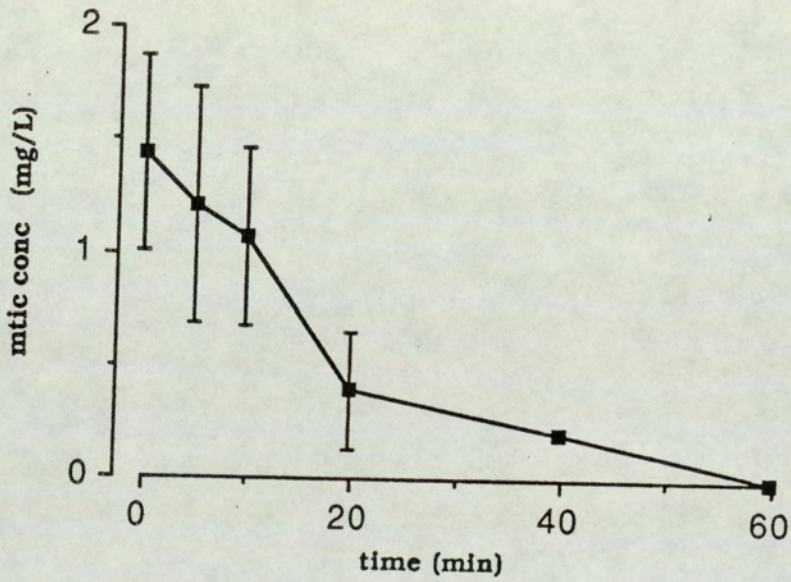
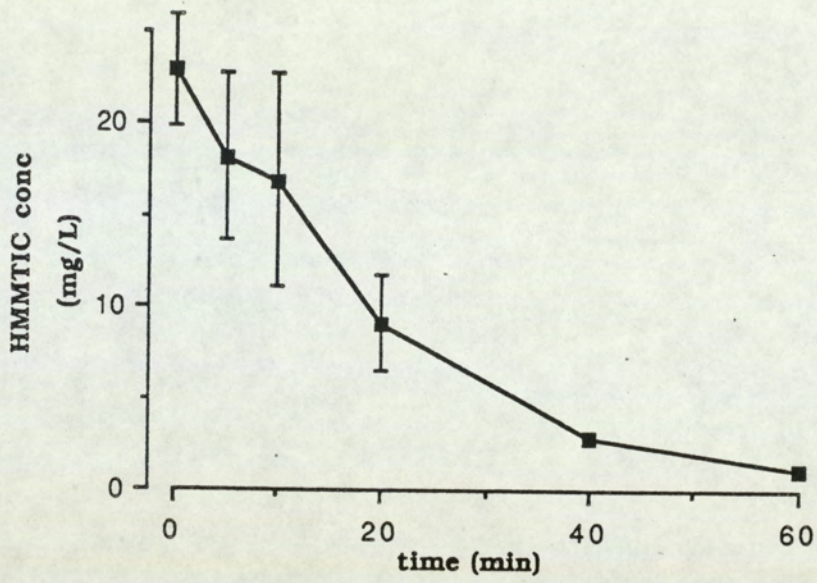


Fig.72 Time course of the a) disappearance of HMMTIC and b) appearance of MTIC (n=4  $\pm$  1 S.D.)

The metabolism of MTIC was also studied in the presence and absence of microsomes. The disappearance of the substrate in microsomal incubations was monitored up to 20min and compared with that in incubations without microsomes. MTIC readily decomposed in the incubation medium with a  $t_{1/2}$   $5.5 \pm 0.5$ min and no MTIC was detectable after 15min (fig.73). The rate of degradation of MTIC in the presence of viable microsomes was not significantly different from that in the absence of viable microsomes. In addition, the AUC of MTIC (20mg/L) in the presence and absence of microsomes were respectively  $129.2 \pm 4$  and  $125 \pm 10$  mg.min/L. These results show that MTIC is not a substrate for metabolism in vitro.

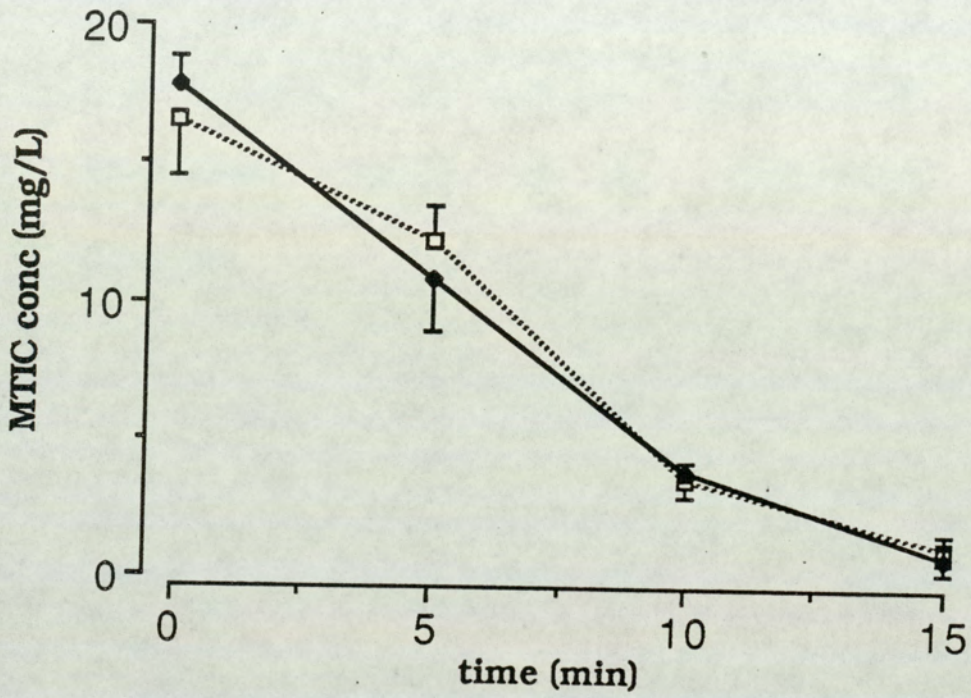
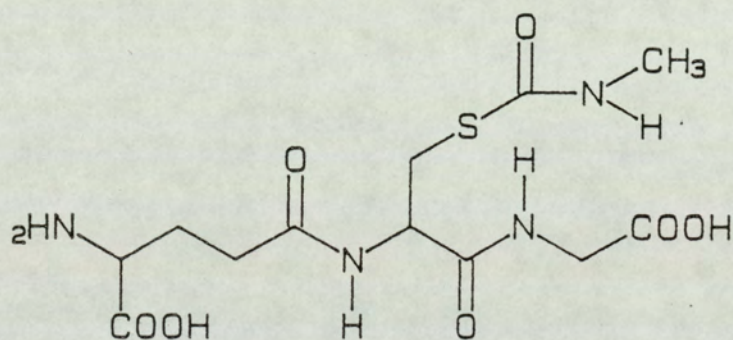


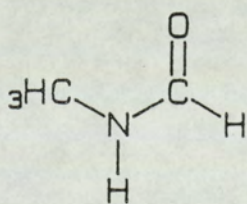
Fig.73 Time course of the disappearance of MTIC in the presence ( □ ) and absence ( ● ) of microsomes (n=4 ± 1 S.D.)

### 3.8.1 Investigation of the release methyl isocyanate from temozolomide

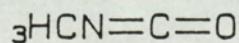
As outlined in the introduction, cleavage of the 2,3 and 4,5 bonds of temozolomide would generate methyl isocyanate, which has been implicated in the cytotoxicity of nitrosoureas, such as CCNU and BCNU towards TLX5 lymphoma cells (Gibson and Hickman, 1979). Methyl isocyanate has been postulated as a reactive hepatotoxic intermediate of experimental antitumour agent N-methylformamide in mouse hepatocytes (Shaw et al, 1988 and Shaw, 1988), presumably by its ability to carbamoylate intracellular proteins. Its glutathione conjugate,



**a** S-(N-methylcarbamoyl)glutathione



**b** N-methylformamide



**c** Methyl isocyanate

Fig.74 Structure of a) S-(N-methyl-carbamoyl)-glutathione, b) N-methylformamide and c) methyl isocyanate

S-(N-methylcarbamoyl)glutathione, has been synthesized (Threadgill et al, 1987; Han et al, in preparation). It was found that this conjugate was cytotoxic towards TLX5 cells and hepatocytes, perhaps due to its ability to liberate methyl isocyanate (Han et al). Segal et al (1989) have shown that methyl isocyanate can form methylcarbamoyl adducts with adenine and cytosine; moreover, the reaction of methyl isocyanate with calf thymus DNA yielded N<sup>4</sup> methylcarbamoyl adduct with cytosine (Segal et al, 1989). In view of the potent toxicity of methyl isocyanate, the hypothesis was tested if methyl isocyanate is generated chemically from temozolomide. The experimental set-up was a modification of that reported by Newman and Farquhar (1987). Methyl isocyanate was derivatized and measured as N-methyl propyl carbamate by GC.

Experiments were conducted using caracemide (NSC-253272), a compound known to generate methyl isocyanate (Newman and Farquhar, 1987) as a positive control.

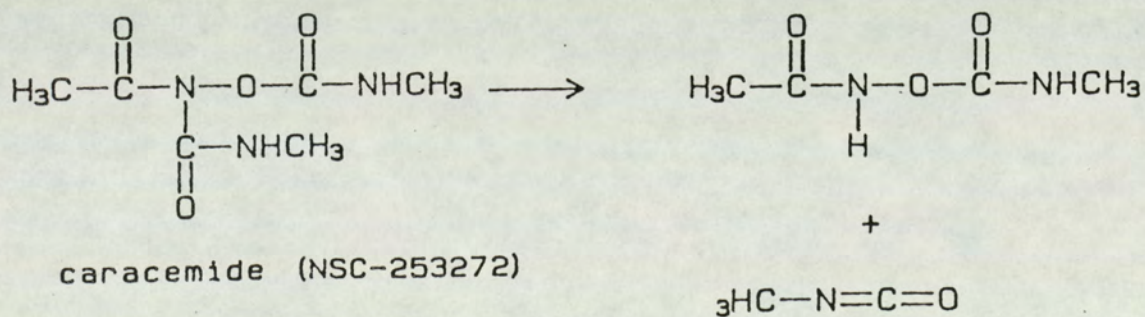


Fig.75 Proposed chemical generation of methyl isocyanate from caracemide (NSC-253272)

Indeed, after incubating with phosphate buffer for 30min, methyl isocyanate was formed from caracemide (20mM). The concentration of substrate used in these experiments was high in order to increase the detectability of reactive methyl isocyanate. Under identical incubation conditions, temozolomide did not liberate methyl isocyanate (fig.76). The results presented here establish that methyl isocyanate is unlikely to be a product of the chemical degradation of temozolomide.



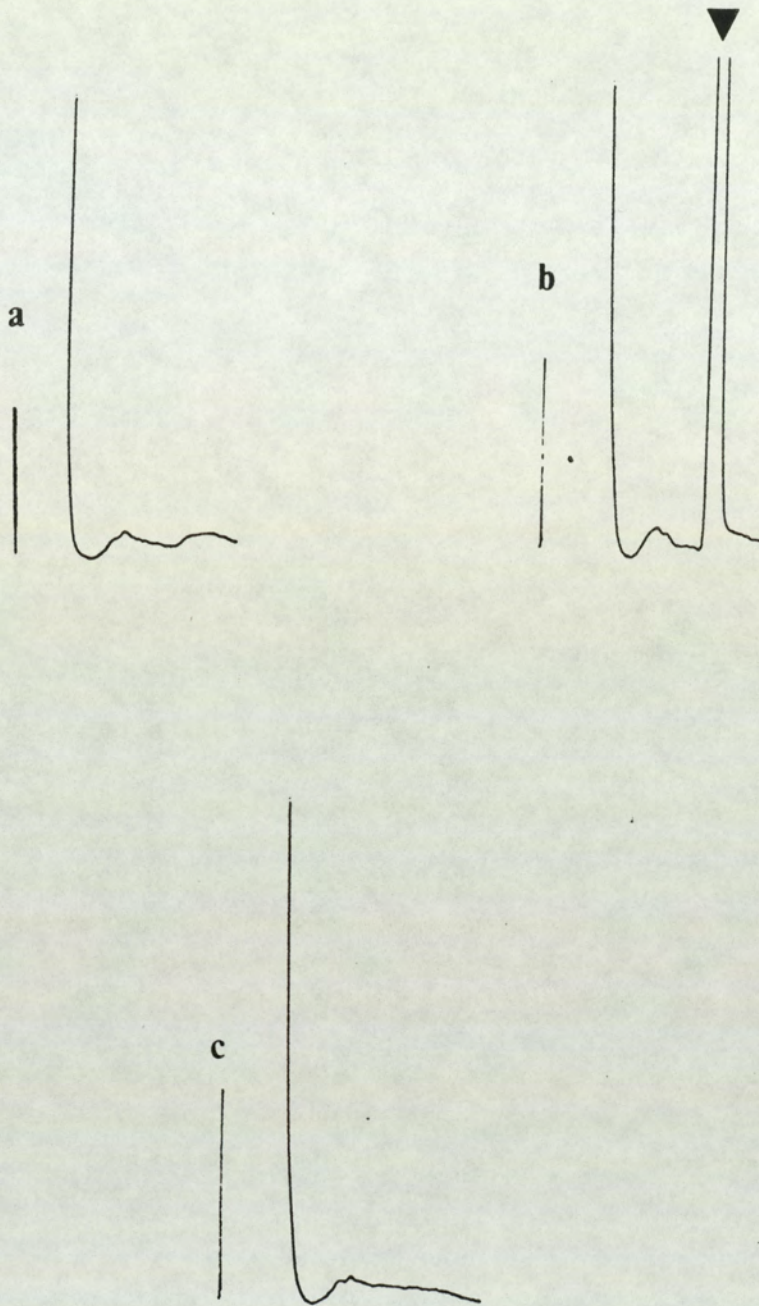


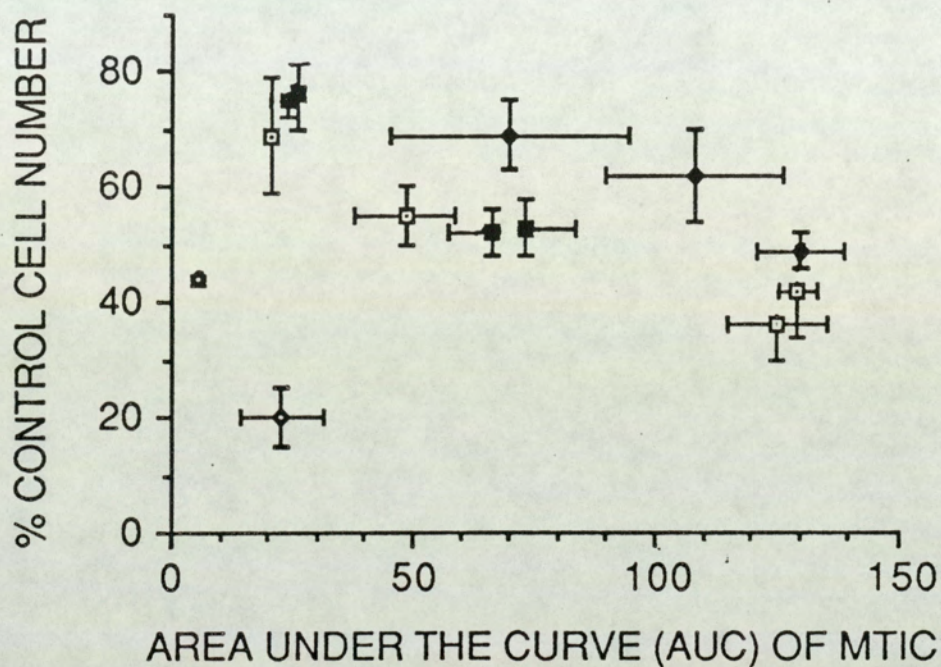
Fig.76 GC chromatograms of an incubation of a) DMSO  
b) caracemide (20mM) and c) temozolomide (20mM)  
The arrow indicates the presence of a carbamoylating species

### 3.8.2. Discussion

The formation of MTIC from DTIC, temozolomide and HMMTIC was determined in mixtures incubated for periods of 60min under conditions identical to those used in the bioassay (section 2.7 and 3.7).

The results presented here establish that MTIC is formed from DTIC, temozolomide and HMMTIC. In the case of DTIC, MTIC is formed only in the presence of viable microsomes fortified with co-factors whilst in the case of temozolomide or HMMTIC, MTIC is liberated by chemical degradation. The AUC for temozolomide and MTIC either in the presence and absence of microsomes were not significantly different, indicating that the release of MTIC was a chemical process. It has been postulated that temozolomide is a stable prodrug of labile monomethyltriazene MTIC (Stevens, et al, 1987). Indeed, this study leaves no doubt that MTIC is generated from temozolomide upon chemical degradation. In addition, methyl isocyanate is unlikely to be a product of chemical degradation; this result is congruent with the biochemical studies conducted on mitozolomide (Horgan and Tisdale, 1984). In that study, it was shown that glutathione reductase, chymotrypsin and gamma-glutamyltranspeptidase were not inhibited by mitozolomide, suggesting an absence of carbamoylating species. The extent of generation of MTIC either chemically from temozolomide or metabolically from DTIC corresponds to the degree of cytotoxicity seen with the equivalent amount of MTIC incubated on its own (fig.77). Furthermore, MTIC is not a substrate for further

metabolic activation. One can therefore argue that it is via MTIC that temozolomide and DTIC exert their cytotoxicity at least in vitro. However, there is no correlation between the extent of MTIC formed from HMMTIC with its in vitro cytotoxicity, indicating that MTIC alone cannot be accounted for the cytotoxicity of HMMTIC in vitro. It has been suggested by some workers that N-(hydroxymethyl) compounds may be the ultimate or proximate cytotoxic metabolites of dimethyltriazenes (Vaughan et al, 1984). Certain N-(hydroxymethyl)-amines and -amides related to N-(hydroxymethyl)-N-methyltriazenes have the ability to form potentially toxic electrophilic imines or iminium ions either themselves or after conjugation (reviewed by Overton et al, 1985) (fig.78). The difference between the cytotoxicity of hydroxymethyl-methyltriazenes and monomethyltriazenes may be due to that hydroxymethyl-methyltriazenes, in theory, are capable of forming an iminium ion (Soloway et al, 1983; Hemens et al, 1984)). However, there is no previous evidence to suggest the formation of an iminium ion from the hydroxymethyl-methyltriazenes can occur under physiological conditions. However, it has been shown that such a reactive moiety is formed during chemical reactions of acetate and benzoate esters of N-(hydroxymethyl)-methyltriazenes (Hemens et al, 1984) (fig.79).



- MTIC
- ◆ DTIC
- TEMOZOLOMIDE
- ◇ HMMTIC

Fig.77 Correlation between TLX5 cell growth and  $[AUC]_{MTIC}$

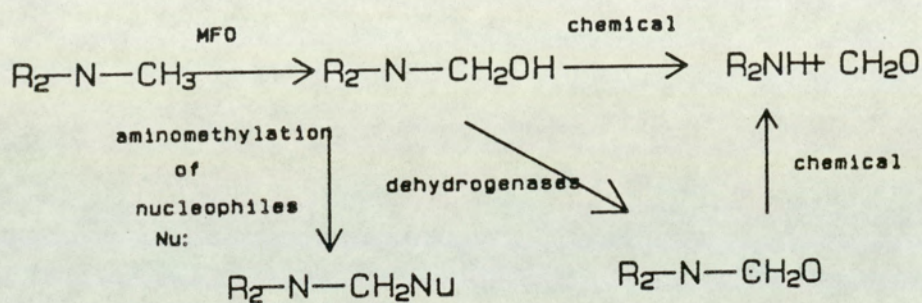


Fig.78 Proposed metabolic pathway of oxidative N-demethylation

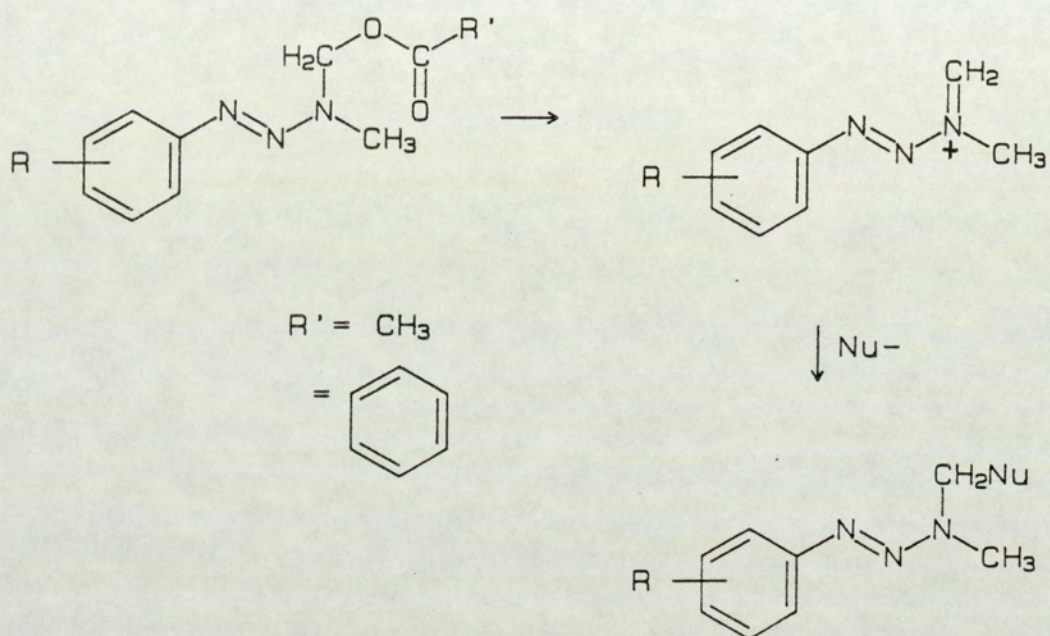


Fig.79 Proposed mechanism of the formation of an iminium ion from an N-(acyloxymethyl)triazenes

### 3.9 Studies of the metabolism of temozolomide in vivo

Temozolomide does not undergo metabolism when incubated in vitro with liver fractions. Instead, chemical decomposition seems to play an important rôle in its in vitro cytotoxicity towards TLX5 cells (see sections 3.6, 3.7 and 3.8). The preparation of subcellular fractions, such as microsomes or 10,000g supernatant, used in the in vitro metabolic studies bears little resemblance to the physiological conditions in vivo in intact animals. In order to test the hypothesis that temozolomide is also metabolically inert in vivo, metabolism studies were carried out in patients who entered the phase I clinical study and in mice using [<sup>14</sup>C]methyl labelled and unlabelled temozolomide. The studies were designed to identify i) the major route of excretion and ii) the nature of potential biotransformation of the drug. The amount of radioactivity was quantified by scintillation counting and the amount of unchanged drug excreted in urine was measured by the HPLC method described in section 2.4.1.

#### 3.9.1 Excretion of drug-derived radioactivity

Fig.80 shows the time-course of the cumulative excretion of drug-derived radioactivity in the urine and in expired air. Fig.81 shows the time-course of the cumulative excretion of unchanged temozolomide in urine over a period of 72hr. The majority of the dose was eliminated in the first 16hr (figs.80 and 81). Renal excretion was the major route of elimination and accounted for 52<sub>+7</sub>% of the injected radioactivity and 39<sub>+6</sub>% was due

to the unchanged drug (fig.82). The percentage of the dose expired as  $^{14}\text{CO}_2$  was  $30\pm 9\%$ . In addition, a small amount of radioactivity was also detected in the faeces ( $3\pm 3\%$ ) and the carcass ( $8\pm 2\%$ ).



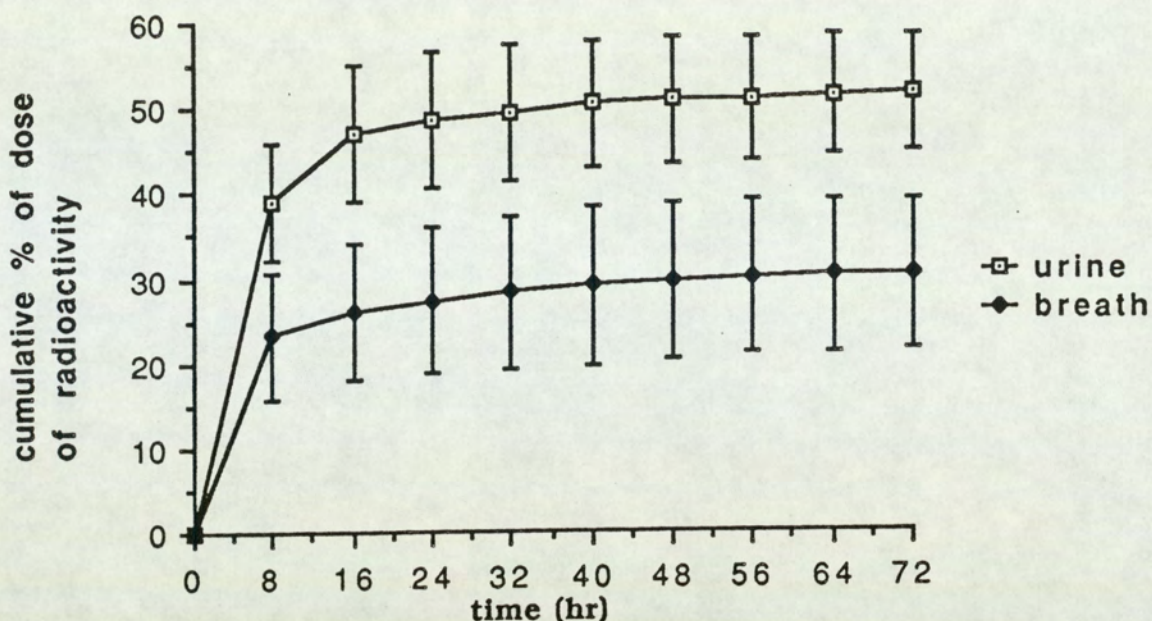


Fig.80 Cumulative amount of radioactivity excreted in urine and exhaled in breath over 72hr following an i.p. injection of  $^{14}\text{C}$  labelled temozolomide (40mg/Kg) (n=6 animals  $\pm$  1 S.D.)

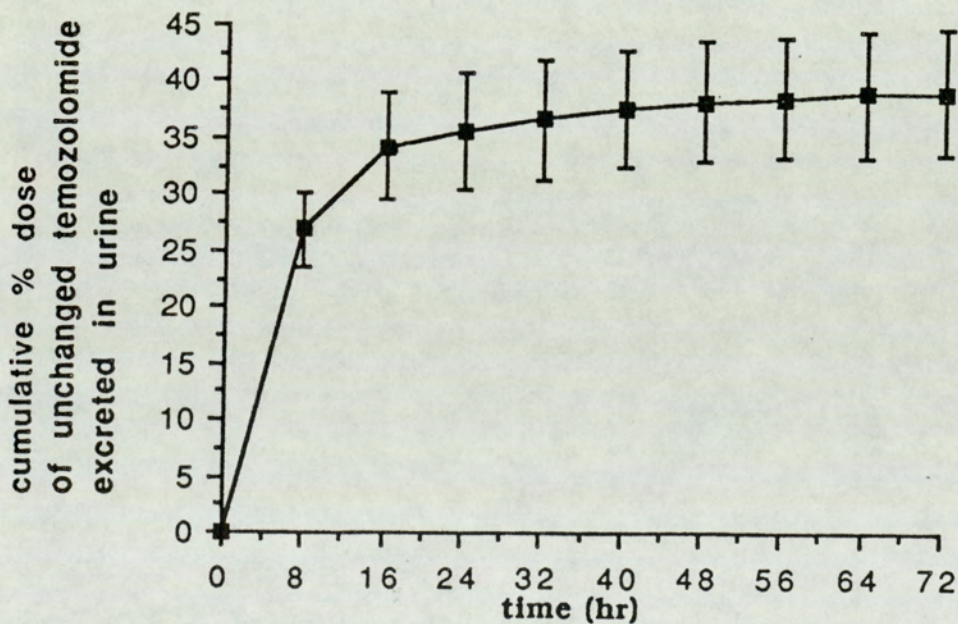


Fig.81 Cumulative amount of unchanged temozolomide excreted in urine over 72hr following an i.p. injection (n=6 animals  $\pm$  1 S.D.)

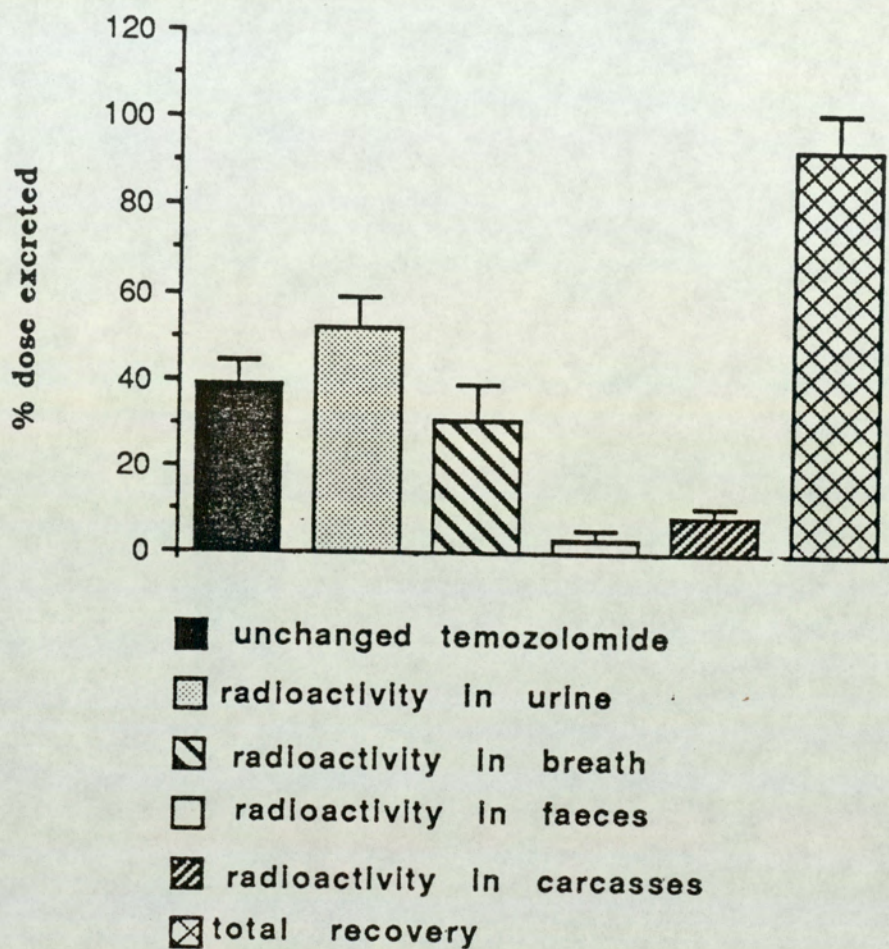


Fig.82 Total excretion balance of temozolomide  
(n=6 animals  $\pm$  1 S.D.)

### 3.9.2. Characterization of urinary metabolites

In order to gain insight into the chemical nature of possible biotransformation products, urine samples obtained from mice and patients were analyzed by HPLC, TLC and combined HPLC/radiochromatography. Fig.83c shows the HPLC chromatogram of an ethylacetate extract of a urine sample from a mouse, which had received a single i.p. dose of temozolomide (40mg/Kg). Fig.83b shows the chromatogram of the same sample omitting the internal standard. Fig.83a shows the HPLC chromatogram of an ethylacetate extract of a urine sample collected 24hr prior to administration of the drug. As shown in fig.83b&c, temozolomide was identified in the urine on the basis of chromatographic retention time. In addition, its UV absorbance at four wavelengths (280, 300, 320 and 350nm) was indistinguishable from that of authentic temozolomide. There were no other peaks found in the extract. However, a major urinary product was detected on TLC autoradiography and HPLC/radiochromatography. This urinary product had a retention time of 1.8min (fig.84). Since it was not detected using the UV detector at 325nm, a wavelength near to the  $\lambda_{max}$  of temozolomide, it is unlikely that this compound closely resembles temozolomide in structure.

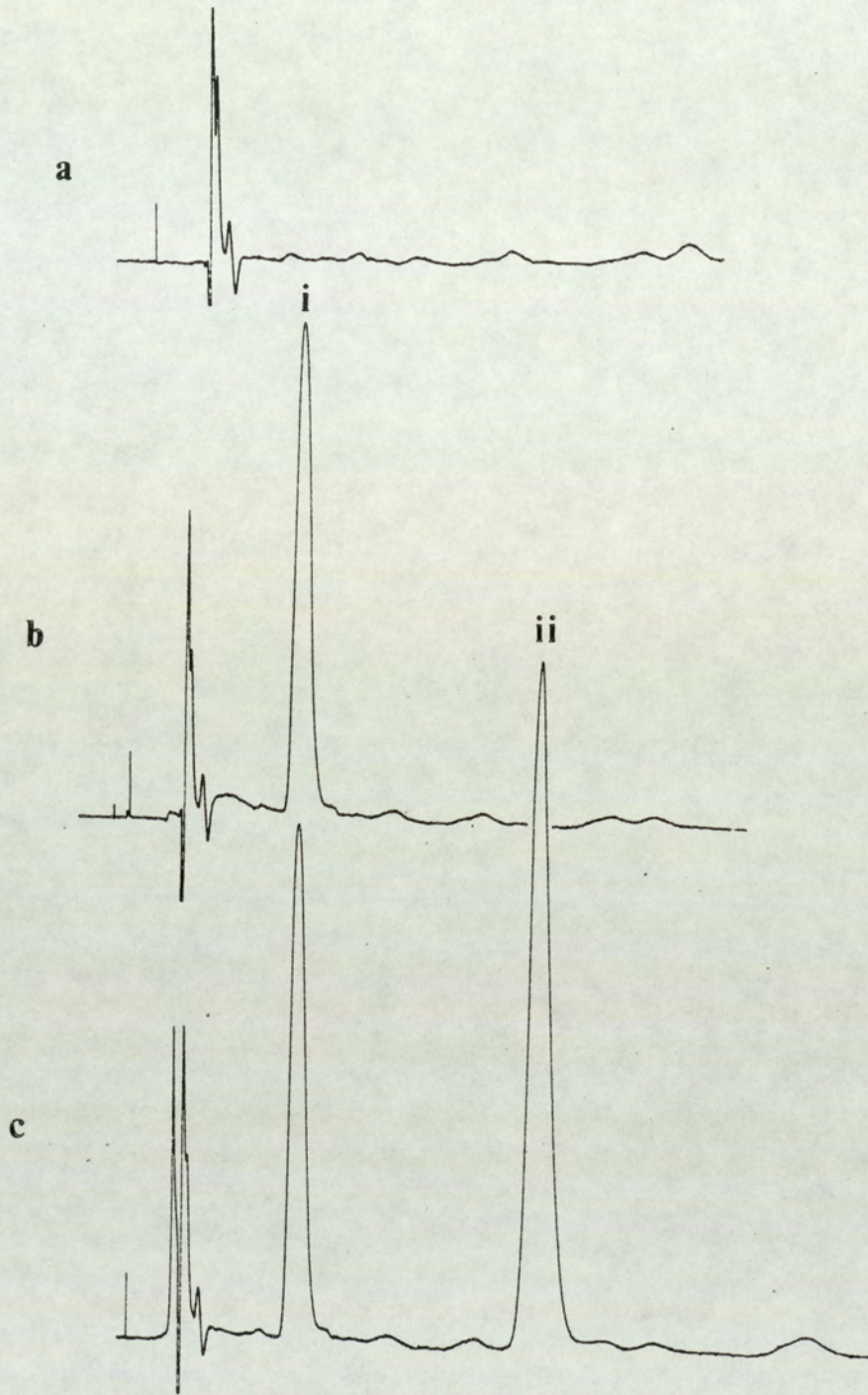


Fig.83 HPLC chromatograms of an ethylacetate extract of a urine sample a) collected 24hr prior to drug administration, b) collected 24hr after dosing omitting the internal standard c) with the internal standard. i) temozolomide, ii) internal standard. Mobile phase, 5% methanol in 0.5% acetic acid (15min) followed by washing period (20min) with 40% methanol in 0.5% acetic acid. Detection wavelength, 325nm. Flow rate, 1ml/min

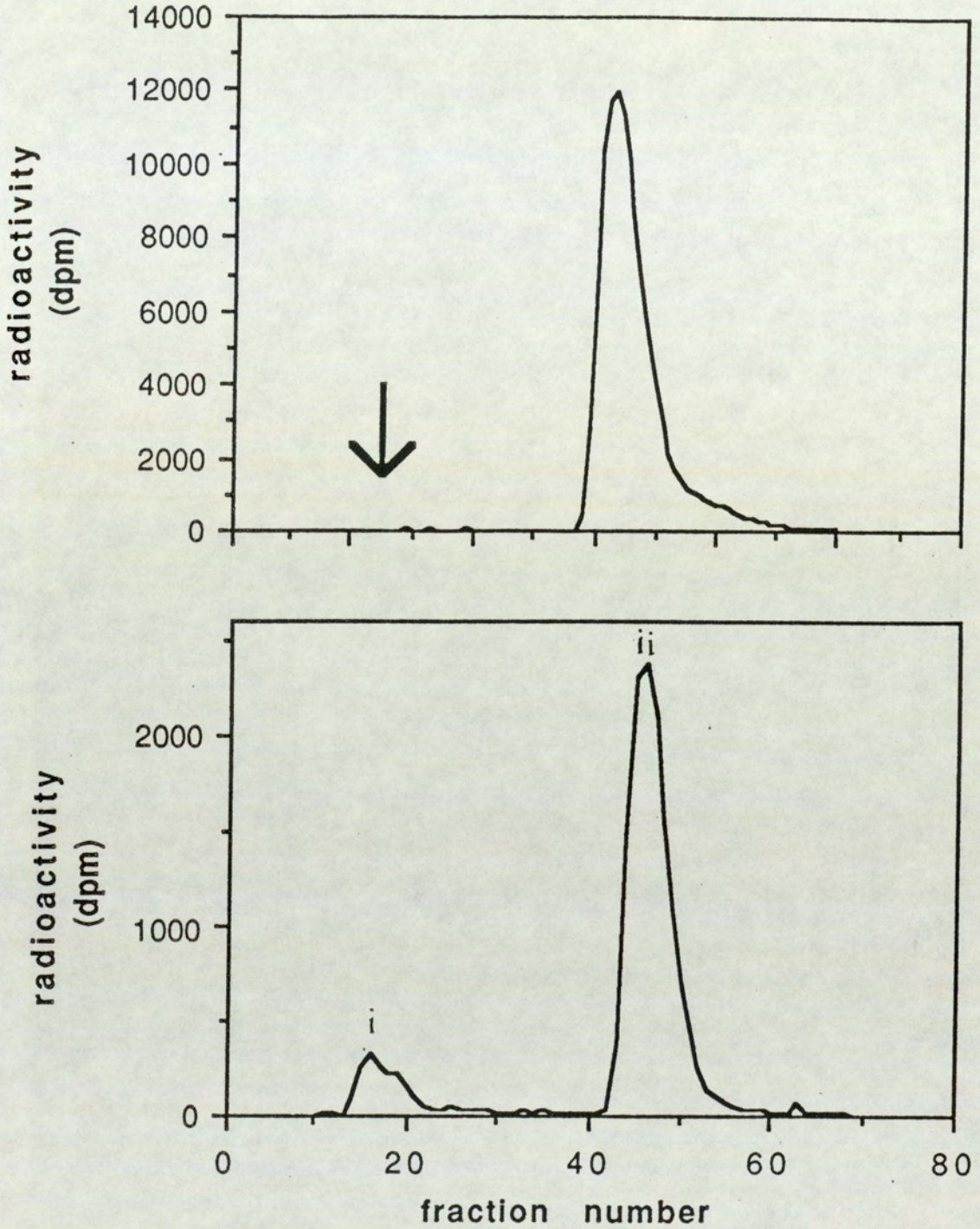


Fig.84 HPLC radiochromatography of a) [ $^{14}\text{C}$ ] labelled temozolomide b) a pooled urine extract of 6 mice which had received the labelled material i) urinary product, ii) temozolomide

An alternative explanation for the inability to detect this compound at 325nm may be that the concentration of this product was well below the detection limit (0.5mg/L). Horton (1983) has shown that monomethyltriazenes can interact with glutathione and speculated that the ultimate end-product is S-methylglutathione (fig.85). Temozolomide, upon chemical decomposition, generates MTIC (section 3.7.1). Therefore, S-methyl-N-acetyl-cysteine is a likely candidate for the material found in the urine. The synthesis of this compound was attempted initially by reacting S-methyl-cysteine with excess acetic anhydride at room temperature for 3 days in the presence of pyridine. This synthetic route was not satisfactory in that it was difficult to separate the product from pyridine during the purification stage. Thomson et al (1963) synthesized S-ethyl mercapturate as a potential urinary metabolite of bromoethane. In accordance with the method used by Thomson et al (1963), S-methyl-N-acetyl-cysteine was synthesized by reacting S-methyl-cysteine with excess acetic anhydride in the presence of 4N NaOH. Fig.86 shows the high field NMR spectrum of S-methyl-N-acetyl-cysteine. A singlet at 1.85ppm, with an integration value equivalent to 3 protons, indicates the presence of an acetyl group.

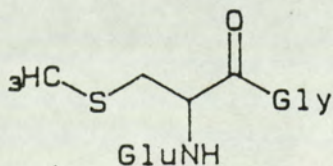


Fig.85 Structure of S-methylglutathione

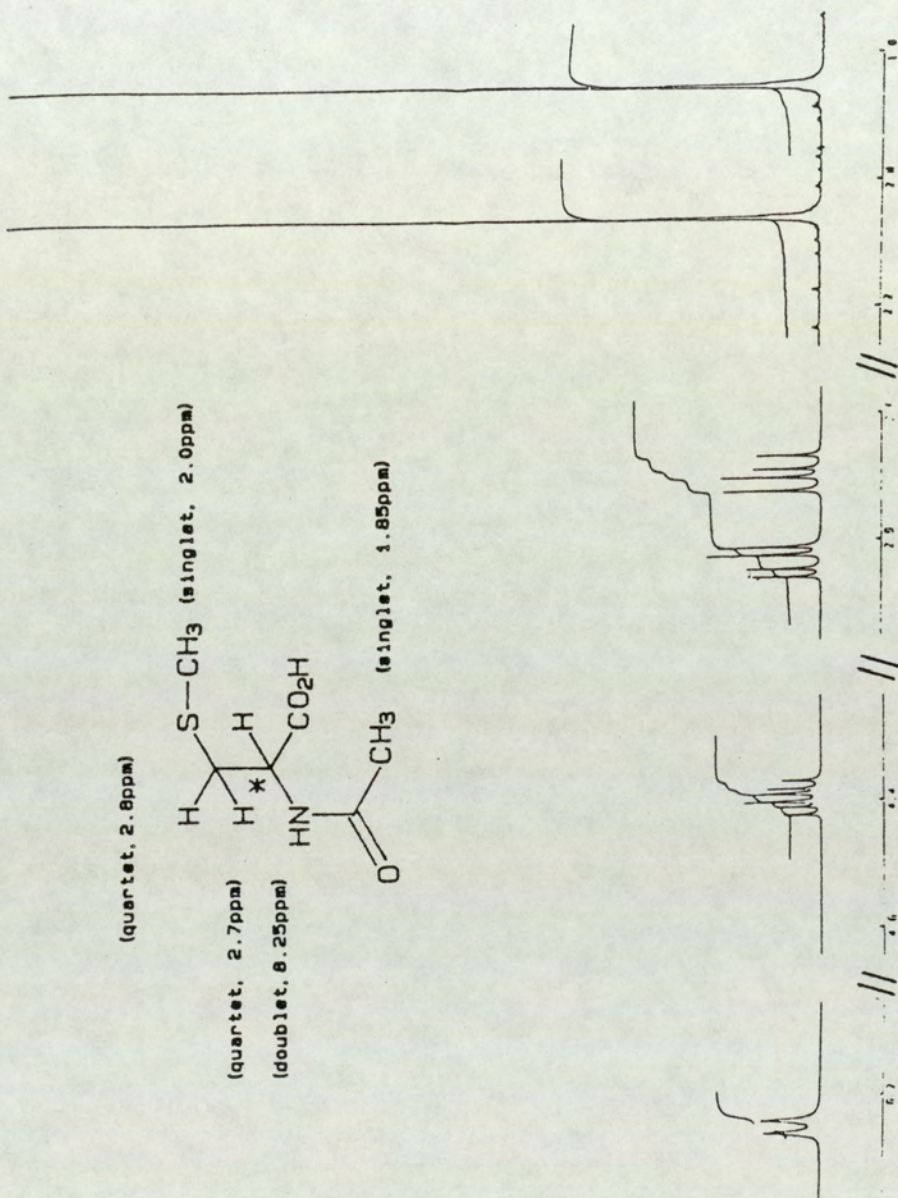


Fig. 86 High field  $^1\text{H}$  NMR spectrum of S-methyl-N-acetylcysteine

TLC analysis using solvent system butanol/acetic acid/water (3:1:1) indicated that the unidentified urinary product did not possess the same chromatographic property as N-acetyl-S-methyl-cysteine (table 7). Due to insufficient material present in urine, further characterization of this urinary product was not attempted.

Compounds	R.F. value
N-acetyl-S-methyl-cysteine	0.3
S-methyl-cysteine	0.49
temozolomide	0.39
unidentified product	0.24

Table 7. Rf values for the standard S-methyl-N-acetyl-cysteine, S-methyl-cysteine, temozolomide and the urinary product

Metabolic studies were also carried out in mice receiving temozolomide at the LD<sub>10</sub>. Fig.87 shows the HPLC chromatogram of an extract of pooled urine of 12 mice which had received temozolomide (450mg/Kg) via p.o. route. Two peaks were identified: one of them had a retention time identical to temozolomide (3.4min) and the other one had the same retention time (1.8min) as the unidentified product found by radiodetection in the urine of a mouse which had received [<sup>14</sup>C]methyl temozolomide (40mg/Kg) via i.p. route. This metabolite was isolated and purified by HPLC for subsequent CIMS and FABMS analyses. Mass spectral



analyses performed by Dr. Peter Farmer and Mr. John Lamb failed to give any interpretable spectra in an attempt to reveal the identity of this urinary product, possibly due to the presence of impurities and the compound is not amenable to mass spectral analysis. The relative UV absorbance of this metabolite at four wavelengths (280, 300, 320 and 350nm) was almost identical to that of temozolomide. This result suggests that this urinary product has an intact triazene or tetrazinone structure.

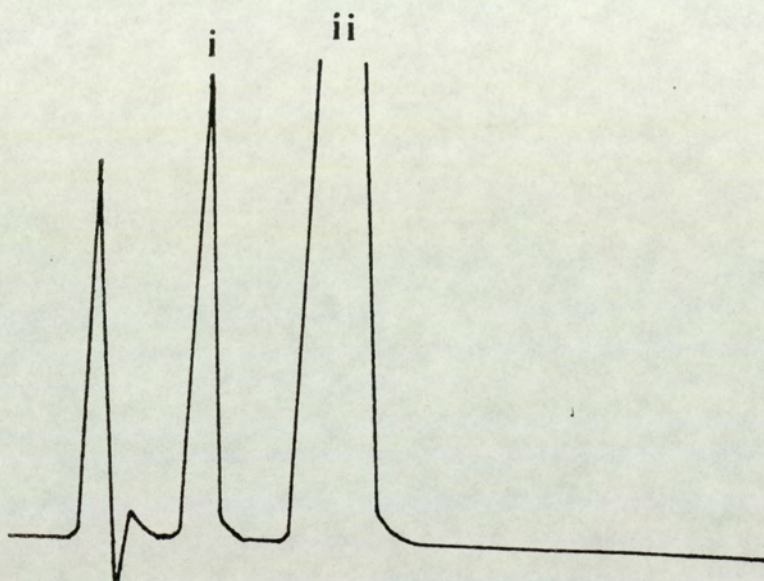


Fig.87 HPLC chromatogram of a pooled urine extract of 12 mice which had received LD<sub>10</sub> dose of temozolomide via p.o. route i) urinary product ii) temozolomide. Mobile phase, 5% methanol in 0.5% acetic acid, followed by a washing period as described in fig.83. Detection wavelength, 325nm. Flow rate, 1m/min

Subsequent isolation and purification of this product were carried out using patients' urine samples because a larger yield could be obtained from this source. Fig.88 shows the HPLC chromatogram of an ethylacetate extract of a urine sample of a patient who had received temozolomide at 700mg/m<sup>2</sup> via p.o. route. Three peaks were identified on the HPLC chromatogram: in addition to temozolomide and the unidentified urinary product found in mice, a peak with a retention time, 8min, was present in the chromatogram.

Further experiments were designed to prove that the peaks which had the retention times 1.8 and 8min found in the HPLC chromatogram were genuine metabolites. Firstly, as shown in fig.89a, they were not present in the urine sample of the same patient prior to drug administration, and after the administration of dexamethasone and metoclopramide. Secondly, they were not present in urine samples collected from normal volunteers (fig.89c&d). Thirdly, they were not formed when temozolomide was incubated with urine for 12hr (fig.90); hence, they were not products of the chemical degradation of temozolomide.

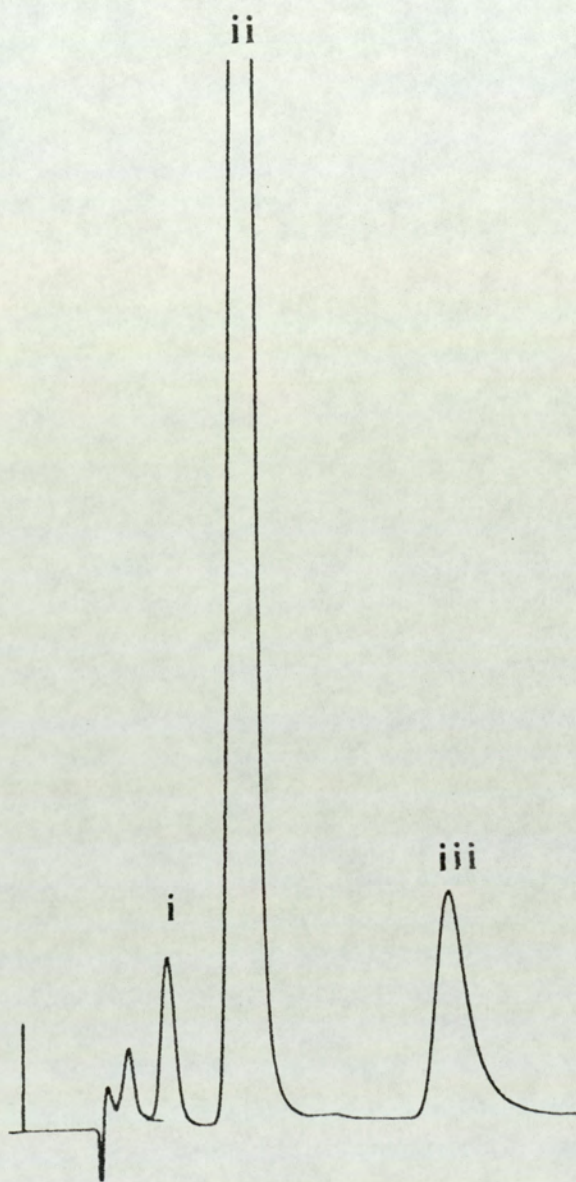


Fig.88 HPLC chromatogram of an ethylacetate extract of a urine sample of a patient (V.S.), who had received 700mg/m<sup>2</sup> of temozolomide via p.o. route i) metabolite I, ii) temozolomide, iii) metabolite II Mobile phase, 5% methanol in 0.5% acetic acid, followed by a washing period as described in fig.83. Detection wavelength, 325nm. Flow rate, 1ml/min

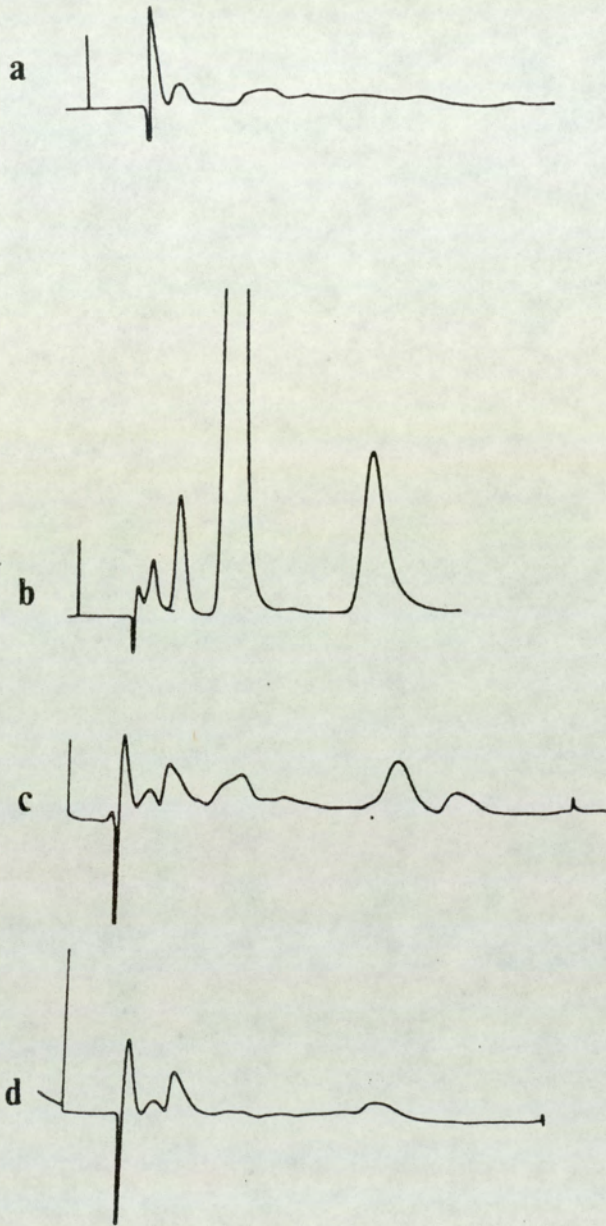


Fig.89 HPLC chromatograms of an ethylacetate extract of a urine sample of a) a patient (V.S.) prior to temozolomide treatment and after receiving dexamethasone (8mg) and metoclopramide (100mg), b) after administration of temozolomide at 700mg/m<sup>2</sup>, c,d) of 2 healthy subjects (F.K, D.G.)

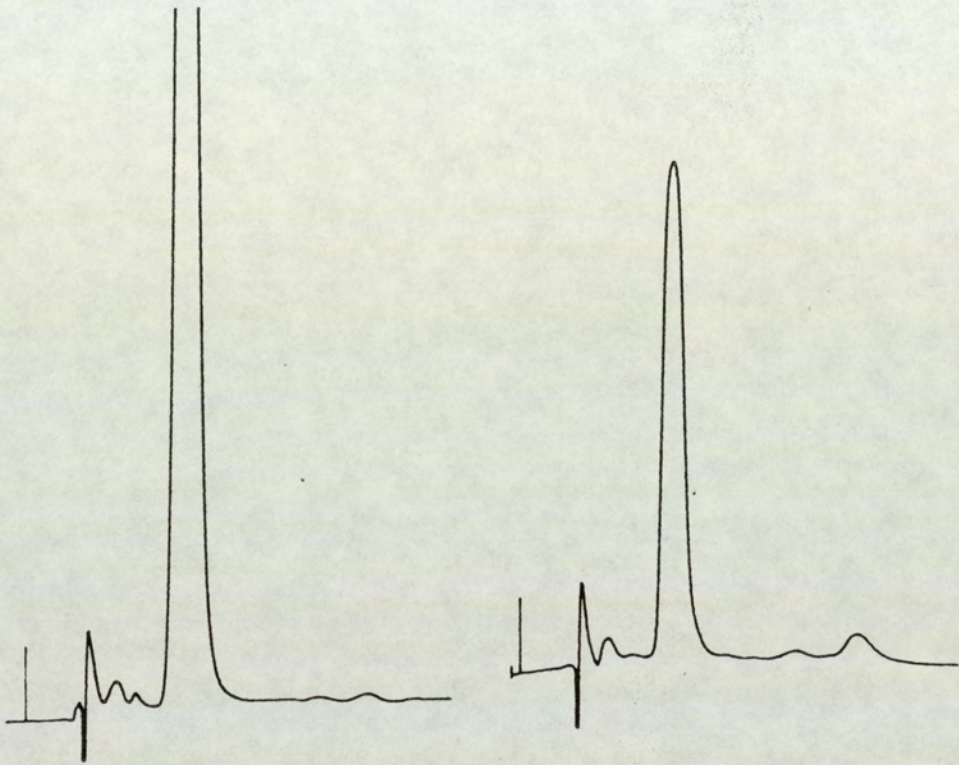


Fig.90 HPLC chromatogram showing the degradation of temozolomide after 12hr incubation with urine at 37°C

Fig.91 shows the effect of differing pH values on the extraction efficiency of these metabolites, designated as metabolite I (1.8min) and metabolite II (8min). It is shown that as the pH value of urine sample was increased from 2 to 4, the peak height of metabolite II decreased but the extraction efficiency of metabolite I was not affected. The peaks corresponding to both metabolites completely disappeared from the ethylacetate extract when the pH of the aqueous phase was increased from 2 to 6. This observation is presumably due to ionization of the metabolites in the aqueous phase and not degradation because the peaks re-appeared in the ethylacetate extract when pH of the aqueous phase was re-acidified (pH2). This result shows unambiguously that both metabolites were acidic in nature. In view of the extraction efficiency at different pH values obtained in this study, the approximate pKa values were assigned to metabolite II and I which were respectively in the region of 3 and 4.5. Furthermore, when the urine was pre-treated with 4N NaOH, temozolomide together with its metabolites disappeared from the ethylacetate extract, suggesting that these metabolites behave chemically like temozolomide, which is unstable under alkaline conditions (fig.44 and see section 3.3). In addition, their UV absorbances at four wavelengths was identical to that of temozolomide. The results obtained from the chemical and chromatographic studies suggest strongly that the metabolites possess an intact tetrazinone ring. In addition, small amounts of these two metabolites were also found in the plasma of the same patient following

drug administration.



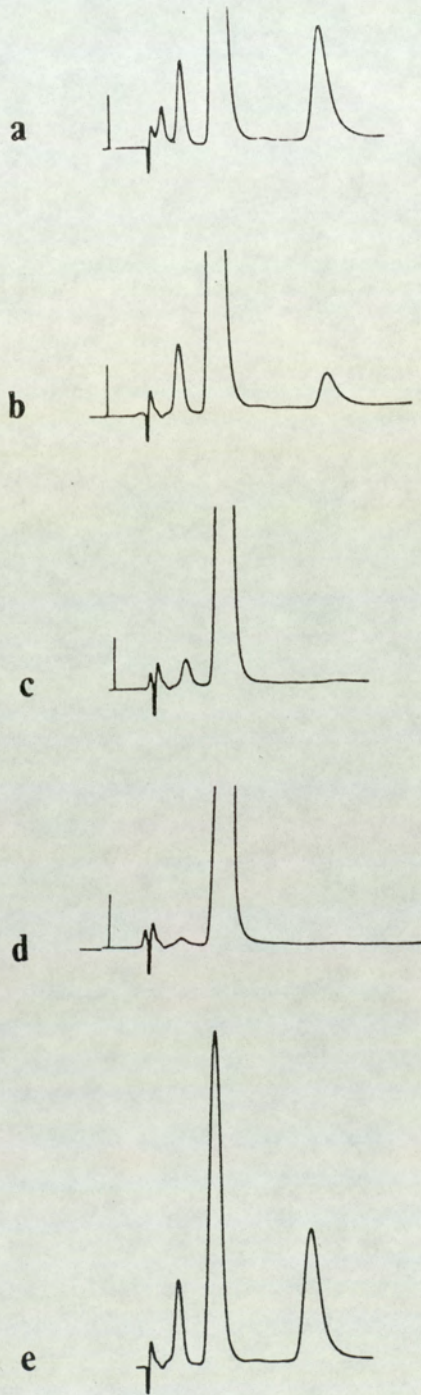


Fig.91 Effect of pH in the urine layer on the extraction efficiency of the metabolites at pH a)1-2, b) 3, c) 4, d) 5 and e) re-acidified the urine with 1N HCl (pH2)

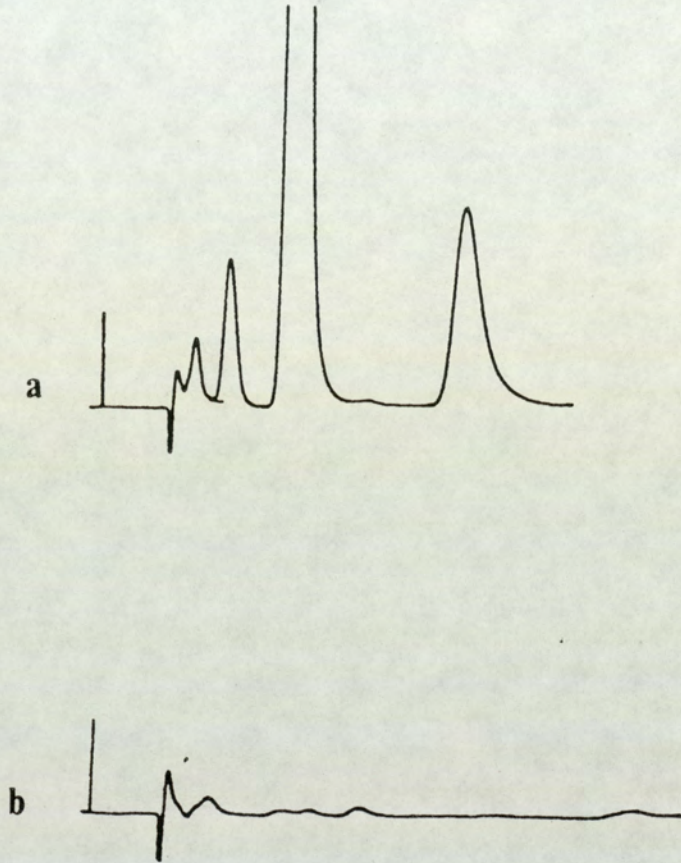


Fig.92 HPLC chromatograms of a) an acidic extract of a patient's urine (V.S.) b) after pre-treatment with 4N NaOH for 2min at room temperature and the aqueous layer was re-acidified for solvent extraction and analyzed by HPLC

3.9.2.1 Isolation and structural characterization of metabolite II

The metabolism of rilmafazone, a novel 1H-1,2,4-triazoyl benzophenone derivative, has been studied in the monkey (fig.93, Koike, et al, 1988). It was found that the drug undergoes ring cyclization as a result of desglycylation and successive N-demethylation in the carboxamide group (fig.93). Hydrolysis of the carboxamide group led to the formation of a carboxylic acid derivative. The structure of this metabolite was fully elucidated by EIMS. Given that temozolomide possesses a functional group similar to rilmafazone and that dimethylmitozolomide has been shown to undergo N-demethylation in the carboxamide functional group (Horspool, 1988; Horspool et al, 1989; fig.94), it is conceivable that one of the metabolites found in the patient's urine is the carboxylic acid derivative of temozolomide. This metabolite was synthesized by acid hydrolysis of temozolomide using a mixture of concentrated H<sub>2</sub>SO<sub>4</sub> and HNO<sub>2</sub> prepared in situ as described in section 2.1.4.1. Metabolite II has a HPLC retention time (fig.95) and a TLC R<sub>f</sub> value identical to those of the synthetic 3-methyl-2,3-dihydro-4-oxoimidazo[5,1-d]tetrazine-8-carboxylic acid. Using TLC solvent systems (see section 2.4.5.1) acetone/acetic acid/water (7:1:2) and benzene/methanol/acetic acid (45:8:8), the R<sub>f</sub> values were respectively 0.6 and 0.07. On the basis of the chromatographic properties discussed so far, it is likely that metabolite II is the carboxylic acid derivative of temozolomide.

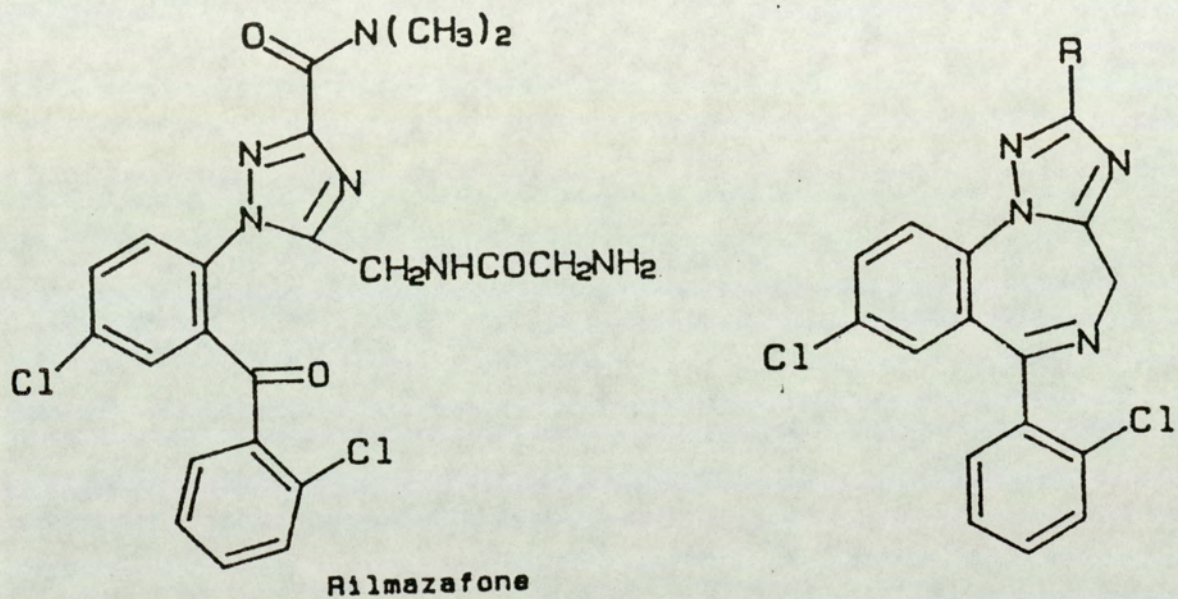


Fig.93 Structures of rilmazafone and its metabolites

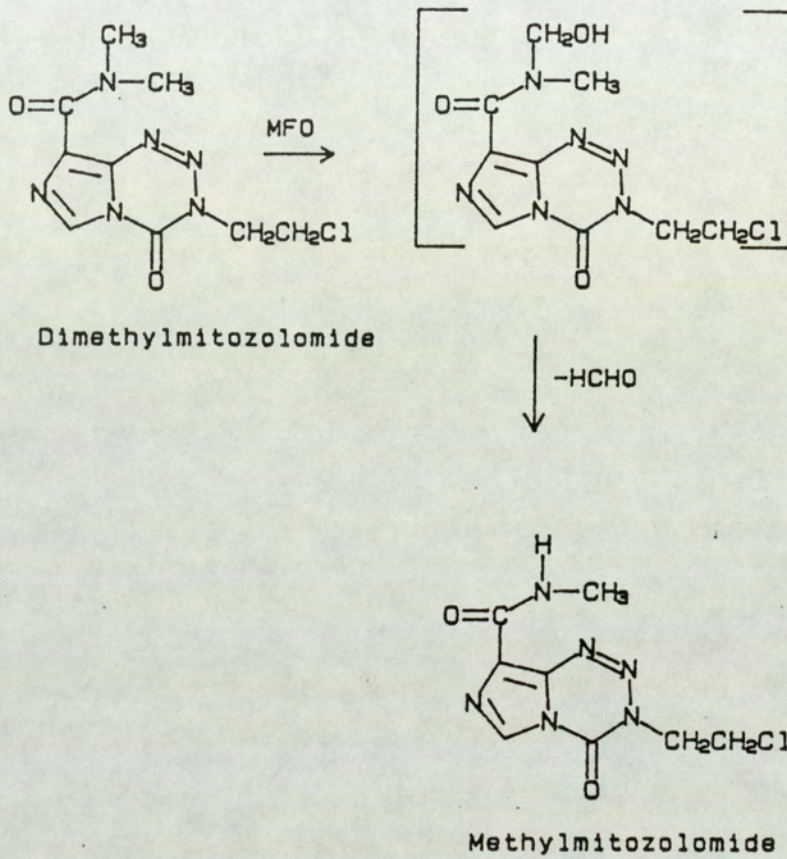


Fig.94 Proposed metabolic pathway of dimethylmitozolomide

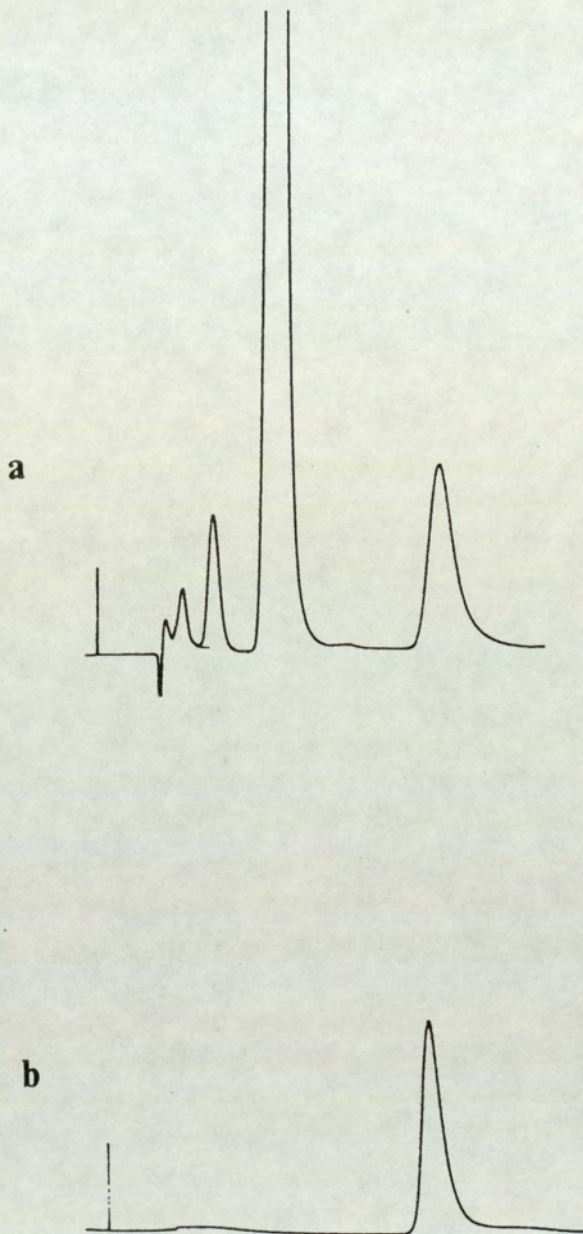


Fig. 95 HPLC chromatograms of an ethylacetate extract of  
a) a patient's urine (V.S.) and b) of the  
authentic 3-methyl-2,3-dihydro-4-oxoimidazo  
[5,1-d]tetrazine-8-carboxylic acid

The isolation and purification of this metabolite were achieved by solvent extraction, solid-phase extraction and repeated HPLC purifications as described in section 2.9.5.1. Metabolite II was extracted into ethylacetate with an extraction efficiency of  $64.3 \pm 12.5\%$  (n=6); therefore, this metabolite seems to be amenable to continuous solvent extraction using the apparatus as described in fig.20. Fig.96 and 97 show that temozolomide and metabolite II were completely removed from urine following continuous extraction with ethylacetate for 72hr. The absence of metabolite I in the ethylacetate extract could possibly be due to its instability in boiling ethylacetate. Metabolite II was subsequently purified by passage through C<sub>18</sub> sep-pak cartridges; it was eluted with a mixture of methanol and 0.5% acetic acid (50:50). The metabolite was isolated and further purified by HPLC (see section 2.11.6.1). The procedures described above yielded a pure sample, which was confirmed by the presence of a single peak on HPLC utilizing UV detection at 205 and 325nm (fig.98).

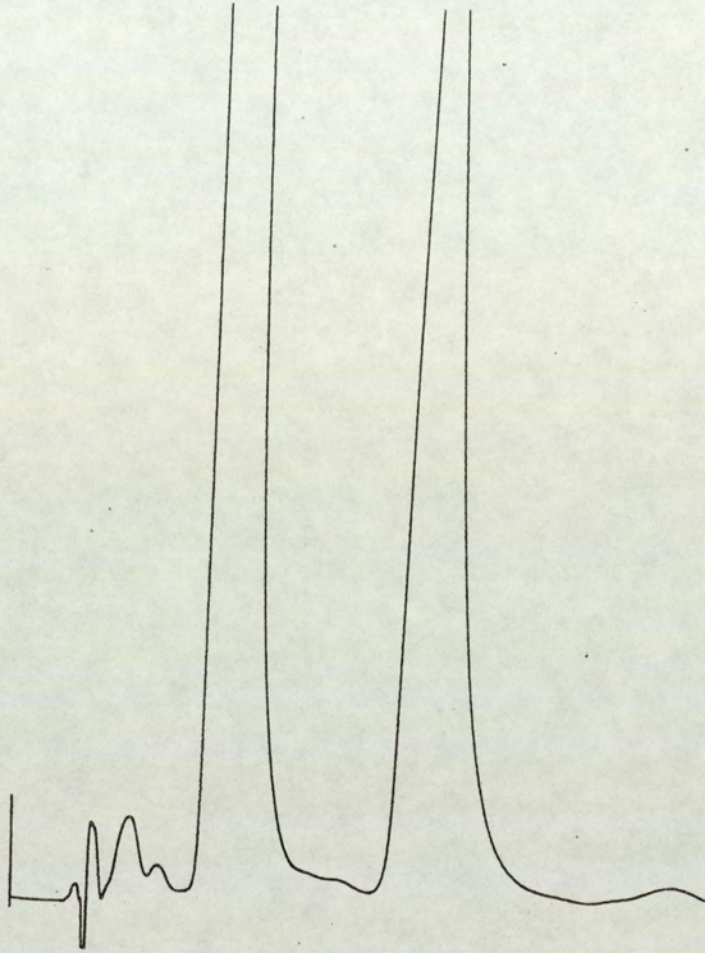


Fig.96 HPLC chromatogram of the ethylacetate layer of a urine sample (200-300ml) after 72hr continuous extraction



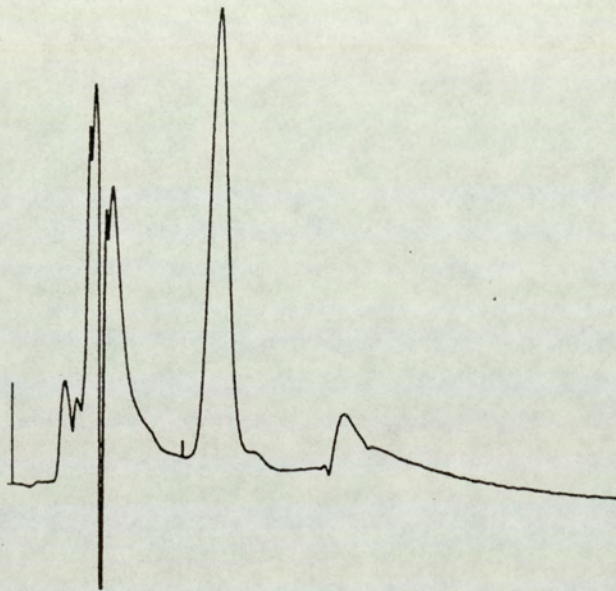


Fig.97 HPLC chromatogram of the urine layer after 72hr continuous extraction

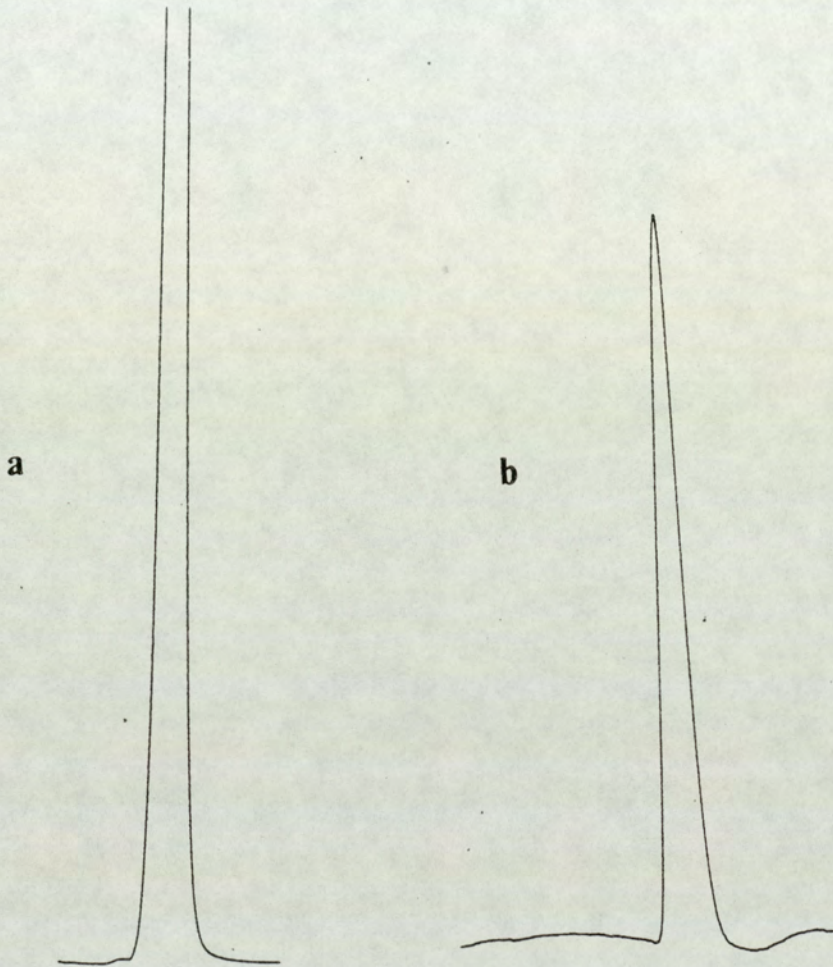


Fig.98 HPLC chromatogram of metabolite II isolated from urine detected at UV at a) 325nm and b) 205nm

The structure of the isolated material was elucidated by high field  $^1\text{H}$  NMR and high resolution MS. HPLC was performed on the isolate before and after MS and NMR analyses to ensure it did not undergo decomposition. Figs. 99 and 100a show the high field  $^1\text{H}$  NMR spectra of temozolomide and the authentic carboxylic acid derivative. In the NMR spectrum of temozolomide, the singlets at 3.9ppm and 8.8ppm correspond to the N-methyl and the imidazole protons respectively; and the doublet at 7.8ppm indicates the presence of the carboxamide protons. Unlike the NMR spectrum of temozolomide, only the singlets at 3.9 and 7.8ppm were present in the spectrum of the carboxylic acid derivative. Fig. 100b shows the NMR spectrum of metabolite II. Metabolite II has an NMR spectrum identical to the synthetic analogue.

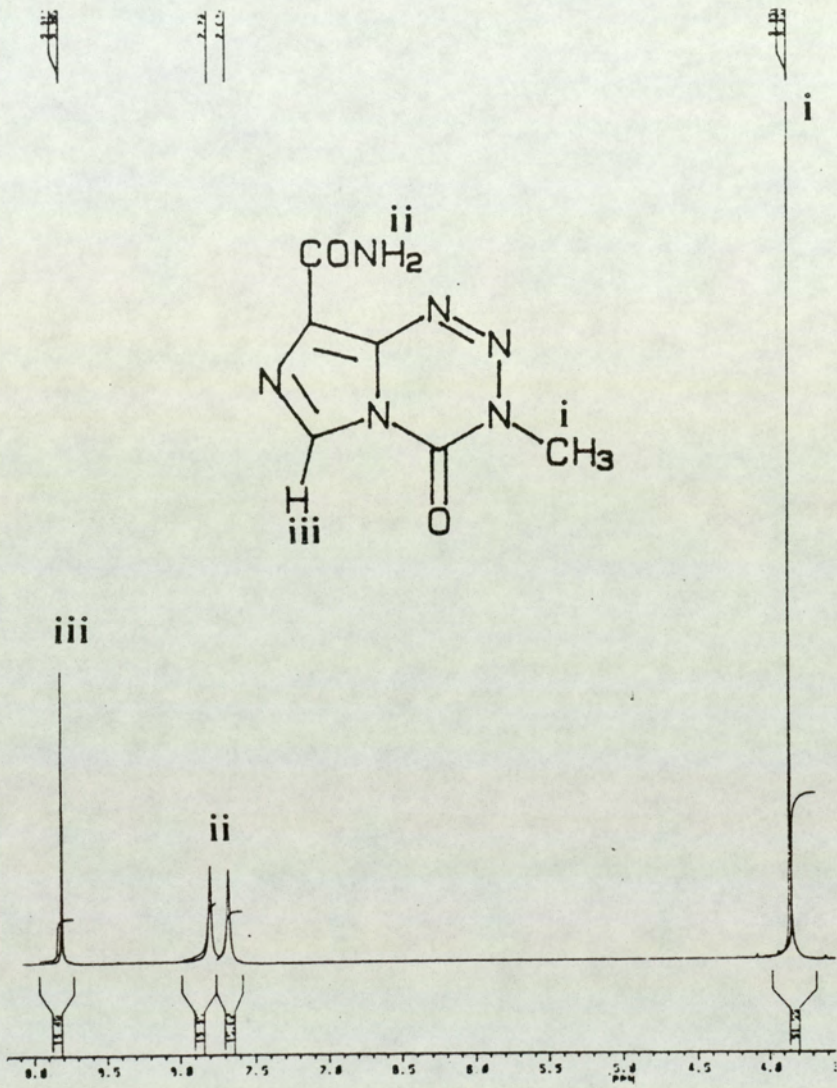


Fig.99 High field <sup>1</sup>H NMR spectrum of temozolomide  
i) N-methyl signal, ii) carboxamide signals,  
iii) imidazole proton signal

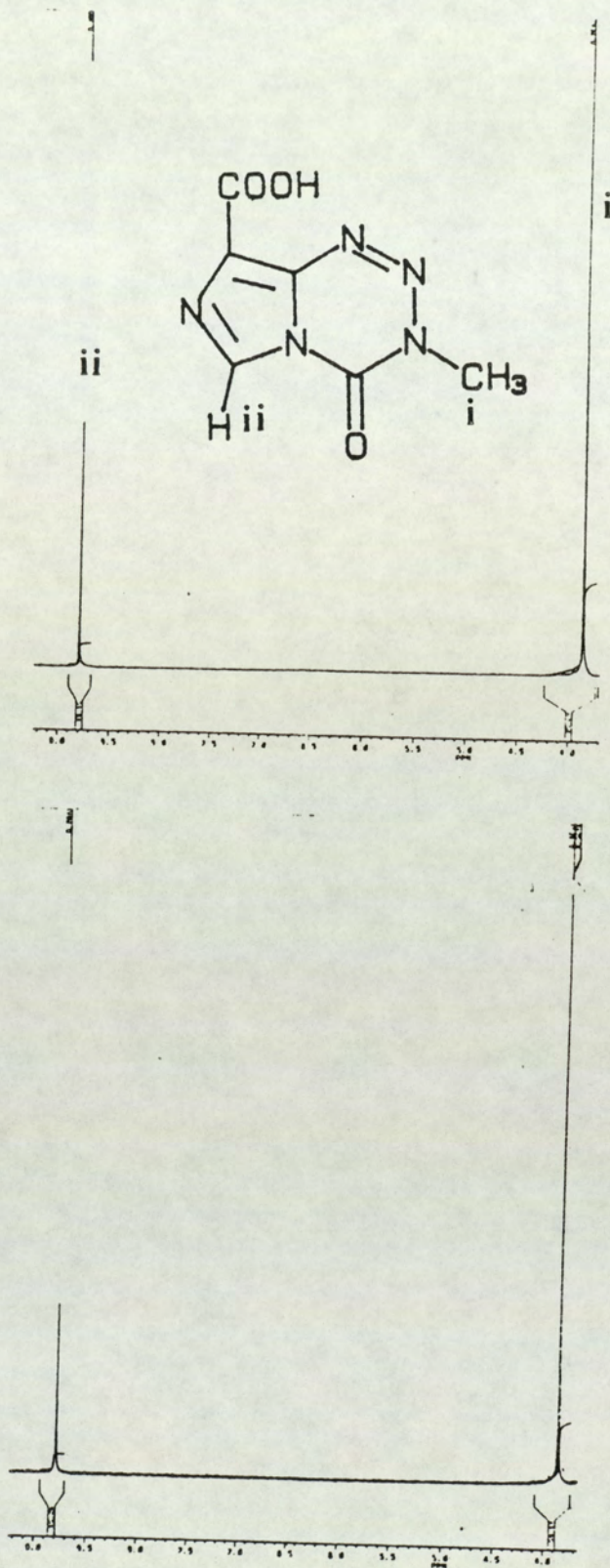


Fig.100 High field <sup>1</sup>H NMR spectra of a) the authentic 3-methyl-2,3-dihydro-4-oxoimidazo[5,1-d]tetrazine-8-carboxylic acid and b) metabolite II  
i) N-methyl signal, ii) imidazole proton signal

The identity of the metabolite was confirmed by EIMS. Fig.101 shows the EIMS of temozolomide and fig.102a shows the EIMS of the authentic carboxylic acid derivative of the drug. Both temozolomide and the carboxylic acid derivative undergo ring cleavage yielding the fragment ions  $m/z$  137 and 138 respectively indicating the loss of  $C_2H_3NO$ . In addition, in the case of the carboxylic acid derivative, a minor fragment ion,  $m/z$  151, indicates the loss of  $COOH$ . Metabolite II isolated from the patients' urine has a mass spectral fragmentation pattern identical to that of the synthetic derivative. Compounds possessing an NNN linkage have a characteristic U.V.  $\lambda_{max}$  in the region of 320nm (see section 3.3). The UV spectral analysis of metabolite II indicates the presence of such a linkage in the molecule (fig.103, see section 3.3). The results obtained in this study characterize unambiguously the structure of metabolite II as the carboxylic acid derivative of temozolomide.

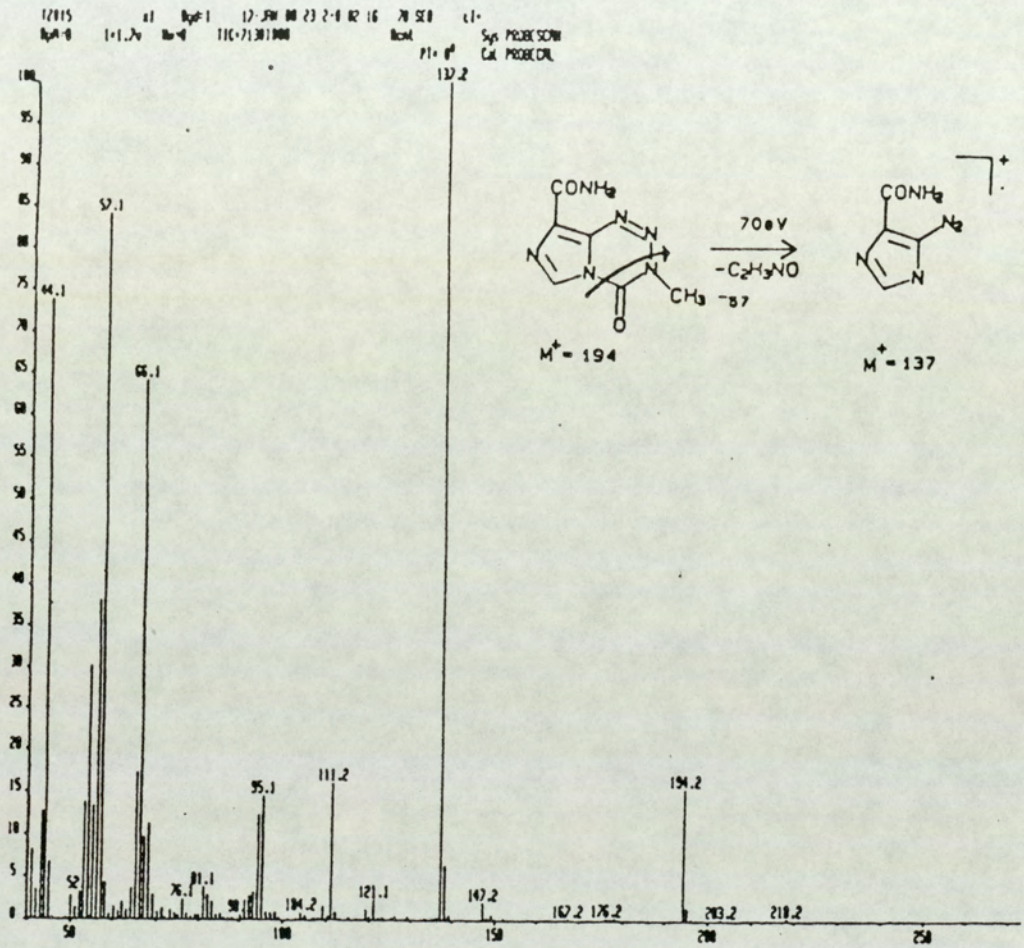


Fig.101 EIMS spectrum of temozolomide

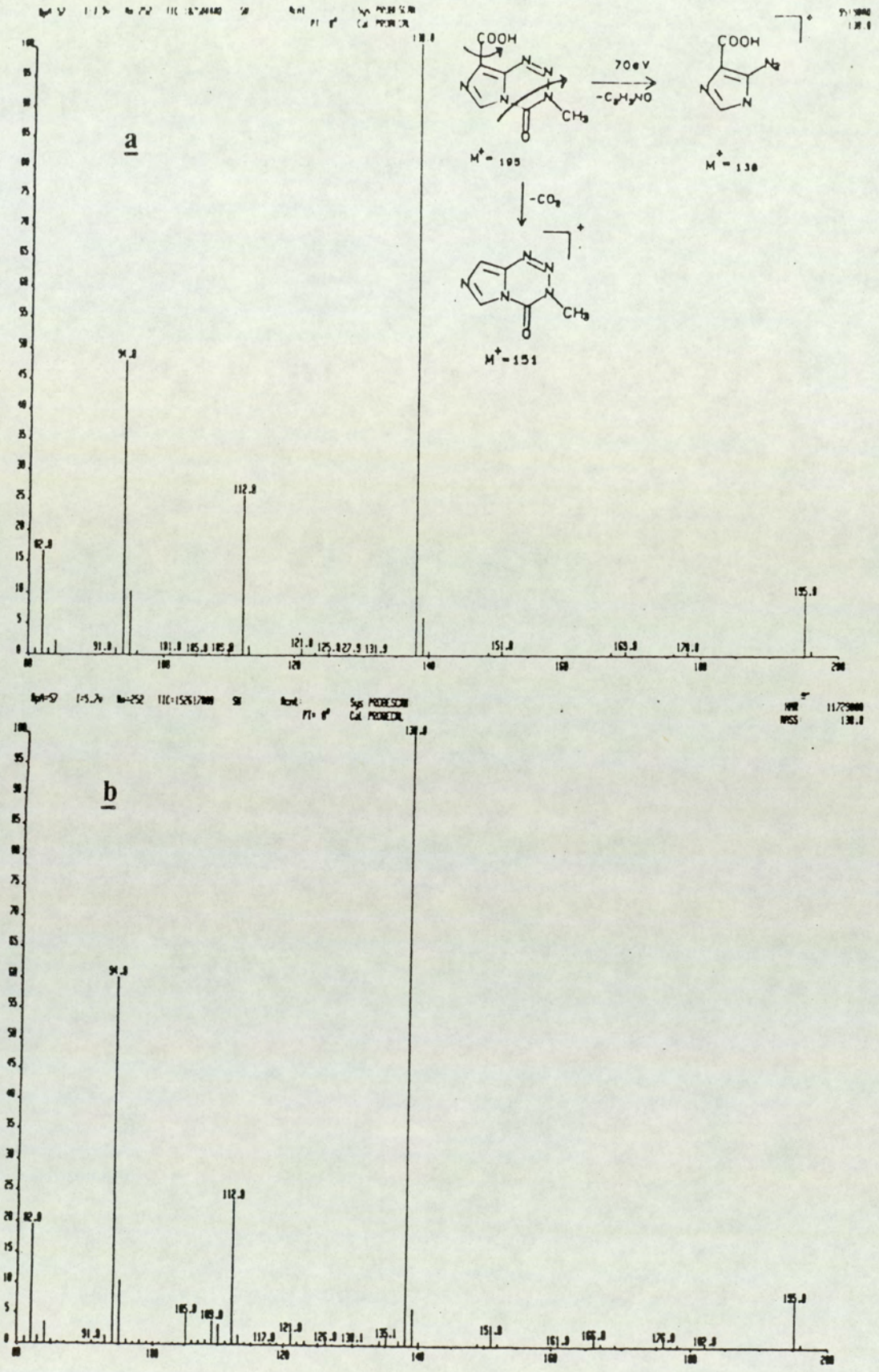


Fig.102 EIMS spectrum of a) authentic 3-methyl-2,3-dihydro-4-oxoimidazo[5,1-d]tetrazine-8-carboxylic acid and b) metabolite II



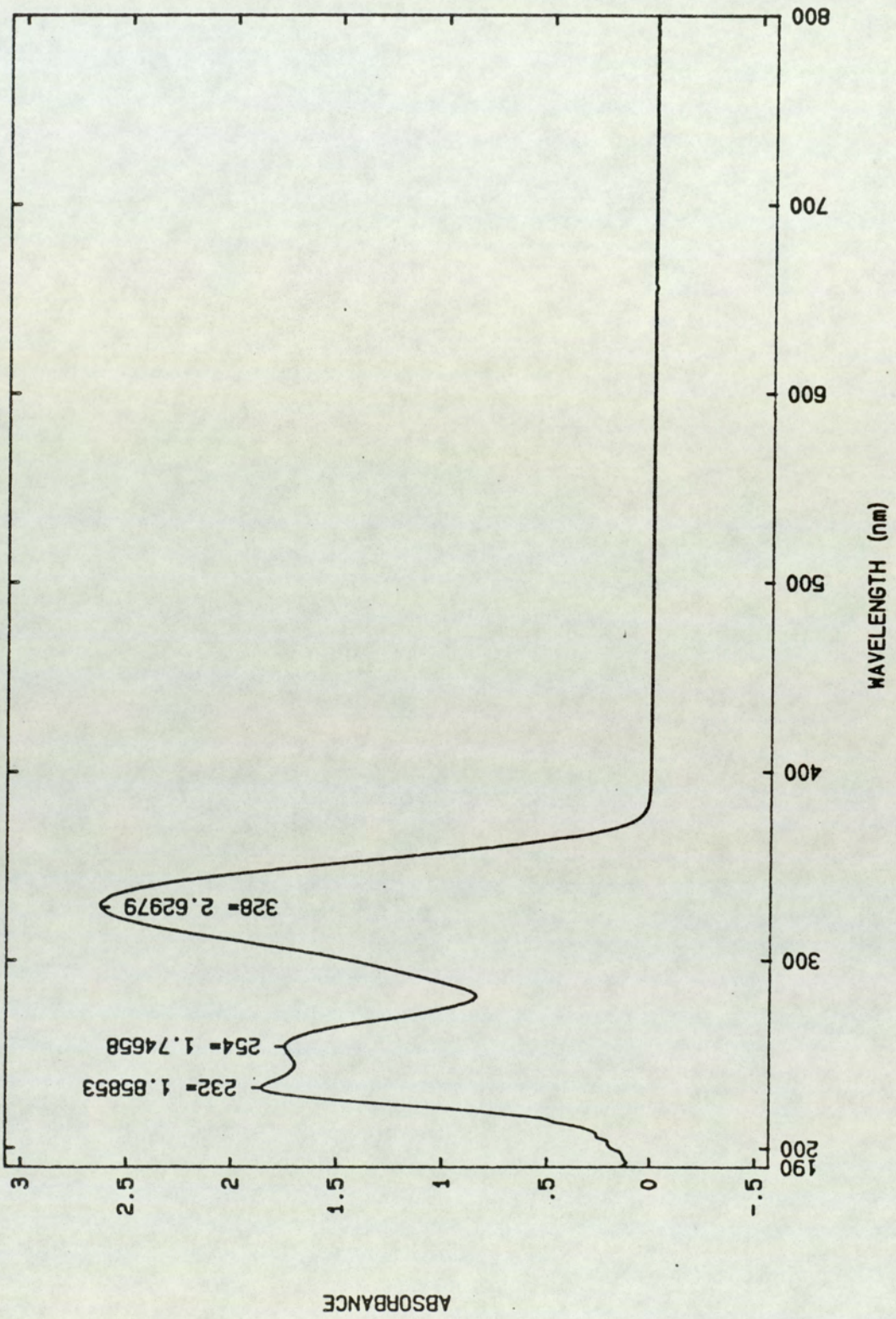


Fig.103 UV spectrum of metabolite II

### 3.9.2.2 Isolation and structural characterization of metabolite I

Initial isolation and purification procedures of metabolite I were achieved by repeated solvent extraction with ethylacetate at room temperature, solid phase extraction and isolation by HPLC. Although the extraction efficiency for this metabolite was poor ( $20.4 \pm 2.4\%$ ;  $n=6$ ), its recovery after solvent extraction as described in section 2.11.6.2 was good ( $>70\%$ ). Following this procedure, the metabolite was purified using  $C_{18}$  sep-pak cartridges and acetic acid (0.5%) as eluting solvent and yielded the metabolite and a trace amount of temozolomide as impurity. Metabolite I was subsequently separated from temozolomide by means of semi-preparative HPLC as described in section 2.11.6.2.

Listed in the following section are the physicochemical properties of metabolite I, which are reminiscent of a conjugate, perhaps a glucuronide: i) it is mildly acidic with a  $pK_a$  value of approximately 4.5, which is near to the values of other glucuronides reported in the literature (Dutton, 1966) ii) it can be extracted into ethylacetate only with low efficiency as compared to the extraction efficiency of temozolomide and metabolite II, iii) it is very water soluble, whereas temozolomide has a low water solubility (Slack, J.A., personal communication). In addition, UV analysis at four wavelengths and chemical reaction with alkali (see section 3.9.2) reveal that metabolite I probably possesses an intact tetrazinone ring. Furthermore, metabolite I gives

an orange colour reaction on the TLC with Pauly's reagent. This result indicates tentatively the presence of an imidazole ring in the molecule (fig.104). A positive colorimetric test with Tollen's reagent (naphthoresorcinol) lent further support to the suggestion that it may be a glucuronide (fig.105). Glucuronides, in general, are susceptible to acid hydrolysis (Dutton, 1966). As shown in fig.106, metabolite I decomposed in boiling concentrated HCl; however, there is no evidence of the appearance of other peaks indicating the presence of product of hydrolysis in the HPLC chromatogram. This result might reflect the instability of the aglycone in acid, if indeed there was a glucuronide. The metabolite was resistant to hydrolysis by glucuronidase/sulphatase (fig.107).

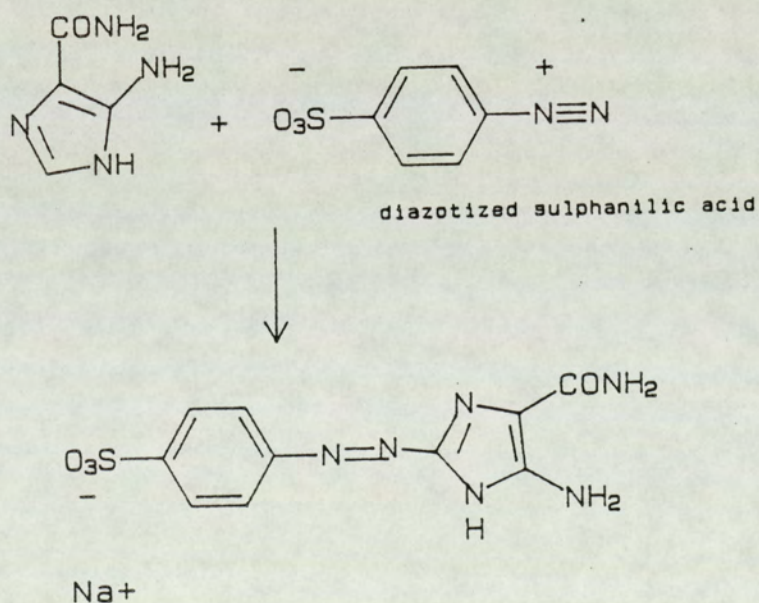


Fig.104 Principle of Pauly's reaction

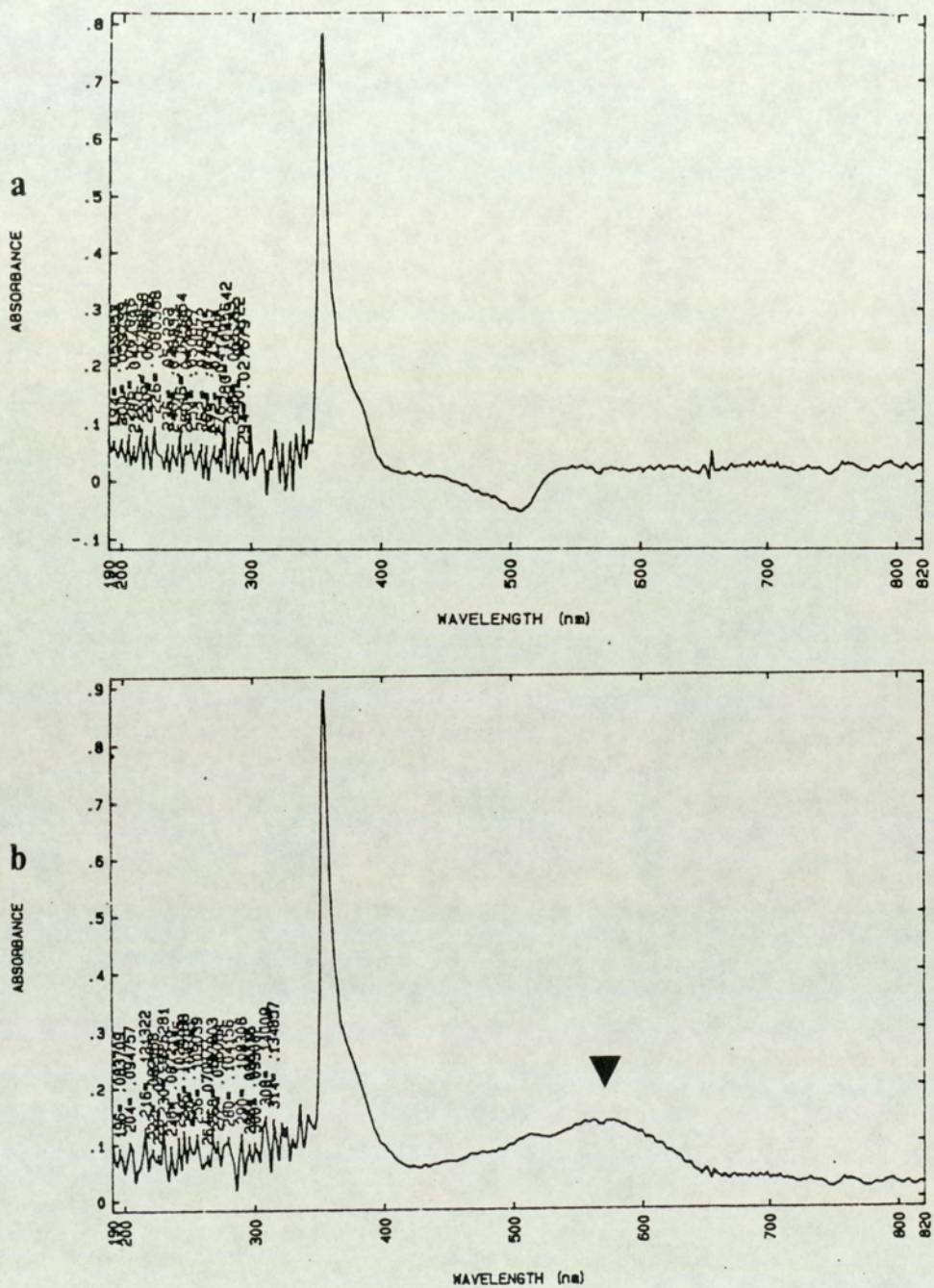


Fig.105 UV spectra of an ethylacetate extract of an acidic incubation of naphthoresorcinol with a) temozolomide and b) with metabolite I showing an absorbance at 570nm

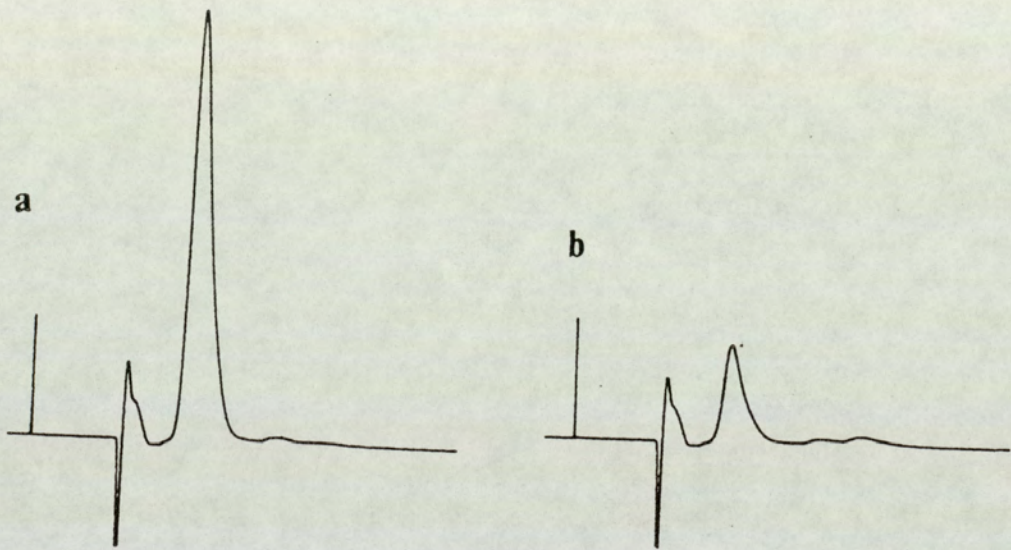


Fig.106 HPLC chromatogram of metabolite I a) before and b) after acid hydrolysis

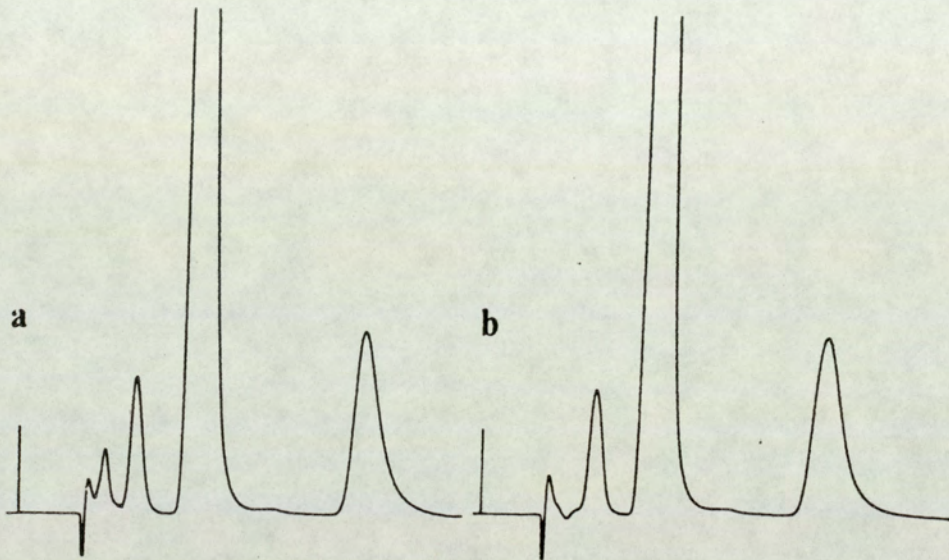


Fig.107 HPLC chromatogram of an ethylacetate extract of patient's urine a) before and b) after the treatment with glucuronidase and sulphatase

Some N-glucuronides have been known to be resistant to enzymic hydrolysis (Dutton, 1966) and it is conceivable that glucuronidation might have occurred at the carboxamide group. An example of this type of glucuronide is that of meprobamate, which is a centrally acting analgesic (Yamamoto et al, 1962; fig.108). It was found that N-glucuronidation occurred in the carbamate group (-OCONH<sub>2</sub>) of the molecule (Yamamoto et al, 1962).

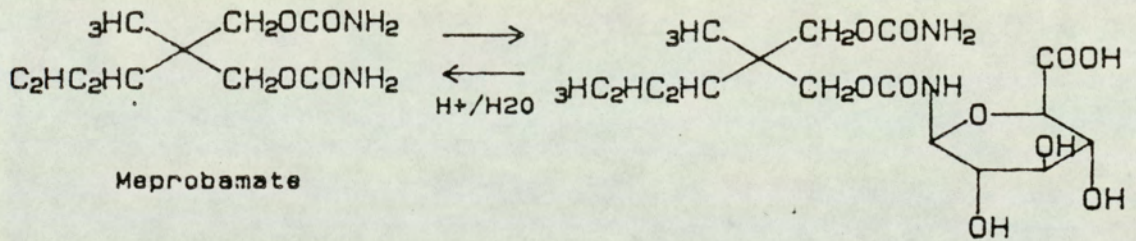


Fig.108 Structures of meprobamate and its glucuronic acid metabolite

If N-glucuronidation did occur in temozolomide, one should, in theory, be able to elucidate the structure of this molecule using EIMS after derivatization or "soft" ionization mass spectrometry, such as, CIMS, FDCI and FABMS; the latter has been used successfully to characterize a number of glucuronides, for examples, those of doxylamine, indomethacin and ketoprofen (Lay et al, 1986; Van Breemen et al, 1988). However, none of these modes of mass spectral analysis gave an interpretable and satisfactory spectrum. The possible explanations for the lack of mass spectral features may be due to the instability and poor volatility. In order to increase its volatility and to increase the retention time on the HPLC column for further purification, the acidic group was derivatized with diazomethane generated in situ by reacting N-methyl-N-nitroso-p-toluenesulphonamide (Diazald) with potassium hydroxide (see section 2.11.7.1). Metabolite I is not amenable to derivatization by this method. Fig.109 shows that the metabolite decomposes during derivatization yielding more than one derivatized products.



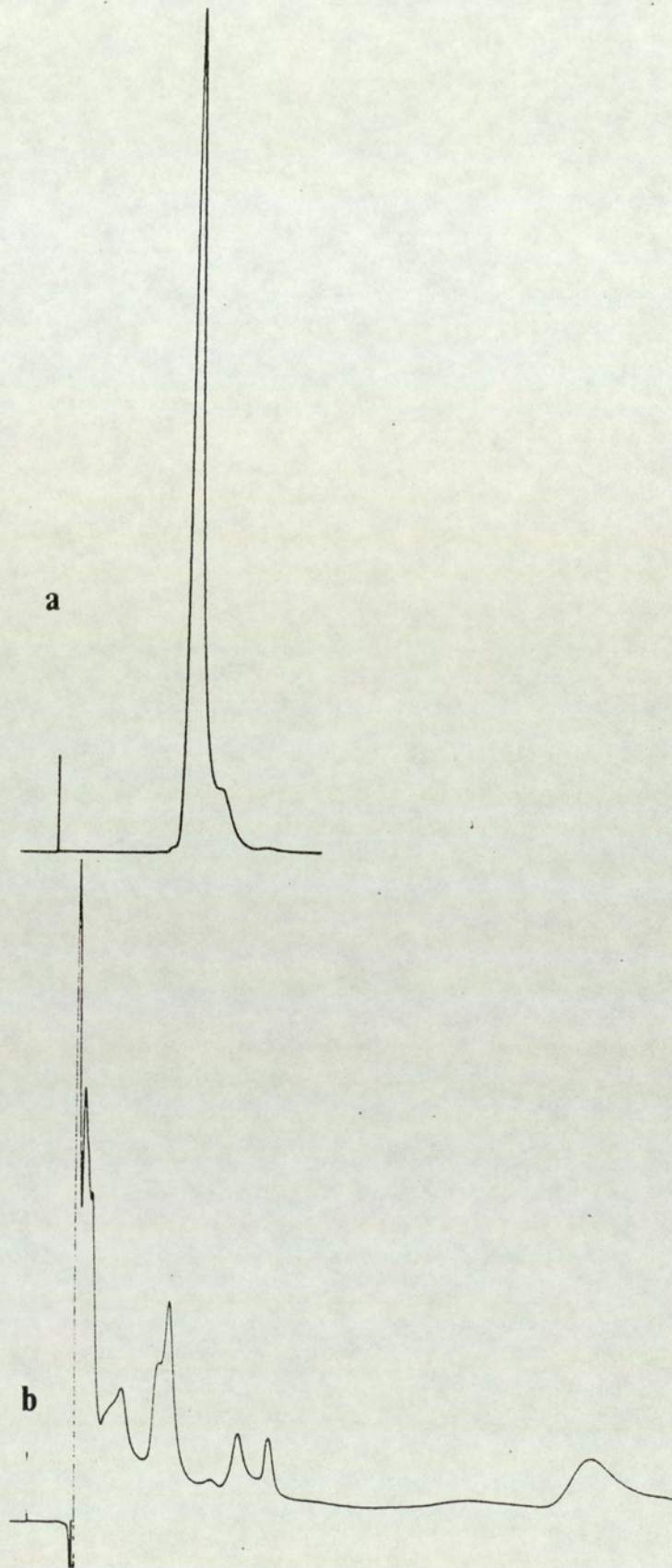


Fig.109 HPLC chromatograms of metabolite I a) before and b) after derivatizing with diazomethane

Further purification steps were necessary in order to obtain a purer sample of metabolite I to elucidate its structure by high field NMR and UV spectroscopy. As discussed in section 3.9.2, metabolite I is mildly acidic. It is, therefore, possible to take advantage of this property to purify it by ion exchange chromatography. Such a purification procedure allows the ionized metabolite, due to a change in pH, to be selectively retained on the column by ionic interaction with the sorbent. A Dowex (Cl<sup>-</sup>) resin was used and equilibrated with a counter ion with a lower selectivity. In this case, formate counter ion was chosen in order to allow the ionized metabolite to displace the counter ion with minimum competition for the charged sorbent. Figs.110-112 show the effect of pH of the formate buffer solutions on the elution of metabolite I from the anionic column. When the pH was above 4, the metabolite was retained on the column, presumably because it was ionized. As seen in fig.111b and 112a, metabolite I was completely eluted from the column as the pH was decreased presumably it was mainly in its unionized form. The collected eluent was then passed through a Dowex cationic exchange column to remove the majority of the formate salt. The eluent collected from the cationic column was freeze-dried and analyzed by high field <sup>1</sup>H NMR. As shown in fig.113, the resultant isolate consisted mainly of ammonium formate: a broad signal at 7.37ppm indicates the presence of an ammonium ion and the proton signal at 2.5ppm is due to formate proton. The ammonium formate present in the extract was finally removed by repeated HPLC purification

procedures using a 25cm C<sub>18</sub> column as described in section 2.11.6.2.

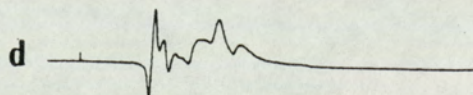
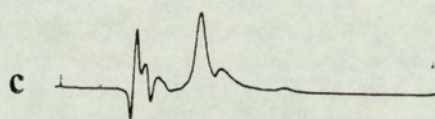
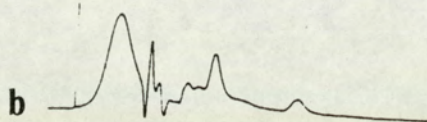
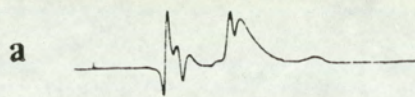


Fig.110 HPLC chromatograms of the eluents from the anionic exchange column at pH a,b) 6 and c,d) 5

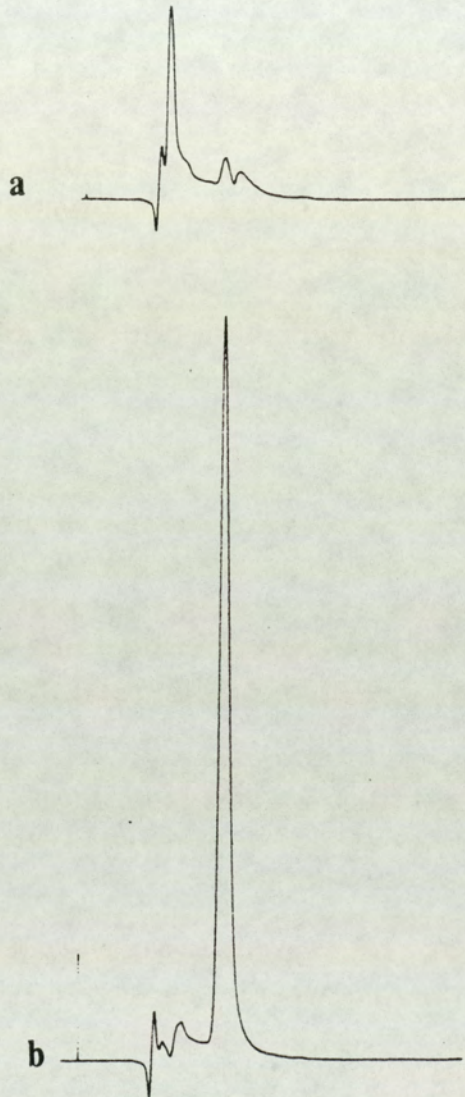


Fig.111 HPLC chromatograms of eluents from the anionic column at pH a) 5 and b) 4

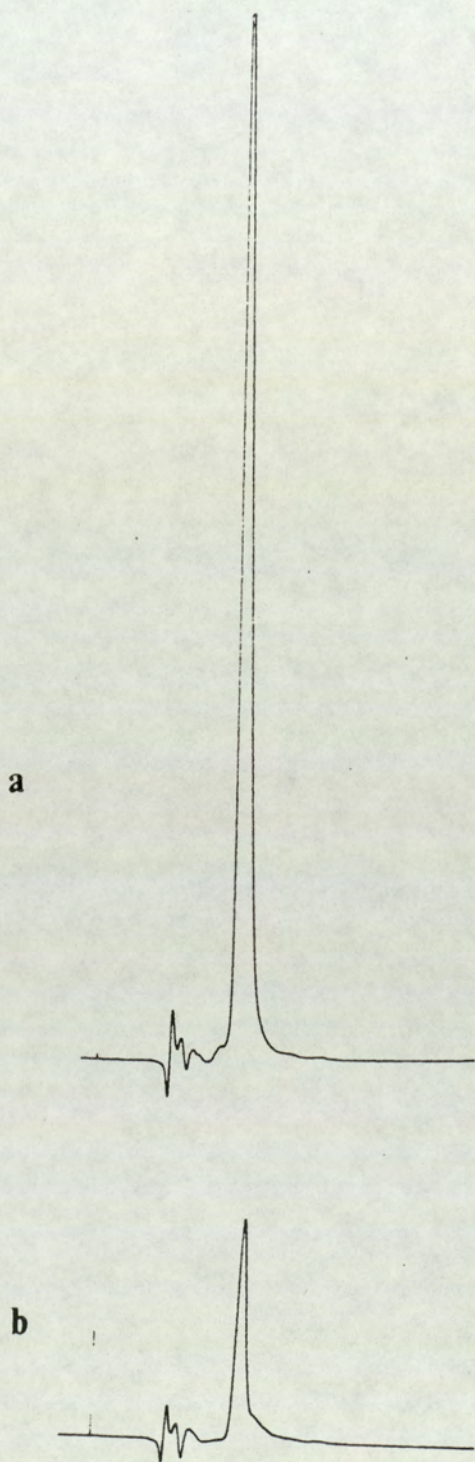


Fig.112 HPLC chromatograms of eluents from the anionic column at pH a) 4 and b) 3

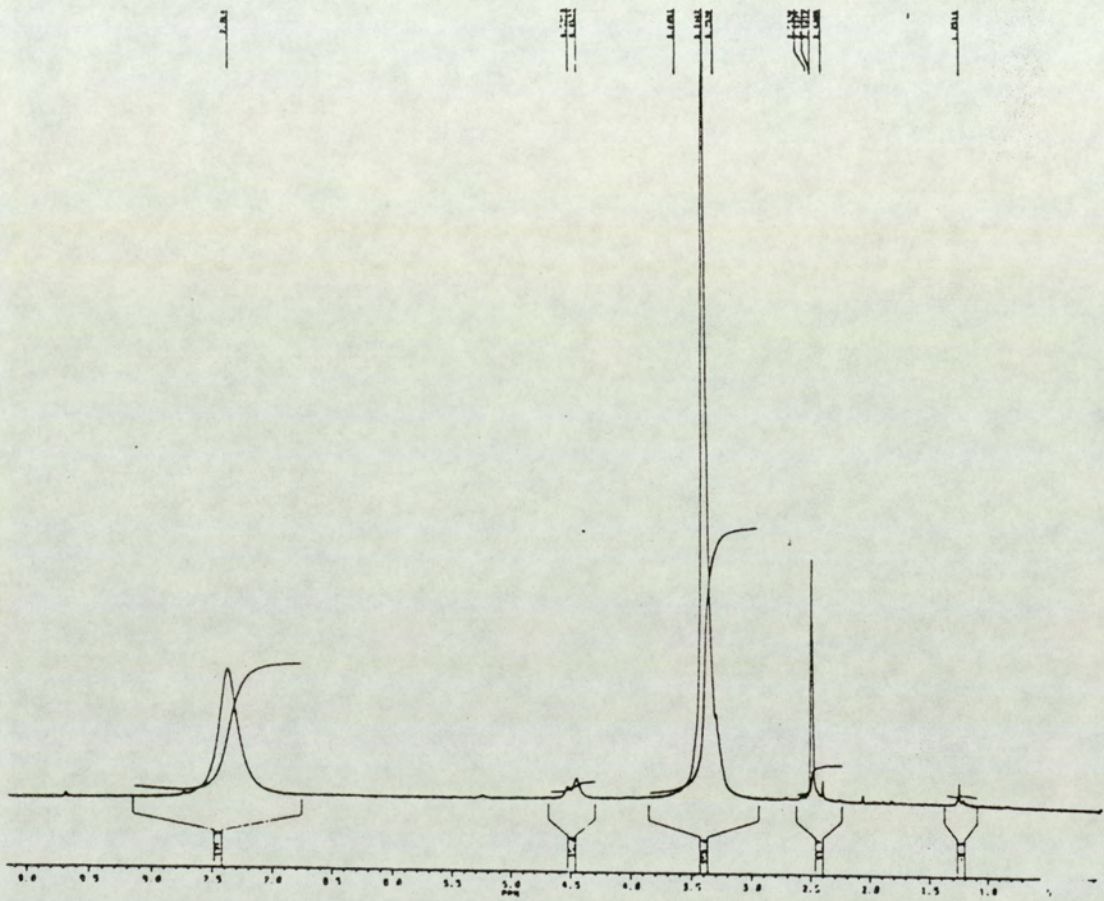


Fig.113 High field  $^1\text{H}$  NMR of the freeze dried extract collected from the anionic and cationic exchange columns

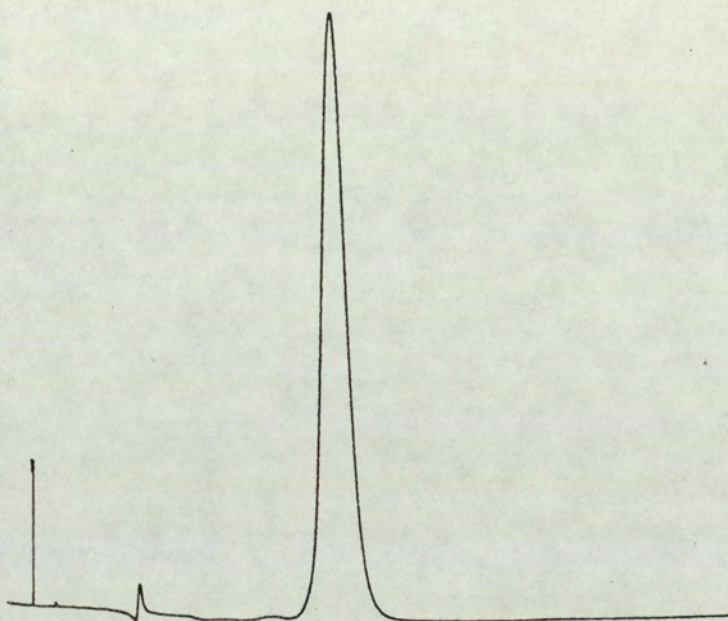


Fig.114 HPLC chromatogram of metabolite I eluted with 0.5% acetic acid using a 12.5cm RP select B column



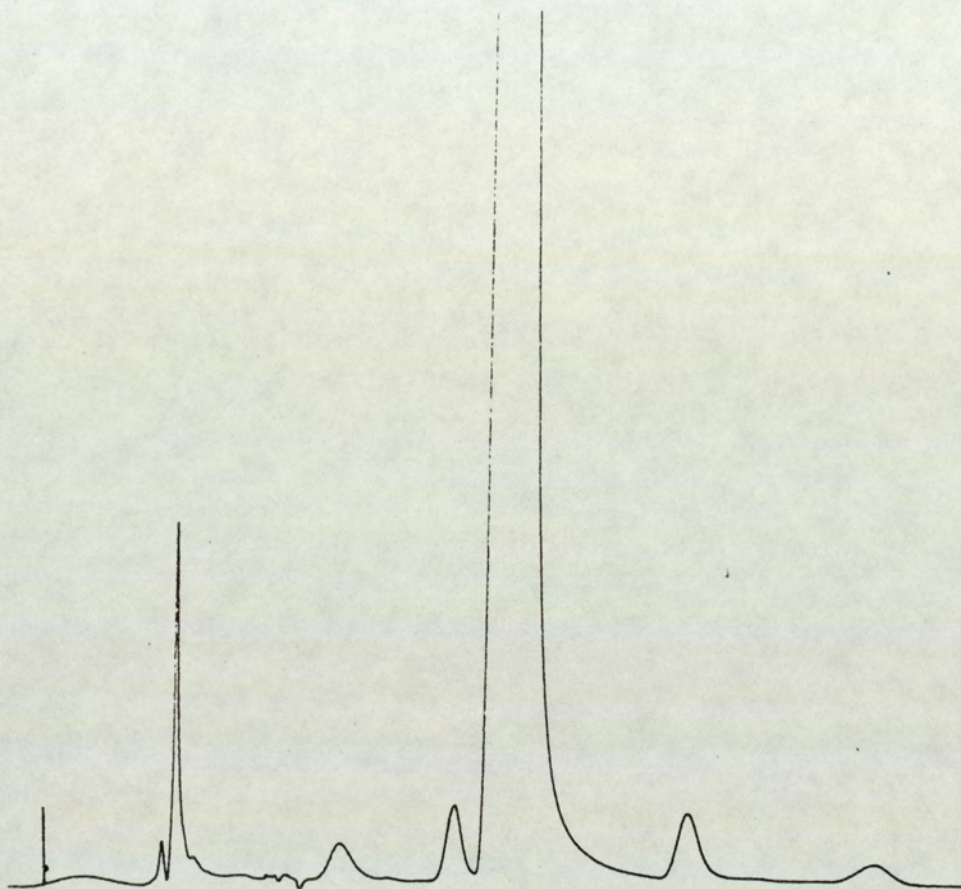


Fig.115 HPLC chromatogram of metabolite I eluted with 0.5% acetic acid using a 25cm RP select B column

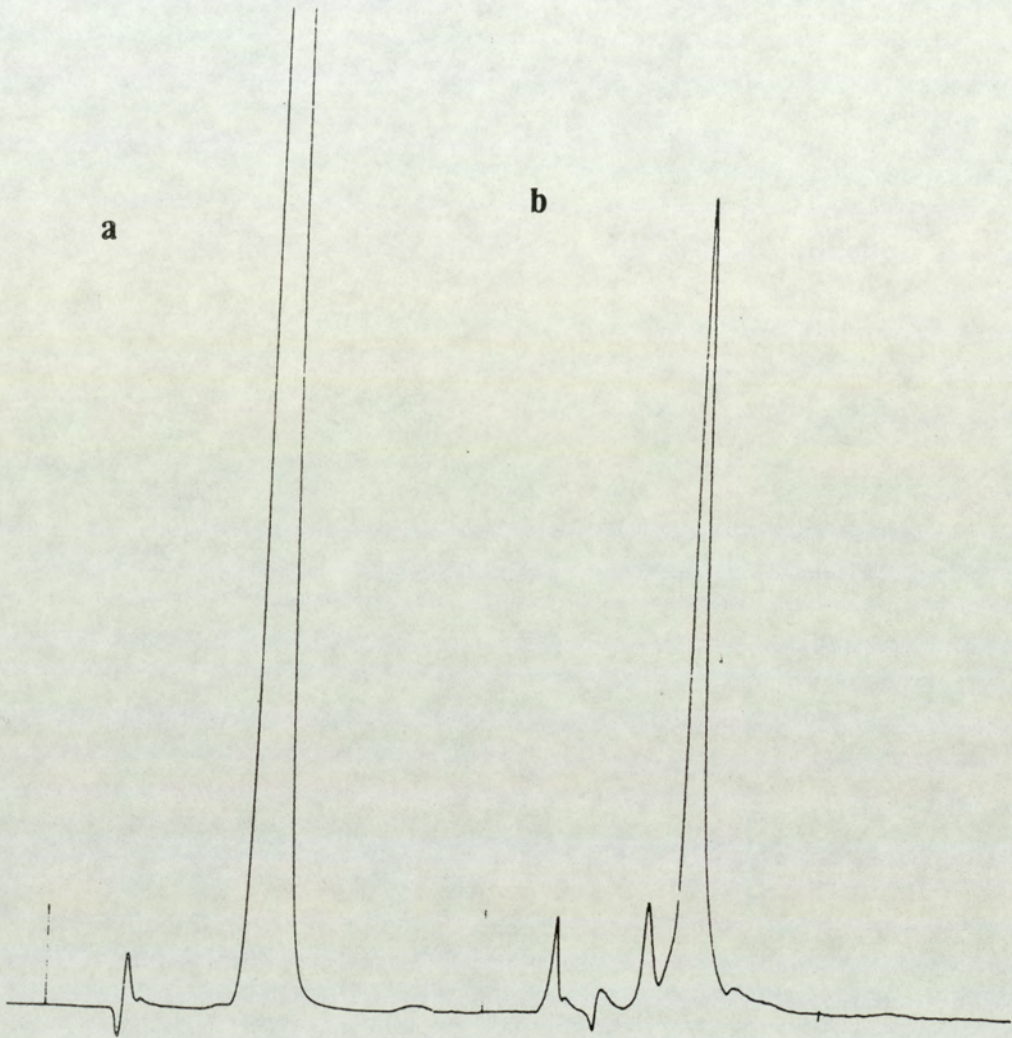


Fig.116 HPLC chromatogram of metabolite I after repeated HPLC purification detected by UV at a) 325nm and b) 205nm

Fig.117 shows the high field NMR spectrum of metabolite I. HPLC analysis was performed before and after NMR analysis to ascertain that the metabolite did not decompose. The salient features of the NMR spectrum of metabolite I was compared with those of temozolomide (fig.99 and section 3.9.2.1) and on this basis interpreted as follows: a singlet at 8.09ppm which indicates the presence of the imidazole proton; a doublet at 7.3ppm represents the protons in the carboxamide group (fig.118). The absence of the temozolomide N-methyl protons at 3.9ppm shows unambiguously that metabolism had occurred at this position of the temozolomide molecule. In addition, a number of aliphatic protons were also present between 0.86-1.69ppm: proton signals between 0.86-0.9 and 1.02-1.09ppm, which represents the equivalent of 1 (J=7.4Hz) and 4 protons (J=6.98Hz) respectively; three singlets at 1.13 (1H), 1.22(1H) and 1.69ppm (6H) were also present. Since the metabolite co-eluted with the radiolabelled urinary product found in mice, one could speculate that it retains a carbon atom in the N<sub>3</sub> position, possibly in the form of -N-CH<sub>2</sub>-. If the molecule was conjugated at this position, the carbon atom would become a prochiral centre thus rendering the methylene protons non-equivalent (Williams and Fleming, 1980). Under these circumstances, the presence of the two protons would be split due to mutual coupling and coupling possibly with the conjugation molecule.

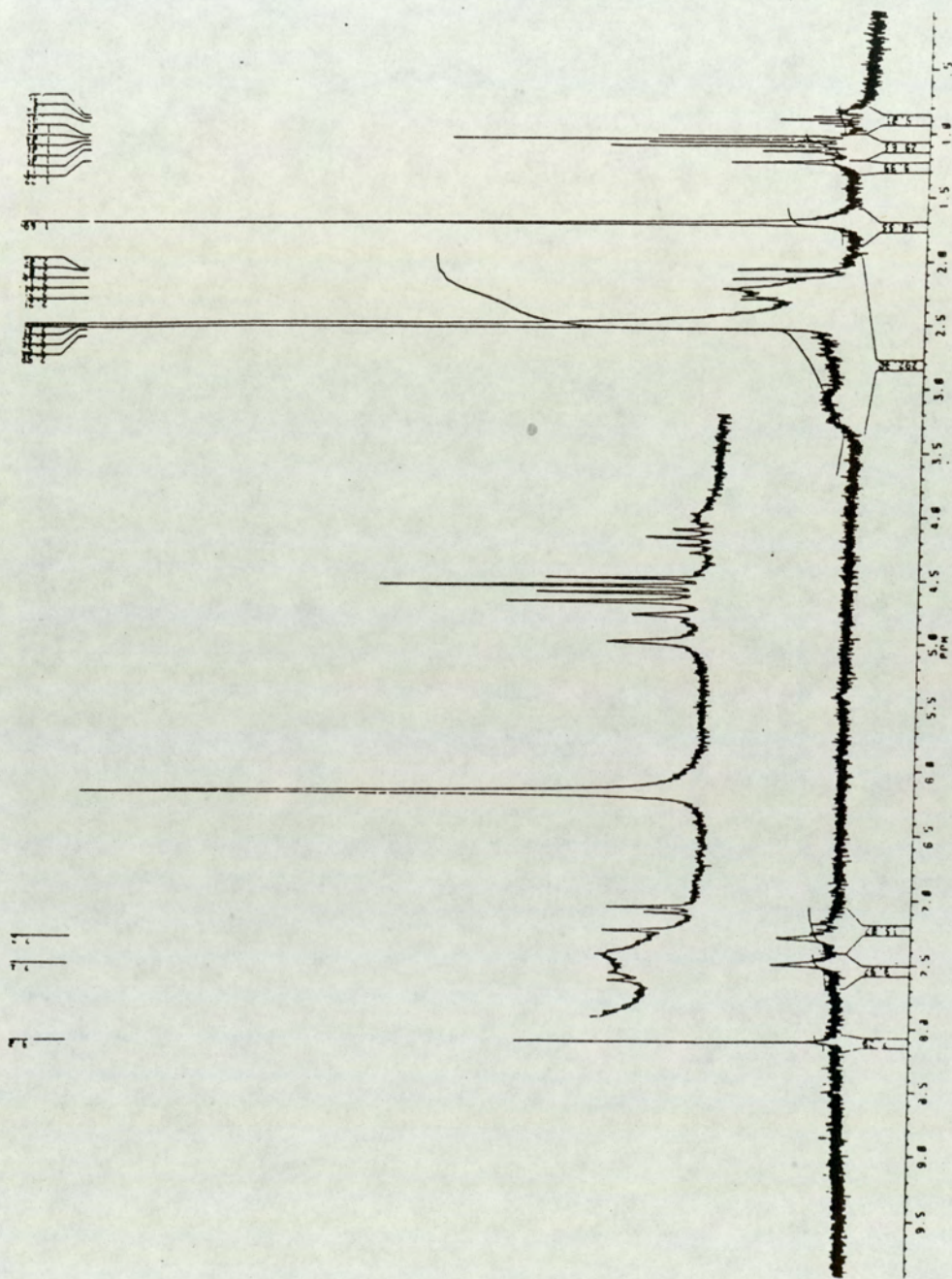


Fig.117 High field  $^1\text{H}$  NMR of metabolite I after pulsing for 4hr; water peak was suppressed by continuous secondary irradiation

The fact that most of the proton signals are further upfield relative to the N-methyl protons (3.9ppm) suggests that the methylene protons, if there are any, are positioned adjacent to an electron-donating group. There is no firm evidence that metabolite I is a glucuronide because of the absence of  $\beta$ -anomeric protons which usually occur between 5-6ppm (Wilson and Nicholson, 1988). Furthermore, the lack of proton signals corresponding to the  $\beta$ -D-glucuronyl moiety between 3-4ppm (Verweij and Kientz, 1981; Gallice et al, 1985; Monti, et al, 1985; Nicholson and Wilson, 1987; Wilson and Nicholson, 1988) provides further evidence that metabolite I is not a glucuronide. Fig.118 shows that metabolite I possesses a UV absorbance ( $\lambda_{\text{max}} = 322\text{nm}$ ) almost identical to that of metabolite II and temozolomide. These results show unambiguously that metabolite I is a metabolic derivative of temozolomide with an intact imidazotetrazinone ring.

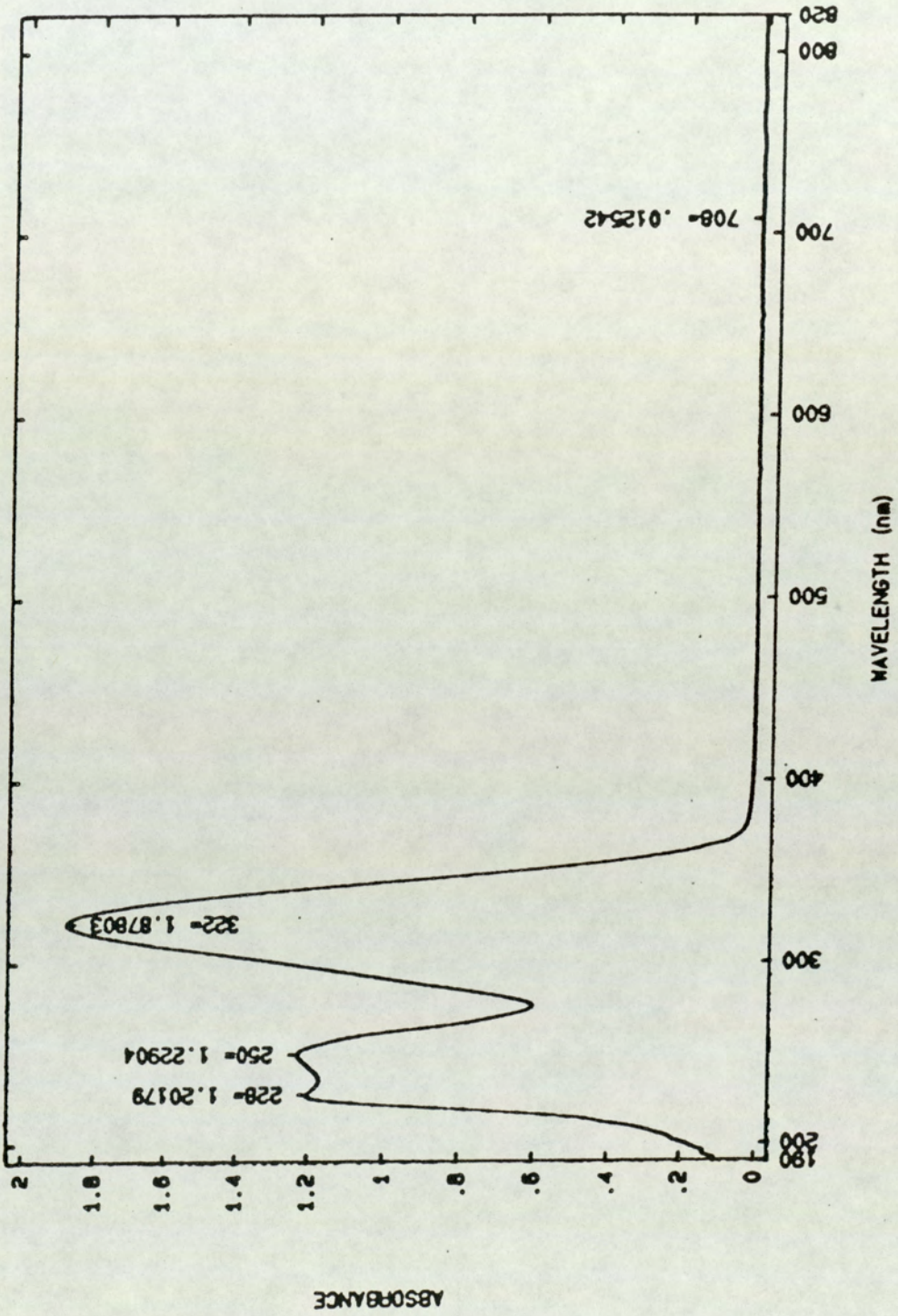


Fig.118 UV spectrum of metabolite I

### 3.9.3 Investigation of the cytotoxicity of metabolite I and II towards TLX5 cells.

As discussed in section 3.7.1, temozolomide does not require metabolic activation by microsomes to exert its cytotoxicity in vitro. Metabolite I and II are only formed in vivo, perhaps their formation is catalyzed by non-hepatic enzymes. Here, the hypothesis is tested that metabolites I and II are cytotoxic towards TLX5 lymphoma cells. Fig.119 shows the effect of metabolite I on the growth of TLX5 lymphoma cells. The concentration of the metabolite was determined by HPLC using temozolomide as the standard. Assuming that metabolite I has the same extinction coefficient as temozolomide, the concentration calculated should be a reflection of the approximate amount of the metabolite present. As shown in fig.120, metabolite I is not toxic towards TLX5 cells at concentrations of up to 20mg temozolomide equivalent/L. In contrast, metabolite II has an  $IC_{50}$  almost identical to that of temozolomide (fig.120 and 121).

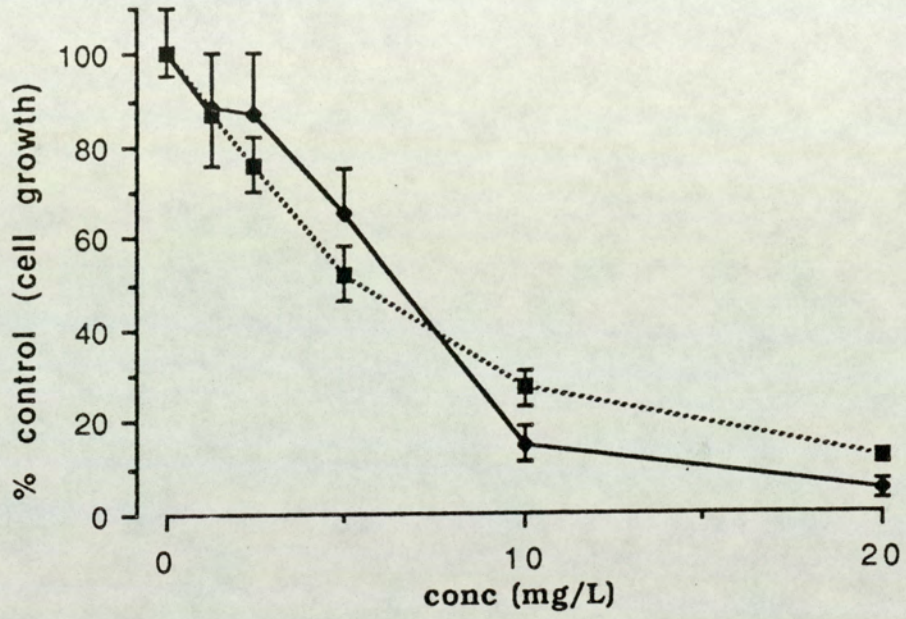


Fig.119 Cytotoxicity of temozolomide ■ and metabolite II ◆ against TLX5 lymphoma cells (n=4 ± 1 S.D.)



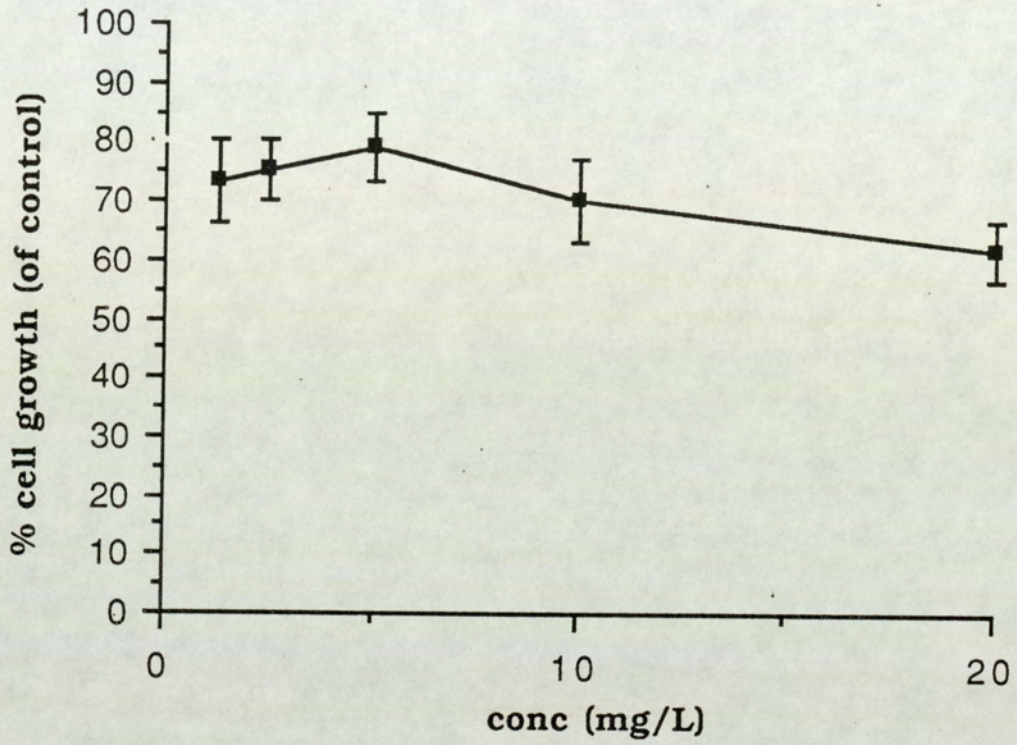
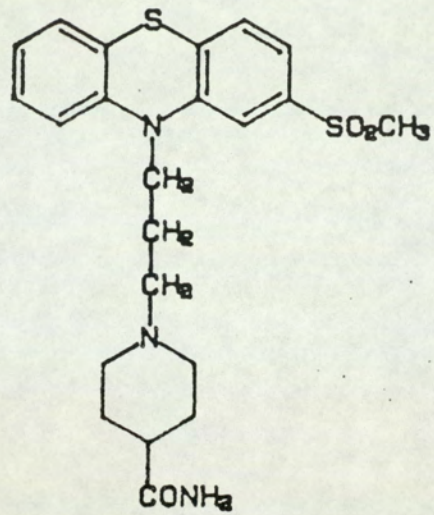


Fig.120 Lack of cytotoxicity of metabolite I against TLX5 lymphoma cells (n=4  $\pm$  1 S.D.)

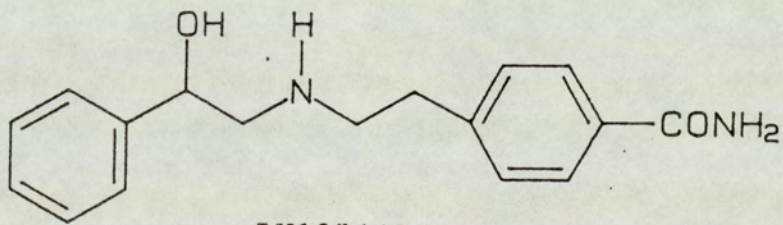
#### 3.9.4. Discussion

In this study, renal excretion was found to be the major route of elimination of unchanged temozolomide and its metabolites. A major urinary product, with a retention time 1.8min, was identified by HPLC and HPLC/radiochromatography in the urine of mice which had received temozolomide at 40mg/Kg and LD<sub>10</sub>. The same metabolite was also found in the urine of patients. An additional metabolite, with a retention time of 8min, was found only in patient's urine.

Metabolite II was fully characterized as the carboxylic acid derivative of temozolomide generated probably by hydrolysis of the carboxamide group. This type of metabolic hydrolysis is not well-documented, only a few examples have been reported in the literature. The first example of a drug which undergoes primary amide hydrolysis was metopimazine, a phenothiazine derivative used primarily as an antiemetic (fig.121, Testa and Jenner, 1978). Most recent examples are Rilmafazone (Koike et al, 1988; section 3.9.2.1), and LY195448 (Ho et al, 1988; Engineer et al, 1988). The former is a novel triazolyl benzophenone derivative, which possesses potential benzodiazepine properties. LY195448 is a benzamide derivative, which has been shown to possess broad spectrum antitumour activity in animals and is synergistic with several known anticancer drugs, for examples, 5-fluorouracil and doxorubicin. The absence of metabolite II in mouse urine might indicate that there is a species difference in the metabolism of temozolomide at the carboxamide group. Unlike the



Metopimazine



LY195448

Fig.121 Structures of metopimazine and LY195448

carboxylic acid derivative of mitozolomide (Horspool, 1988), the carboxylic acid derivative of temozolomide has been shown here to possess pronounced antineoplastic activity in vitro with almost the same  $IC_{50}$  as the parent compound. This is an interesting observation because at physiological pH the acid ( $pK_a \sim 3$ ) is ionized to form a carboxylate ion which decreases the ability of the molecule to diffuse across membranes. If the initiation of cytotoxicity is via attack at an intracellular target, one might expect to see decreased cytotoxicity in an ionisable derivative of temozolomide. In this case, the cytotoxicity of metabolite II is almost comparable to that observed with temozolomide. One might, therefore, argue that the cytotoxicity of metabolite II may be mediated via the cell membranes. Certainly, more experiments are required to support this contention.

The structure of metabolite I was not fully elucidated. However,  $^1H$  NMR and UV spectroscopy reveal some important features of this molecule: a UV  $\lambda_{max}$  at 328nm indicates the presence of an NNN linkage in the molecule; the presence of the imidazole and carboxamide protons indicates that the metabolite has an unchanged imidazocarboxamide structure; the absence of the N-methyl signal on the NMR spectrum indicates that the site of metabolism is at this position of the molecule. One could speculate that temozolomide undergoes N-methyl oxidation perhaps catalyzed by non-hepatic enzymes, because this metabolite was not found in metabolism experiments in vitro using liver fractions (section 3.6). The formation of

$^{14}\text{CO}_2$  in the breath of mice which had received [ $^{14}\text{C}$ -methyl]temozolomide might result from oxidative N-demethylation and chemical degradation of temozolomide. The synthesis of N-desmethyl temozolomide has not been achieved using the synthetic route as described in section 1.3.1 (Baig, G.U., personal communication). Since metabolite co-eluted with a urinary product found in the study using labelled material, it is likely that it still retains the methyl carbon in the molecule, probably as  $-\text{NCH}_2-$ . It is, therefore, conceivable that metabolite I is conjugated via this methylene group to an endogenous molecule which renders it acidic and water soluble. However, the lack of signals of the  $\beta$ -anomeric protons and the glucuronic acid protons on the  $^1\text{H}$  NMR and the resistance to hydrolysis by  $\beta$ -glucuronidase indicate that metabolite I is not a glucuronide. Since metabolite is not enzymically hydrolyzed by sulphatase, it is unlikely to be a sulphate conjugate. Metabolite I is also probably not a taurine conjugate which has the characteristic proton signals at 1.5 and 3.5ppm (Case, 1973). The lack of proton signals at 1.8, 2-2.8 and 4.4ppm also indicate the metabolite is not a mercapturate (Nicholson et al, 1985; Kestell et al, 1986; Nicholson and Wilson, 1987; and see fig.86). Conjugation with some other unusual endogenous molecules cannot be ruled out. Unlike metabolite II, metabolite I is not cytotoxic in vitro towards TLX5 lymphoma cells. The lack of cytotoxicity of this compound might be attributed to the absence of an intact N-methyl group as shown by  $^1\text{H}$  NMR. Structure-activity analysis of a

number of dialkyl phenyl- or imidazo- triazenes has revealed the importance of at least one methyl group in the N<sub>3</sub> position for antitumour activity (see introduction section 1.2.3). The results obtained in this study appear to be consistent with these findings. The small amount of radioactivity found in faeces might be indicative of biliary excretion; however, since the drug was administered via the i.p. route, it is possible that the drug diffused into the gastrointestinal tract. Hence, the chemical nature of the faecal radioactivity remains speculative. Temozolomide has been shown to react readily with calf thymus DNA (Bull and Tisdale, 1987). Therefore, the radioactivity found in the carcasses could possibly be due to alkylation of intracellular targets via the formation of the reactive MTIC.

### 3.10 Murine pharmacokinetics in vivo

Pharmacokinetics of temozolomide in vivo has been performed previously in mice (Goddard, 1985; Slack et al, 1986) at doses of 10mg/Kg and 20mg/Kg via the i.p. route. In that study, only the parent compound was analyzed and MTIC could not be detected because of its instability in the mobile phase used in that study (see section.2.4.1). The pharmacokinetic evaluation accompanying the phase I clinical trial commenced in 1987 with a starting dose of 50mg/m<sup>2</sup> given by i.v. infusion and higher doses, given by the p.o. route (Slack et al, 1989). As discussed in section 3.8.2, it has been demonstrated that temozolomide undergoes chemical decomposition to liberate the MTIC. In order to test the hypothesis that chemical decomposition is an important route of disposition of temozolomide and that MTIC is generated in vivo, experiments were designed to examine the pharmacokinetics of temozolomide and its metabolite, MTIC, in plasma and tumour tissue. In addition, the in vivo pharmacokinetics of MTIC at the same dose are also investigated in order to compare with that of temozolomide. In vivo screening studies using transplanted s.c. TLX5 lymphoma had demonstrated that temozolomide had an optimal antitumour and therapeutic activity at a dose of 40mg/Kg (Stevens et al, 1987). On the basis of this information, the pharmacokinetics of temozolomide in CBA/CA mice bearing TLX5 tumour implanted s.c. was conducted at this dose. Unlike in the previous study (Goddard, 1985), here temozolomide was administered to mice via i.v. route in order to ensure that all the administered drug entered

the body, hence providing a realistic profile of the distribution of drug in plasma and tumour.

The individual experimental data are tabulated in Appendices II, III, IV and the pooled results are tabulated in tables 8 and 9.

Figs.122b&c show the HPLC chromatograms of the plasma samples collected after 5 and 10min of drug administration. Two peaks were identified in the plasma with retention times identical to those of temozolomide and MTIC, they were not found in the plasma of a mouse receiving DMSO in normal saline only (fig.122a). Fig.123 shows a semi-log plot of plasma concentration of temozolomide and MTIC versus time. The correlation coefficient for the line were  $0.96 \pm 0.03$  ( $n=4$ ). On the basis of these results, the data was described by a simple one-compartment open model. This model assumes instantaneous distribution of the dose throughout a single compartment where the levels of drug decline in an exponential manner, indicating that the elimination follows first order kinetics (Rowland and Tozer, 1981; Gibaldi and Perrier, 1980). Temozolomide had an elimination  $t_{1/2}$  of  $0.66 \pm 0.07$ hr, which is consistent with that obtained for the decomposition of the drug in plasma in vitro (see section 3.4). The drug was rapidly distributed to the tumour tissue with the maximum concentration,  $54.3 \pm 23.7$ mg/Kg, achieved 15min after drug administration (fig.128). The AUC of temozolomide in the tumour was almost comparable to that achieved in plasma, with the values respectively  $72.04 \pm 16.01$  mg.hr/Kg and  $64.93 \pm 11.85$  mg.hr/L (fig.128). The maximum concentration



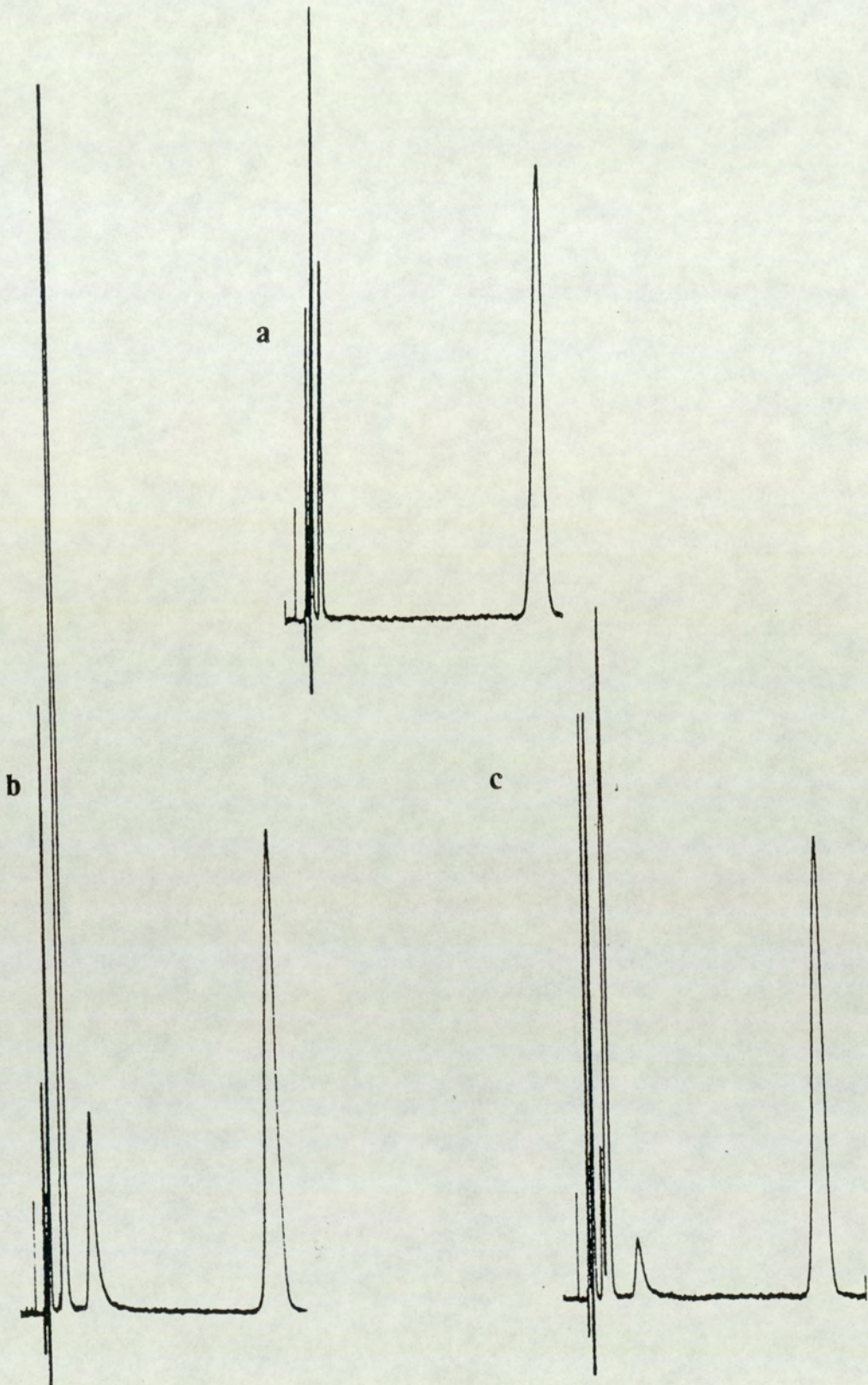


Fig.122 HPLC chromatograms of a sample of plasma of a mouse which had received a) DMSO/normal saline, b) temozolomide 5min and c) 10min after drug administration

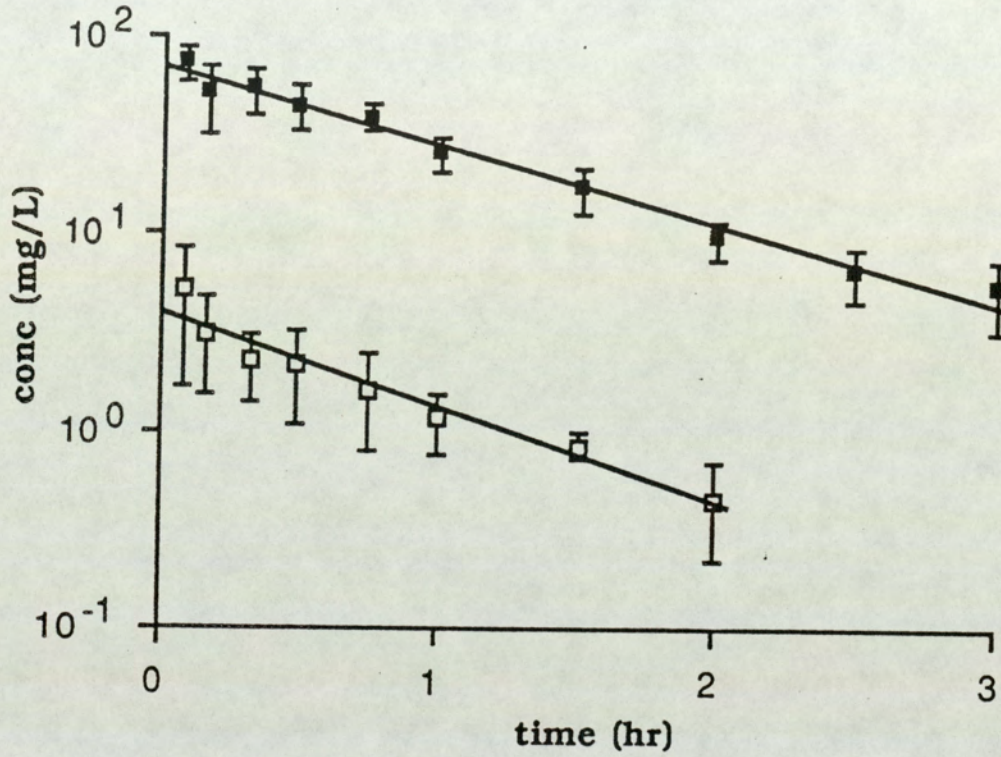


Fig.123 In vivo murine plasma pharmacokinetics of temozolomide and its major metabolite MTIC after a single i.v. bolus injection at 40mg/Kg (n=4 animals  $\pm$  1 S.D.)

temozolomide ■

MTIC □

of MTIC,  $5.14 \pm 3.46$  mg/L, was achieved 5min after the administration of temozolomide, but MTIC was not detected in the tumour, possibly due to its extreme lability and reactivity towards nucleophiles. The AUC of MTIC in the plasma was  $2.9 \pm 0.9$  mg.hr/L. By comparison of the AUC and clearance values obtained for temozolomide and MTIC, it was found that  $19.6 \pm 6.2\%$  of temozolomide was converted to MTIC. When MTIC was given to mice at 40mg/Kg by the i.v. route, the drug rapidly disappeared from the plasma with an AUC of  $0.9 \pm 0.2$  mg.hr/L, which is significantly less than that of MTIC generated from temozolomide (figs.124 and 125). MTIC was not detected in the plasma beyond 15min after drug administration and in the tumour at any time point. Fig.126a&b show that there is no observable degradation of MTIC in normal saline for up to 3hr when the prepared solution was stored on ice. In addition, Metabolite I was detected in the tumour (fig.127).

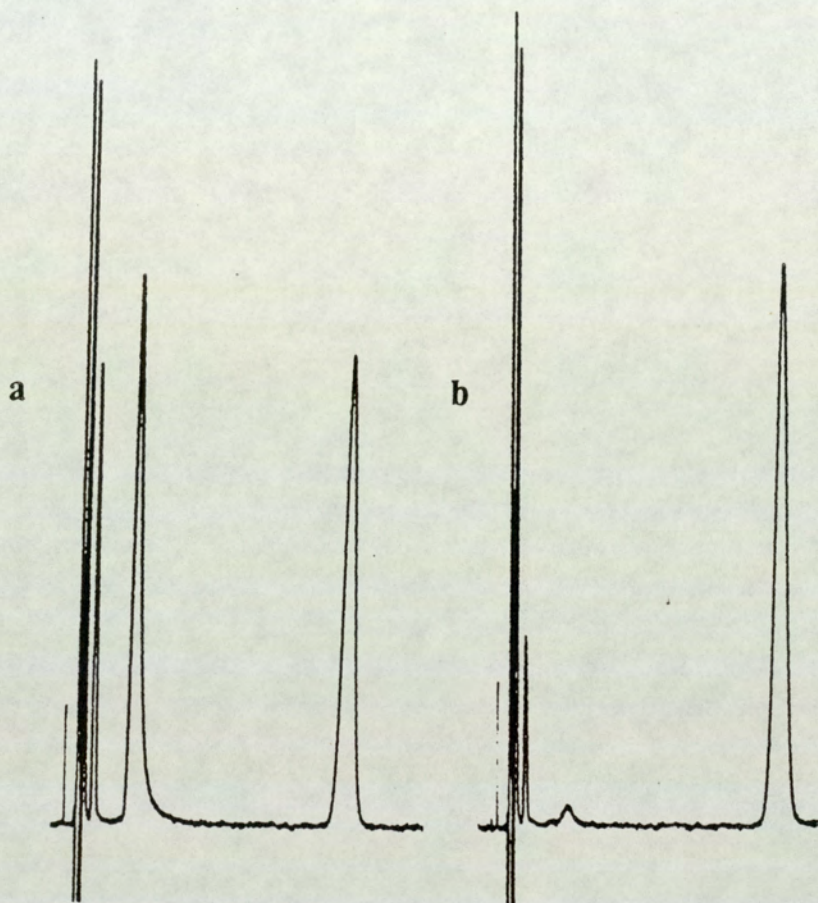


Fig.124 HPLC chromatograms of a sample of plasma of a mouse which had received MTIC a) 5min and b) 10min after drug administration

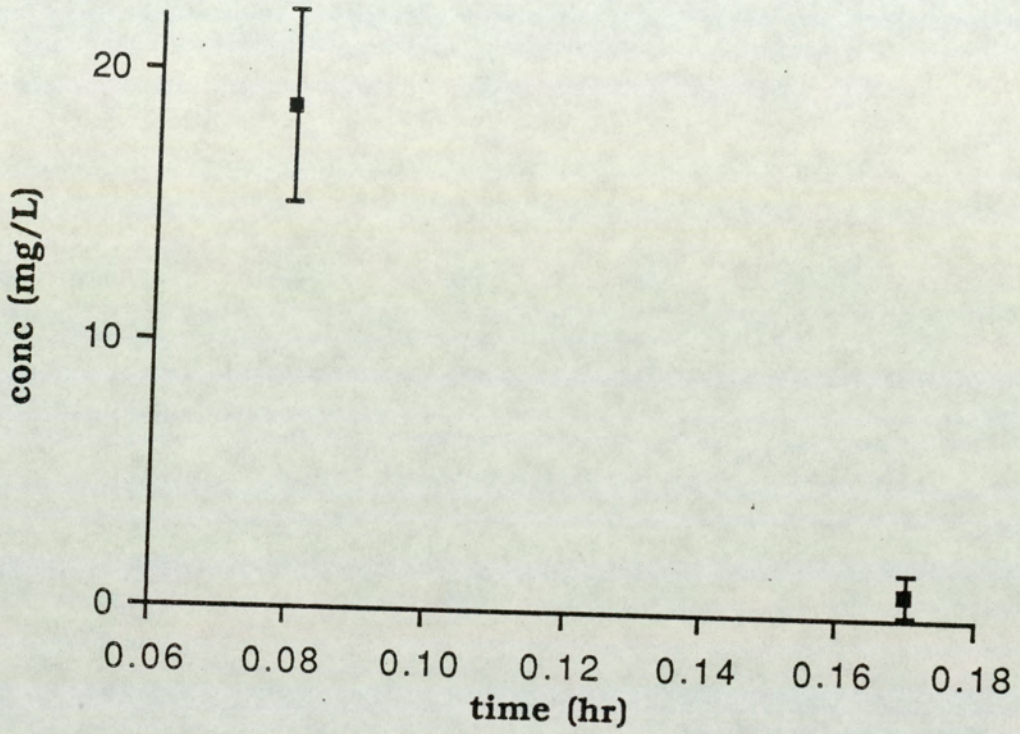


Fig.125 In vivo plasma pharmacokinetics of MTIC after a single i.v. bolus injection at 40mg/Kg (n=4 animals  $\pm$  1 S.D.)

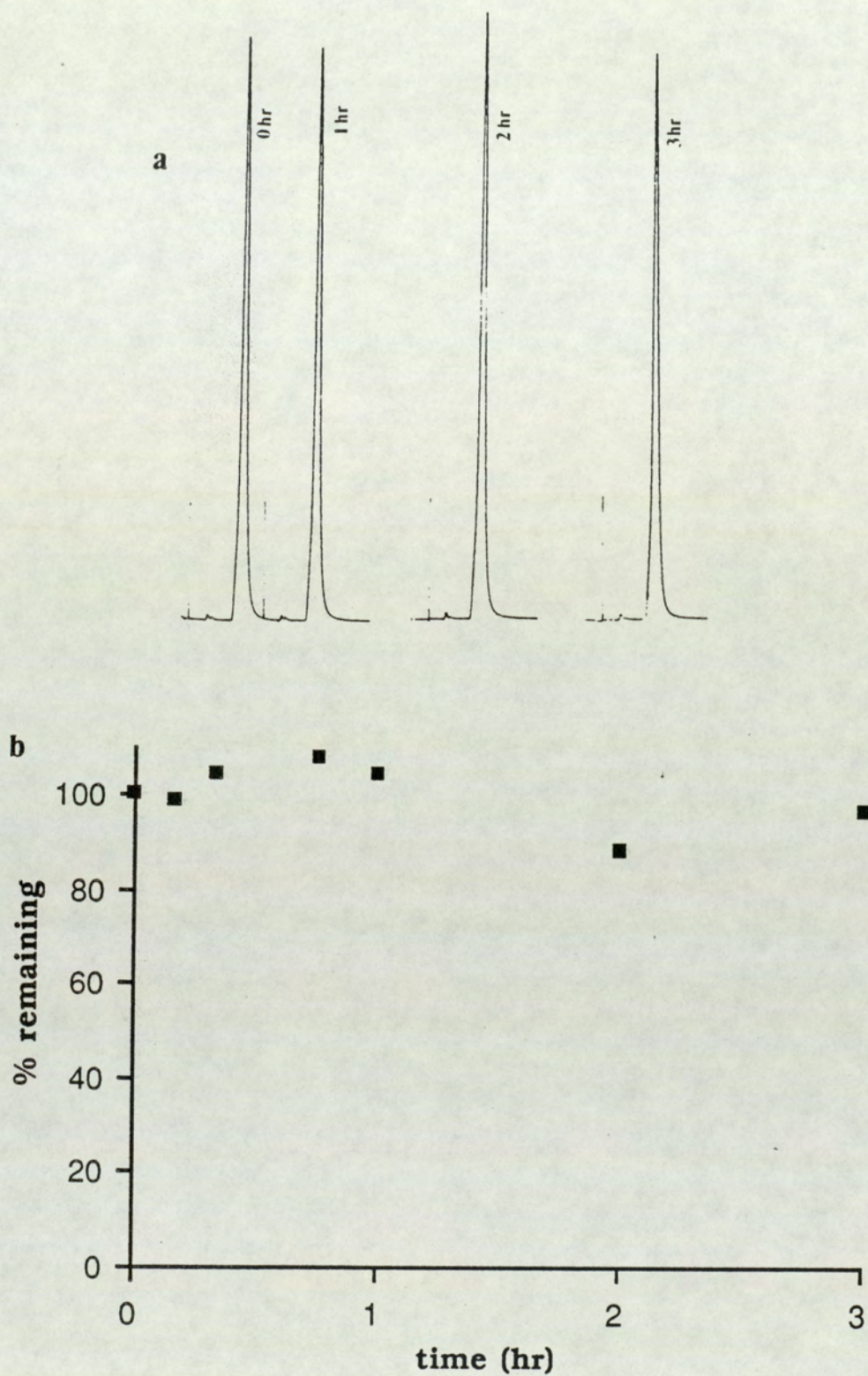


Fig.126 a) HPLC chromatograms b) a graph showing the stability of MTIC in normal saline on ice/water

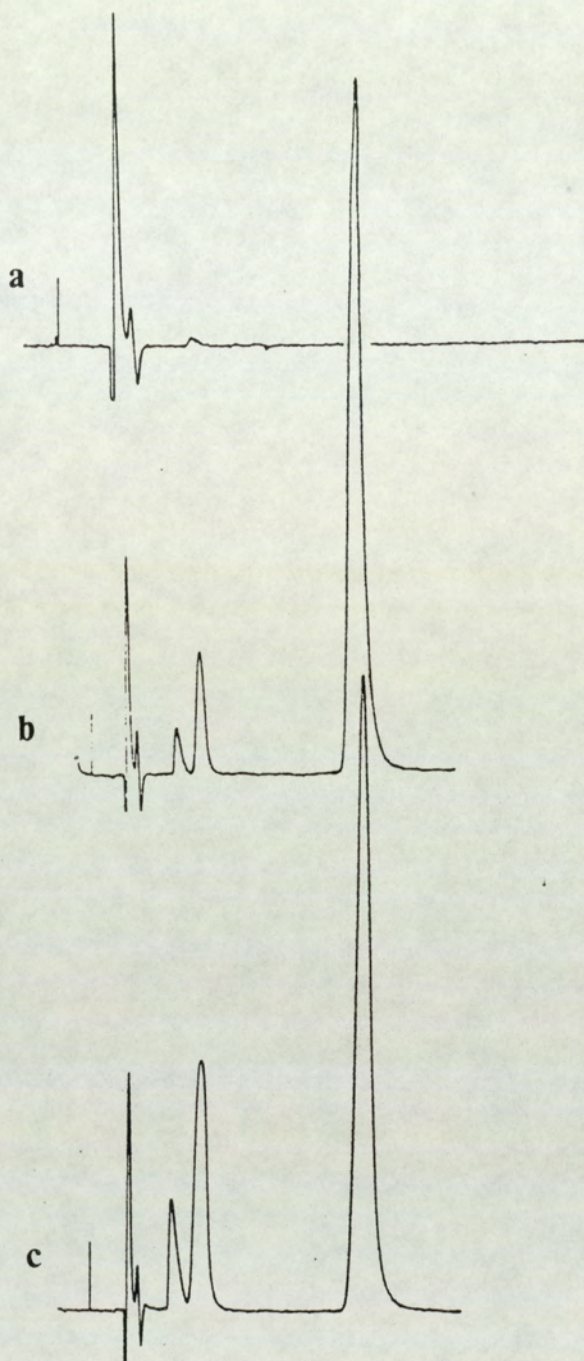


Fig.127 HPLC chromatograms of a) a sample of tumour of a mouse received DMSO/normal saline, b) 5min and c) 10min after the administration of temozolomide

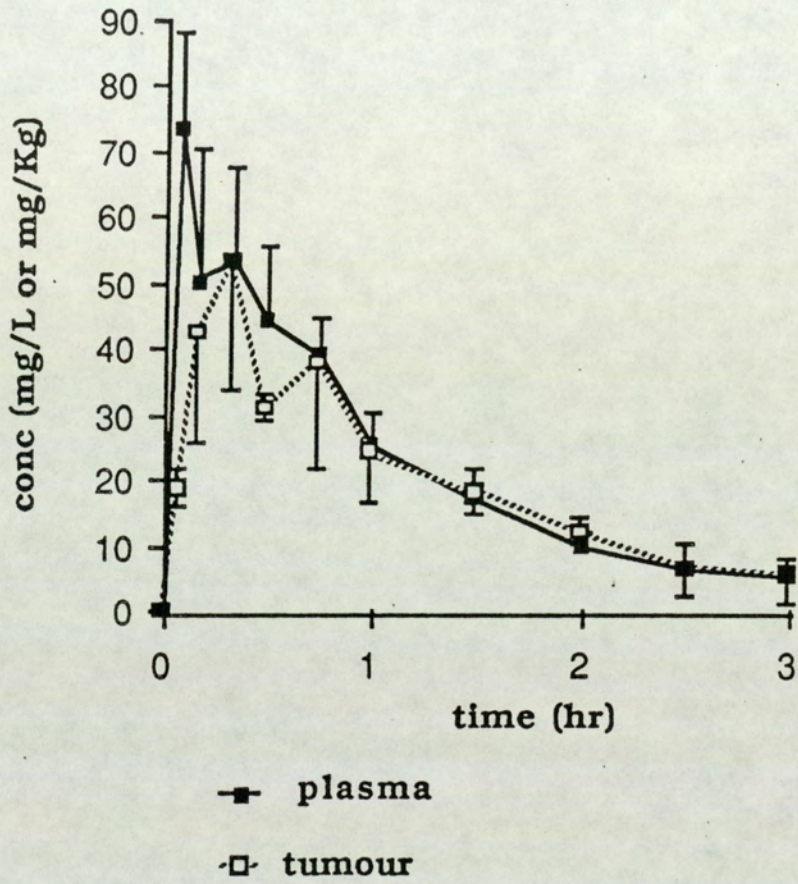


Fig.128 In vivo tumour and plasma pharmacokinetics of temozolomide after a single i.v. bolus injection at 40mg/Kg (n=4 animals  $\pm$  1 S.D.)



### 3.10.1 Discussion

Following i.v. administration, the pharmacokinetics of temozolomide in mice could be described by a single one compartment open model. This observation is supported by the lack of an apparent distribution phase and its elimination follows first order kinetics. The volume of distribution calculated is less than the total body water (0.018-0.025L for mice) (Goddard, 1985; Curry, 1982). The elimination  $t_{1/2}$  was  $0.66 \pm 0.07$  hr which is comparable to that obtained in vitro decomposition in plasma (section 3.4). This result is consistent with the interpretation that chemical decomposition is an important route for the elimination of temozolomide in vivo and that MTIC is probably formed as an intermediary of this process. Indeed, MTIC is detected in plasma with a maximum concentration,  $5.14 \pm 3.46$  mg/L, achieved 5 min immediately after the administration of temozolomide. A plot of plasma concentration of MTIC versus time is linear and parallel to that of temozolomide (fig.124). This observation probably reflects a quicker elimination of MTIC from the plasma than that of temozolomide (Gibaldi and Perrier, 1980; Rowland and Tozer, 1981). When MTIC was given to mice at 40mg/Kg via i.v. route, it eliminates readily from the plasma with an elimination  $t_{1/2}$  less than 2min. This result is congruent with that found in vitro degradation studies (see section 3.4), suggesting that chemical decomposition plays an important rôle in its elimination in vivo.

Since temozolomide produced similar screening results to those obtained with DTIC (Stevens et al, 1987), it is of

interest to compare the pharmacokinetics of temozolomide with that seen for DTIC. As discussed at the beginning of this section, the kinetics of temozolomide can be described by a single compartment model with a peak plasma concentration of  $73.45 \pm 14.72$  mg/L and an elimination  $t_{1/2}$  of just over half an hour. In both animals and man (Breithaupt et al, 1982; Skibba et al, 1969; Loo et al, 1968a&b), the kinetics of DTIC can best be described by a two-compartment model with a rapid distribution phase preceding a slower elimination phase. Following a single i.v. bolus injection of DTIC at 40mg/Kg, a dose used throughout the present kinetic studies, the plasma  $t_{1/2}$  of DTIC was 12.7min in mice (Rutty et al, 1980). The peak plasma concentration of MTIC generated metabolically in mice was equivalent to 7.98mg/L (Rutty et al, 1980), which is similar to that obtained in this study with temozolomide,  $5.14 \pm 3.46$  mg/L. Temozolomide may possess distinct pharmacokinetic advantages over DTIC: temozolomide produces relatively sustained levels of the parent drug in plasma when compared with DTIC. In addition, the plasma kinetics of temozolomide also reflect a similarly high tumour concentration as observed in this study (fig.127). TLX5 lymphoma cells cannot bioactivate and metabolize DTIC (see section 3.7). Therefore, in the case of DTIC, the exposure of the tumour to MTIC is solely dependent upon the labile metabolites in circulation such as MTIC and HMMTIC. Unlike DTIC, temozolomide is capable of generating MTIC in situ upon chemical decomposition (see section 3.7.1 and 3.8.1). MTIC and HMMTIC have a  $t_{1/2}$  of 2 and 16min

respectively (see section 3.4 and 3.8). When MTIC was given at 40mg/Kg via i.v. route to mice, the plasma AUC calculated was significantly less than that generated from temozolomide. One can, therefore, argue that the metabolic generation of HMMTIC and MTIC may not produce the comparable levels of MTIC in tumour in comparison with that produced from temozolomide. In addition, unlike DTIC (Loo et al, 1968), temozolomide possesses excellent bioavailability when given by p.o. route (Goddard, 1985; Slack et al, 1986; Slack et al, 1989).

Dose (mg/Kg)	$t_{1/2}$ (hr)	Cpmax (mg/L)	AUC (mg.hr/L)	Vd (L)	Cl (L/hr)	fm
40	0.66	73.45	64.93	0.0098	0.0011	0.196
	$\pm 0.07$	$\pm 14.77$	$\pm 11.85$	$\pm 0.002$	$\pm 0.002$	$\pm 0.062$

Table 8 Summary of the pharmacokinetic parameters of temozolomide in CBA/CA mice

Dose (mg/Kg)	$t_{1/2}$ (hr)	Cpmax (mg/L)	AUC (mg.hr/L)	Vd (L)	Cl (L/hr)
40	0.26	18.70	0.088	0.033	0.85
	$\pm 0.006$	$\pm 3.57$	$\pm 0.16$	$\pm 0.011$	$\pm 0.12$

Table 9 Summary of the pharmacokinetic parameters of MTIC in CBA/CA mice

Section 4  
General Discussion

#### 4 General Discussion

The aim of the present study is concerned with the elucidation of the pharmacokinetic properties and the metabolism of an imidazotetrazinone, temozolomide (section 1.4). The results obtained in the previous sections will now be discussed in a broader context with a view to elucidating its mode of action. Fig.128 depicts the proposed pathways of metabolic and chemical decomposition for DTIC and temozolomide. Integral to this scheme is the generation of MTIC from temozolomide and DTIC, which seems to be important in the mechanism of cytotoxic action of these two antineoplastic agents. Temozolomide has been postulated to be a stable prodrug of MTIC in that MTIC should be generated upon chemical decomposition of temozolomide (section 1.3.1 and 1.3.4). The mechanism of decomposition of temozolomide is thought to involve an initial nucleophilic attack at C<sub>4</sub> to generate the linear monomethyltriazene MTIC which is also a metabolite of DTIC (sections 1.3.1 and 1.3.4). The results obtained in the in vitro and in vivo metabolic and pharmacokinetic studies (sections 3.8 and 3.10) leave no doubt about the suggestion MTIC is generated chemically from temozolomide. In vivo screening data shows that temozolomide possesses comparable and, in some cases, superior antitumour activity to DTIC (Langdon et al, 1985a&b; Stevens et al, 1987). The biochemical study conducted by Tisdale (1985) has shown that temozolomide, like monomethyltriazene, can induce cell differentiation in human leukaemia line K562. Furthermore, a line of the L1210 leukaemia, which has been made

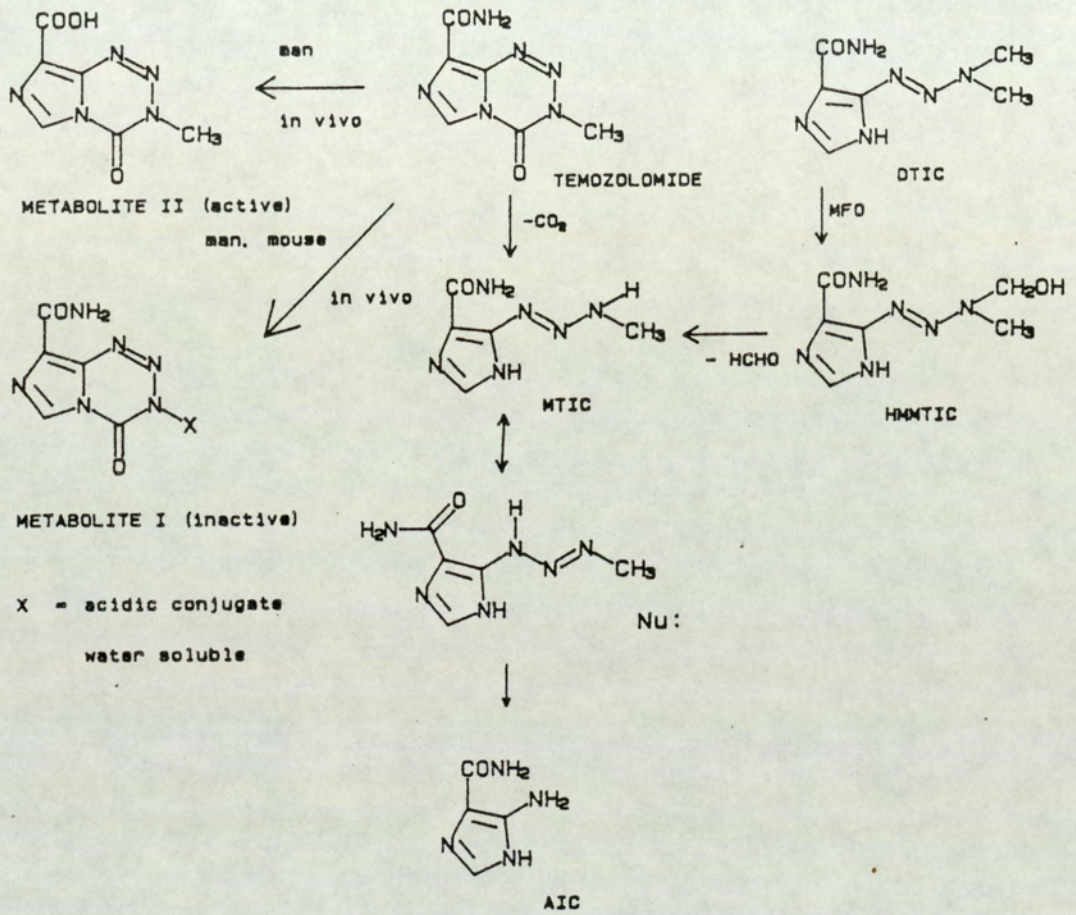


Fig.129 Proposed metabolic and decomposition pathways of temozolomide and DTIC

resistant to DTIC, is also resistant to temozolomide (Stevens et al, 1987). The results obtained in these studies suggest some commonality of mechanism of action shared by these two agents. DTIC is only active in the presence of microsomes and cofactors with the concomitant generation of MTIC (sections 3.7 and 3.8.1). Temozolomide, under physiological conditions, decomposes chemically to MTIC (sections 3.8 and 3.10), which is cytotoxic in its own right (section 3.5). Like the monomethyltriazenes (Gibson et al, 1986a,b), methylation of O<sup>6</sup>-guanine may be an important lesion caused by temozolomide in vitro (Tisdale, 1986; Bull and Tisdale, 1987; Catapano et al, 1987). It is, therefore, conceivable that it is via MTIC, that temozolomide and DTIC exert their cytotoxicity (sections 3.7.1 and 3.8.2). Temozolomide and MTIC do not undergo biotransformation (sections 3.6 and 3.8). Instead, chemical decomposition plays an important rôle in their disposition in vitro and in vivo (section 3.8 and 3.9). In contrast, their structural analogues 3-methylbenzotriazinone (section 3.6) and 1-(4-acetyl-phenyl)-3-methyltriazene (Farina et al, 1982) are metabolized in vitro by liver fractions. This is an interesting observation because the metabolic fate of these monomethyltriazenes apparently differs considerably depending on the presence of either an imidazole ring or a phenyl ring in position 1 of the triazene linkage, even though the ring system does not appear to affect significantly the antitumour activity of certain dialkylaryltriazenes (Audette et al, 1973; Connors et al,



1976). It has been suggested that the generation of a monomethyltriazene could not account for the selective cytotoxicity exerted by a dimethyltriazene (Hickman, 1978; Gescher et al, 1980). Farina et al (1982) hypothesized that the genuine selective cytotoxic species could be a stable hydroxymethyltriazene which, in theory, can form a potentially electrophilic imine or iminium ion (Overton et al, 1986; sections 3.8.2; fig.78) and therefore might react with nucleophiles present in the biophase. However, the results obtained in sections 3.6 and 3.8 show that such a hypothesis does not hold true for the monomethyltriazenes examined in this study: MTIC is not metabolized to form the corresponding stable hydroxymethyltriazene derivative and neither does temozolomide, its stable prodrug, undergo such a biotransformation in vitro. The results obtained in the structure-activity analysis of the 3-alkyl-substituted imidazotetrazinones resemble those obtained with aryldialkyltriazenes (section 1.2.3) in that only the 3-methyl analogue or in the case of the dialkyltriazenes, only compounds which can be metabolically converted to a monomethyltriazene, displayed antitumour activity. Ethazolastone and diethyltriazenes and compounds with a higher number of carbon atoms in the alkyl chain are inactive. Though there is good evidence to suggest that the different pharmacological activities of dimethyltriazenes and diethyltriazenes could, at least in part, be due to different metabolism (Farina et al, 1986), it is difficult to explain the lack of antitumour activity of ethazolastone (CCRG 82019), the 3-ethyl analogue of

temozolomide, by means of the concept of metabolism proposed by Farina et al (1986). Ethazolastone is not metabolized by hepatic post-mitochondrial supernatant (fig.129). In addition, analogous to temozolomide (section 3.8 and 3.9), ethazolastone, should, in theory, be able to undergo ring-opening to afford the corresponding linear monoethyltriazene, which is also an alkylating agent. It has been postulated by several authors that the difference in biological activity of the methyl and ethyl analogues of imidazotetrazinones and imidazo- or aryl- triazenes could possibly be attributed to biochemical difference between the monomethyl and monoethyl analogues (Gibson et al, 1986a&b; Bull and Tisdale, 1987; Tisdale, 1985a,b, 1987, 1988, 1989). It was postulated that the selective toxicity of the monomethyltriazene may be a direct consequence of its ability to cause a lethal DNA lesion by O<sup>6</sup>-methylation and the lack of antitumour activity of monoethyltriazene may be explained by its inability to cause a DNA-damaging lesion (Gibson et al, 1986a,b). The importance of alkylation of the imidazotetrazinones at the O<sup>6</sup>-position in determining cytotoxicity has also been postulated by Tisdale and co-worker (Tisdale, 1987; Bull and Tisdale, 1987); and the lack of cytotoxicity of ethazolastone may suggest that the ethyl analogue may produce an alternative cytotoxic lesion (Tisdale, 1987; Bull and Tisdale, 1987). Furthermore, contrary to the observation made by Gescher et al (1981), Horton (1983) also found that a monomethyltriazene can be selectively cytotoxic towards TLX5 sensitive line but not the resistant line. The

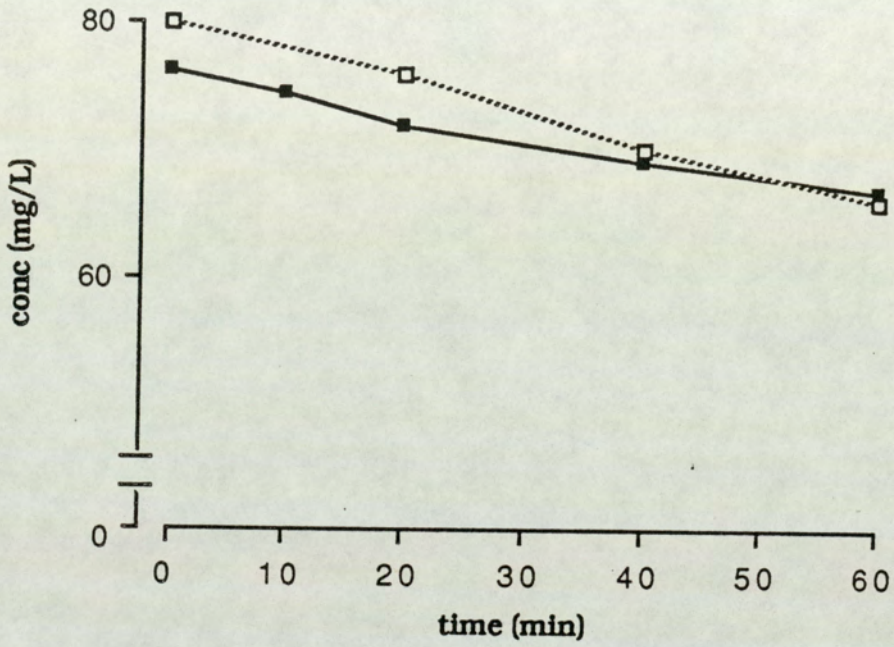


Fig.130 Time course of disappearance of ethazolastone in the presence of viable and deactivated post-mitochondrial supernatant (n=4). C.V. of each data point was less than 10%

results obtained in this study in conjunction with those obtained in the biochemical mechanistic studies (Bull and Tisdale, 1987; Gibsons et al, 1986a&b; Tisdale, 1985a&b, 1987, 1988, 1989) are consistent with the postulation that generation of a monomethyltriazene is an important determinant for selective cytotoxicity of temozolomide and DTIC. Although there is overwhelming evidence to suggest the involvement of a monomethyltriazene in the antitumour activity of dimethyltriazenes, there are some examples published in the literature which show that under certain circumstances, some dimethyltriazenes are active per se without metabolic activation (Giraldi et al, 1981; Sava et al, 1982; Farina et al, 1985; Sava et al, 1988). Indeed, DTIC has been used in local therapy in patients with advanced malignant melanoma and soft tissue sarcoma of the extremities and tumour regression has been observed (Aigner et al, 1983). Recently, Saunders et al (1986) suggested that metabolism plays little rôle in the cytotoxic action of DTIC towards Chinese hamster ovary cells in vitro. It was found that in the dark, DTIC can decompose to form 2-azahypoxanthine which is usually formed via the light-catalyzed pathway (see section 1.2.1). 2-Azahypoxanthine also possesses growth inhibitory properties. It was, therefore, postulated by these authors that the growth inhibition by DTIC could be due to the accumulation of 2-azahypoxanthine (Saunders et al, 1986).

The results obtained in sections 3.7.1 and 3.8 show unambiguously that the dimethyltriazene DTIC is not cytotoxic towards TLX5 cells in the absence of microsomes.

In the presence of microsomes, DTIC brings about a significant decrease in cell growth which correlates with the extent of MTIC generated by metabolism (sections 3.7 and 3.8). The metabolism of DTIC also appears to be species dependent (sections 3.7.1 and 3.8). Using mouse and human microsomes, it was found that there was a measurable difference in the extent of MTIC formed metabolically from DTIC. This result is in agreement with the in vivo data obtained by Ruddy et al (1981). As discussed before, if the generation of MTIC is an essential determinant for antitumour activity of temozolomide and DTIC, it appears that temozolomide might provide a pharmacokinetic advantage over DTIC in that the generation of MTIC is not metabolically mediated (section 3.8 and 3.9). In the in vivo pharmacokinetic study, an attempt was made to determine whether temozolomide possesses such a pharmacokinetic advantage over DTIC. The kinetics of the drug can best be described by an one-compartment open model which assumes instantaneous distribution of the dose throughout the whole body (section 3.10). Indeed, temozolomide is extensively distributed into the tumour (section 3.10). Temozolomide can chemically decompose in situ to form MTIC in vitro and in vivo (sections 3.8 and 3.10). Though MTIC has not been detected in tumour, it is possible to simulate the theoretical levels of MTIC which could be achieved after administration of temozolomide in plasma and tumour (fig.130). The individual values in fig.130 are computed using the  $f_m$  value experimentally obtained in section 3.10. This model is based on the

assumption that temozolomide can decompose chemically in situ inside the tumour to form MTIC as observed in the plasma (section 3.10). As discussed in section 3.10.1, unlike temozolomide, DTIC require metabolic activation to generate MTIC. The exposure of the tumour to MTIC is dependent on circulating levels of MTIC or its precursor, HMMTIC. When MTIC was given to mice via the i.v. route at 40mg/Kg (section 3.10), the plasma AUC was significantly less than that for MTIC generated from temozolomide. Hence, it is unlikely that metabolic generation from DTIC may produce the levels of MTIC produced from temozolomide. Most importantly, patients are less efficient in metabolizing DTIC to MTIC than mice (section 3.8, Ruddy et al, 1980, see fig.131). It is therefore likely an advantage in administering temozolomide to the patients because predictable levels of MTIC can be attained. In the phase I clinical evaluation of temozolomide conducted between 1987-1989, it was found that the dose limiting toxicities in patients were myelosuppression, in particular thrombocytopenia, nausea, vomiting, gastro-intestinal disturbances and in one case alopecia (Newlands et al, 1989; Slack, J.A. and C.P. Quarterman, personal communication); the maximum tolerated dose (MTD) was 750mg/m<sup>2</sup>. Temozolomide was also given to patients at day x 5 schedule with a starting dose of 150mg/m<sup>2</sup> (Quarterman, C.P., personal communication).

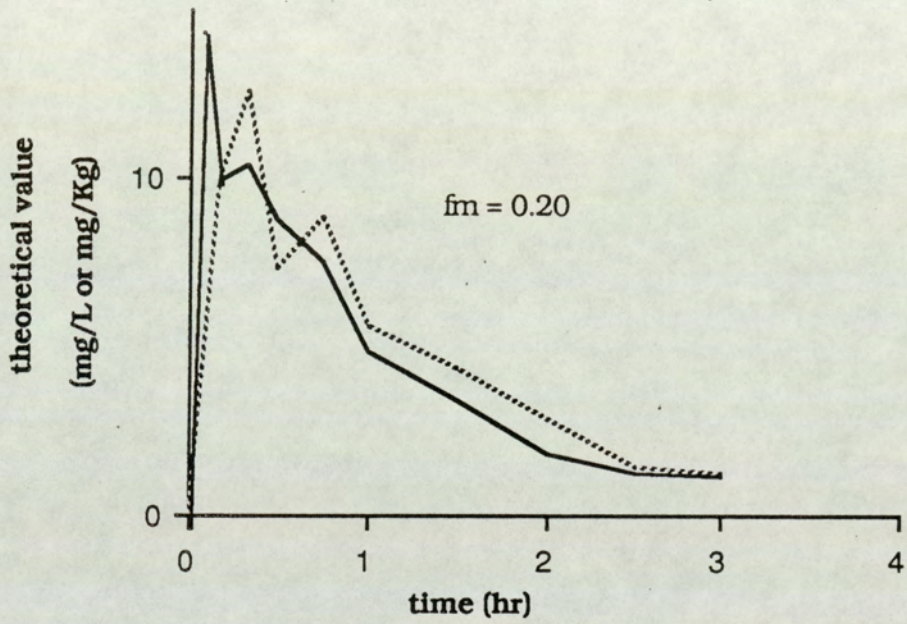


Fig.131 Computer simulation of the amount of MTIC generated from temozolomide in plasma and tumour. The theoretical values were computed on the basis of the  $f_m$  value obtained experimentally in section 3.10

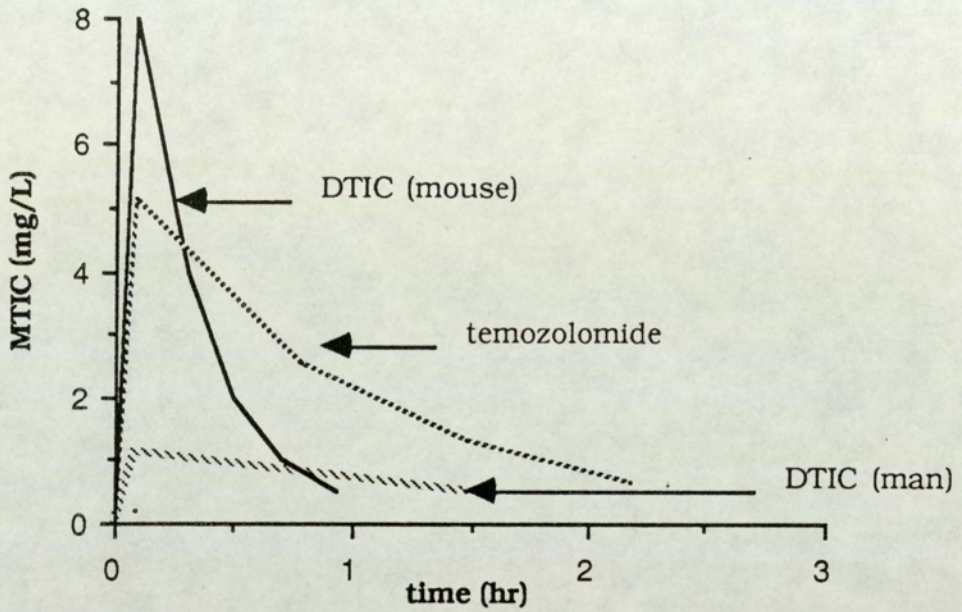


Fig.132 Computer simulation of the amount MTIC generated metabolically from DTIC and chemically from temozolomide. The theoretical values were computed on the basis of the results obtained in section 3.10 and Ruddy et al (1981)



Although temozolomide is metabolically inert in vitro (section 3.6) in the presence of hepatic fractions, under physiological conditions the drug has been shown to undergo metabolism to afford two metabolites (section 3.9). One of these metabolites (metabolite II) has been identified unambiguously as the 8-carboxylic acid derivative of temozolomide (section 3.9.2.1). The structure of the other acidic and water soluble metabolite has not been fully elucidated. However, the interpretation of the <sup>1</sup>H NMR spectrum suggests that the site of metabolism is at the N-methyl group (section 3.9.2.2). In addition, the metabolism of temozolomide appears to be species dependent because metabolite II was only found in patients' plasma and urine but not in the urine of mice. Unlike metabolite II, which has a IC<sub>50</sub> comparable to that of temozolomide, metabolite I is devoid of cytotoxic activity in vitro (section 3.9.3). This result is in accordance with the contention, as previously discussed in this section, that the N-methyl group is important for cytotoxicity, because metabolite I does not possess an intact N-methyl moiety.

In conclusion, the results presented in this thesis have helped to elucidate the mode of action of imidazotetrazinones and imidazotriazenes by means of metabolism and pharmacokinetics. It has been previously proposed (Stevens et al, 1987 and Langdon et al, 1985a&b) that temozolomide may be a clinical alternative to DTIC in that the active species is generated by chemical decomposition. In this study, it has been shown that temozolomide is, indeed, a stable pro-drug of MTIC; and the

use of such a stable tetrazinone ring to deliver a chemically labile monomethyltriazene seems to be an attractive approach in drug design in that the generation of the active species is chemically mediated and hence bypassing metabolism. The results obtained from the metabolism studies of temozolomide and 3-methylbenzotriazinone constitute a contribution towards how chemicals possessing the NNN linkage can be metabolized. Indeed, the in vitro metabolism of these two structurally similar compounds differ considerably when an imidazole ring is substituted by a phenyl ring. Furthermore, the metabolism of temozolomide to metabolite I which is presumably a deactivation product may be an important determinant in the antitumour activity, toxicity and clinical usefulness of the drug.

SECTION 5

APPENDICES

Appendix I

Data for the correlation between cytotoxicity and AUC of MTIC generated from temozolomide, DTIC, HMMTIC in vitro

Substrate (conc)	% control (cell number)	AUC <sub>MTIC</sub> (mg.min/L)
MTIC (act) (20mg/L)	42 <sub>+8</sub>	129.2 <sub>+4.1</sub>
MTIC (deact) (20mg/L)	36 <sub>+6</sub>	125.3 <sub>+10.1</sub>
MTIC (act) (10mg/L)	55 <sub>+5</sub>	48.5 <sub>+10.5</sub>
MTIC (act) (5mg/L)	69 <sub>+10</sub>	20.6 <sub>+1.3</sub>
HMMTIC (deact) (20mg/L)	20 <sub>+5</sub>	23.8 <sub>+8.6</sub>
HMMTIC (deact) (10mg/L)	44 <sub>+1</sub>	5.8 <sub>+0.6</sub>
DTIC (act) (80mg/L)	49 <sub>+3</sub>	130.1 <sub>+8.9</sub>
DTIC (act) (40mg/L)	62 <sub>+8</sub>	108 <sub>+18.6</sub>
DTIC (act) (20mg/L)	69 <sub>+6</sub>	69.8 <sub>+24.9</sub>
Temozolomide (deact)(20mg/L)	53 <sub>+5</sub>	73.3 <sub>+10</sub>
Temozolomide (act)(20mg/L)	52 <sub>+4</sub>	66.7 <sub>+9.4</sub>
Temozolomide (deact)(10mg/L)	76 <sub>+6</sub>	26.4 <sub>+1</sub>
Temozolomide (act)(10mg/L)	75 <sub>+3</sub>	24.1 <sub>+4.3</sub>

act: in the presence of activated microsomes  
deact: without microsomes

Appendix II

In vivo pharmacokinetics of temozolomide at 40mg/Kg

FILE NAME -  
DISK -

LTP/MAS  
LTAUC  
TEMOZOLOMIDE  
Mouse-40mg/kg I.V.

DATE (DD MM YY)

MAY-JUNE 1989

MEAN WEIGHT (g)  
MEAN DOSE ADMINISTERED (mg)

18.040  
0.720

-----  
KINETIC PARAMETERS DERIVED FOR TEMOZOLAMIDE  
-----

TRAPEZOIDAL AUC (ng·hr/L)	=	75.9287
MAXIMUM PLASMA CONC. (ng/L)	=	76.5600
CLEARANCE (L/hr) (ASSUMING F=1 & TRAPEZOIDAL AUC)	=	0.0094
VOLUME OF DISTRIBUTION (L) (ASSUMING F=1 & TRAPEZOIDAL AUC)	=	0.0081

-----  
N.B. - ASSUMED SINGLE COMPARTMENT MODEL

ELIMINATION HALF LIFE (hr)	=	0.5979
ELIMINATION RATE CONSTANT (1/hr)	=	-1.1591
R	=	-0.9724

-----  
KINETIC PARAMETERS DERIVED FOR MTIC  
-----

TRAPEZOIDAL AUC (ng·h/l)	3.9930
CLEARANCE OF METABOLITE (l/h) (SEE FILE MCBYPK1/C008)	0.0489
FRACTION OF DRUG CONVERTED TO METABOLITE	0.2712

-----

TEMZOLOMIDE				MTIC			
MEAN TIME (hr)	CONC (ng/L)	LN CONC (ng/L)	TRAP AUC	MEAN TIME (hr)	CONC (ng/L)	LN CONC (ng/L)	TRAP AUC
0.08	75.580	4.338		0.08	3.890	2.185	
0.17	63.810	4.153	6.308	0.17	5.210	1.651	0.635
0.33	59.080	4.079	9.815	0.33	3.240	1.176	0.676
0.50	59.400	4.084	10.071	0.50	3.730	1.316	0.592
0.75	43.330	3.759	12.841	0.75	2.740	1.008	0.809
1.00	25.320	3.232	8.581	1.00	0.770	-0.261	0.439
1.50	23.910	3.174	12.308	1.50	1.020	0.020	0.448
2.00	10.970	2.395	8.720	2.00	0.280	-1.273	0.325
2.50	8.700	2.163	4.915	2.50	0.000	ERR	0.070
3.00	4.510	1.528	3.323	3.00	0	ERR	0.000

75.56

76.98865 -AUC(TRAP)

3.99295

-----  
KINETIC PARAMETERS DERIVED FOR TENZOLOLMIDE  
-----

TRAPEZOIDAL AUC (mg.hr/L)	=	72.3769
MAXIMUM PLASMA CONC. (mg/L)	=	56.4300
CLEARANCE (L/hr) (ASSUMING F=1 & TRAPEZOIDAL AUC)	=	0.3099
VOLUME OF DISTRIBUTION (L) (ASSUMING F=1 & TRAPEZOIDAL AUC)	=	0.9085

-----  
N.B. - ASSUMED SINGLE COMPARTMENT MODEL

ELIMINATION HALF LIFE (hr)	=	0.5979
ELIMINATION RATE CONSTANT (1/hr)	=	-1.1591
R	=	-0.9724

-----  
KINETIC PARAMETERS DERIVED FOR MTIC  
-----

TRAPEZOIDAL AUC (mg.hr/L)	2.3121
CLEARANCE OF METABOLITE (L/hr) (SEE FILE M03XPK1/009)	0.0489
FRACTION OF DRUG CONVERTED TO METABOLITE	0.1502

-----



TEMOZOLOMIDE				MTIC			
MEAN TIME (hr)	CONC (mg/L)	LN CONC (lg/L)	TRAP AUC	MEAN TIME (hr)	CONC (mg/L)	LN CONC (lg/L)	TRAP AUC
0.08	56.430	4.033		0.08	1.710	0.535	
0.17	71.720	4.272	5.767	0.17	2.450	0.896	0.197
0.33	68.490	4.227	11.217	0.33	1.290	0.657	0.347
0.50	51.710	3.946	10.217	0.50	1.700	0.531	0.305
0.75	44.750	3.801	12.059	0.75	1.140	0.131	0.355
1.00	32.540	3.482	7.662	1.00	1.320	0.278	0.308
1.50	16.120	2.780	12.165	1.50	0.760	-0.274	0.520
2.00	7.130	1.964	5.813	2.00	0.000	ERR	0.190
2.50	6.650	1.896	3.448	2.50	0.000	ERR	0.000
3.00	3.540	1.254	2.550	3.00	0	ERR	0.000
55.43			72.8768 -AUC (TRAP)	2.21205			

-----  
KINETIC PARAMETERS DERIVED FOR TEMOZOLOMIDE  
-----

TRAPEZOIDAL AUC (ng.hr/L)	=	57.8113
MAXIMUM PLASMA CONC. (ng/L)	=	69.1200
CLEARANCE (L/hr) (ASSUMING F=1 & TRAPEZOIDAL AUC)	=	0.0125
VOLUME OF DISTRIBUTION (L) (ASSUMING F=1 & TRAPEZOIDAL AUC)	=	0.0107

-----  
N.B. - ASSUMED SINGLE COMPARTMENT MODEL  
-----

ELIMINATION HALF LIFE (hr)	=	0.5979
ELIMINATION RATE CONSTANT (1/hr)	=	-1.1591
R	=	-0.9724

-----  
KINETIC PARAMETERS DERIVED FOR MTIC  
-----

TRAPEZOIDAL AUC (ng.hr/L)	3.2612
CLEARANCE OF METABOLITE (1/h)	0.0489
FRACTION OF DRUG CONVERTED TO METABOLITE	0.2215

-----

TEMOZOLOMIDE				MTIC			
MEAN TIME (hr)	CONC (ng/L)	LN CONC (ng/L)	TRAP AUC	MEAN TIME (hr)	CONC (ng/L)	LN CONC (ng/L)	TRAP AUC
0.08	69.130	4.236		0.08	2.750	1.012	
0.17	35.040	3.556	4.688	0.17	3.340	1.206	0.274
0.33	51.000	3.932	6.893	0.33	2.690	0.986	0.482
0.50	37.490	3.624	7.522	0.50	2.150	0.765	0.411
0.75	32.350	3.477	8.730	0.75	1.760	0.565	0.489
1.00	22.320	3.105	6.834	1.00	1.630	0.489	0.424
1.50	13.780	2.623	9.025	1.50	0.840	-0.174	0.617
2.00	10.460	2.348	6.060	2.00	0.710	-0.342	0.388
2.50	6.430	1.861	4.223	2.50	0.000	ERR	0.178
3.00	8.960	2.192	3.848	3.00	0	ERR	0.000
69.13			57.81125 -AUC (TRAP)	3.2612			

-----  
KINETIC PARAMETERS DERIVED FOR FEMOZOLEMICE  
-----

TRAPEZOIDAL AUC (ug.hr/L)	=	52.1257
MAXIMUM PLASMA CONC. (ug/L)	=	91.6700
CLEARANCE (L/hr) (ASSUMING F=1 & TRAPEZOIDAL AUC)	=	0.0138

VOLUME OF DISTRIBUTION (L) (ASSUMING F=1 & TRAPEZOIDAL AUC)	=	0.0119
--	---	--------

-----  
N.B. - ASSUMED SINGLE COMPARTMENT MODEL  
-----

ELIMINATION HALF LIFE (hr)	=	0.5979
ELIMINATION RATE CONSTANT (1/hr)	=	-1.1591
R	=	-0.9724

-----  
KINETIC PARAMETERS DERIVED FOR MTIC  
-----

TRAPEZOIDAL AUC (ug.h/l)	2.0484
CLEARANCE OF METABOLITE (l/h) (SEE FILE MCBXPK1/C08)	0.0489
FRACTION OF DRUG CONVERTED TO METABOLITE	0.1391

-----

TEMOZOLOMIDE				MTIC			
MEAN TIME (hr)	CONC (ug/L)	LN CONC (ug/L)	TRAP AUC	MEAN TIME (hr)	CONC (ug/L)	LN CONC (ug/L)	TRAP AUC
0.08	91.670	4.518		0.08	7.210	1.975	
0.17	32.740	3.519	5.642	0.17	1.520	0.419	0.393
0.33	35.000	3.555	5.499	0.33	1.260	0.231	0.222
0.50	30.930	3.428	5.596	0.50	1.130	0.122	0.203
0.75	34.770	3.549	8.200	0.75	0.870	-0.139	0.250
1.00	20.330	3.022	6.913	1.00	0.870	-0.139	0.218
1.50	15.650	2.750	9.045	1.50	0.740	-0.301	0.403
2.00	7.870	2.063	5.380	2.00	0.350	-1.050	0.273
2.50	4.010	1.389	2.970	2.50	0.000	ERR	0.088
3.00	5.510	1.707	2.320	3.00	0	ERR	0.000

91.67

52.1257 -AUC(TRAP)

2.0484

Appendix III

In vivo tumour pharmacokinetics of temozolomide

TIME (h)	Wt bijoux (g)	Bijoux + HCl (g)	Wt Tissue bijoux + HCl (mg)	Ht residue (g)	Ht residue bijoux + residue (g)	Ht residue (g)	Wt total homog (g)	Ht 0.25ml homog (g)	Conc homog (mg/l)	Tem conc in tissue (ug/g tissue)
0.08	4.5350	6.5303	294.80	4.6122	0.0772	2.7155	0.2376	2.370	22.970	
0.17	4.5240	6.5193	195.10	4.5668	0.0428	2.5502	0.2457	2.370	32.757	
0.33	4.4248	6.4201	224.40	4.4687	0.0439	2.6784	0.2480	3.020	36.337	
0.50	4.4370	6.4323	196.20	4.4735	0.0365	2.6576	0.2230	2.480	37.660	
0.75	4.6046	6.5999	221.50	4.6663	0.0617	2.6577	0.2429	2.370	29.268	
1.00	4.4001	6.3954	242.40	4.4676	0.0675	2.6728	0.2533	2.050	22.310	
1.50	4.5177	6.5130	256.10	4.6404	0.1227	2.6313	0.2464	2.050	21.370	
2.00	4.4400	6.4353	269.00	4.4966	0.0566	2.7103	0.2369	1.280	13.610	
2.50	4.5338	6.5291	329.80	4.5786	0.0398	2.7879	0.2362	0.480	4.295	
3.00	4.5296	6.5249	177.40	4.5837	0.0541	2.6212	0.2469	0.370	5.536	

---

TUMOUR CONCENTRATION			
TIME	MEAN	LN CONC	TRAP
(hr)	CONC	(mg/Kg)	AUC
	(mg/Kg)		
0.08	22.970		
0.17	32.757	3.489	2.508
0.33	36.337	3.593	5.528
0.50	37.660	3.629	6.290
0.75	29.268	3.376	8.366
1.00	22.310	3.105	6.447
1.50	21.370	3.062	10.920
2.00	13.610	2.611	8.745
2.50	4.295	1.457	4.476
3.00	5.536	1.711	2.458

---

---

55.73723 -AUC(TRAP)

TIME (h)	Wt bijoux (g)	Bijoux + HCl (g)	Wt bijoux + Tissue (g)	Wt Tissue + HCl (g)	Wt bijoux + residue (g)	Wt residue (g)	Wt total (g)	Wt 0.25ml homog (g)	Conc homog (µg/l)	TEA CONC in tissue (µg/g tissue)
0.08	4.6682	6.6635	7.0227	359.20	4.7513	0.0831	2.7740	0.2402	2.370	19.050
0.17	4.5310	6.5263	6.6841	157.80	4.5901	0.0591	2.5966	0.2432	2.150	36.367
0.33	4.6724	6.6677	6.7852	117.50	4.7785	0.1061	2.5093	0.2414	4.130	91.341
0.50	4.5898	6.5851	6.7720	186.90	4.5647	-0.0251	2.7099	0.2563	2.670	37.761
0.75	4.5110	6.5063	6.7095	203.20	4.6126	0.1016	2.5995	0.2461	2.520	32.749
1.00	4.4339	6.4292	6.6635	234.30	4.5603	0.1264	2.6058	0.2468	2.150	24.222
1.50	4.4465	6.4418	6.6232	181.40	4.5270	0.0805	2.5988	0.2502	2.070	29.632
2.00	4.5517	6.5470	6.7454	198.40	4.4998	-0.0519	2.7482	0.2436	0.870	12.368
2.50	4.3994	6.3947	6.5793	184.60	4.4776	0.0782	2.6043	0.2412	0.120	1.755
3.00	4.4792	6.4745	6.6272	152.70	4.6541	0.1749	2.4757	0.2432	0.030	0.540



---

TUMOUR CONCENTRATION			
TIME	MEAN	LN CONC	TRAP
(hr)	CONC	(mg/Kg)	AUC
	(mg/Kg)		
0.08	19.050		
0.17	36.367	3.594	2.494
0.33	91.341	4.515	10.217
0.50	37.761	3.631	10.974
0.75	32.749	3.489	8.814
1.00	24.222	3.187	7.121
1.50	29.638	3.389	13.465
2.00	12.368	2.515	10.502
2.50	1.755	0.562	3.531
3.00	0.500	-0.693	0.564

---

67.6802 -AUC(TRAP)

TIME (h)	Wt bijoux (g)	Bijoux + HCl (g)	Wt bijoux + HCl (g)	Bijoux + Tissue (g)	Wt Tissue (mg)	Wt bijoux + residue (g)	Wt residue (g)	Wt total (g)	Wt homog (g)	Conc homog (mg/l)	Tea conc in tissue (ug/g tissue)
0.08	4.6366	6.6313	6.8726	241.30	4.7513	0.1147	2.6239	0.2402	2.370	26.823	
0.17	4.4990	6.4943	6.9381	443.80	4.5333	0.0343	2.9074	0.2455	8.730	57.306	
0.33	4.6543	6.6496	7.0592	409.60	4.7320	0.0977	2.8098	0.2533	8.190	55.450	
0.50	4.5670	6.5623	6.9123	350.00	4.6235	0.0565	2.7914	0.2583	5.173	39.931	
0.75	4.5697	6.5650	6.9934	428.40	4.6070	0.0373	2.8890	0.2549	7.220	47.754	
1.00	4.4253	6.4206	6.9931	572.50	4.4798	0.0545	3.0159	0.2562	5.070	25.062	
1.50	4.4978	6.4931	6.8649	371.80	4.5447	0.0469	2.8228	0.2570	2.420	17.873	
2.00	4.5900	6.5853	6.9922	406.90	4.6432	0.0532	2.8516	0.2531	2.050	14.191	
2.50	4.5745	6.5698	6.9463	376.50	4.6262	0.0517	2.8227	0.2584	1.510	10.953	
3.00	4.4896	6.4849	7.0799	595.00	4.5267	0.0371	3.0558	0.2570	1.300	6.495	

-----			
TUMOUR CONCENTRATION			
TIME	MEAN	LN CONC	TRAP
(hr)	CONC	(mg/Kg)	AUC
-----			
0.08	26.823		
0.17	57.306	4.048	3.786
0.33	55.450	4.015	9.020
0.50	39.931	3.687	8.107
0.75	47.754	3.866	10.961
1.00	26.062	3.260	9.227
1.50	17.873	2.883	10.984
2.00	14.191	2.653	8.016
2.50	10.953	2.394	6.286
3.00	6.495	1.871	4.362

-----  
70.74904 -AUC(TRAP)

TIME (h)	Wt bijoux (g)	Bijoux + HCl (g)	Bijoux + Tissue (g)	Wt Tissue (mg)	Wt bijoux + residue (g)	Wt residue (g)	Wt total homog (g)	Wt 0.25ml homog (g)	Conc homog (mg/l)	Tem conc in tissue (ug/g tissue)
0.08	4.6549	6.6592	6.9203	270.10	4.7664	0.1115	2.6565	0.2382	2.050	21.161
0.17	4.5639	6.5592	6.8738	314.60	4.6365	0.0726	2.7399	0.2480	8.730	76.644
0.33	4.4905	6.4858	6.8310	345.20	4.5497	0.0592	2.7839	0.2230	8.190	74.046
0.50	4.5588	6.5541	7.0026	448.50	4.6229	0.0641	2.8823	0.2429	5.173	34.216
0.75	4.6323	6.6276	6.8955	257.90	4.7489	0.1166	2.6392	0.2533	7.220	72.923
1.00	4.4578	6.4531	6.7812	328.10	4.5141	0.0563	2.7697	0.2464	5.070	43.424
1.50	4.5125	6.5078	6.8321	324.30	4.5972	0.0847	2.7375	0.2369	2.420	21.557
2.00	4.6428	6.6381	6.9760	337.90	4.7101	0.0673	2.7685	0.2362	2.050	17.777
2.50	4.5798	6.5751	6.8948	319.70	4.6523	0.0725	2.7451	0.2425	1.510	13.367
3.00	4.5482	6.5435	6.8360	292.50	4.5910	0.0428	2.7476	0.2379	1.300	12.833

---

TIME (hr)	MEAN CONC mg/Kg	LN CONC mg/Kg	TRAP AUC
0.08	21.161		
0.17	76.644	4.339	4.401
0.33	74.046	4.305	12.055
0.50	34.216	3.533	9.202
0.75	72.230	4.280	13.306
1.00	43.424	3.771	14.457
1.50	21.557	3.071	16.245
2.00	17.777	2.878	9.834
2.50	13.367	2.593	7.786
3.00	12.833	2.552	6.550

---

93.83594

Appendix IV

In vivo pharmacokinetics of MTIC

-----					
MTIC					
MEAN TIME (hr)	CONC ( $\mu\text{g/L}$ )	LN CONC ( $\mu\text{g/L}$ )	TRAP AUC	MEAN TIME (hr)	CONC ( $\mu\text{g/L}$ )
-----					
0.08	16.670	2.314		0.08	1.710
0.17	0.430	-0.244	0.770	0.17	2.450

-----  
0.7695 -AUC(TRAP)

-----  
KINETIC PARAMETERS DERIVED FOR TEMOZOLOMIDE  
-----

TRAPEZOIDAL AUC ( $\mu\text{g}\cdot\text{hr/L}$ ) = 0.7695

MAXIMUM PLASMA CONC. ( $\mu\text{g/L}$ ) = 16.6700

CLEARANCE (L/hr)  
[ASSUMING F=1 & TRAPEZOIDAL AUC] = 0.9357

VOLUME OF DISTRIBUTION (L)  
[ASSUMING F=1 & TRAPEZOIDAL AUC] = 0.0392

-----  
N.B. - ASSUMED SINGLE COMPARTMENT MODEL

ELIMINATION HALF LIFE (hr) = 0.0290

ELIMINATION RATE CONSTANT (1/hr) = -23.8688

R = -1.0000  
-----

-----					
MTIC					
MEAN				MEAN	
TIME	CDAC	LN CONC	TRAP	TIME	CONC
(hr)	(ug/L)	(ug/L)	AUC	(hr)	(ug/L)
-----					
0.08	17.910	2.895		0.08	1.710
0.17	2.090	0.737	0.900	0.17	2.450
-----					
0.9 -AUC (TRAP)					

-----  
 KINETIC PARAMETERS DERIVED FOR TEMOZOLOMIDE  
 -----

TRAPEZOIDAL AUC (ug.hr/L)	=	0.9000
MAXIMUM PLASMA CONC. (ug/L)	=	17.9100
CLEARANCE (L/hr)	=	0.8000
[ASSUMING F=1 & TRAPEZOIDAL AUC]		
VOLUME OF DISTRIBUTION (L)	=	0.0335
[ASSUMING F=1 & TRAPEZOIDAL AUC]		

-----  
 N.B. - ASSUMED SINGLE COMPARTMENT MODEL

ELIMINATION HALF LIFE (hr)	=	0.0290
ELIMINATION RATE CONSTANT (1/hr)	=	-23.8688
R	=	-1.0000

-----

-----						
MTIC						
MEAN				MEAN		
TIME	CONC	LN CONC	TRAP	TIME	CONC	LN CONC
(hr)	(ug/L)	(ug/L)	AUC	(hr)	(ug/L)	(ug/L)
-----						
0.08	23.950	3.176		0.08	1.710	0.536
0.17	0.640	-0.446	1.107	0.17	2.450	0.996

-----  
1.10655 -AUC(TRAP)

-----  
KINETIC PARAMETERS DERIVED FOR MTIC  
-----

TRAPEZOIDAL AUC (ug.hr/L)	=	1.1066
MAXIMUM PLASMA CONC. (ug/L)	=	23.9500
CLEARANCE (L/hr) [ASSUMING F=1 & TRAPEZOIDAL AUC]	=	0.6995
VOLUME OF DISTRIBUTION (L) [ASSUMING F=1 & TRAPEZOIDAL AUC]	=	0.0174

-----  
N.B. - ASSUMED SINGLE COMPARTMENT MODEL

ELIMINATION HALF LIFE (hr)	=	0.0172
ELIMINATION RATE CONSTANT (1/hr)	=	-40.2473
R	=	-1.0000

-----



MEAN		M <sup>2</sup> IC			MEAN	
TIME	CONC	LN CONC	TRAP	TIME	CONC	
(hr)	(µg/L)	(µg/L)	AUC	(hr)	(µg/L)	
0.08	16.250	2.789		0.08	1.710	
0.17	0.430	-0.844	0.751	0.17	2.450	

0.7506 -AUC-TRAP)

KINETIC PARAMETERS DERIVED FOR TEMOZOLOMIDE

TRAPEZOIDAL AUC (µg.hr/L)	=	0.7506
MAXIMUM PLASMA CONC. (µg/L)	=	16.2500
CLEARANCE (L/hr) [ASSUMING F=1 & TRAPEZOIDAL AUC]	=	0.9592
VOLUME OF DISTRIBUTION (L) [ASSUMING F=1 & TRAPEZOIDAL AUC]	=	0.0402

N.B. - ASSUMED SINGLE COMPARTMENT MODEL

ELIMINATION HALF LIFE (hr)	=	0.0290
ELIMINATION RATE CONSTANT (1/hr)	=	-23.8689
R	=	-1.0000

SECTION 6  
REFERENCES

## 6 References

Aigner, K., Hild, P., Breithaupt, H., Hundeiker, M., Schwemmle, K., Henneking, K., Illing, L.L., Merker, G., Paul, E., Broddkorb, J., Jungbluth, A., (1983). Isolated extremity perfusion with DTIC. An experimental and clinical study. *Anticancer Res.* 3: 87-94.

Anderson, T., McMenemy, M.G., Schein, P.S., (1975). Chlorozotocin 2-[3-(2-chloroethyl-3-nitrosoureido)-D-glucopyranose, an antitumour agent with modified bone marrow toxicity. *Cancer Res.*, 35: 761-765.

Audette, R.C.S., Connors, T.A., Mandel, H.G., Merai, K., Ross, W.C.J. (1973). Studies on the mechanism of action of the tumour inhibitory triazenes. *Biochem. Pharmacol.*, 22: 1855-1864.

Auerbach, C., Moutschen-Dahmen, M., Moutschen, J., (1977). Genetic and cytogenetical effects of formaldehyde and related compounds. *Mutation Res.* 39: 317-362.

Baig, G.U., (1986). Ph.D. thesis, University of Aston in Birmingham.

Baig, G.U., Stevens, M.F.G., (1987). Antitumour imidazotetrazines. Part 12. Reaction of mitozolomide and its 3-alkyl congeners with oxygen, nitrogen, halogen and carbon nucleophiles. *J. Chem. Soc. Perkin. Trans. I.*: 665-670.

Bill, C.A., Gescher, A., Hickman, J.A., (1988). Effects of N-methylformamide on the growth, cell cycle, and glutathione status of murine TLX5 lymphoma cells. *Cancer Res.*, 48: 3389-3393.

Bombaugh, K.J. (1978). Column selection in HPLC. In *GLC and HPLC determination of therapeutic agents. Part I* (Ed. Tsuji, K., Morozowich, W.). Merck Decker, Inc. p. 83-133.

Boyle, W., (1968). An extension of the <sup>51</sup>Cr release assay for the estimation of mouse cytotoxins. *Transplantation* 6: 761-764.

Bratton, A.C., Marshall, E.C., Jr., (1939). A new coupling component for sulfanilamide determination. *J. Biol. Chem.*, 128: 537-550.

Breithaupt, H., Dammann, A., Aigner, K., (1982). Pharmacokinetics of dacarbazine (DTIC) and its metabolite 5-aminoimidazole-4-carboxamide (AIC) following different dose schedules. *Cancer Chemother. Pharmacol.*, 9: 103-109.

British Pharmacopoeia (1980).

- Brodie, A.E., Babson, J.R., Reed, D.J. (1980). Inhibition of tubulin polymerization by nitrosourea-derived isocyanates. *Biochem. Pharmacol.*, 29: 652-654.
- Brindley, C.J., Antoniw, P., Newlands, E.S., (1986). Plasma and tissue disposition of mitozolomide in mice. *Br. J. Cancer*, 53: 91-97.
- Bull, V.L., Tidsdale, M.J., (1987). Antitumour imidazotetrazines-XVI. Macromolecular alkylation by 3-substituted imidazotetrazinones. *Biochem. Pharmacol.*, 36(19): 3215-3220.
- Burchenal, J.H., Dagg, M.K., Beyer, M., Stock, C.C., (1956). Triazenes as antitumour agents. *Proc. Soc. Exp. Biol. Med.*, 91: 398-403.
- Case, D.E., (1973). The place of nuclear magnetic resonance spectroscopy in drug metabolism studies. *Xenobiotica*, 3(7): 451-471
- Catapano, C.V., Broggin, M., Erba, E., Ponti, M., Mariani, L., Citti, L., D'Incalci, M., (1987). *In vitro* and *in vivo* methazolastone-induced DNA damage and repair in L-1210 leukaemia sensitive and resistant to chloroethylnitrosoureas. *Cancer Res.*, 47(18): 4884-4889.
- Cheng, C.C., Elslager, E.F., Werbel, L.M., Prierbe, S.R., Leopold, W.R. III., (1986). Pyrazole derivatives 5: synthesis, antineoplastic activity of 3-(2-chloroethyl),3,4-dihydro-4-oxopyrazolo [5,1-d]1,2,3,5 tetrazine-8-carboxamide and related compounds. *J. Med. Chem.*, 29: 1544-1547.
- Clark, D.A., Barclay, R.K., Stock, C.C., Rondestvedt, C.S., (1955). Triazenes as inhibitors of mouse sarcoma 180. *Proc. Soc. Exp. Biol. Med.*, 90: 484-489.
- Comis, R.L., (1976). DTIC (NSC-45388) in malignant melanoma: a perspective. *Cancer Treat. Rep.*, 60(2): 165-175.
- Connors, T.A., Goddard, P.M., Merai, K., Ross, W.C.J., Wilaman, D.E.V., (1976). Tumour inhibitory triazenes: structural requirements for an active metabolite. *Biochem. Pharmacol.*, 25: 241-246
- De Bruijn, E.A., Van Oosterom, A.T., Tjaden, U.R. (1987). The influence of ethanol on cyclophosphamide pharmacokinetics and metabolism in tumour-bearing rats. *Pharmac. Ther.* 33: 171-177.
- Dhondt, J.L., Cartigny, B., Farriaux, J.P., (1974). Etude des derives imidazoles urinaires pour chromatographie sur couche-nince. *Clin. Chim. Acta*,

50: 297-300.

Dive, C., Workman, P., Watson, J., (1987). Further evidence that flow cytoenzymological carbamoylation by chloroethylnitrosourea-derived isocyanates. *Br. J. Cancer*, 56(2): 222.

Dolfini, E., Martini, A., Donelli, M.G., Morasca, L., Garatiini, S., (1973). Methods for tissue culture evaluation of the cytotoxic activity of drugs active through the formation of metabolites. *European J. Cancer*, 9: 375-378.

Druckery, H., (1973). Specific carcinogenic and tetratogenic effects of "indirect" alkylating methyl and ethyl compounds and their dependency on stages of oncogenic developments. *Xenobiotica*, 3: 274-303.

Edge, G., Gilbert, K., (1979). [7+2] and [1+2] cycloaddition reactions of diazo-azoles with isocyanates to azolo[5,1-d]1,2,3,5 tetrazine 4(3H)ones. *Tet. Letters*, 44: 4253-4257.

Engineer, M.S., Raber, M.N., Newman, R.A. (1988). Clinical Pharmacology of LY195448. *Proceedings of AACR*, 29: 195

Erickson, L.C., Bradley, M.O., Ducore, J.M., Ewig, R.A.G., Kohn, K.W., (1980a). DNA crosslinking and cytotoxicity in normal and transformed human cells treated with antitumour nitrosoureas. *Proc. Natl. Acad. Sci.*, 77(1): 467-471.

Erickson, L.C., Laurent, G., Sharkey, N.A., Kohn, K.W., (1980b). DNA-cross-linking and monoadduct repair in nitrosourea treated human tumour cells. *Nature*, 288(28/25): 727-729.

Farina, P., Gescher, A., Hickman, J.A., Horton, J.K., D'Incalci, M., Ross, D., Stevens, M.F.G., Torti, L., (1982). Studies of the mode of action of antitumour triazenes and triazines-IV. The metabolism of 1-(4-acetyl-phenyl)3,3-dimethyl triazene. *Biochem. Pharmacol.* 31(10): 1887-1892.

Farina, P., Benfenati, E., Reginato, R., Torti, L., D'Incalci, M., Threadgill, M., Gescher, A., (1983). Metabolism of the anticancer agent 1-(4-acetylphenyl)-3,3-dimethyltriazene. *Biomed. Mass. Spectrom.* 10:485-488.

Farina, P., Benfenati, E., Lassiani, L., Nisi, C., D'Incalci, M., (1985). High performance liquid chromatographic assay for the determination of p-(3,3-dimethyl-1-triazeno)benzoic acid in mouse plasma. *J. Chromatography.* 345: 323-331.

Farina, P., Torti, L., Urso, R., Horton, J.K., Gescher, A., D'Incalci, M., (1986). Comparison of metabolism and activity of an arylldimethyltriazene and an arylldiethyltriazene. *Biochem. Pharmacol.* 35(2): 209-215.

Fiore, D., Jackson, A.J., Didolkar, M., Dandu, V.R., (1985). Simultaneous determination of dacarbazine, its photolytic degradation product, 2-azahypoxanthine, and the metabolite, 5-aminoimidazole-4-carboxamide in plasma and urine by high-pressure liquid chromatography. *Anticmicrobial Agents and Chemotherapy*, 27(6): 977-979.

Fodstad, Ø., Aamdal, S., Pihl, A., Boyd, M.R., (1985). Activity of mitozolomide (NSC 353451). A new imidazotetrazine, against xenograft from human melanomas, sarcomas, and lung and colon carcinomas. *Cancer Res.*, 45: 1778-1786.

Gallice, P., Monti, J.P., Crevat, A., Durand, C., Murisasco, A., (1985). A compound from uremic plasma and from normal urine isolated by liquid chromatography and identified by nuclear magnetic resonance. *Clin. Chem.*, 31(11): 30-34.

Geran, R.I., Greenberg, N.H., MacDonald, M.M., Schumacher, A.M., Abbott, B.J., (1972). Protocols for screening chemical agents and natural products against animal tumours and other biological systems. *Cancer Chemother. Rep.*, 3(2): 1-103.

Gerulath, A.H., Loo, T.L., (1972). Mechanism of action of 5-(3,3-dimethyl-1-triazeno)imidazole-4-carboxamide in mammalian cells in culture. *Biochem. Pharmacol.*, 21: 2335-2343.

Gescher, A., Threadgill, M.D., (1987). The metabolism of triazene antitumour drugs. *Pharm. Ther.*, 32: 191-205.

Gibaldi, M., Perrier, D., (1982). *Pharmacokinetics*. (2nd. Ed.).

Gibson, N.W., Hickman, J.A., (1982). The rôle of isocyanates in the toxicity of antitumour haloalkylnitrosoureas. *Biochem. Pharmacol.*, 31(17): 2795-2800.

Gibson, N.W., Erickson, L.C., Hickman, J.A., (1984a). Effects of the antitumour agents 8-carbamoyl-3-(2-chloroethyl)imidazo-[5,1-d]-1,2,3,5-tetrazin-4(3H)one on the DNA of murine L1210 cells. *Cancer Res.*, 44: 1767-1771.

Gibson, N.W., Hickman, J.A., Erickson, L.C. (1984b). DNA cross-linking and cytotoxicity in normal and transformed human cells treated in vitro with 8-carbamoyl-3-(2-chloroethyl)imidazo-[5,1-d]-1,2,3,5-

tetrazin-4(3H)one. *Cancer Res.*, 44: 1772-1775.

Gibson, N.W., Erickson, L.C., (1985). The effects of pretreatment of human tumour cells with MNNG on the DNA cross-linking and cytotoxicity of mitozolomide. *Br. J. Cancer*, 52: 251-258.

Gibson, N.W., Hartley, J., LaFrance, R.J., Vaughan, K., (1986a). Differential cytotoxicity and DNA-damaging effects produced in human cells of the Mer<sup>+</sup> and Mer<sup>-</sup> phenotypes by a series of alkyltriazenylimidazoles. *Carcinogenesis*. 7(2): 259-265.

Gibson, N.W., Hartley, J., LaFrance, R.J., Vaughan, K., (1986b). Differential cytotoxicity and DNA-damaging effects produced in human cells of the Mer<sup>+</sup> and Mer<sup>-</sup> phenotypes by a series of 1-aryl-3-alkyltriazenes. *Cancer Res.*, 46: 4999-5003.

Giraldi, T., Nisi, C., Sava, G., (1975). Investigation on the oxidative N-demethylation of aryltriazenes in vitro. *Biochem. Pharmacol.* 24:1793-1797.

Giraldi, T., Sava, G., Cuman, R., Nisi, C., Lassiani, L., (1981). Selectivity of the antimetastatic and cytotoxic effects of 1-p-(3,3-dimethyl-1-triazeno)benzoic acid potassium salt, (+)-1,2-di(3,5-dioxopiperazin-1-yl)-propane and cyclophosphamide in mice bearing Lewis lung carcinoma. *Cancer Res.* 41:2524-2528.

Goddard, C., (1985). Ph.D. thesis, University of Aston in Birmingham.

Goddard, C., Slack, J.A., Stevens, M.F.G., (1985a). Antitumour imidazotetrazines. Part IX. The pharmacokinetics of mitozolomide in mice. *Br. J. Cancer*, 52: 37-41.

Goddard, C., Slack, J.A., Griffin, M., Baig, G., Stevens, M.F.G., (1985b). Preclinical studies on CCRG 81045. *Proc. Amer. Assoc. Cancer Res.*, 26: 1396.

Goth, R., Rajewsky, M.F., (1974). Persistence of O<sup>6</sup>-ethylguanine in rat-brain DNA: correlation with nervous system-specific carcinogenesis by ethylnitrosourea. *Proc. Nat. Acad. Sci.* 71(3): 630-643.

Gundersen, S., Aamdal, S., Fodstad, Ø., (1987). Mitozolomide (NSC 353451), a new drug in the treatment of malignant melanoma, phase II trial in patients with advanced disease. *Br. J. Cancer*, 55: 433-435.

Guttenplan, (1984). Mutagenesis and O<sup>6</sup>-ethylguanine levels in DNA from N-Nitroso-N-ethylurea treated *Salmonella Typhimurium*: evidence for a high mutational efficiency of O<sup>6</sup>-ethylguanine. *Carcinogenesis*, 5: 55-59.

Hano, K., Akashi, A., Yamamoto, I., Narumi, S., Horii, Z., Ninomiya, I., (1965). Antitumour activity of 4(or5)-amino-imidazole-5(or4)-carboxamide derivatives. *Gann* 56: 417-420

Hano, K., Asashi, A., Yamamoto, I., Narumi, S., Iwata, H., (1968). Further investigation on the carcinostatic activity of 4(or5)-amino-imidazole-5(or4)-carboxamide derivatives: structure activity relationships. *Gann* 59: 207-216.

Hansch, C., Smith, N., Engle, R., Wood, H., (1972). Quantitative structure-activity relationships of antineoplastic drugs: nitrosoureas and triazenoimidazoles. *Cancer Chemother. Rep.*, 56; 443-456.

Harding, M., Northcott, D., Smyth, J., Stuart, N.S.A., Green, E., Newlands, E., (1988). Phase II evaluation of mitozolomide in ovarian cancer. *Br. J. Cancer*, 57: 113-114.

Harris, A.L., Karran, P., Lindahl, T., (1983). O<sup>6</sup>-methylguanine-DNA methyltransferase of human lymphoid cells: structural and kinetic properties and absence in repair-deficient cells. *Cancer Res.*, 43: 3247-3252.

Hatheway, G., Hansch, C., Kim, K.H., Milstein, S.R., Schmidt, C.L., Smith, R.N., Quinn, F.R., (1978). Antitumour (X-aryl)-3,3,dialkyltriazenes. I) Quantitative structure-activity relationships vs L1210 leukaemia in mice. *J. Med. Chem.*, 21(6): 563-

Hearse, D.J., (1984). Microbiopsy metabolite and paired flow analysis: a new rapid procedure for homogenisation, extraction and analysis of high energy phosphates and other intermediates without any errors from tissue loss. *Cardiovascular Research*, 18: 384-390.

Hemens, C.M., Manning, H.W., Vaughan, K., LaFrance, R.J., Tang, Y., (1984). Opening chain nitrogen compounds. Part V. Hydroxymethyltriazenes: synthesis of some new alkyl homologues of the antitumour 3-methyl-3-hydroxymethyl triazenes and preparation of the derived acetoxymethyl, benzoyloxymethyl and methoxymethyltriazenes. *Can. J. Chem.* 62: 741-748.

Hickman, J.A., Stevens, M.F.G., Gibson, N.W., Langdon, S.P., Fizames, C., Lavelle, F., Atassi, G., Lunt, E., Tilson, R.M., (1985). Experimental antitumour activity against murine tumour model systems of 8-carbamoyl-3(2-chloroethyl)imidazo [5.1,d-] 1,2,3,5 tetrazin-4(3H)one (mitozolomide) a novel broad spectrum agent. *Cancer Res.*, 45, 3008-3013.

Hill, D.L., (1975). Microsomal metabolism of



triazenylimidazoles. *Cancer Res.*, 35, 3106-3110.

Ho, D.H., Covington, W., Lin, J.R., Brown, N., Kraflkoff, I.H., Newman, R.A., (1988). Disposition and metabolism of LY195448, (R)-4-[3-(2-hydroxy-2-phenyl)ethylamino-3-methylbutyl]benzamide in mice. *Proceedings of AACR*, 29: 485.

Hora, J.F., Eastman, A., Bresnick, E., (1983). O<sup>6</sup>-Methylguanine Methyltransferase in rat liver. *Biochemistry*, 22: 3759-3763.

Horgan, C.M.T., Tisdale, M.J., (1984). Antitumour imidazotetrazinones IV- an investigation into the mechanism of antitumour activity of a novel and potent antitumour agent, mitozolomide (CCRG 81010, M&B 39505, NSC 353451). *Biochem. Pharmacol.* 33(14) 2185-2192.

Horgan, C.M.T., Tisdale, M.J., (1985). Antitumour imidazotetrazines VIII- uptake and decomposition of a novel antitumour agent mitozolomide (CCRG 81010, M&B 39565, NSC 353451) in TLX5 mouse lymphoma in vitro. *Biochem. Pharmacol.* 34(2):217-221.

Horspool, K.R., (1988). Ph.D. thesis, Aston University.

Horspool, K.R., Quarterman, C.P., Slack, J.A., Gescher, A., Stevens, M.F.G., Lunt, E., (1989). Metabolism and murine pharmacokinetics of 8-(N,N-dimethylcarboxamide) analogue of the experimental antitumour drug mitozolomide (NSC353451). *Cancer Res.* in press.

Horton, J.K., (1982). Ph.D. thesis, University of Aston.

Horton, J.K., Stevens, M.F.G., (1981a). Triazenes and related products. Part 23. New photo-products from 5-diazoimidazole-4-carboxamide (diazotIC). *J.C.S. Perkins I*, 1433-1436.

Horton, J.K., Stevens, M.F.G., (1981b). A new light on the photo-decomposition of the antitumour drug DTIC. *J. Pharm. Pharmacol.*, 33: 808-811.

Householder, G.E., Loo, T.L., (1969). Elevated urinary excretion of 4-amino-imidazole-5-carboxamide in patients after intravenous injection of 4-(3,3-dimethyl-1-triazeno)-imidazole-5-carboxamide. *Life Sci.*, 8(1): 533-536.

Householder, G.E., Loo, T.L., (1971). Disposition of 5-(3,3-dimethyl-1-triazeno)imidazole-4-carboxamide; a new antitumour agent. *J. Pharm. Exp. Ther.* 179(3): 386-395.

Julliard, M., Vernin, G., Metzger, J., (1980). Triazenes III. A convenient synthesis of triazenes with potential

antitumour activity. *Synthesis*, 116-117.

Kestell, P., Brindley, C., Antoniow, P., Slack, J.A., Newlands, E., (1985). Tissue disposition of radiolabelled mitozolomide in mice. *Br. J. Cancer*, 52: 437-8.

Keilhues, P., Kolar, G.F., Margison, G.P., (1976). Interaction of carcinogen 3,3-dimethyl-1-phenyltriazeno with nucleic acids of various rat tissues and the effect of a protein-free diet. *Cancer Res.* 36: 2189-2193.

Kohn, K.W., (1977). Interstrand cross-linking of DNA by 1,3-bis (2-chloroethyl)-1-nitrosourea and other 1-(2-haloethyl) -1-nitrosourea. *Cancer Res.*, 37: 1450-1454.

Koike, M., Norikura, R., Iwatani, K., Sugeno, K., Takahashi, S., Nakagawa, Y., (1988). Structure determination of metabolites of rilmazafone, a 1H-1,2,4-triazolyl benzophenone derivative in monkey urine. *Xenobiotica*, 18(3): 257-268.

Kolar, G.F., Carubelli, R., (1979). Urinary metabolite of 1-(2,3,6-trichlorophenyl) 3,3-dimethyltriazeno with an intact diazoamino structure. *Cancer Letts.* 7: 209-214.

Kolar, G.F., Maurer, M., Wildschütte, M., (1980). 5-(3-hydroxy-methyl-3-methyl-1-triazeno)imidazole-4-carboxamide is a metabolite of 5-(3,3-dimethyl-1-triazeno)imidazole-4-carboxamide (DIC, DTIC, NSC-45388). *Cancer Letts.* 10: 235-241.

Kolar, G.F., (1984). Triazenes. In *Chemical Carcinogenesis*. American Chemical Society Monograph 182. 2: 869-914.

Krstulovic, A.M., Brown, P.R., (1982). Reversed-phase High Performance Liquid Chromatography. Theory, Practice and Biomedical Application.

Krüger, F.W., Preussmann, R., Nieplelt, N., (1971). Mechanism of carcinogenesis with 1-aryl-3,3-dialkyl triazenes-III. In vivo methylation of RNA and DNA with 1-phenyl-3,3-[<sup>14</sup>C]-dimethyltriazeno. *Biochem. Pharmacol.*, 20: 529-533.

Langdon, S.P., Stevens, M.F.G., Stone, Gibson, N.W., Baig, G.U., Hickman, J.A., Newton, C.G., Lunt, E., (1985a). CCRG 81045- an antitumour imidazotetrazinones with potential as a clinical alternative to DTIC. *Br. J. Cancer*, 52: 3.

Langdon, S.P., Stone, R., Stevens, M.F.G., Gibson, N.W., Chubb, D., Hickman, J.A., Lavelle, F., Fizames, C., (1985b). CCRG 81045- a novel imidazotetrazinone with broad spectrum activity against murine tumours. *Proc. Amer. Assoc. Cancer Res.* 26: 1006.

- Lay Jr., J.O., Korfmacher, W.A., Miller, D.W., Siitonen, P., Holder, C.L., Gosnell, A.B., (1986). Desorption chemical ionization and fast atom bombardment mass spectrometric studies of the glucuronide metabolites of doxylamine. *Biomed. Envir. Mass Spec.* 13: 627-632.
- Levin, V.A., Stearns, J., Byrd, A., Finn, A., Weinkham, R.J., (1979). Effect of phenobarbital pretreatment on the antitumour activity of BCNU, CCNU and FCNU and on the plasma pharmacokinetics and biotransformation of BCNU. *J. Pharmacol. Exp. Ther.*, 2081-2086.
- Levin, V.A., (1981). Clinical pharmacology of nitrosoureas. In nitrosoureas: current status and future development. Ed. Prestagkyo, A.W., Schein P.S.). Academic Press. New York: 171-180.
- Lin, Y.T., Loo, T.L., (1972). Preparation and antitumour activity of derivatives of 1-phenyl-3,3-dimethyltriazene. *J. Med. Chem.*, 15(2): 201-203.
- Loo, T.L., Stasswender, E.A., (1967). Colorimetric determination of dialkyltriazenoimidazoles. *J. Pharm. Sci.*, 56: 1016-1018.
- Loo, T.L., Tanner, B.B., Householder, G.E., Shepard, B.J., (1968a). Some pharmacokinetic aspects of 5-(dimethyl triazeno)-imidazole-4-carboxamide in the dog. *J. Pharm. Sci.*, 57(12): 2126-2131.
- Loo, T.L., Luce, J.K., Jardine, J.H., Frei III, E., (1968b). Pharmacologic studies of the antitumour agents 5-(dimethyltriazeno)-imidazole-4-carboxamide. *Cancer Res.*, 28: 2448-2453.
- Loo, T.L., Householder, G.E., Gerulath, A.H., Saunders, P.H., Farquhar, D.L., (1976). Mechanism of action and pharmacologic studies with DTIC (NSC 45388). *Cancer Treat. Rep.*, 60: 149-152.
- Lowe, P.R., Schwalbe, C.H., Whiston, C.D., Stevens, M.F.G., (1985). Antitumour imidzotetrazinones: the crystal and molecular structure of mitozolomide and five of its analogues. *J. Pharm. Pharmacol.* 37: 136p.
- Lowe, P.R., Schwalbe, C.H., Stevens, M.F.G., (1985), Antitumour imidazotetrazinones. Part 5 <sup>1</sup> crystal and molecular structure of 8-carbamoyl 1,3-(2-chloroethyl) imidzo[5,1-d]-1,2,3,5-tetrazin-4(3H)-one (mitozolomide). *J. Chem. Soc. Perkins Trans.* 2: 357-
- Lowry, O.H., Rosebrough, N.J., Ferr, A.L., Randall, R.J., (1951). Protein measurement with the folin Phenol reagent. *J. Biol. Chem.*, 193: 265-275.
- Lunn, J.M., Harris, A.L., Brown, P.M., Pierpoint, C.,

- Golding, B.T., (1986). Potentiation of the cytotoxic action of DTIC involvement of O<sup>6</sup>-methylguanine-DNA methyltransferase. *Br. J. Cancer*, 54(1): 186-
- Lunn, J.M., Harris, A.L., (1988). Cytotoxicity of 5-(3-methyl-1-triazeno)imidazole-4-carboxamide (MTIC) on Mer<sup>+</sup>REM<sup>-</sup> and Mer<sup>-</sup> cell lines: differential potentiation by 3-acetamidobenzamide. *Br. J. Cancer*, 57: 54-58.
- Major, R.E., (1976). Liquid-solid (adsorption chromatography). In *Practical performance liquid chromatography*. (Ed. Simpson G.C.F.). Heyden and Son Ltd. p.89-108.
- Marsh, C.A., (1963). D-glucuronic acid and its glycosides. In *Glucuronic acid. Free and combined chemistry, biochemistry, pharmacology and medicine*. Ed. Dutton, G.J. Acad. Press: 4-119.
- McKeage, M.J., Roberts, P.B., (1989). Mitozolomide-induced sensitisation of mammalian cells in vitro to radiation. *Br. J. Cancer*, 60:182-184.
- Meers, L., Janzer, R.C., Kleihues, P., Kolar, G.F., (1986). In vivo metabolism and reaction with DNA of the cytostatic agent 5-(3,3-dimethyl-1-triazeno)-imidazole-4-carboxamide (DTIC). *Biochem. Pharmacol.*, 35(19): 3243-3247.
- Mehta, J.R., Ludlum D.B., Renard, A., Verly, W.G., (1981). Repair of O<sup>6</sup>-ethylguanine in DNA by a chromatin fraction from rat liver: Transfer of the ethyl group to an acceptor protein. *Proc. Natl. Acad. Sci.*, 78(11): 6766-6770.
- Metelmann, H-R., Von Hoff, D.D., (1983). In vitro activation of dacarbazine (DTIC) for a human tumor cloning system. *Int. J. Cell Cloning*. 1: 24-32.
- Mitchell, E.P., Schein, P.S., (1986). Contributions of nitrosoureas to cancer treatment. *Cancer Treat. Rep.*, 70: 31-41.
- Mihich, E., (1981). In *New Leads in Cancer Therapeutics*; ed. E. Mihich. G.K. Hall Medical Publishers, Boss, Mass.
- Mizuno, N.S., Humphrey, E.W., (1972). Metabolism of 5-(3,3-dimethyl-1-triazeno)-imidazole-4-carboxamide (NSC 45388) in human and animal tumour tissue. *Cancer Chemother. Rep.*, 56(1): 465-472.
- Montgomery, J.A., (1959). The relation of anticancer activity to chemical structure- A review. *Cancer Res.*, 19(5): 447-463.
- Montgomery, J.A., (1976). Experimental studies at

Southern Research Institute with DTIC (NSC-45388).  
Cancer Treat. Rep. 60: 125-134.

Monti, J.P., Gallice, Crevat, A., Murisasco, A., (1985).  
Identification by nuclear magnetic resonance and mass  
spectrometry of a glucuronic acid conjugate of  
O-hydroxybenzoic acid in normal urine and uremic plasma.  
Clin. Chem., 31/10: 1640-1643.

Mraz, J., Turecek, F., (1987). Identification of  
N-acetyl-S-(N-methylcarbamoyl)cysteine a human metabolite  
of N,N-dimethylformamide and N-methylformamide. J.  
Chromatography 414: 399-404.

Nash, T., (1953). The colorimetric estimation of  
formaldehyde by means of the Hantzsch reaction. Biochem.  
J., 55: 416-421.

Nature (1979). U.S. studies identify formaldehyde as  
carcinogenic. 281: 625.

Newell, D., Gescher, A., Harland, S., Ross, D., Rutty,  
C., (1987). N-methyl antitumour agents- a distinct class  
of anticancer drugs. Cancer Chemother. Pharmacol., 19:  
91-102.

Newlands, E.S., Blackledge, G., Slack, J.A., Goddard, C.,  
Brindley, C.J., Holden L., Stevens, M.F.G., (1985).  
Phase I clinical trial of mitozolomide.  
Cancer Treat. Rep., 69(7-8): 801-805.

Newlands, E.S., Slack, J., Blackledge, Stuart, N.,  
Quarterman, C., Hoffman, R., Stevens, M.F.G., (1989).  
Sixth NCI-EORTC symposium on new drugs in cancer therapy.  
Amsterdam. March 7-10. 419.

Newman, R.A., Farquhar, D., (1987). Release of methyl  
isocyanate from the antitumour agent caracemide  
(NSC-253272). Investigational New Drugs 5: 267-271.

Nicholson, J.K., Wilson, I.D., (1987). The detection of  
drug metabolites in biological samples by high resolution  
proton NMR spectroscopy. In Drug metabolism from  
molecules to man. Ed. Benford, D.J., Bridges, J.W.,  
Gibson, G.G.: 189-207.

Olsson, M., Lindahl, T., (1980). Repair of alkylated  
DNA in Escherichia Coli. J. Biol. Chem., 255:  
10569-10571.

Overton, M., Hickman, J.A., Threadgill, M.D., Vaughan,  
K., Gescher, A., (1985). The generation of potentially  
toxic, reactive iminium ions from the oxidative  
metabolism of xenobiotic N-alkyl compounds. Biochem.  
Pharmacol. 34: 2055-2061.

Panasci, L.C., Fox, P.A., Schein, P.S. (1977).

Structure activity studies of methylnitrosourea antitumour agents with reduced murine bone marrow toxicity. *Cancer Res.*, 37: 3321-3328.

Pool, B.L., (1979a). Microsomal mediated metabolism of dialkylaryltriazenes I. Demethylation of ring halogenated 3,3-dimethyl-1-phenyl triazenes. *J. Cancer Res. Clin. Oncol.*, 93: 215-220.

Pool, B.L., (1979b). Microsomal mediated metabolism of dialkyltriazenes II. Isolation and identification of metabolites of 3,3-dimethyl-1-phenyl triazene. *J. Cancer Res. Clin. Oncol.* 93: 221-231.

Pratt, W.B., Rudden, R.W., (1979). *The anticancer drugs.* Oxford University Press, U.K.

Preussmann, R., Von Hodenberg, A., Hengy, H., (1969a). Mechanism of carcinogenesis with 1-aryl-3,3-dialkyl triazenes. Enzymatic dealkylation by rat liver microsomal fraction in vitro. *Biochem. Pharmacol.*, 18: 1-13.

Preussmann, R., Druckery, H., Ivankovic, S., Von Hodenberg, A., (1969b). Chemical structure and carcinogenicity of aliphatic hydrazo, azo, and azoxy compounds and of triazenes, potential in vivo alkylating agents. *Ann. N.Y. Acad. Sci.* 163: 687-714.

Preussman, R., Hodenberg, A., (1970). Mechanism of carcinogenesis II, in vitro alkylation of guanosine RNA and DNA with arylmonoalkyltriazenes to form 7-alkylguanine. *Biochem. Pharmacol.* 19: 1505-1508.

Rajewsky, M.F., (1982). Pulse-carcinogenesis by ethylnitrosourea in the developing rat nervous system: molecular and cellular mechanisms. In: *Chemical Carcinogenesis.* Ed. Nicolini, C. Plenum Press. New York. 363-379.

Rapoport, I.A., (1946). Carbonyl compounds and the chemical mechanism of mutation. *C.R. Acad. Sci. (URSS)*. 54: 65-67.

Ross, W.E., Shipley, N., (1980). Relationship between DNA damage and survival in formaldehyde-treated mouse cells. *Mutation Res.* 79: 277-283.

Ross, D., Farmer, P.B., Gescher, A., Hickman, J.A., Threadgill, M.D., (1981). The formation and metabolism of N-hydroxymethyl compounds-I. The oxidative N-demethylation of N-dimethyl derivatives of arylamines, aryltriazenes, arylformamidines and arylureas including the herbicide monuron. *Biochem. Pharmacol.* 31(22): 3621-3627.

Ross, D. (1982). Ph.D. thesis, Aston University.

Ross, D., Farmer, P.B., Gescher, A., Hickman, J.A., Threadgill, M.D., (1983). The formation and metabolism of N-hydroxymethyl compounds-III. The metabolic conversion of N-methyl and N,N,-dimethylbenzamides to N-hydroxymethyl compounds. *Biochem. Pharmacol.* 32(11): 1773-1781.

Rowlands, M., Tozer, T.N. (1980). *Clinical Pharmacokinetics. Concept and application.*

Rutty, C.J., Abel, G., (1980). *In vitro* cytotoxicity of the methylmelamines. *Chem.-Biol. Interactions.* 29: 235-246.

Rutty, C.J., Newell, D.R., Vincent, R.B., Abel, G., Goddard, P.M., Harland, S.J., Calvert, A.H., (1980). The species dependent pharmacokinetics of DTIC. *Br. J. Cancer.*, 48: 140.

Sava, G., Giraldi, T., Lassiani, L., Nisi, C., (1982). Metabolism and mechanism of the antileukaemic action of isomeric aryl dimethyl triazenes. *Cancer Treat. Rep.* 66: 1751-1755.

Sava, G., Zorzet, S., Perissin, L., Giraldi, T., Lassiani, L., (1988). Effects of an inducer and an inhibitor of hepatic metabolism on the antitumour action of dimethyl triazenes. *Cancer Chemother. Pharmacol.*, 21: 241-245.

Schein, P.S., (1981). In *Cancer and Chemotherapy 3: Antineoplastic agents*; eds. Crooke, S.T., Prestayko, A.W. Academic Press, New York. 37-48.

Schmall, B., Cheng, C.J., Fujimura, S., Gersten, N., Grunberger, D., Weinstein, B.I., (1973). Modification of Proteins by 1-(2-chloroethyl)-3-cyclohexyl-1-nitrosourea (NSC 79037) *in vitro*. *Cancer Res.*, 33: 1921-1924.

Segal, A., Solomon, J.J., Li, F., (1989). Isolation of methylcarbamoyl-adducts of adenine and cytosine following *in vitro* reaction of methyl isocyanate with calf thymus DNA. *Chem.-Biol. Interactions*, 69: 359-372.

Shaw, A.J., Gescher, A., Mraz, J., (1988). Cytotoxicity and metabolism of hepatotoxic N-methylformamide and related formamides. *Tox. Appl. Pharmacol.* 95: 162-170.

Shaw, A.J., (1988). Ph.D. thesis, Aston University.

Shealy, F.Y., Struck, R.F., Holum, L.B., Montgomery, J.A., (1961). Synthesis of potential anticancer agents XXIX. 5-diazo-imidazole-4-carboxamide and 5-diazo-v-triazole-4-carboxamide. *J. Org. Chem.* 26: 2396-2401.

Shealy, F.Y., Krauth, C.A., Montgomery, J.A., (1962a). Imidazoles. I coupling reactions of diazoimidazole-4-carboxamide. *J. Org. Chem.* 27: 2150-2154.

Shealy, F.Y., Montgomery, J.A., Laster Jr., W.R., (1962b). Antitumour activity of triazenoimidazoles. *Biochem. Pharmacol.* 2: 674-676.

Shealy, Y.F., Clayton, S.G., Krauth, C.A., Caster, Jr., W.R., Shortnacy, A.T., (1968). Imidazoles. V. 5(or4)-(3-alkyl-3-methyl-1-triazeno)imidazole-4(or5)-carboxamides. *J. Pharm. Sci.*, 57: 1562-1568.

Shealy, Y.F., O'Dell, C.A., Krauth, C.A., (1975). 5-[3-(2-chloroethyl)-1-triazenyl-1-]imidazole-4-carboxamide and a possible mechanism of action of 5-[3,3-bis(2-chloro-ethyl)-1-triazenyl]-imidazole-4-carboxamide. *J. Pharm. Sci.* 64: 177-180.

Singer, B., (1979). N-nitroso alkylating agents: formation and persistence of alkyl derivatives in mammalian nucleic acids as contributing factors in carcinogenesis. *JNCI*, 62(6): 1329-1339.

Skibba, J.L., Beal, D.D., Bryan, G.T., (1969a). A sensitive method for the determination of plasma and urinary 4(5)-amino-5(4)-imidazole carboxamide. *Biochem. Med.* 3: 150-157.

Skibba, J.L., Ramirez, G., Beal, D.D., Bryan, G.T., (1969b). Preliminary clinical trial and the physiologic disposition of 4(5)-(3,3-dimethyl-triazeno)-imidazole-5(4)-carboxamide in man. *Cancer Res.*, 29: 1944-1951.

Skibba, J.L., Beal, D.D., Ramirez, G., Bryan, G.T., (1970). N-demethylation of the antineoplastic agent 4(5)-(3,3-dimethyl-1-triazeno)imidazole-5(4)-carboxamide by rats and man. *Cancer Res.*, 30: 147-150.

Skibba, J.L., Bryan, G.T., (1971). Methylation of nucleic acids and urinary excretion of <sup>14</sup>C-labelled 7-methylguanin by rats and man after administration of 4(5)-3,3-dimethyl-1-triazeno)-imidazole-5(4)-carboxamide. *Tox. App. Pharm.* 18: 707-719.

Slack, J.A., Goddard, C., (1985). Antitumour imidazotetrazines. VII. Quantitative analysis of mitozolomide in biological fluids by high performance liquid chromatography. *J. Chromatography (Biomed. App.)*, 337: 178-181.

Slack, J.A., Goddard, C., Stevens, M.F.G., Baig, G.U., Griffin, M.J., (1986). The analysis and murine pharmacokinetics of a new antitumour agent CCRG 81045. *J. Pharm. Pharmacol.*, 38: 63p.



3-4-chlorophenyl-1-methylurea in cotton. *Phytochemistry*.  
11: 2701-2708.

Tate, P.S., Briele, H.A. (1986). Reversed-phase high performance liquid chromatography of 5-(3,3-dimethyl-1-triazeno)imidazole-4-carboxamide and metabolites. *J. Chromatography*. 374: 421-424.

Testa, B., Jenner, P., (1976). *Drug Metabolism- Chemical and Biochemical Aspects*. Vol.I

Thomson, A.E.R., Barnsley, E.A., Young, L., (1963). Biochemical studies of Toxic agents. 14. The biosynthesis of ethylmercapturic acid. *Biochem J.*, 86: 145-152.

Tisdale, M.J., (1985a). Antitumour imidazotetrazines-XI: Effect of 8-carbamoyl-3-methyl imidazo-[5,1,d]-1,2,3,5-tetrazin-4(3H)one [CCRG 81045, M&B 39831, NSC 362856] on poly ADP ribose metabolism. *Br. J. Cancer*, 52: 789-792.

Tisdale, M.J., (1985b). Induction of haemoglobin synthesis in the Human Leukaemia cell line K562 by monomethyl triazines and imidazotetrazinones. *Biochem. Pharmacol.*, 34(12); 2077-2082.

Tisdale, M.J., (1987). Antitumour Imidazotetrazines-XV. Rôle of guanine O<sup>6</sup> alkylation in the mechanism of cytotoxicity of imidazotetrazinones. *Biochem. Pharmacol.*, 36(4): 457-462.

Tisdale, M.J., (1988). Antitumour imidazotetrazines and gene expression. *Acta Oncologica*, 27: 511-516.

Tisdale, M.J., (1989). Antitumour imidazotetrazines -XVIII. Modification of the level of 5-methylcytosine in DNA by 3-substituted imidazotetrazinones. *Biochem. Pharmacol.* 38(7): 1097-1101.

Tong, W.P., Ludlum, D.B., (1981). Formation of the Cross-linked base, diguanylethane, in DNA treated with N,N'-bis(2-chloroethyl)-N-nitrosourea. *Cancer Res.*, 41: 380-382.

Threadgill, M.D., Axworthy, D.B., Baillie, T.A., Farmer, P.B., Farrow, K.C., Gescher, A., Kestell, P., Pearson, P.G., Shaw, A.J., (1987). Metabolism of N-methylformamide in mice: primary kinetic deuterium isotope effect and identification of S-(N-methylcarbamoyl)glutathione as a metabolite. *J. Pharmacol. Exp. Ther.*, 242: 312-319.

Van Breemen, R.B., Stogniew, M., Fenselau, C., (1988). Characterization of acyl-linked glucuronides by electron impact and fast atom bombardment mass spectrometry. *Biomed. Envir. Mass Spec.* 17: 97-103.

Slack, J.A., Newlands, E.S., Blackledge, G.R.P., Quarterman, C.P., Stuart, N.S.A., Hoffman, R., Stevens, M.F.G., (1989). Phase I clinical pharmacokinetics of temozolomide (CCRG81045, NSC362856). Proceedings of AACR, 30: 250.

Smith, R.L., Williams, R.T., (1963). Implications of the conjugation of drugs and other endogenous compounds. In Glucuronic acid free and combined. Chemistry, biochemistry, pharmacology and medicine. Ed. Dutton, G.J. Acad. Press: 457-491.

Soloway, A.H., Brumbaugh, R.J., Wittiak, D.T., (1983). Carbinolamines and related structures-potential alkylating metabolites of clinically active anticancer drugs. J. Theor. Biol. 102: 361-373.

Spasova, M.K., Golovinsky, E.V., (1985). Pharmacobiochemistry of arylalkyltriazenes and their application in cancer chemotherapy. Pharmac. Ther., 27: 333-352.

Stevens, M.F.G., (1983). DTIC-springboard to new antitumour drugs. In. Structure activity relationships of antitumour agents. Ed. Reinhoudt, D.N., Connors, T.A.; Pinedo, H.M., Vandepoll, K.W. Developments in pharmacology. Martinus Nijhoff Publishers. 183-218.

Stevens, M.F.G., Hickman, J.A., Stone, R., Gibson, N.W., Baig, G.U., Lunt, E., Newton, C.G. (1984). Antitumour imidazotetrazines. 1, synthesis and chemistry of 8-carbamoyl-3-(2-chloroethyl)-imidazo-[5,1-d]1,2,3,5-tetrazin-4(3H)one- a novel broad spectrum antitumour agent. J. Med. Chem. 27: 196-201.

Stevens, M.F.G., Hickman, J.A., Langdon, S.P., Chubb, D., Vickers, L., Stone, R., Baig, G., Goddard, C., Slack, J.A., (1987). Antitumour activity and pharmacokinetics in mice of 8-carbamoyl-3-methyl-imidazo[5,1-d]1,2,3,5-tetrazin-4(3H)one (CCRG 81045, M&B 39831)- a novel drug with potential as an alternative to dacarbazine. Cancer Res. 47: 5846-5852.

Stevens, M.F.G., (1987). In: New avenues in developmental cancer chemotherapy. Ed. Harrap, Kenneth R., Connors, Thomas A. Acad. Press. 335-354.

Stone, R., (1981). Ph.D. thesis, University of Aston.

Swenberg, J.A., Kerns, W.D., Mitchell, R.I., Gralla, E.J., Pavkov, K.L., (1980). Induction of squamous cell carcinoma of the rat nasal cavity by inhalation exposure to formaldehyde vapor. Cancer Res. 40: 3398-3402.

Tanaka, F.S. et al (1972). An unstable hydroxymethyl intermediate formed in the metabolism of

Van Oosterom, A.T., Stoter, G., Bono, A.V., Splinter, T.A.W., Fossa, S.D., Verbaeys, A., De Mulder, P.H.M., De Pauw, M., Sylvester, R., (1989). Mitozolomide in advanced renal cancer. A phase II study in previously untreated patients from the EORTC genito-urinary cancer co-operative group. *Eur. J. Cancer Clin. Oncol.* 25(8):1249-1250

Vaughan, K., Stevens, M.F.G., (1978). Monoalkyltriazenes. *Chem. Soc. Rev.*, 7(3): 377-397.

Vaughan, K., Tang, Y., Llanos, G., Horton, J.K., Simmonds, R.J., Hickman J.A., Stevens, M.F.G., (1984). Studies of the mode of action of antitumour triazenes and triazines. 6. 1-Aryl-3-(hydroxymethyl)-3-methyl triazenes: synthesis, chemistry and antitumour properties. *J. Med. Chem.* 27:357-363.

Venditti, J.M., (1976). Antitumour activity of DTIC (NSC-45388) in animals. *Cancer Treat. Rep.* 60(2): 135-139.

Verweij, A., Kientz, C.S., (1981). High-performance liquid chromatographic separation, isolation and identification of 1,2,3-thiadiazole-5-carboxaldoxime glucuronide in rabbit urine. *J. Chromatography*, 226: 165-173.

Wheeler, G.P., Bowden, B.J., Grimsley, J.A., Lloyd, H.H., (1974). Inter-relationships of some chemical, physiological and biological activities of several 1-(2-haloethyl)-1-nitrosoureas. *Cancer Res.*, 34, 194-210.

Williams, D.H., Fleming, I., (1980). Spectroscopic methods in organic chemistry. 3rd ed.

Wilman, D.E.V., Goddard, P.M., (1980). Tumour inhibitory triazenes 2. Variation of antitumour activity with an homologous series. *J. Med. Chem.* 23: 1052-1054.

Wilson, I.D., Nicholson, J.K., (1988). Solid phase extraction chromatography and NMR spectroscopy (SPEC-NMR) for the rapid identification of drug metabolites in urine. *J. Pharm. Biomed. Anal.*, 6(2): 151-165

Woolley, D.W., Shaw, E., (1951). Some imidazo-1,2,3-triazines and their biological relationships to the purine. *J. Biol. Chem.* 189: 401-410.

Workman, P., Lee, F.Y.F., (1984). Experimental antitumour activity and mechanism of action of the novel anticancer agent CCRG 81010. *Br. J. Cancer* 50: 251.

Yamamoto, A., Yoshimura, H., Tsukamoto, H., (1962).

Metabolism of drugs. XXVIII. Metabolic fate of meprobamate (1). Isolation and characterization of metabolites. Bull. Pharm. Chem. 10: 522-528.